Title
A Ring Expansion Strategy Toward the Synthesis of Hetisine-Type C20-Diterpenoid Alkaloids

Author
Kisunzu, Jessica Kristine

Publication Date
2014

Peer reviewed|Thesis/dissertation

A Ring Expansion Strategy Toward the Synthesis of Hetisine-Type C_{20}-Diterpenoid Alkaloids

by

Jessica Kristine Kisunzu

A dissertation submitted in partial satisfaction of the
requirements for the degree of
Doctor of Philosophy
in
Chemistry
in the
GRADUATE DIVISION
of the
UNIVERSITY OF CALIFORNIA, BERKELEY

Committee in charge:

Professor Richmond Sarpong, Chair
Professor K. Peter C. Vollhardt
Professor Wenjun Zhang

Spring 2014

Abstract

A Ring Expansion Strategy Toward the Synthesis of Hetisine-Type C_{20}-Diterpenoid Alkaloids

by

Jessica Kristine Kisunzu

Doctor of Philosophy in Chemistry

University of California, Berkeley

Professor Richmond Sarpong, Chair

A benzyne insertion ring expansion strategy toward the synthesis of hetisine-type C_{20}-diterpenoid alkaloids has been developed. The first chapter of this manuscript presents an introduction to C_{20}-diterpenoid alkaloids and previous synthetic work toward selected target core structures. The second and third chapters outline our ring expansion strategy for the synthesis of the core of the natural product cossonidine and efforts to complete its total synthesis.

An overview of the structural and biological properties of C_{20}-diterpenoid alkaloids is provided, as well as a survey of the synthetic studies that have been carried out thus far toward natural products containing the hetidine and hetisine-type framework. The two existing syntheses of a hetisine-type diterpenoid alkaloid are also described. This review outlines some of the salient structural challenges associated with the synthesis of these compounds, as well as the strategies applied to their construction.

An approach involving a ring expansion was developed to access a tricyclic motif conserved in the hetidine and hetisine frameworks. The acyl-alkylation of aryne intermediates by insertion into C–C sigma bonds was applied to several β-ketoesters and aryne precursors to investigate the efficacy of this transformation on complex systems. Three tricyclic intermediates were synthesized that contain functional handles at the appropriate positions for C–N bond formation to construct the hetisine core.

With a sequence in place to arrive as several desired tricyclic intermediates, they were then employed to investigate C–N bond formation. A range of conditions was explored, and the desired azabicycle was accessed in 3 steps from the tricyclic scaffold. The requisite [2.2.2] bicycle was then formed in 2 steps to complete the hetisine core. Finally, the synthetic sequence was modified in order to introduce a methyl group necessary for completion of the natural product target. This methylation pathway has been successful in providing the full hetisine core en route to the synthesis of the natural product cossonidine.

To my family, both immediate and extended,
for their continued love and support.

TABLE OF CONTENTS

Acknowledgements

First, I thank God for sustaining me through my time here at UC Berkeley and for reminding me that "He who began a good work in you will carry it on to completion until the day of Christ Jesus" (Phil. 1:6).

I want to thank Professor Richmond Sarpong for the opportunity to work with him and to target such cool and complex natural products over the last 5 years. I have appreciated and learned from his ideas, support, encouragement, and enthusiasm for chemistry during this time.

The research described in these pages couldn't have gone this far without the people I worked with directly. I am grateful to Dr. Ethan Fisher, Dr. Toshihiro Kiho, and Kyle Clagg, my (no longer an) undergrad, who were all wonderful to work with and played a big part in pushing the project forward.

I have had the opportunity to face all of the hurdles and pass all of the milestones of graduate school with the Sarpong class of 2014—Amy Hamlin, Rebecca Murphy, Erica Schultz, and Gary Gallego. Their friendship has meant a lot to me and I'm excited to see where these next stages of life take us.

Outside of my graduating class, I have been able to work with many others in the Sarpong group who have provided a fun and intellectually stimulating work environment, and helped me to grow as a synthetic chemist and as a person. Dr. Alison Narayan and Dr. Jessica Herrick were mentors and sources of advice to me during our overlapping graduate careers. Dr. Terry Lebold was not only a great person to work with in lab, but also pioneered some of the early work that I have been able to use in my research. I had the chance to sit and work next to Chris Marth, and our friendship and various conversations, chemistry-related and otherwise, have meant a lot to me. I'm grateful to other members of the Sarpong lab: Jack Lee, Sidney Wilkerson-Hill, Jason Pflueger, and Zach Hallberg, for research discussions and for their encouragement. I also want to acknowledge Chris Marth, Dr. Vincent Lindsay, Paul Leger, and Zach Hallberg for the time and effort they put into thesis edits.

My thanks go to my qualifying exam and dissertation committee members Professors Dean Toste, Robert Bergman, Peter Vollhardt, Nancy Amy, and Wenjun Zhang for their time and feedback as I moved through my graduate study.

Many other relationships have developed over the years since I have moved to Berkeley. Specifically, I'm thankful for the continued friendship of Chelsea Gordon and Miles Johnson from the very beginning. I also want to thank my Richmond and Berkeley church families, especially Shaunna Foster, Krystal Johnson, Alie and Walter Graf, Christine Purba, and Lucien-Nahum Isaac, for their fellowship and support.

Finally, I would like to give a big thank you to my parents and my brother for their constant love and presence over the years. Knowing that they were there for me has been a source of strength even when things were particularly challenging. I especially enjoyed being able to live only an hour away from my brother for a couple years, giving us the chance to see each other more often than before.

Chapter 1. Hetidine and Hetisine-Type C_{20}-Diterpenoid Alkaloids

1.1 Introduction

The hetidine and hetisine-type C_{20}-diterpenoid alkaloids are highly caged natural products that are members of the diterpenoid alkaloid family. They have been of interest to the synthetic community due to their complex structures, as well as to biologists and chemical biologists as a result of their biological implications and unique binding capabilities. This chapter will outline the structural classifications of the C_{20}-diterpenoid alkaloids, as well as their isolation, biosynthesis, and bioactivity. Synthetic studies toward these compounds and the two existing completed syntheses of the hetisine-type alkaloid nominine will be discussed.

1.2 Isolation, bioactivity, and structure

Alkaloids are nitrogen-containing compounds that can be divided into two broad types according to their biogenesis: (1) "true alkaloids" are derived directly from amino acids, and (2) "pseudo (or crypto-) alkaloids" are derivatives most often of terpenoid or steroidal origin, and have the nitrogen atom introduced at a later stage from methylamine, ethylamine, or β-aminoethanol.[1a] Alkaloid-containing extracts from plants have been used as both medicines and poisons for many years, making their biological mode of action a subject of interest. As many of their structures have been elucidated by degradation studies, X-ray crystallography, and total synthesis, synthetic chemists have also been drawn to their complexity.

Structurally, the diterpenoid alkaloids are classified as C_{18}, C_{19}, or C_{20}, according to the number of carbons in the core framework. The C_{20}-diterpenoid alkaloid family of natural products contains over 400 compounds.[1b] These compounds have been isolated from many different species of plants, the majority of which belong to the *Aconitum* and *Delphinium* genera, from the Ranunculaceae (or buttercup) family, and the *Spiraea* genus in the Rosaceae family of shrubs. In many countries, plants that contain significant levels of diterpenoid alkaloids have been used in traditional medicine for the treatment of sepsis, plaque, rheumatoid arthritis, and pain.[1a] More recently, the bioactivity of specific diterpenoid alkaloids has been increasingly studied and has been the topic of review by Wang and coworkers.[1c] Compounds in the diterpenoid alkaloid family span a range of strength in binding certain receptors, as well as several modes of action. Levels of oxygenation and ester functionalization correlate to reactivity and toxicity, with more highly oxygenated and acylated compounds having a strong effect on the central nervous system (CNS), due to interaction of the natural products with voltage-gated sodium ion channels.[1c,2] Compounds that are less decorated exhibit a weaker CNS effect, but still influence other systems. C_{20}-diterpenoid alkaloids, specifically, have been shown to possess cytotoxicity against certain cell lines, antiparasite and insect antifeedant activity, and to also have an effect on murine blood flow.[1c]

Wang and Liang divided the C_{20}-diterpenoid alkaloids into four major classes according to their carbon skeletons.[1a] The atisane class (**A**, Figure 1-1) is characterized by the [2.2.2] bicycle on the right-hand portion of the compounds. In place of this [2.2.2] bicycle, alkaloids in the kaurane structural class (**B**) contain a [3.2.1] bicycle. The rearranged class (**C**) is defined by the rearrangement of rings on the right-hand portion of the framework as viewed in Figure 1-1. Finally, the bisditerpenoid class (**D**) is derived from condensation of two C_{20}-diterpenoid alkaloids or one each of the C_{19} and C_{20} compounds.

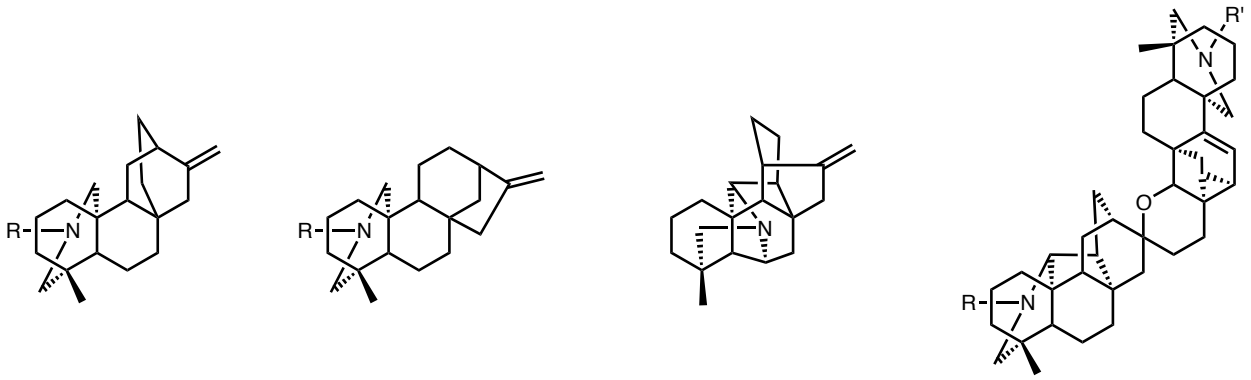

Figure 1-1. The four structural classes of C_{20}-diterpenoid alkaloids.

Within the atisane class, there are eight further subdivisions that are delineated according to the C–C and C–N bonds that are present (Figure 1-2). For example, the denudatine type (**AII**) contains an additional C20–C7 bond as compared to the general atisane structure. The hetidine type (**AIV**) contains an additional C20–C14 bond, and an additional N–C6 bond formation leads to the hetisine structure (**AVII**). Bond scission creates a distinction as well, seen in the case of the cardionidine subtype (**AV**), which contains a 6,7-*seco*-hetidine core.

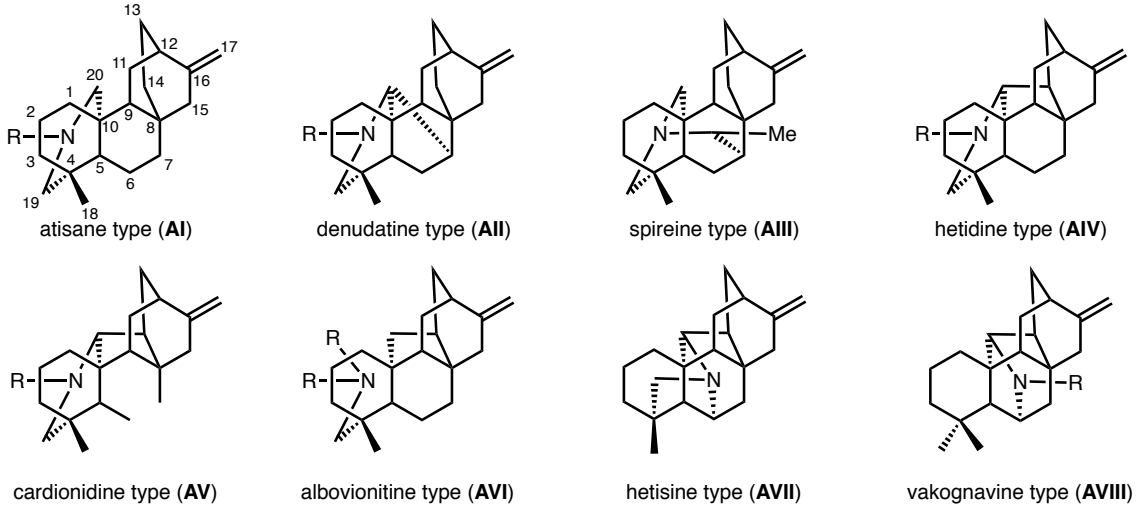

Figure 1-2. Structural divisions of the atisane class.

1.3 Proposed Biosynthesis and degradation studies

C_{20}-Diterpenoid alkaloids arise biosynthetically from geranylgeranyl pyrophosphate (GGPP, **1.1**, Scheme 1-1)[1a,b] via enzyme-mediated cyclizations. It is proposed that initial cyclization delivers *ent*-copalyl diphosphate (**1.2**), which then further cyclizes with the loss of pyrophosphate to give carbocation **1.3**. At this point, several pathways are operative, although the exact sequence is unknown. Loss of a proton coupled with an alkyl shift (red arrows) forms the [3.2.1] bicycle characteristic of alkaloids in the kaurane class (**1.5**). Alternatively, a hydride shift (in blue) followed by an alkyl shift to form the tertiary carbocation and loss of a proton arrives instead at the [2.2.2] bicycle that is present in the atisane class (**1.9**). Recent computational studies by Tantillo suggest that several alkyl and hydride shifts happen in a

concerted fashion to avoid secondary carbocations.[3] The hydrocarbon framework is then oxidized and nitrogen is incorporated from L-serine in the form of β-aminoethanol.[4]

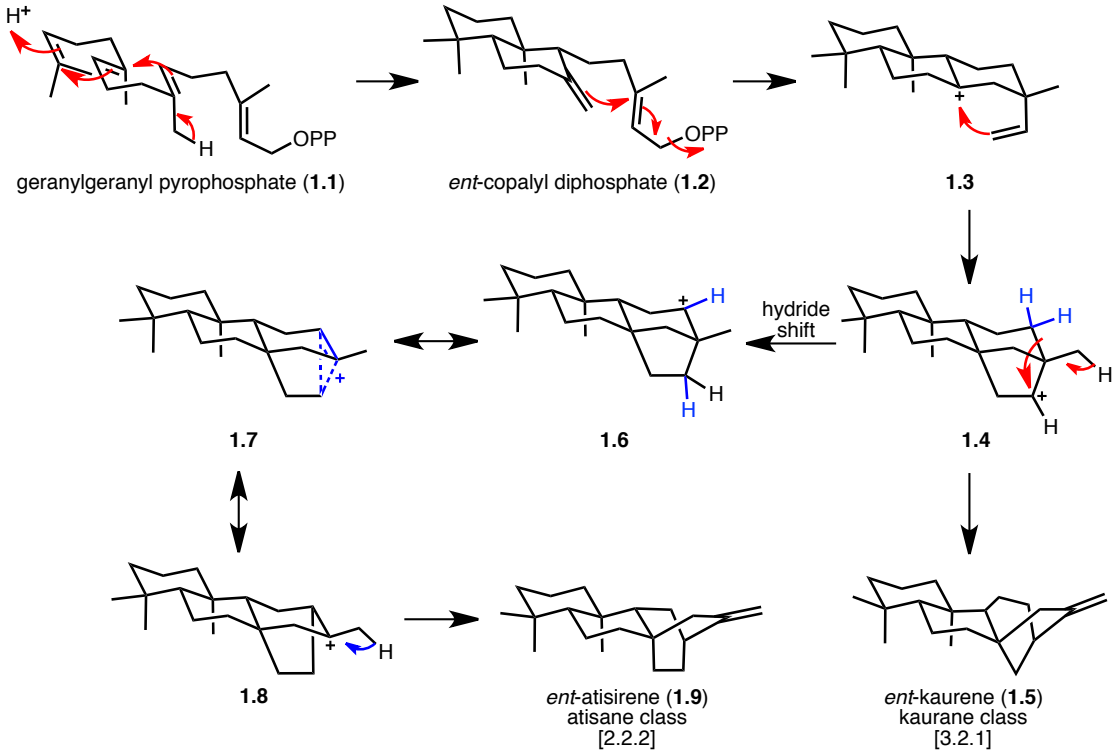

Scheme 1-1. Proposed biosynthetic pathway for diterpenoid alkaloids in the atisane and kaurane classes.

Many C_{20}-diterpenoid alkaloids contain the hetidine (**AIV**) or hetisine (**AII**) core framework. The two carbon skeletons are related biogenetically and arise from *ent*-atisirene (**1.9**, Scheme 1-2).[1a] Oxidation of **1.9** to an intermediate such as **1.10** allows for incorporation of the nitrogen atom. Formation of the C20–C14 bond occurs first (i.e., **1.11**→ **1.12**) followed by N–C6 bond formation to arrive at the hetisine framework. The isolation of compounds like talassimine (**1.14**) also lends insight into the possible pathways that link the two structural cores.

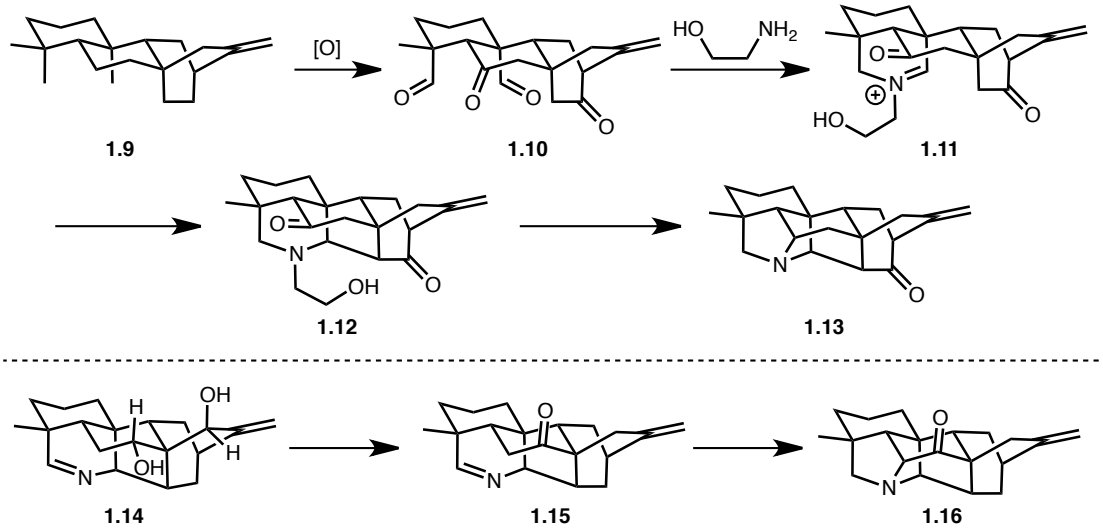

Scheme 1-2. Biogenetic relationship between the hetidine and hetisine cores.

From the onset of isolation and identification of C_{20}-diterpenoid alkaloids, degradation studies were performed to confirm the structures and probe the connectivity between compounds and structural classes. For the hetisine-type alkaloids, seminal work in this area was accomplished by Okamoto and coworkers.[5,6] Starting from kobusine (**1.17**, Scheme 1-3), they investigated the cleavage and reformation of the C14–C20 and N–C6 bonds, as these are key bonds that establish the relationship between the hetidine, hetisine, and atisine cores.

Subjection of kobusine to reducing conditions (sodium in *n*-propanol) followed by acylation gave acetate **1.18** (Scheme 1-3). Treatment of **1.18** with phenyl chloroformate in *o*-dichlorobenzene at reflux delivered carbamate **1.19** in 90% yield, where the N–C6 bond has been cleaved. Interestingly, it was observed that hydrolysis of the carbamoyl group resulted in reformation of the N–C6 bond (to yield **1.18**) when the C6–C7 double bond was in place as in **1.19**. Therefore, reduction of the C6–C7 double bond was necessary in order to achieve further manipulation. This observation is of note because forming the strained azabicycle of the hetisines from the hetidines is a significant challenge. Synthetic planning could therefore benefit from mimicking this type of innate reactivity.

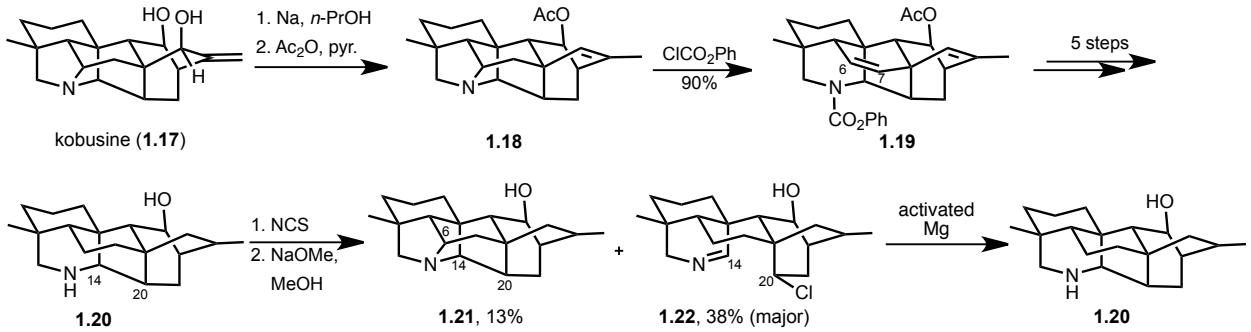

Scheme 1-3. Degradation studies on kobusine.

From carbamate **1.19**, sequential reductions of the tri- and di-substituted double bonds resulted in a fully saturated framework (not shown). Removal of the acetyl group proceeded without complication, and cleavage of the carbamate was accomplished in two steps to arrive at amine **1.20**. In order to cleave the C14–C20 bond (see **1.20** for numbering) to arrive at the

atisine-type core, polycycle **1.20** was first converted to the chloramine, then treated with sodium methoxide in methanol at reflux to deliver chloroimine **1.22** in 38% yield. Among the compounds isolated from the crude mixture was **5** in which the N–C6 bond was reformed, presumably through a Hoffman-Löffler-Freytag-type mechanism. This transformation again provides insight into the importance of proximity and potential reactivity of key atoms that could be exploited in the synthesis of hetisine-type natural products (i.e, **1.20→1.21**). Imine **1.22** could then be reduced to the secondary amine (not shown) or treated with activated magnesium to reform the C14–C20 bond (**1.20**). Through these chemical conversion studies, Okamoto and coworkers were able to learn about the intrinsic reactivity of kobusine-derived caged structures. This knowledge may be applied to the synthesis of related hetisine and hetidine-type diterpenoid alkaloids.

1.4 Synthetic approaches to hetisine-type diterpenoid alkaloids

Model Studies Toward the Hetidine/Hetisine Core

The following literature review has been previously published in *Organic & Biomolecular Chemistry*.[7] Retrosynthetic analysis of the C_{20}-diterpenoid alkaloid core often focuses on deconstructing two structural units: the nitrogen-containing rings and the all-carbon [2.2.2] bicycle containing an exomethylene on the right hand portion (Figure 1-3, bold). In most of the existing studies and syntheses of hetidine and hetisine-type alkaloids, the azabicycle is often constructed first, with the [2.2.2] bicycle formed at a later stage. This overview of the synthetic work toward these compounds therefore begins with a discussion of the strategies employed to form the azabicycle, followed by C–C bond formation to construct the [2.2.2] bicycle, and completion of the core.

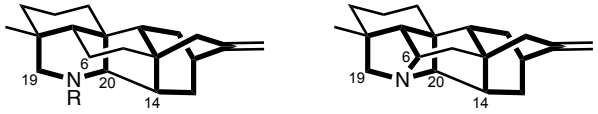

hetidine-type (**AIV**) hetisine-type (**AVII**)

Figure 1-3. Structural cores of interested and targeted motifs.

The general tetracyclic structure **1.23** (see Figure 1-4) was identified by Pelletier[8] as a versatile intermediate that was used in various early synthetic studies toward diterpenoid alkaloids in the atisane or kaurane class.[9] While this seminal work was not directed specifically at the hetidine or hetisine frameworks, much of the work that followed from other investigators adopted similar intermediates (e.g., **1.24**) as targets (*vide infra*).

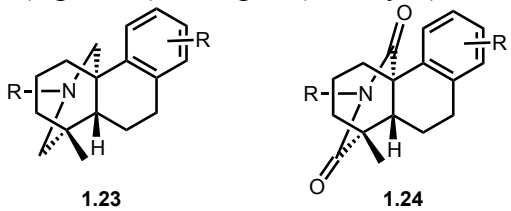

1.23 **1.24**

Figure 1-4. Key tricyclic intermediates.

Bickelhaupt

One of the earliest reported model studies toward the hetisine-type diterpenoid alkaloids was reported by van der Baan and Bickelhaupt in 1975.[10] In studying the reactivity of

cyanopyridinediols such as **1.27** (Scheme 1-4), which they could easily prepare from ethyl cyclohexanone-2-carboxylate (**1.25**) and malononitrile or cyanoacetamide (**1.26**),[11] they observed that alkylation of these diols (e.g., with allyl bromide) occurred exclusively at the carbon atom bearing the cyano group to give compounds such as **1.28**. Protection of the imide nitrogen followed by Cope rearrangement delivered imide **1.29** in which the quaternary center at C10 was now in place. Bromohydroxylation of the terminal olefin group and subsequent protection of the secondary hydroxyl as a tetrahydropyran ether gave **1.30**, which was now poised for cyclization. Treatment of **1.30** with NaH in DMF gave the cyclized product (**1.31**) via initial deprotonation of the vinyl nitrile. Imide **1.32**, bearing an additional carbonyl group, was accessed by THP-cleavage and oxidation. This compound maps closely onto **1.24** (Figure 1-4), and contains the 2 C–N bonds present in the hetidine structural core, with a functional handle at C6, should the hetisine-type alkaloids be of interest as targets.

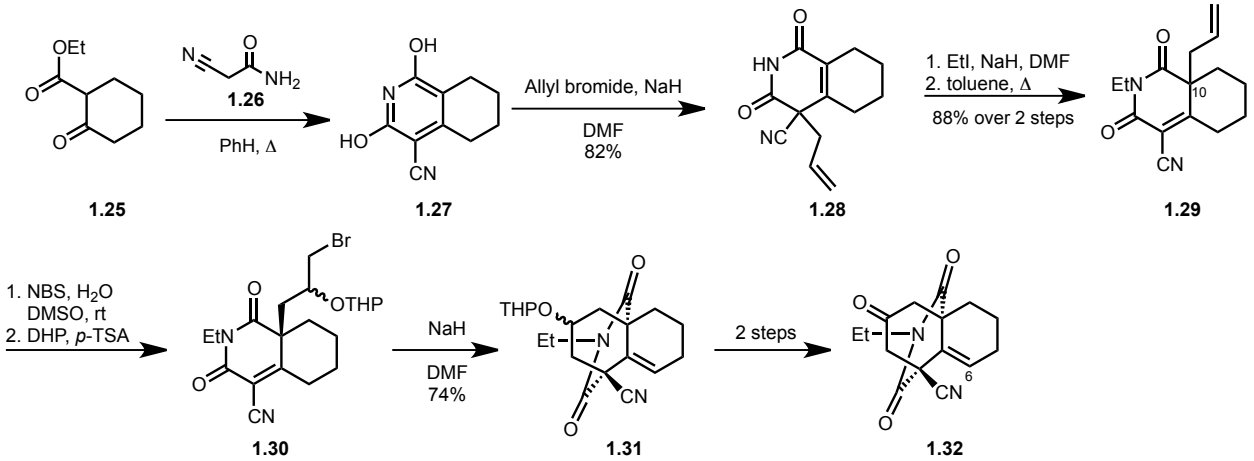

Scheme 1-4. Bickelhaupt tricycle formation *via* a cyanopyridinediol.

Winkler

In 2001, the Winkler group reported a methodology that they posited could be used to access a different portion of the hetisine azabicycle.[12] To demonstrate their strategy, Winkler and Kwak began with vinylogous amide **1.33**, which was used to access 1,5-diene **1.34** in 3 steps (Scheme 1-5). Irradiation of amide **1.34** gave "crossed" photoadduct **1.35** in good yield. Heating **1.35** in ethanol followed by the addition of catalytic pyridinium *p*-toluenesulfonate delivered tricycle **1.37** via sequential retro-Mannich/Mannich reactions. This azabicyclic[3.2.1]octanone has the same decalin system as the Bickelhaupt model system (**1.32**), but with the pyrrolidine ring in place rather than the piperidine (compare **1.32** to **1.37**). Superimposed onto the hetisine core, the C–N bonds resident in **1.37** correspond to the N–C6 and N–C20 bonds of the hetisines.

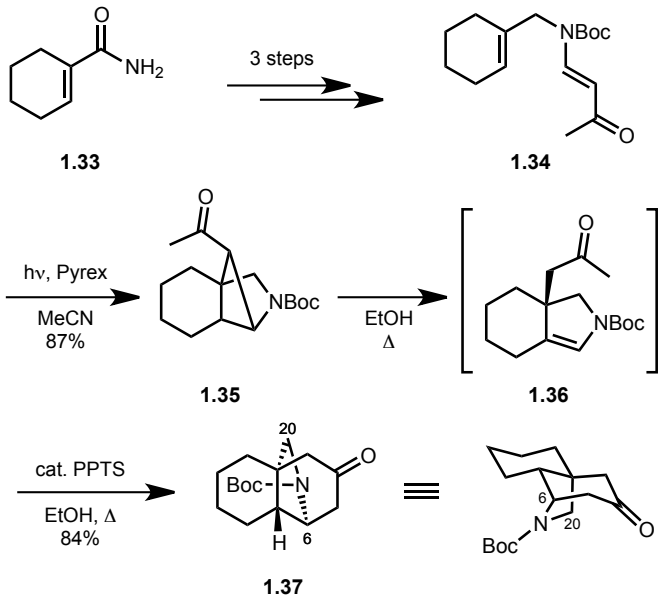

Scheme 1-5. Winkler's photochemical approach.

Mander

Mander and coworkers investigated several model systems of the hetisine and hetidine structural cores. Herein we highlight two—one that contains the desired N–C20 bond (forming a piperidine ring) and one that has the N–C6 bond forged (to access the requisite pyrrolidine ring).[13,14] The first of these sequences was published by Williams and Mander in 2003[15,16] and utilized a silver(I)-promoted bridgehead arylation. Starting from azabicycle **1.38**, which was accessed via a double Mannich reaction, they were able install the piperidine ring at the onset (Scheme 1-6). The addition of aryl acetylide **1.39** to **1.38** provided access to the desired diastereomer of the adduct (**1.40**) in 64% yield. From this adduct, they were able to access cyclization precursor **1.41** in 3 steps. At this point, numerous silver(I) salts and solvents were screened to effect bridgehead arylation. Ultimately, silver 2,4,6-trinitrobenzenesulfonate (**1.42**) in nitromethane emerged as the optimal combination for delivering arylated product **1.43**. This substrate contains the 6-6-6 tricycle present in the natural product core and is analogous to the tetracyclic intermediate utilized by Pelletier (for example see **1.23**, Figure 1-4).

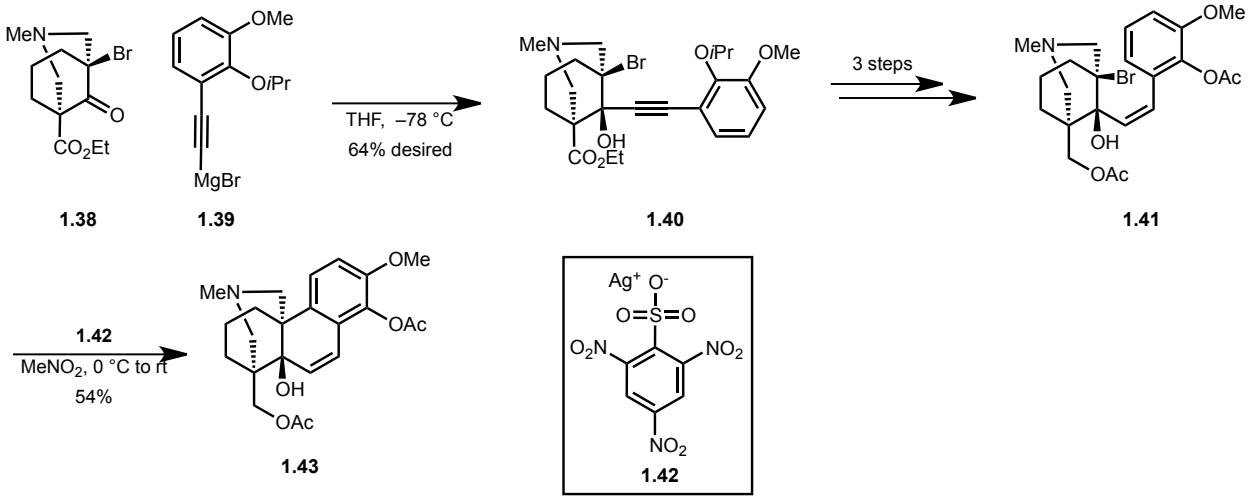

Scheme 1-6. Williams and Mander's approach.

Several years later, Mander and Hutt reported another approach to the hetisine structural core, this time focusing on the installation of the pyrrolidine ring containing the N–C6 bond.[17] Key to this sequence was a reductive acylation as well as a Lewis acid-catalyzed 1,6-addition of a carbamate to form the N–C6 bond. Enone **1.44** was accessed in 8 steps from commercial starting materials using known procedures (Scheme 1-7). At this juncture, reducing metal conditions were employed to reduce the enone, followed by quenching with methyl cyanoformate, to afford a β-ketoester (not shown). Subsequent protection of the β-ketoester gave MOM enol ether **1.45**. Vinylogous carbonate **1.45** was reduced to methylene alcohol **1.46** using lithium and NH_3 with complete diastereoselectivity. From this point, Mander and Hutt were able to install the requisite nitrogen atom in 3 steps through oxime formation and subsequent dehydration to the nitrile (**1.47**). Enone **1.48** was accessed in a 6-step sequence, which left them poised to test a conjugate addition to form the C–N bond. While basic and strongly acidic conditions resulted in no reaction or decomposition of **1.48**, it was found that milder Lewis acidic conditions—namely, $FeCl_3$ and TMSCl—delivered the desired pyrrolidine (**1.49**), albeit in 21% yield. In this way, Hutt and Mander were able to demonstrate the utility of a 1,6-conjugate addition strategy, as well as highlight the use of methyl cyanoformate in the context of a reductive acylation that provided a critical substituent for the natural product scaffold.

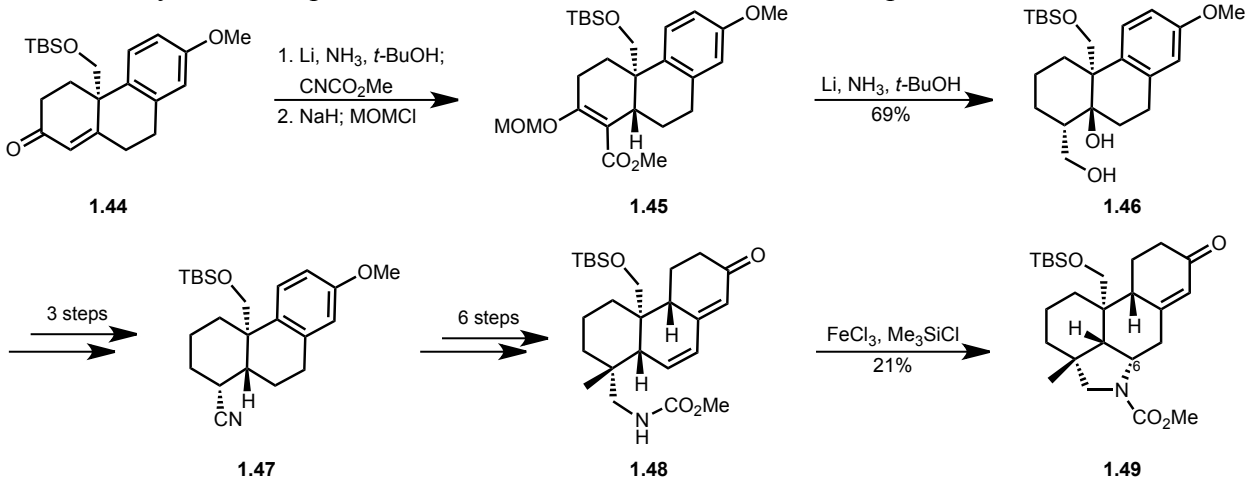

Scheme 1-7. Hutt and Mander's approach.

Okamoto

In 1985, Shibanuma and Okamoto reported an approach to the hetisine core with kobusine (**1.17**) as the specific target.[18] Starting from tetrahydrophenanthol (**1.50**, Scheme 1-8), they were able to access amine **1.51** in 7 steps. This compound was used to access the azabicycle. The first key step was the formation of the N–C6 bond. This was accomplished by treatment of amine **1.51** with lead tetraacetate, which resulted in aziridine **1.52**. Without purification, aziridine **1.52** could be treated with benzyl chloroformate to effect a regioselective ring opening to provide benzyl carbamate **1.53**. Reduction of chlorocarbamate **1.53** with Raney Ni gave secondary amine **1.54**. At this stage, Shibanuma envisioned forming the N–C19 bond (see **1.54**) using a Hofmann–Löffler–Freytag (HLF) reaction. The HLF transformation is often used to form 5-membered azacycles via an N-halo intermediate. Treatment of amine **1.54** with NCS provided the requisite *N*-chloro compound (not shown) that was then submitted to photoirradiation under acidic conditions (400 W high-pressure Hg lamp, trifluoroacetic acid) to provide **1.56** via alkyl chloride intermediate **1.55**.

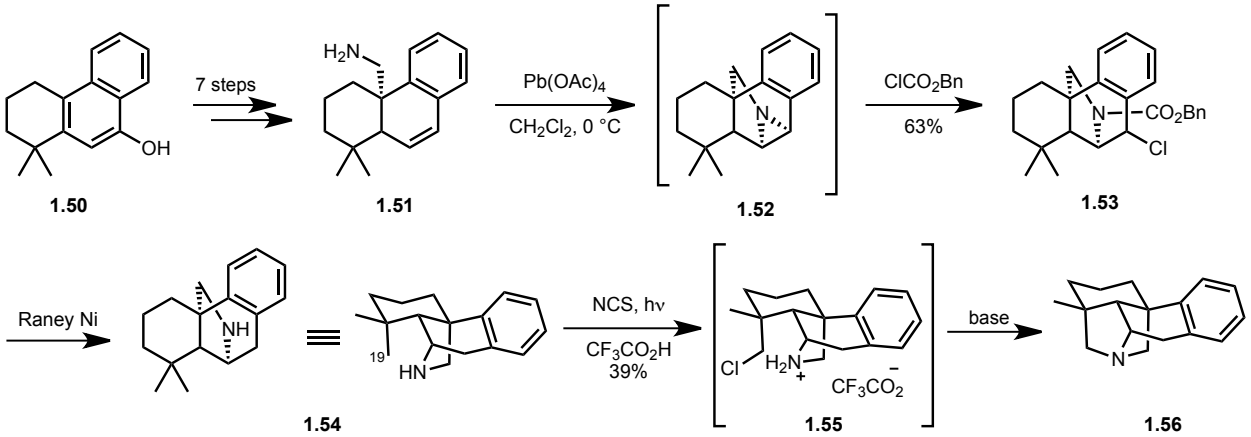

Scheme 1-8. Shibanuma and Okamoto's HLF approach to the azabicycle.

Sarpong

In 2013, the Sarpong group reported a synthesis of the hetidine core that could potentially be used to also access hetisine targets.[19] They proposed that the hetisine core could arise from the hetidine core through a formal dehydrogenative C–N bond forming reaction (Figure 1-5) as suggested by the degradation studies published by Okamoto (see **20➔21**, Scheme 1-3).[5,6]

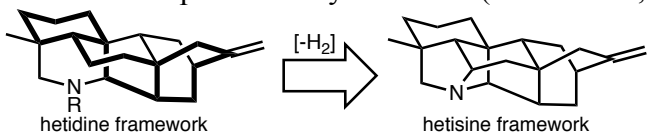

Figure 1-5. Proposed formation of hetisines from hetidines.

Within the hetidine framework, the Sarpong group recognized a fused 6-7-6 carbocycle (see bolded bonds, Figure 1-5) and proposed that tetracycle **1.57**, which is representative of the hetidine core, could be accessed from cycloheptadiene **1.58** (Scheme 1-9). Cycloheptadiene **1.58** could arise from an appropriately functionalized indenyl alkyne (**1.59**) using a gallium(III)–catalyzed cycloisomerization reaction.

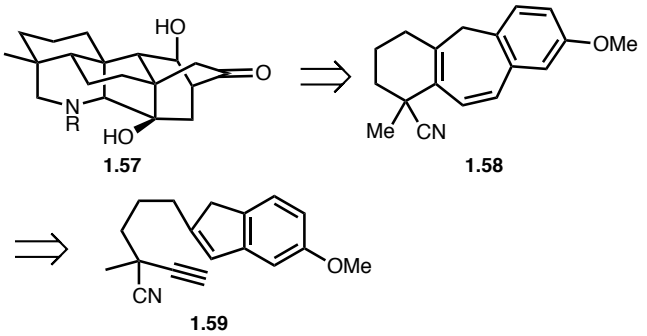

Scheme 1-9. Retrosynthetic analysis of the Sarpong intermediate.

The cycloisomerization of indenyl alkyne **1.59** (Scheme 1-10) proceeded in the presence of gallium(III) iodide to provide 6-7-6 fused carbocycle **1.58** in 89% yield. Cycloheptadiene **1.58** was elaborated to Boc-protected amino alcohol **1.60** over a sequence of 7 steps. Exposure of **1.60** to thionyl chloride effected cyclization to form the piperidine ring (**1.61**). Demethylation of methoxy arene **1.61** and subsequent oxidative dearomatization of the resulting phenol with PIFA ([bis(trifluoroacetoxy)iodo]benzene) provided **1.62,** where the Boc carbamate engaged as the nucleophile. To form the last two C–C bonds and complete the [2.2.2] bicycle, a Michael addition followed by an aldol reaction was enlisted. Thus, the allyl group was converted to an aldehyde (not shown) that cyclized through a Michael addition reaction to provide **1.63**. Finally, reduction of enone **1.63** to a ketone (not shown) and an aldol reaction formed the final C–C bond and provided the hetidine framework (**1.57**). The Sarpong group proposes to use this intermediate to access natural products of both the hetidine and hetisine-type.

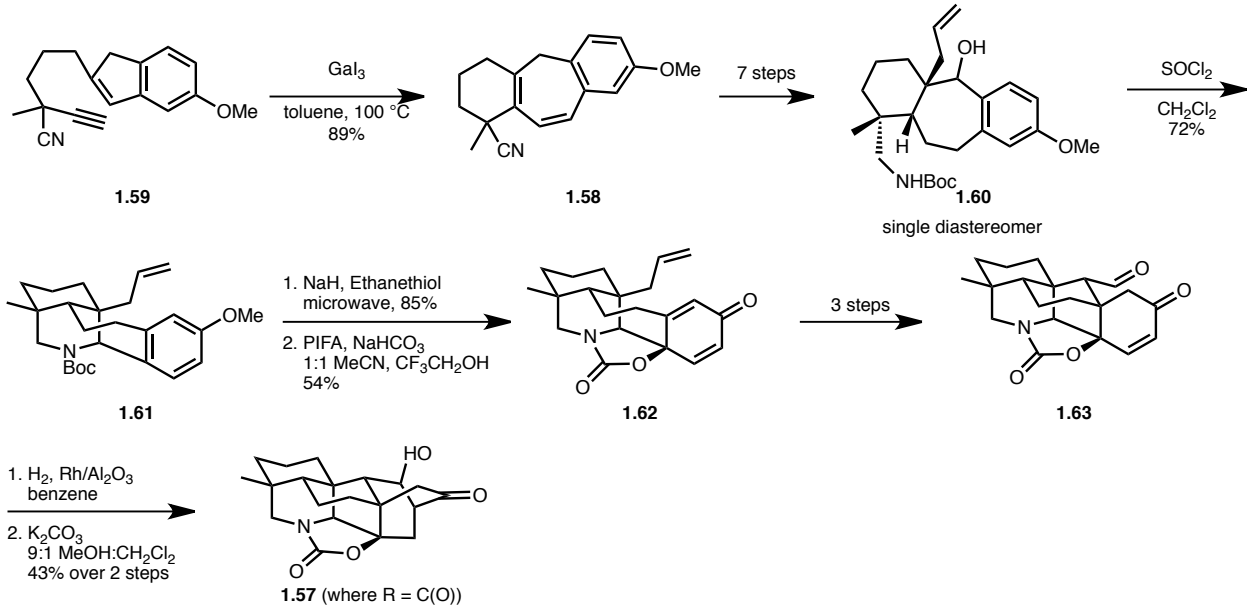

Scheme 1-10. Sarpong's synthesis of the hetidine framework.

As previously stated, structural classifications of the diterpenoid alkaloids are partially guided by the presence or absence of specific C–N bonds. Particularly pertinent to this review, the N–C6 bond differentiates the hetidine and hetisine cores. Therefore, structural analyses and methodologies that address the formation of the azabicycle in different ways are important to understanding the reactivity and conformations of these compounds. Although the strategies and

model studies presented thus far have not led to completed natural product syntheses, they provide insight into the reactivity of these particular scaffolds and the strategies that can be employed for C–N bond formation.

Total Syntheses: Nominine

Muratake and Natsume

Muratake and Natsume reported their first approach toward the natural product nominine (**1.64**) in 2002.[20] In this first approach, they sought to use a strategy similar to a previous approach by Shibanuma and Okamoto where the azabicycle is constructed early in the synthesis. They envisioned accessing the [2.2.2] bicycle at a late stage from functional handles present on hexacyclic compound **1.65** (Scheme 1-11) where all 3 bonds to the basic amine are already installed. Azabicycle **1.65** could arise from functionalization of tricycle **1.66**, where the amine is installed over a series of steps. Tricycle **1.66** could be obtained from a palladium-catalyzed intramolecular arylation, a method previously developed in their group. Using this initial approach, Muratake and Natsume were able to access azabicycle **1.65** (where R = CH_2CH_2OBz), but were unable to use this intermediate to access the [2.2.2] bicycle of the hetisine core.

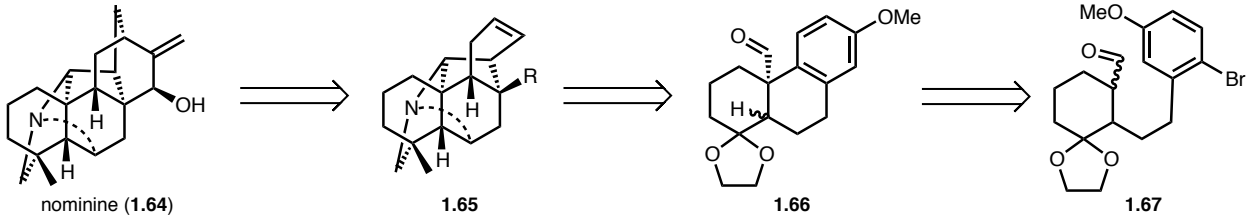

Scheme 1-11. Natsume's first generation retrosynthesis.

The synthesis of azabicycle **1.65** (where R = CH_2CH_2OBz) began with the palladium-catalyzed α-arylation of aldehyde **1.67** (Scheme 1-12) to arrive at tricycle **1.66**. The tricycle was elaborated through a sequence of 6 steps to provide **1.68**. Treatment of **1.68** with boron trifluoride effected an acetal-ene cyclization to forge a key C–C bond between C14 and C20. Transposition of the ketone in **1.69** followed by installation of the methyl group at C4 gave **1.70** over 4 steps. A Nagata reaction with Et_2AlCN was used to install a cyano group (see **1.71**), which provided the nitrogen atom that would be used to construct the azabicycle. The MOM and 2-hydroxyethyl protecting groups at C20 were then removed over a three-step sequence to reveal a hydroxyl group that would be used to form the third and final C–N bond. To access the N–C6 bond and form the pyrrolidine ring, the carbonyl was first protected as a silyl enol ether and the nitrile group was reduced to a primary amine. The primary amine immediately condensed with the incipient ketone generated upon cleavage of the silyl group. Protection of the resulting imine with Boc anhydride gave **1.73**. Reduction of the enamine and selective protection of the primary alcohol provided **1.74**, which on exposure to trifluoroacetic acid revealed a secondary amine. Treatment of the secondary amine with thionyl chloride led to cyclization by displacement of the secondary hydroxyl group at C20 (see **1.74**) to complete the azabicycle.

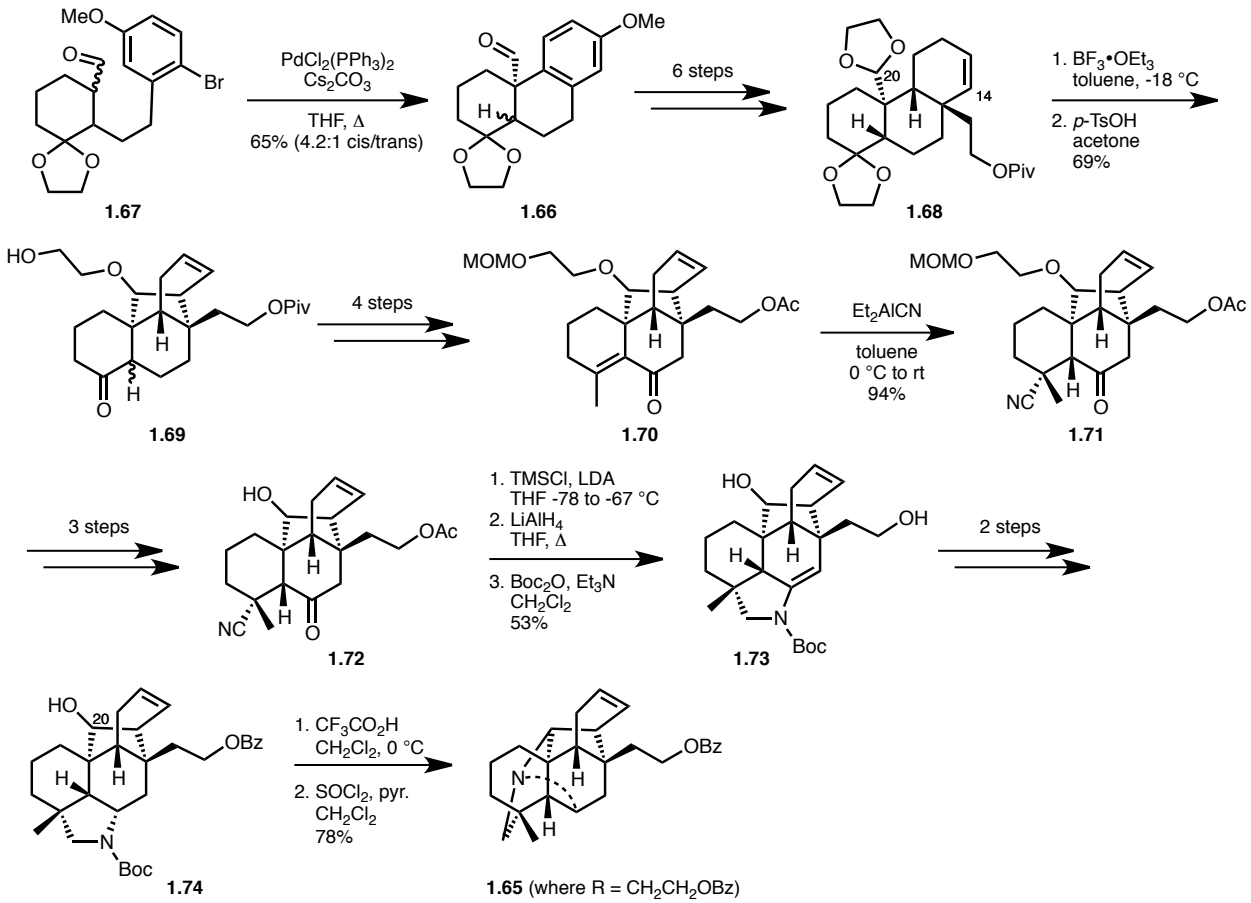

Scheme 1-12. Natsume's first generation synthesis of the azabicyclic core.

Hexacyclic compound **1.65** is composed of almost the entire skeleton of the hetisines, except for the 6-membered ring bearing the exomethylene. Unfortunately, because of the basicity of the tertiary amine, Muratake and Natsume were unable to advance this intermediate any further toward the hetisine core.

In 2004, Muratake and Natsume reported a revised approach to the hetisine core that involved formation of the N–C20 bond last, thus avoiding the need to carry a basic amine through several steps in the synthesis.[21] In this approach, the [2.2.2] bicycle would be constructed before completion of the azabicycle to enable the basic amine to be carried through the majority of the synthesis protected as an amide (Scheme 1-13). Herein we analyze the key insights that led to the first total synthesis of nominine. The initial report was published 2004 and was followed by a series of full papers that were published in 2006.[22]

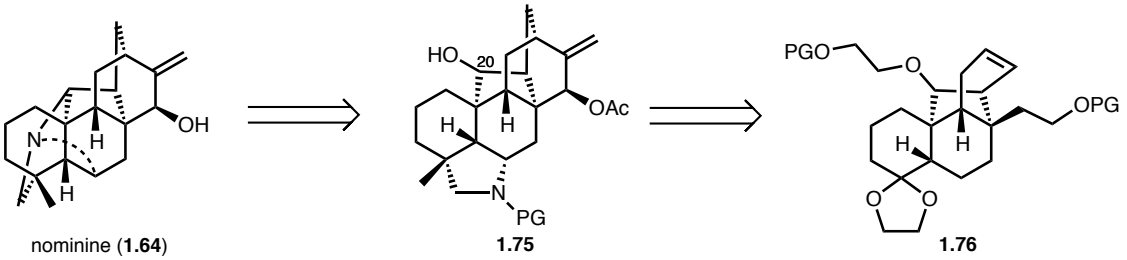

Scheme 1-13. Second generation Natsume synthesis.

In the revised approach to the hetisine core, Muratake and Natsume first explored ways to access the [2.2.2] bicycle directly after the acetal-ene reaction (Scheme 1-14). Allylic oxidation of acetal-ene product **1.77** with chromium trioxide provided a mixture of enones (**1.78** and **1.79**). Each enone was used as a model substrate to study how the [2.2.2] bicycle could be formed.

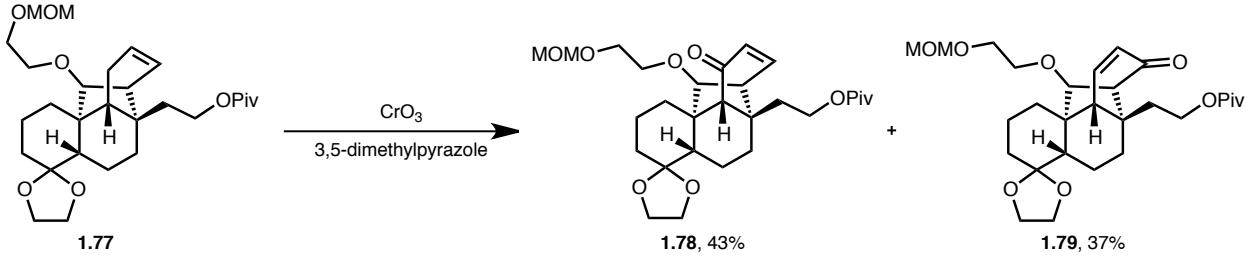

Scheme 1-14. Allylic oxidation of acetal-ene product **1.77**.

Enone **1.78** was advanced to keto-aldehyde **1.80** over a three-step sequence (not shown). Homologation of aldehyde **1.80** with the Ohira-Bestmann reagent provided the desired alkyne (**1.82**) along with a small amount of aldol product **1.83** where the [2.2.2] bicycle had been formed, but in a low 7% yield (Scheme 1-15). Treatment of keto-alkyne **1.82** with LDA and TMSCl followed by carbomercuration with mercuric triflate-N,N,N',N'-tetramethylurea complex [$Hg(OTf)_2(TMU)_2$] led to an aldol reaction upon acidic workup. This sequence provided access to **1.85** where the [2.2.2] bicycle was in place as well as the exomethylene group at C16.

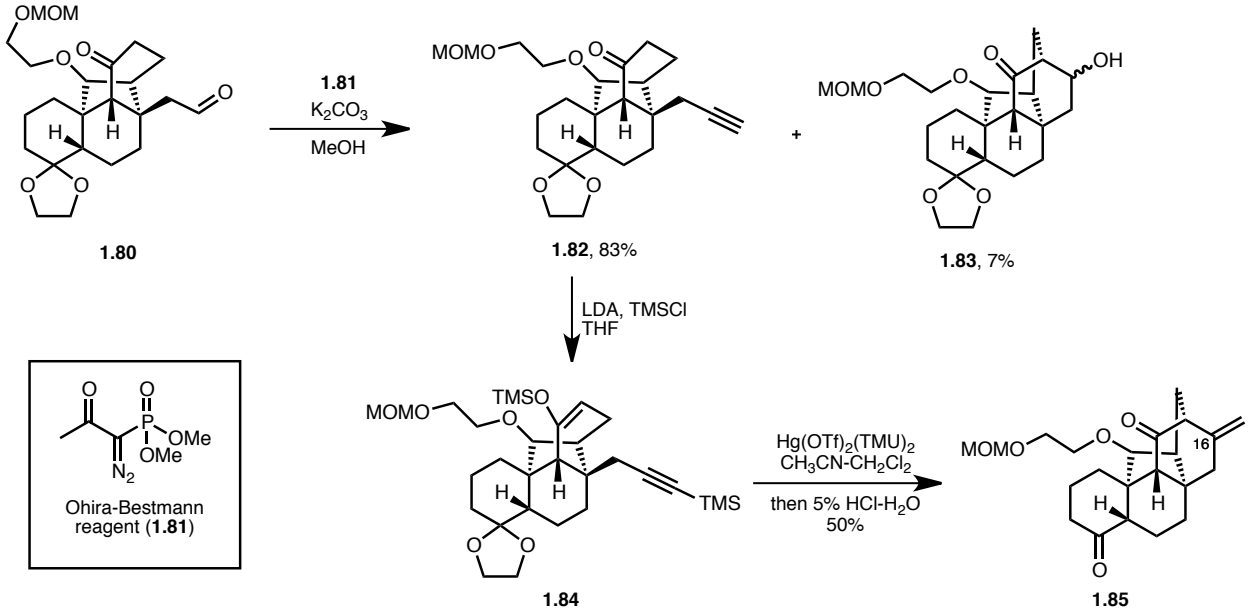

Scheme 1-15. Functionalization of keto-aldehyde **1.80**.

Enone **1.79** was converted to keto-aldehyde **1.86** through the same 3-step sequence used to prepare **1.80** (not shown). Exposure of aldehyde **1.86** to K_2CO_3 in refluxing methanol effected an aldol cyclization to give **1.87** as a mixture of epimers at the hydroxyl bearing C16 position (Scheme 1-16). Aldehyde **1.86** could also be converted to alkyne **1.88** through an Ohira-Bestmann homologation. Carbomercuration of alkyne **1.88** with [$Hg(OTf)_2(TMU)_2$] followed by an aldol cyclization of the resulting ketone (**1.89**) in the presence of LDA provided access to a [2.2.2] bicycle as a single diastereomer (**1.90**, stereochemistry was not determined).

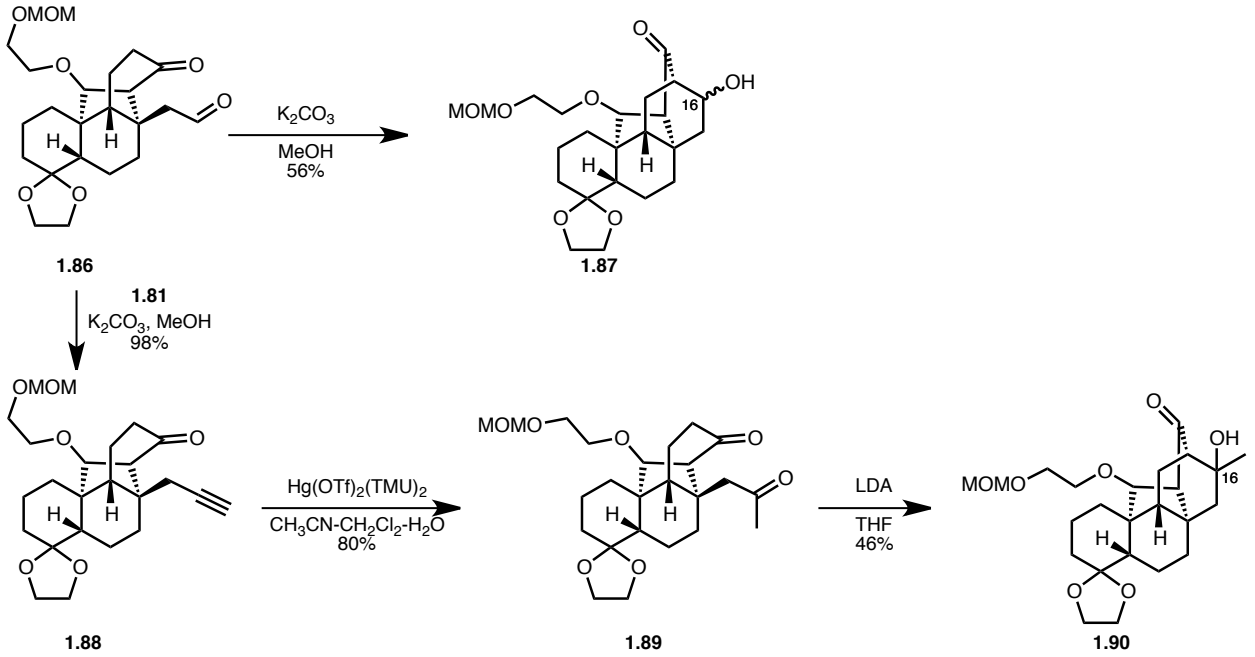

Scheme 1-16. Functionalization of keto-aldehyde **1.86**.

With several strategies to access the [2.2.2] bicycle in hand, Muratake and Natsume next explored ways to install the amine before formation of the [2.2.2] bicycle. The pyrrolidine was installed using a strategy similar to their first reported approach beginning with intermediate **1.71**. In this new approach, the hydroxyl group at C20 remained protected with the MOM and 2-hydroxyethyl protecting groups until the final stages of the synthesis.

The N–C6 bond was forged using the same sequence previously described to access **1.73** and the resulting enamine was protected with either a Boc group or a Cbz group to provide **1.91** and **1.92**, respectively (Scheme 1-17). Reduction of the enamine and protection of the primary hydroxyl group as a benzoate provided **1.93** and **1.94** over 2 steps. Allylic oxidation of the Boc-protected amine substrate (**1.93**) in the presence of chromium trioxide as before gave a mixture of enones **1.95** and **1.97** in 45% and 28% yield, respectively. Using the Cbz protected substrate (**1.94**), the yields for the chromium trioxide oxidation were even lower with only 12% of **1.96** and 6% of **1.98** obtained with a 50% recovery of **1.94**. Because of the low yields associated with the oxidation of Cbz-protected amine substrate **1.94**, only enone **1.95** was carried forward.

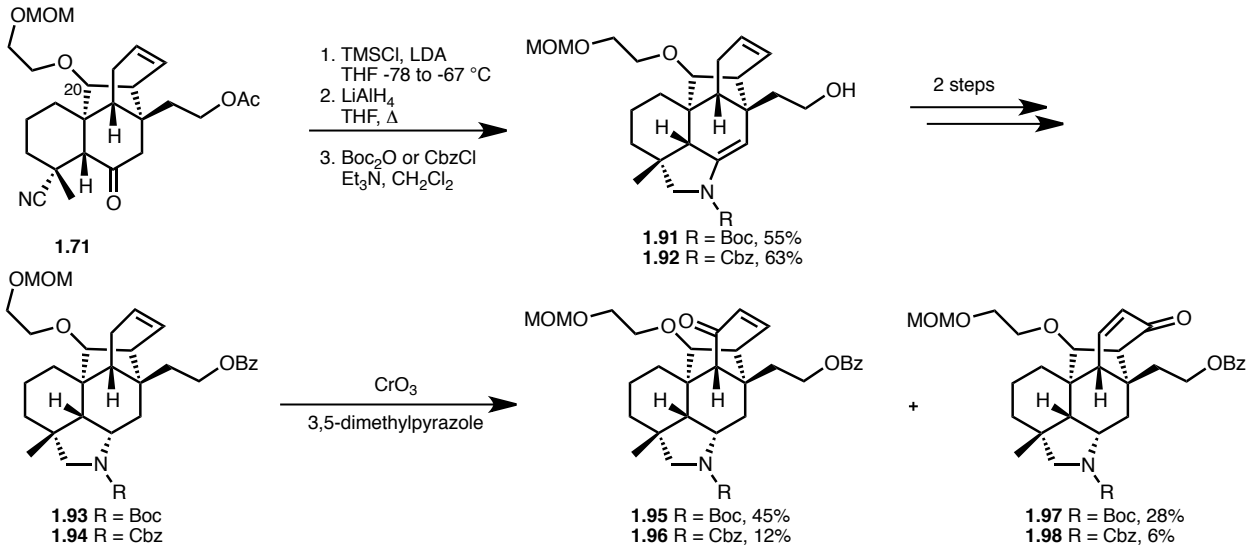

Scheme 1-17. Installation of the nitrogen atom and C–N bond formation.

Enone **1.95** was converted to keto-aldehyde **1.99** using a 3-step sequence (not shown) and treatment of keto-aldehyde **1.99** with Ohira-Bestmann homologation conditions gave 34% yield of the desired alkyne (**1.100**) as well as 55% of aldol product **1.101** as a mixture of diastereomers at C16 (Scheme 1-18). Oxidation of **1.101** to yield diketone **1.102** occurred in the presence of PCC-Al_2O_3 but unfortunately, attempts at a Wittig reaction to install the exomethylene group only returned starting material.

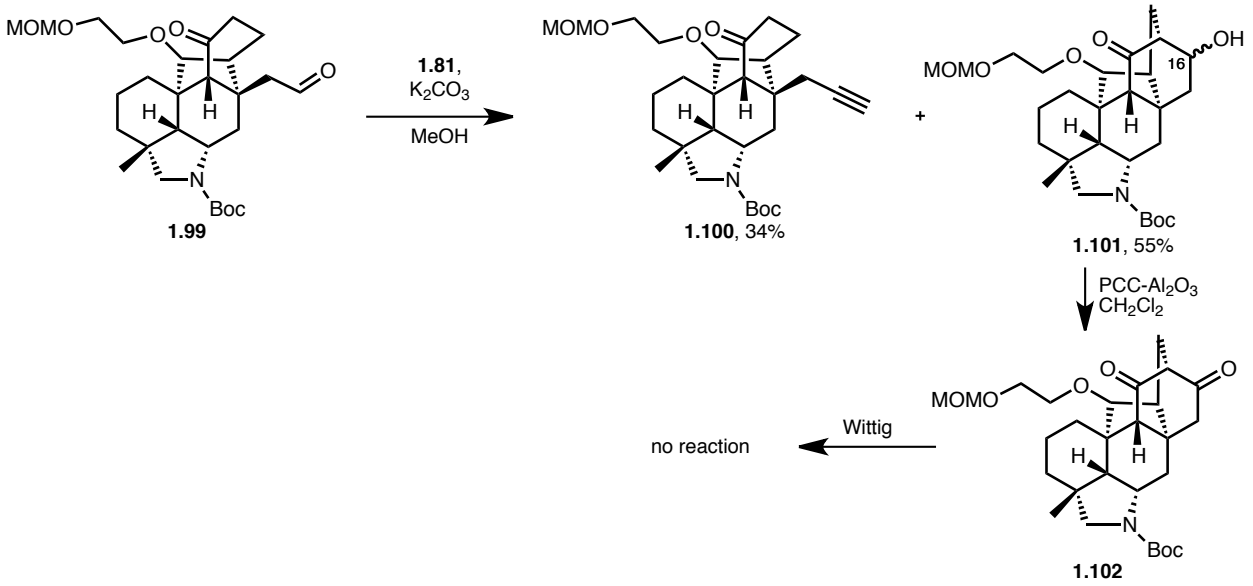

Scheme 1-18. [2.2.2] Bicycle formation *via* an Aldol reaction.

Because the aldol reaction approach to form the [2.2.2] bicycle was low yielding, the use of a radical-mediated methodology to form a similar [2.2.2] bicycle was explored. It was proposed that a radical intermediate obtained from a xanthate-containing compound in the presence of a tethered alkyne (see **1.103**) could be used to access the desired [2.2.2] bicycle containing the exomethylene group. Xanthate **1.103** was obtained from **1.91** through a 5-step sequence (Scheme 1-19). Treatment of xanthate **1.103** with tributyltin hydride in the presence of

catalytic AIBN generated a radical intermediate that cyclized with the alkyne group to provide **1.104** in 85% yield.

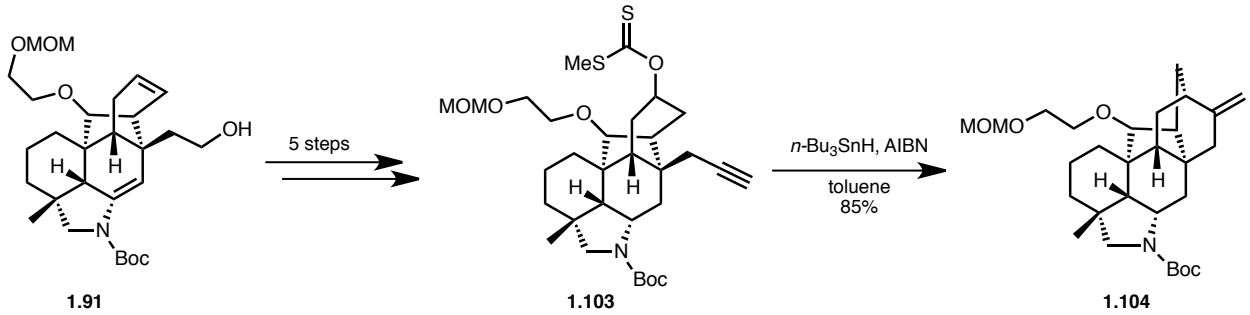

Scheme 1-19. Radical cyclization to form the [2.2.2] bicycle.

Generation of a radical intermediate to access the [2.2.2] bicycle proved to be an effective strategy. Unfortunately, following the cyclization, the MOM and Boc protecting groups could not be removed because of the unexpected instability of the methylene-[2.2.2]bicycle moiety to acidic conditions. The synthesis of the xanthate (not shown) from olefin **1.91** was also low yielding. With these challenges in mind, Muratake and Natsume next explored an enyne radical cyclization from enyne **1.105** where the secondary amine was protected with a Cbz group and the MOM group was removed before the cyclization. This final approach would not require the use of a xanthate to generate the radical intermediate and would avoid the acidic conditions required to cleave the protecting groups. Enyne radical cyclization substrate **1.105** was obtained from **1.92** over a 4-step sequence (Scheme 1-20). Treatment of enyne **1.105** with tributyltin hydride and catalytic AIBN in refluxing toluene provided the [2.2.2] bicycle bearing the exomethylene (**1.106**) in 50% yield. With the [2.2.2] bicycle in place, oxygenation at C15 was introduced and the 2-hydroxyethyl protecting group was removed over a 6-step sequence to give **1.75** (where PG = Cbz). The Cbz group was removed with triethylsilane in the presence of a catalytic amount of palladium(II) acetate and the resulting amino alcohol was treated with thionyl chloride to form the final C–N bond. Cleavage of the acetyl protecting group provided nominine (**1.64**) in a total of 40 steps from commercially available starting materials.

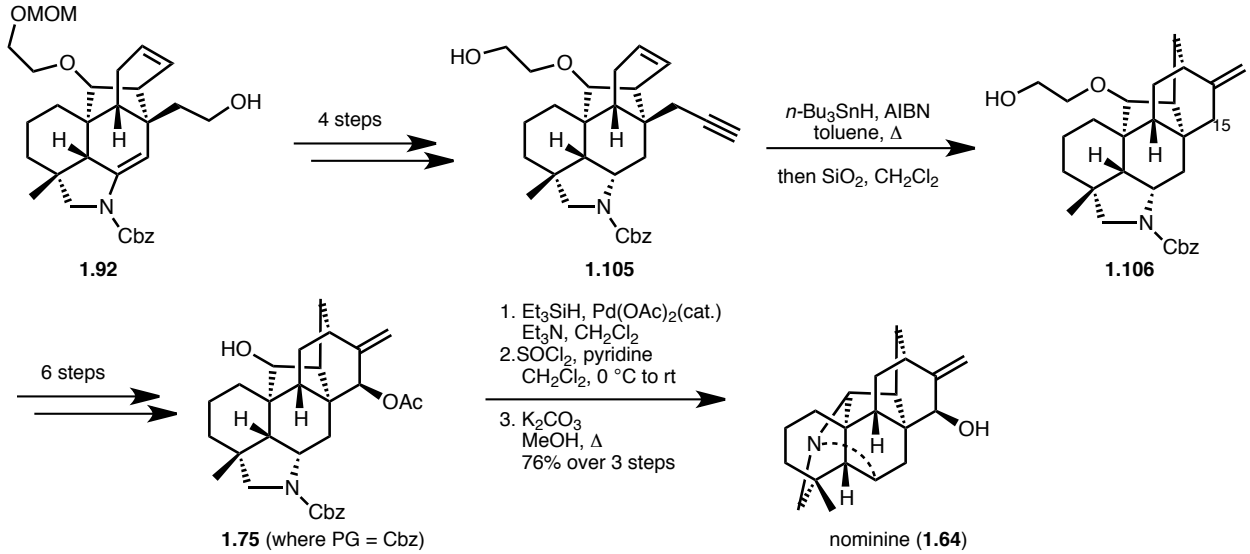

Scheme 1-20. Completion of the first total synthesis of nominine.

Muratake and Natsume completed the first total synthesis of nominine using several key steps including a palladium-catalyzed α-arylation to access a 6-6-6 ring system, an acetal-ene reaction to form the bonds between C14 and C20 and a radical cyclization to access the [2.2.2] bicycle.

Peese and Gin

The Peese and Gin total synthesis of nominine, first reported in 2006,[23] used a convergent, dual-cycloaddition approach to access the hetisine core. They envisioned accessing the bridged pyrrolidine ring of **1.64** using a 1,3-dipolar cycloaddition from an aza-dipole and dipolarophile to form bonds between C5-C6 and C10-C20 simultaneously (Scheme 1-21). The [2.2.2] bicycle could then be assembled using a Diels–Alder reaction between an appropriately placed diene and dienophile to form the final two C–C bonds. Because functional group incompatibility would most likely thwart a tandem cycloaddition, the 1,3-dipolar cycloaddition was explored first, and was then followed by the Diels–Alder from a latent diene and dienophile pair.

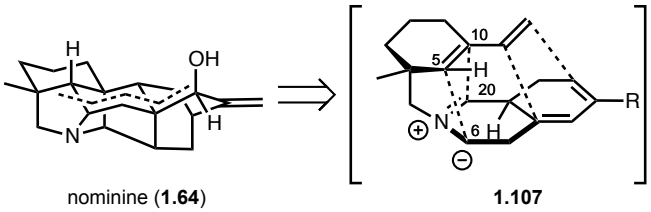

nominine (**1.64**) **1.107**

Scheme 1-21. Cycloaddition approach to the hetidine core.

Peese and Gin first explored the feasibility of using a 1,3-dipolar cycloaddition to access the azabicycle found in the hetisine core.[24] They ultimately decided to use a 3-oxidopyridinium betaine as the aza-dipole because it is significantly more stable than other aza-dipoles, such as azomethine ylides, but still moderately reactive in cycloadditions. Initial investigations began with a 3-oxidopyridinium betaine tethered to a 2-enenitrile dipolarophile (**1.109**, Scheme 1-22). Betaine **1.109** was accessed from furan **1.108** through an aza-Achmatowicz reaction in the presence of bromine. However, heating oxidopyridinium **1.109** to effect the dipolar cycloaddition was unsuccessful. Instead, an intramolecular conjugate addition of the oxidopyridinium followed by rearomatization occurred to provide **1.110** in 73% yield.

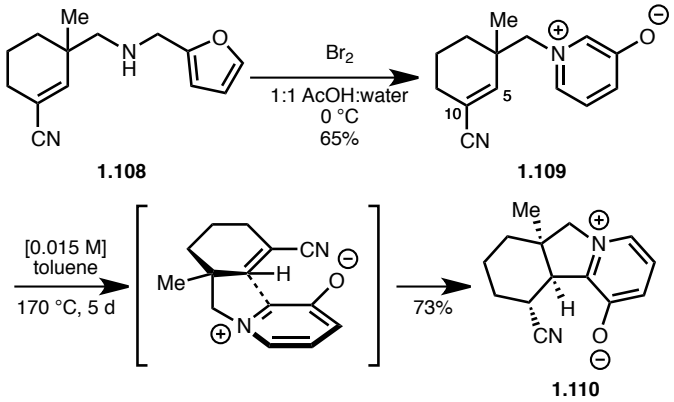

1.108 **1.109** **1.110**

Scheme 1-22. Initial cycloaddition investigations.

In order to suppress the 1,4-conjugate addition pathway, Gin and Peese envisioned a cycloaddition substrate bearing a removable electron deficient group (Z) at C5 rather than at C10

of the dipolarophile (see Figure 1-6). Conjugate addition would then occur at the C10 position leading to a strained bridged [3.3.1] bicycle. It was anticipated that the high barrier associated with the generation of a strained bicycle would possibly suppress the 1,4-conjugate addition pathway and instead favor the 1,3-dipolar cycloaddition pathway.

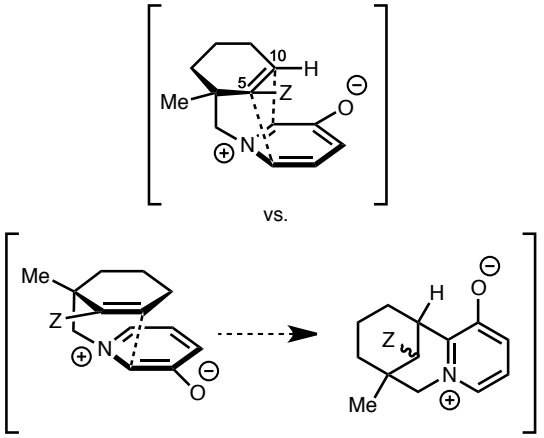

Figure 1-6. [3 + 2] Cycloaddition vs. conjugate addition pathways.

Cycloaddition precursor **1.112** (bearing a phenyl sulfone at C5) was obtained in racemic form in 5 steps from 2-cyano-2-methylcyclohexanone (**1.111**, Scheme 1-23). An enantioselective synthesis of **1.112** was also reported starting from 2-oxo-cyclohexanecarboxylic acid ethyl ester (**1.114**). An asymmetric α-methylation of the (S)-t-butylvaline enamine derivative of **1.114** provided cyclohexanone **1.115** (98:2 er). Enantioenriched **1.112** could then be obtained from **1.115** in 6 additional steps. Heating cycloaddition precursor **1.112** in toluene at reflux provided cycloadduct **1.113** in 70% yield with no trace of a 1,4-conjugate addition product. With the cycloaddition successfully accomplished, the sulfone group could then be removed by reduction of enone **1.113** to olefin **1.116** over 2 steps followed by desulfurization with sodium/mercury amalgam to provide (+)-**1.117**.

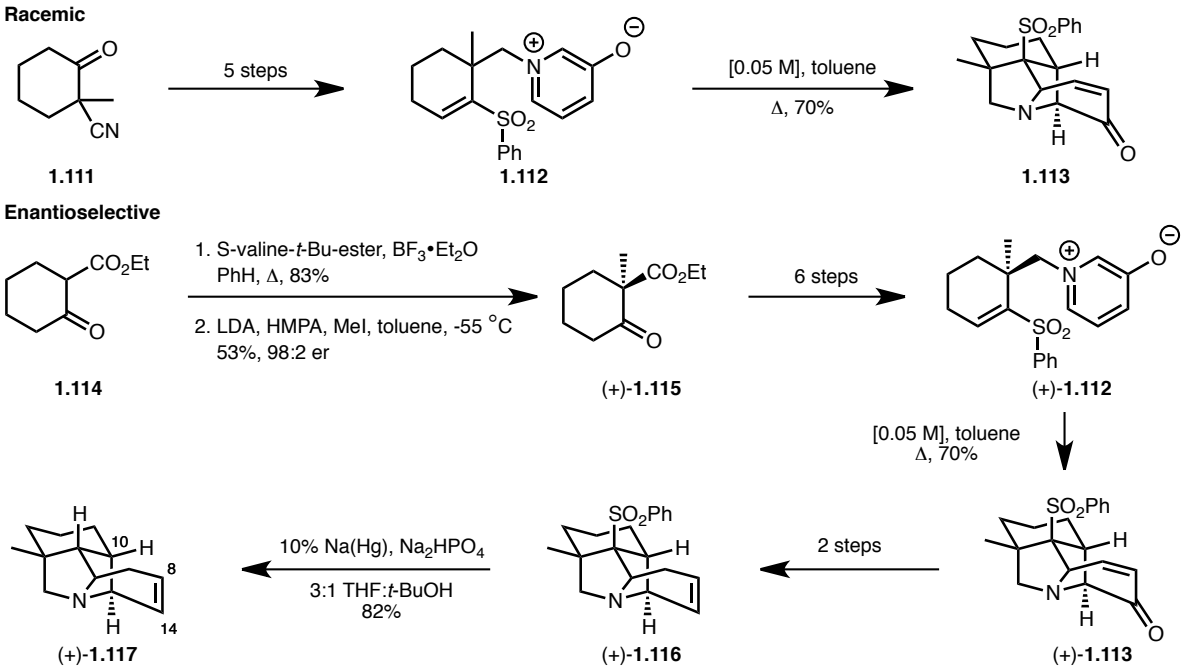

Scheme 1-23. Racemic and enantioselective synthesis of the core azabicycle.

The 1,3-dipolar cycloaddition strategy proved to be effective in generating the azabicycle found in the hetisine-type natural products and Gin and Peese ultimately provided the first example of accessing the azabicycle moiety enantioselectively.[25] From azabicycle **1.117**, installation of the diene group could be envisioned through various annulation strategies at C8–C14 but unfortunately, accessing the dienophile at C10 remained a challenge.

Given the challenge of installing the dienophile after the cycloaddition, Gin and Peese next explored the use of an appropriate functional group handle at C10, which would be installed before the cycloaddition.[31] For this purpose, they chose to introduce a nitro group at C10 (**1.118**). Heating the nitro containing oxidopyridinium betaine in the microwave gave only one regioisomer of cycloadduct **1.119** with no trace of the conjugate addition product. However, the reaction did not proceed past 14% conversion (Scheme 1-24). Furthermore, resubmission of cycloadduct **1.113** to the microwave reaction conditions provided a ~6:1 ratio of betaine **1.118** to cycloadduct **1.113** suggesting that the dipolar cycloaddition reaction is under thermodynamic control.

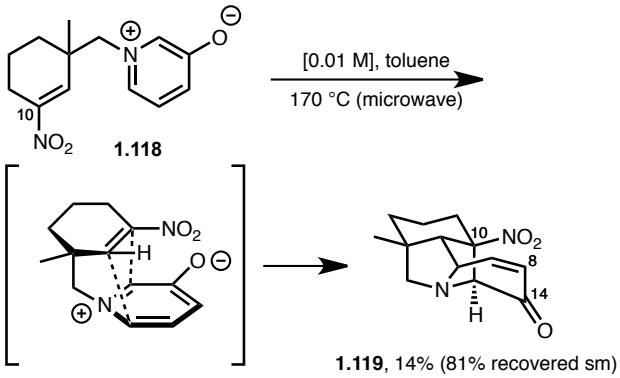

Scheme 1-24. Nitro-containing cycloaddition substrate.

To address the unfavorable equilibrium observed in the dipolar cycloaddition of 3-oxidopyridinium substrate **1.118** to give pyrrolidine adduct **1.119**, Gin and Peese once again decided to redesign the cycloaddition substrate. The use of a 4-oxidoisoquinolinium betaine as the dipole was explored. It was proposed that lowering the energetic cost of breaking aromaticity of the dipole during the cycloaddition would allow for a more thermodynamically favored dipolar cycloaddition. The 4-oxidoisoquinolinium betaine (**1.122**) was accessed using a Staudinger-aza-Wittig reaction between dipole precursor **1.121** and dipolarophile **1.120** followed by a TFA-promoted extrusion of methanol (Scheme 1-25).

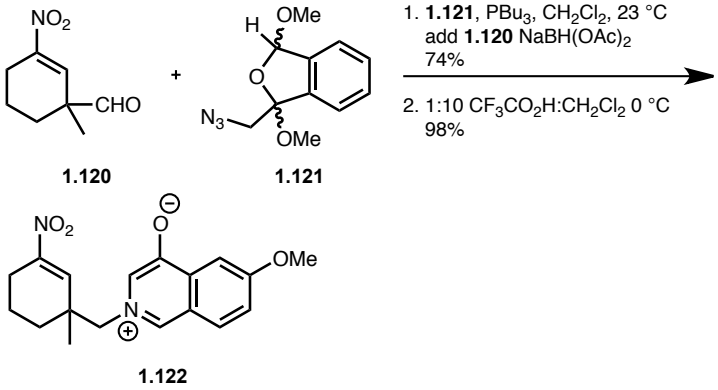

Scheme 1-25. Synthesis of the oxidoisoquinolinium betaine.

Heating betaine **1.122** in toluene at 90 °C in the microwave for 30 min provided a mixture of 3 isomeric products: cycloaddition products **1.123** and **1.124** and intramolecular conjugate addition product **1.125**, in a 4:2:3 ratio (Scheme 1-26). Unfortunately, longer reaction times lead to exclusive formation of **1.125**. Because of the reversibility of the cycloaddition reaction, the reversion of cycloaddition products **1.123** and **1.124** to betaine **1.122** enabled eventual funneling of all the material to the conjugate addition product **1.125**, which is the thermodynamic sink of the reaction.

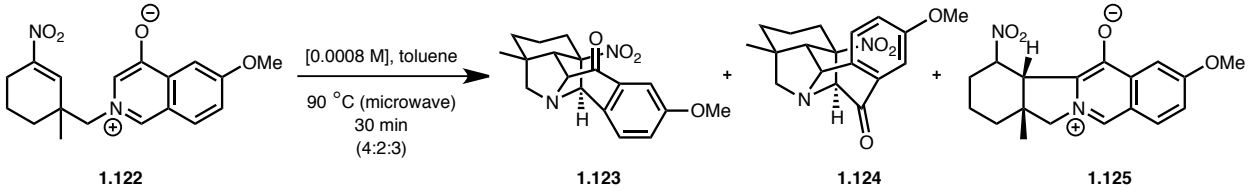

Scheme 1-26. Cyclization results with nitro substrate.

In order to suppress the competing irreversible conjugate addition of **1.122**, one last modification of the dipolarophile component was made. The use of a less activated ene-nitrile as the dipolarophile was re-investigated using the 4-oxidoisoquinolinium as the dipole component. Dipolarophile precursor **1.126** was accessed from cyclohexenone in 3 steps (not shown). The Staudinger-aza-Wittig reaction followed by subsequent extrusion of methanol was used to couple aldehyde **1.126** to azide **1.121** giving access to betaine **1.127**.

Heating cycloaddition precursor **1.127** to 180 °C provided two cycloadducts (**1.128** and **1.129**) as the only products with the undesired regioisomer (**1.129**) being the major product in a ratio of 1:3.6 (desired:undesired) (Scheme 1-27). This ratio remained unchanged over extended reaction times and no conjugate addition products were detected. The observations indicate that the cycloaddition reaction was exothermic and the undesired conjugate addition pathway had

been completely suppressed. Because the cycloaddition was under thermodynamic control, the undesired diastereomer (**1.129**) could be isolated and re-equilibrated using the same reaction conditions to give the same ratio of the desired to undesired diastereomer, which allowed for accumulation of ~20% of **1.128** per re-equilibration of **1.129** with very little loss of material.

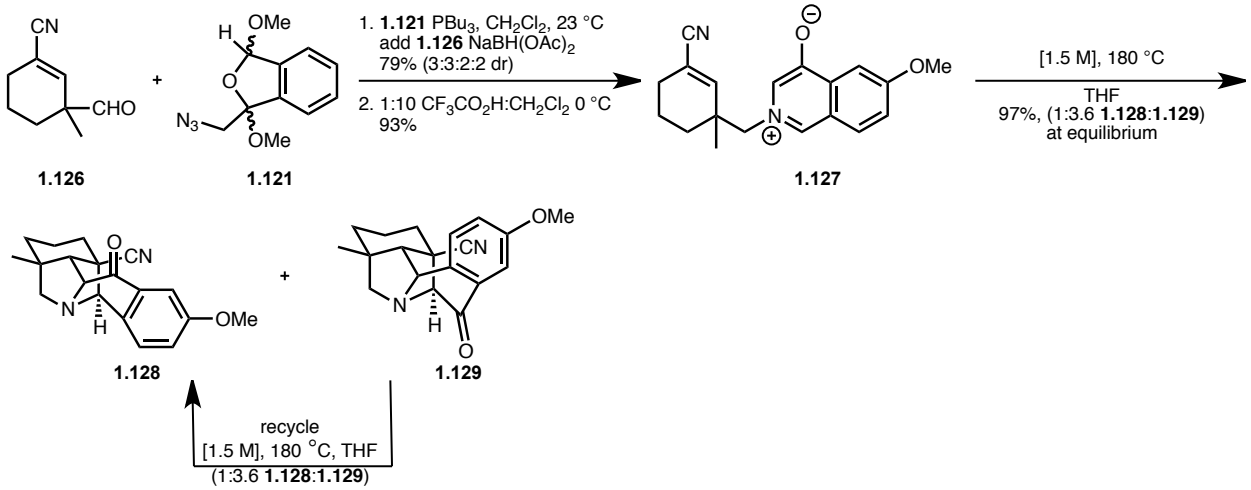

Scheme 1-27. Final cycloaddition substrate bearing a cyano group.

To complete the synthesis of nominine from cycloadduct **1.128**, the benzylic ketone group was removed and the cyano group was converted to the vinyl group that would serve as the dienophile in the [4+2] cycloaddition reaction (Scheme 1-28). To access the diene, a reductive dearomatization using standard Birch reduction conditions was performed on the methoxy arene followed by hydrolysis of the resulting methyl enol ether. It was expected that isomerization of the double bond into conjugation with the ketone would subsequently lead to formation of the requisite diene. All attempts to isomerize **1.131** to a conjugated enone under both acidic and basic conditions led only to returned starting material or decomposition suggesting that **1.131** is thermodynamically favored. In an attempt to form the diene using iminium/enamine intermediates, it was found that by treating **1.131** with pyrrolidine in refluxing methanol, the [4+2] cycloaddition product (**1.134**) could be obtained as the sole product. Although several dienamine species are possible, diene **1.132** is the only one poised for the intramolecular Diels–Alder cycloaddition. Thus, the equilibrating intermediates could be funneled to the irreversible cycloaddition adduct (**1.133**). Ketone **1.134** could then be obtained from **1.133** following enamine hydrolysis. Finally, Wittig olefination of ketone **1.134** followed by allylic oxidation with SeO_2 provided nominine in a total of 15 steps from commercially available materials.

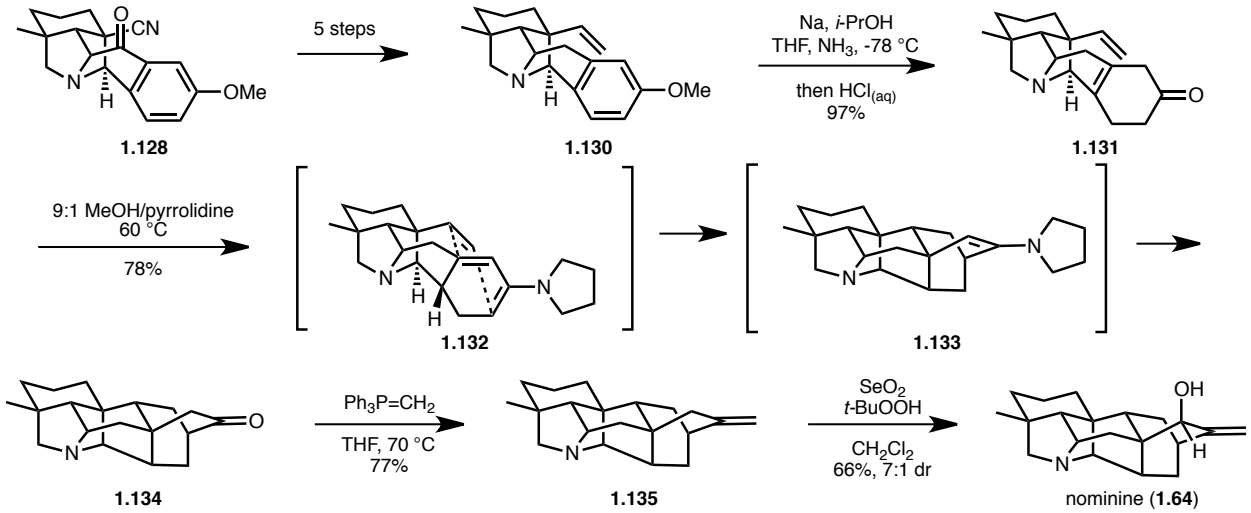

Scheme 1-28. Formation of the [2.2.2] bicycle and total synthesis of nomine.

Gin and Peese also completed an enantioselective synthesis of nominine by setting the stereocenter at C4 of **1.136** using an enantioselective 1,4 conjugate addition of a dialkylzinc reagent into enone **1.136** in the presence CuOTf and chiral N-heterocyclic carbene ligand complex **1.137** (Scheme 1-29). The resulting zinc enolate was then trapped as vinyl triflate **1.138**. A two-step sequence from vinyl triflate **1.138** provided enantioenriched dipolarophile **1.126**, which was then used to access dipolar cycloaddition product **1.128** in enantioenriched form. Recrystallization of **1.128** further increased the enantiopurity to provide material which was used to complete the first enantioselective synthesis of nominine (**1.64**).

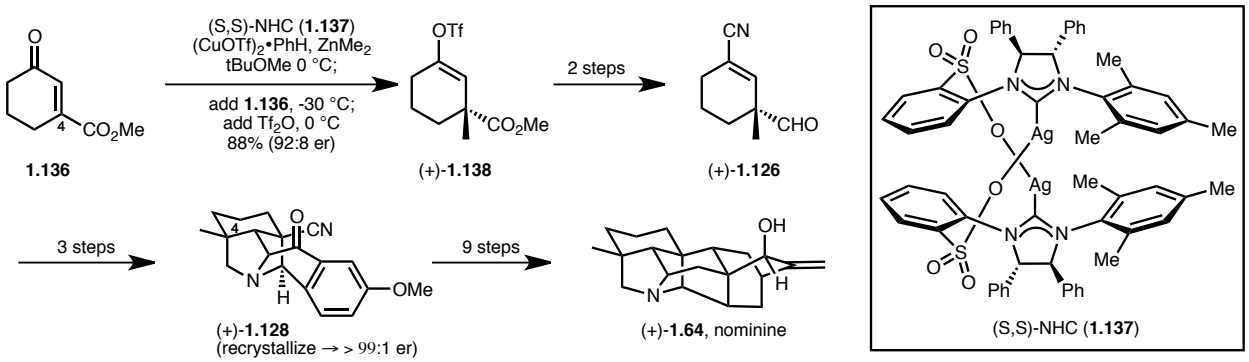

Scheme 1-29. Enantioselective synthesis of nominine.

Gin and Peese reported a very elegant synthesis of nominine, which stands as the shortest and most efficient approach to these molecules to date. By using a convergent dual cycloaddition strategy, they were able to rapidly and efficiently access the hetisine core and thereby set the standard for future syntheses of the hetisines and related frameworks.

1.5 Conclusion

The C_{20}-diterpenoid alkaloid family of natural products consists of a number of complex interconnected structural cores. The bioactivity and structural diversity of these compounds, as well as their sheer complexity have made them attractive targets for synthetic study. Those compounds characterized by the hetidine or hetisine framework have specifically been targeted

through strategies that synthesize the azabicycle or all-carbon [2.2.2] bicycle. To date, only one hetisine-type alkaloid, nominine, has been synthesized.

1.6 References and Notes

[1] For selected reviews on the structure, activity, and study of C_{20}-diterpenoid alkaloids, see the following and references therein: (a) Wang, F. P.; Liang, X. T. In *The Alkaloids: Chemistry and Biology;* G. A. Cordell, Ed.; Elsevier Science: New York, 2002; Vol. 59, pp 1. (b) Cherney, E. C.; Baran, P. S. *Isr. J. Chem.* **2011**, *51,* 391. (c) Wang, F. P.; Chen, Q. H.; Liu, X. Y. *Nat. Prod. Rep.* **2010**, *27,* 529.

[2] Ameri, A. *Prog. Neurobiol.* **1998**, *56,* 211.

[3] Hong, Y. J.; Tantillo, D. J. *J. Am. Chem. Soc.* **2010**, *132,* 5375.

[4] Zhao, P.-J.; Gao, S.; Fan, L.-M.; Nie, J.-L.; He, H.-P.; Zeng, Y.; Shen, Y.-M.; Hao, X.-J. *J. Nat. Prod.* **2009**, *72,* 645.

[5] Yatsunami, T.; Isono, T.; Hayakawa, I.; Okamoto, T. *Chem. Pharm. Bull.* **1975**, *23,* 3030.

[6] Yatsunami, T.; Furuya, S.; Okamoto, T. *Chem. Pharm. Bull.* **1978**, *26,* 3199.

[7] Hamlin, A. M.; Kisunzu, J. K.; Sarpong, R. *Org. Biomol. Chem.* **2014**, *12,* 1846.

[8] Pelletier, S. W.; Page, S. W.; In *The Alkaloids;* M. F. Grundon, Ed.; The Royal Society of Chemistry: London, 1979; Vol. 9, pp 221.

[9] For the use of Pelletier's intermediate in synthesis, see: (a) Meyer, W. L.; Goodwin, T. E.; Hoff, R. J.; Sigel, C. W. *J. Org. Chem.* 1977, **42**, 2761. (b) Meyer, W. L.; Sigel, C. W.; Hoff, R. J.; Goodwin, T. E.; Manning, R. A.; Schroeder, P. G. *J. Org. Chem.* **1977**, *42,* 4131. (c) Kametani, T.; Kato, Y.; Honda, T.; Fukumoto, K. *J. Am. Chem. Soc.* **1976**, *98,* 8185. (d) Satoh, F.; Kametani, T.; Kato, Y.; Honda, T.; Fukumoto, K. *Heterocycles* **1977**, *6,* 1757. (e) Pelletier, S. W.; Parthasarathy, P. C. *Tetrahedron Lett.* **1963**, *4,* 205.

[10] van der Baan, J. L.; Bickelhaupt, F. *J. R. Neth. Chem. Soc.* **1975**, *94,* 109.

[11] van der Baan, J. L.; Bickelhaupt, F. *Tetrahedron* **1974**, *30,* 2447.

[12] Kwak, Y.–S.; Winkler, J. D. *J. Am. Chem. Soc.* **2001**, *123,* 7429.

[13] For Mander's first approach, see: Balgir, B. S.; Mander, L. N.; Prager, R. H. *Aust. J. Chem.* **1974**, *27,* 1245.

[14] For Hutt and Mander's most recent approach, see: Hutt, O. E.; Mander, L. N. *Aust. J. Chem.,* **2008**, *61,* 204.

[15] Williams, C. M.; Mander, L. N. *Org. Lett.* **2003**, *5,* 3499.

[16] Williams, C. M.; Mander, L. N.; Bernhardt, P. V.; Willis, A. C. *Tetrahedron* **2005**, *61,* 3759.

[17] Hutt, O. E.; Mander, L. N. *J. Org. Chem.* **2007**, *72,* 10130.

[18] Shibanuma, Y.; Okamoto, T. *Chem. Pharm. Bull.* **1985**, *33,* 3187.

[19] Hamlin, A. M.; Cortez, F. de J.; Lapointe, D.; Sarpong, R. *Angew. Chem. Int. Ed.* **2013**, *52,* 4854.

[20] Muratake, H.; Natsume, M. *Tetrahedron Lett.* **2002**, *43,* 2913.

[21] Muratake, H.; Natsume, M. *Angew. Chem. Int. Ed.* **2004**, *43,* 4646.

[22] (a) Muratake, H.; Natsume, M. *Tetrahedron* **2006**, *62,* 7056. (b) Muratake, H.; Natsume, M. *Tetrahedron* **2006**, *62,* 7071. (c) Muratake, H.; Natsume, M. *Tetrahedron* **2006**, *62,* 7093.

[23] Peese, K. M.; Gin, D. Y.; *J. Am. Chem. Soc.* **2006**, *128,* 8734.

[24] Peese, K. M.; Gin, D. Y. *Org. Lett.* **2005**, *7,* 3323.

[25] Peese, K. M.; Gin, D. Y. *Chem. Eur. J.* **2008**, *14,* 1654.

Chapter 2. Development of an Aryne Insertion Strategy and Functionalized Tricycle Synthesis

2.1 Introduction

As outlined in Chapter 1, the hetisine-type collection of C_{20}-diterpenoid alkaloids consists of a variety of complex natural products that have inspired a flood of synthetic studies in the years since their isolation. We envisioned developing a route to the general hetisine core, which would start from a versatile intermediate and be utilized to access multiple alkaloid targets. A 6-7-6 tricycle was identified as a conserved structural motif in these alkaloids, and we anticipated that a benzyne insertion approach would provide the opportunity for a divergent synthesis. Our retrosynthetic analysis according to this disconnection, as well as the use of aryne intermediates in natural product synthesis, will be discussed in this chapter. This strategy was applied to access differently substituted 6-7-6 tricyclic frameworks. The development of this synthetic sequence will be detailed herein.

2.2 Analysis of the hetisine-type C_{20}-diterpenoid alkaloids

Our studies focused on cossonidine (**2.1**, Scheme 2-1) as our primary target. Cossonidine, whose structure was first reported in 1996,[1] has not been synthesized previously, nor has its biological activity been studied. In our structural analysis of the hetisine-type diterpenoid alkaloids, we identified a 6-7-6 tricyclic core (**2.1** and **2.2**, bolded bonds) that is conserved throughout the family of natural products and could serve as an initial target structural motif (e.g., compounds like **2.3**). This framework could be then advanced to the completed natural product skeleton via two C–N bond forming reactions. Construction of the [2.2.2] bicycle would then be addressed using a [4+2] cycloaddition, in accordance with the endgame sequence in the Gin synthesis of nominine (see Chapter 1.4). We envisioned accessing the 6-7-6 tricycle (**2.4**) through an aryne insertion into β-ketoester **2.6**. The use of an insertion approach would enable modification of both the hydrindanone derivative that is employed and the aryne precursor in order to introduce various functionalities as required by the target compound.

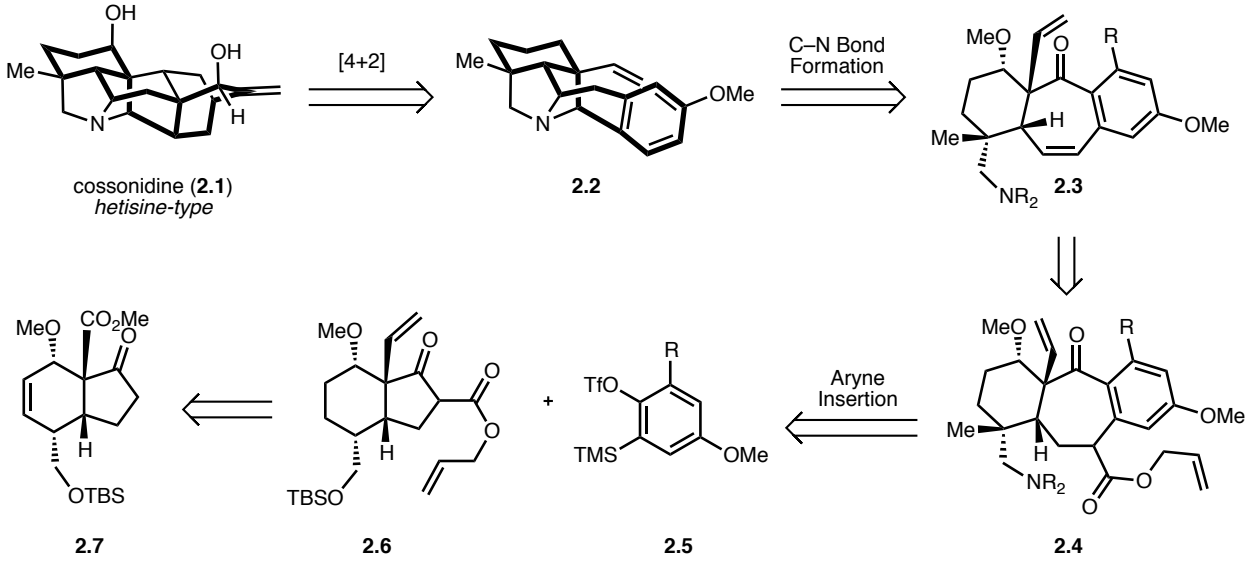

Scheme 2-1. Retrosynthetic analysis of cossonidine and the hetisine-type core.

2.3 Benzyne insertion into C–C sigma bonds

The parent *ortho*-benzyne (**2.8**) was first postulated as a reactive intermediate in 1927 by Bachmann and Clarke, but it wasn't until the ^{14}C labeling studies of John D. Roberts and coworkers in the 1950s, followed by work by Huisgen and Wittig, that proof of its existence was solidified.[2] *o*-Benzynes can be obtained from a variety of precursors such as the ones shown in Figure 2-1.[2,3] Treatment of aryl halides like **2.9** with sodium amide or a similar strong base with heat will generate a benzyne. Similarly, metal-halogen exchange of dihaloarenes or *o*-halotriflates (**2.10** or **2.11**) or the thermolysis of *o*-diazocarbonates (**2.12**) can facilitate a similar elimination reaction. While effective, many of the original methods for generating benzyne intermediates required the use of very harsh conditions (i.e., strong bases, high temperatures) that are often not compatible with more highly functionalized substrates. In 1983, Kobayashi reported the formation of benzyne intermediates through the fluoride-mediated elimination of *o*-silyl triflate precursors (e.g., **2.13**).[4] According to this protocol, benzynes could now be formed at, or even below, room temperature, and in the presence of a variety of functional groups. Since that time, other mild routes to benzyne intermediates have been reported.[5]

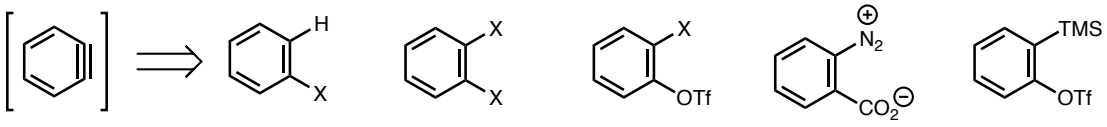

2.8 **2.9** **2.10** **2.11** **2.12** **2.13**

Figure 2-1. Selected precursors to benzyne intermediates (X = halogen).

Direct aryne insertions into C–C sigma bonds have been increasingly investigated in the past 10 years. In 2005, both Stoltz and Yoshida reported the insertion of arynes into C–C sigma bonds. Stoltz and coworkers had been investigating the α-arylation of β-ketoesters with arynes to form all-carbon quaternary centers (Scheme 2-2). In addition to, and sometimes instead of, the expected arylated products, however, they isolated products such as **2.15**, where the aryne had inserted into a C–C bond (see bolded bonds).[6] These transformations were performed by treating the β-ketoester with various *o*-silyl triflate aryne precursors in the presence of CsF in MeCN at 80 °C. Yields ranged from 45–95% depending on the substrate. Selected products **2.17**–**2.19** demonstrate the scope of reaction with the parent benzyne, substituted benzyne intermediates, and insertion into cyclic β-ketoesters.

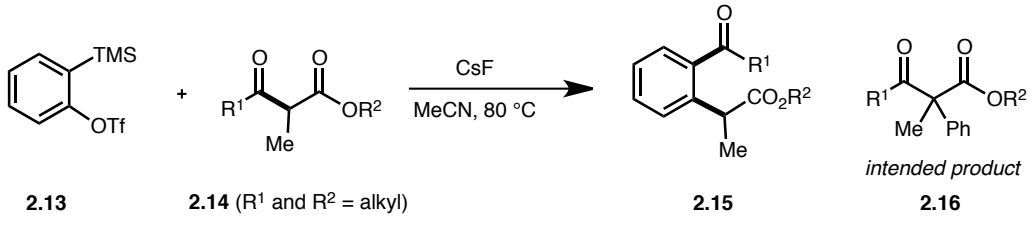

2.13 **2.14** (R^1 and R^2 = alkyl) **2.15** **2.16**

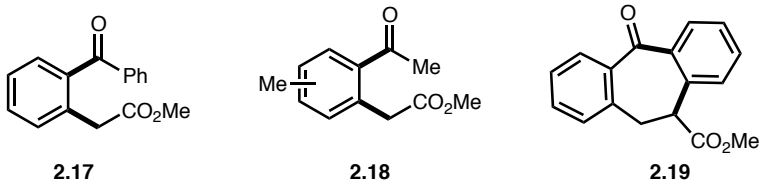

2.17 **2.18** **2.19**

Scheme 2-2. Stoltz acyl-alkylation of aryne intermediates.

Yoshida and coworkers have studied the metal-free insertion of arynes into various sigma bonds where one atom is nucleophilic in nature, while the other is electrophilic (Scheme 2-3).[7] They exploited this polarization in the context of sigma bonds where heteroatoms (N, S, Cl, Br) are the nucleophilic sites in order to arrive at polysubstituted arenes. In the same manner, they investigated the use of β-dicarbonyl substrates (e.g., **2.21**) in which the activated methylene serves as a nucleophile and one of the carbonyl carbons as the electrophile.[8] Treatment of symmetric cyclic and acyclic malonates or β-diketones with aryne precursors in the presence of KF at room temperature indeed provided the desired products (Scheme 2-3). Yields ranged from 49–82% with reaction times of 3–27 hours.

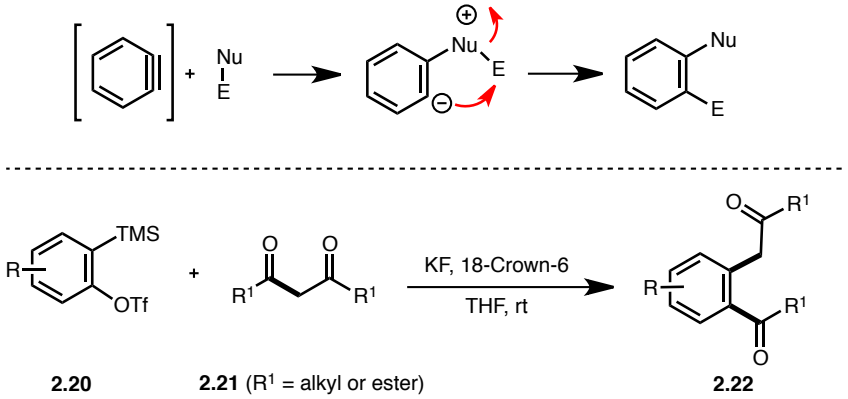

Scheme 2-3. Yoshida sigma-bond insertion strategy and application to C–C bond formation.

Mechanistically, these aryne insertions begin with the addition of the metal enolate to the aryne, resulting in an aryl anion such as **2.23** (Scheme 2-4). The aryl anion then adds into an ester or ketone carbonyl to provide a cyclobutane alkoxide (**2.24**). Collapse of the alkoxide and subsequent C–C bond cleavage give the final substituted arene.

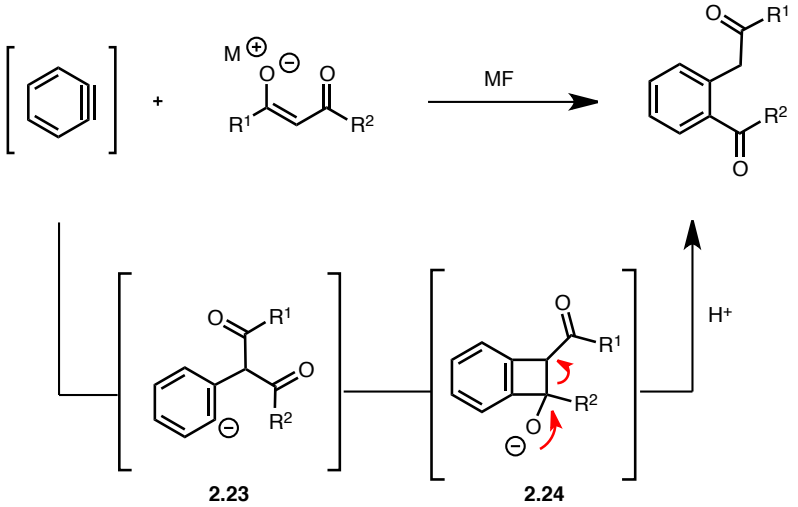

Scheme 2-4. Benzyne insertion mechanism.

Rationalization and prediction of the more electrophilic carbon of unsymmetrically substituted benzyne intermediates has most often been undertaken using both electronic and steric arguments by comparison to empirical trends. With a wide variety of possible substituents and properties, it can quickly become difficult to predict the regioselectivity of nucleophilic

addition. In the investigation of their acyl-alkylation of arynes, Stoltz and coworkers analyzed the regioselectivity of a variety of substituted arynes[9] and found that the presence of a substituent *ortho* to the triple bond resulted in increased electrophilicity at the distal carbon atom (e.g., **2.25**–**2.27**, Figure 2-2, where the arrow indicates the more electrophilic carbon). Intermediates such as **2.28**, with no *ortho* substituent showed poorer selectivity. Akai and coworkers reported in 2011[10] that silylbenzyne intermediates with an *ortho* silicon atom are preferentially electrophilic at the proximal carbon (e.g., **2.29**). This is in contrast to the inherent selectivity for the distal carbon when the directing substituent is alkyl, alkoxy, a halogen, or a bulky group. In their study of indolynes as reactive intermediates,[11,12] Garg and coworkers examined the electrophilicity of 4,5-, 5,6-, and 6,7-indolynes (**2.30**–**2.32**). Other empirical studies include those related to fused ring strain or heteroatom directing groups.[13]

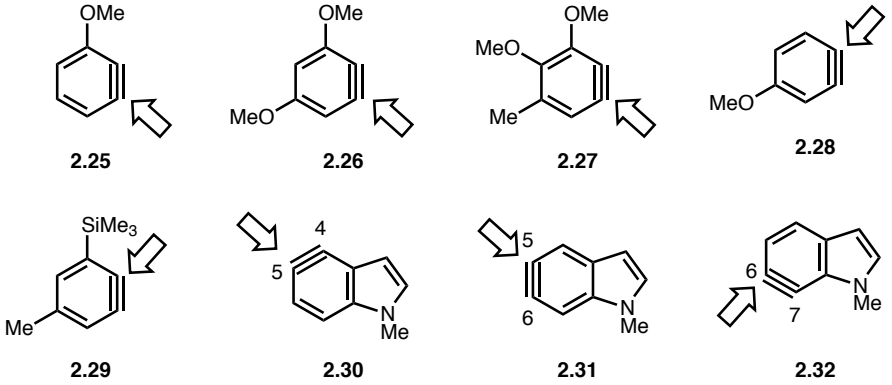

Figure 2-2. Selected aryne intermediates used for probing electrophilicity trends.

To further understand, and subsequently predict, indolyne reactivity, Garg and Houk developed a computational distortion model for the regioselectivity of nucleophilic attack on unsymmetrical arynes.[12, 14] Starting with the investigation of indolyne intermediates, then expanding to substituted benzynes, they found that the regioselectivity is controlled by the relative ease of distorting the aryne intermediate into the transition state necessary for addition (Scheme 2-5). This ease directly corresponds to the internal CCC bond angles at the triple bond termini. Nucleophilic attack is biased to the flatter, more electropositive end of the triple bond, which results in an energetically favorable decrease in ring distortion energy. Greater differences in energy correspond to higher regioselectivity. Unsymmetrical arynes with fused rings or adjacent polar substituents favored addition at the position *meta* to the substituent, and larger differences in bond angle resulted in greater selectivity. Of note, the introduction of a halide substituent can also influence the bond angle to improve, or even overturn,[15] the selectivity.

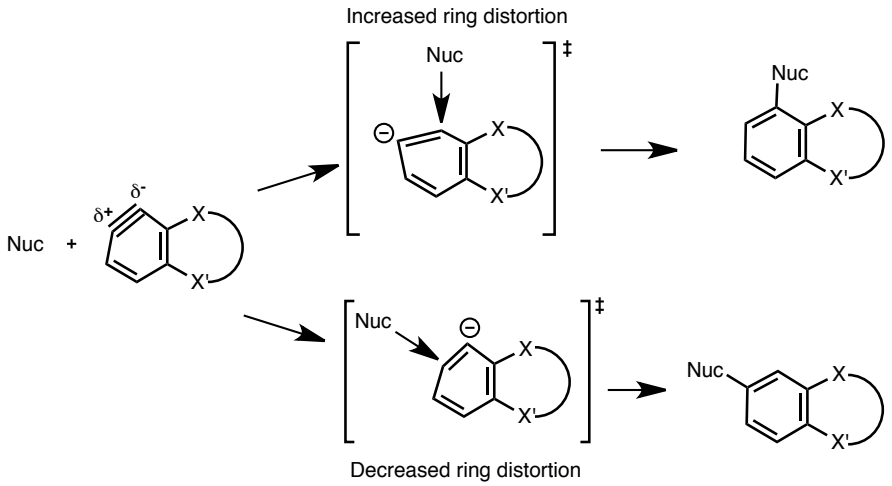

Scheme 2-5. Effect of the position of attack on transition state energy (adapted from Ref. 13).

2.4 Aryne insertion in natural product synthesis

Since their discovery, aryne intermediates have been used in natural product synthesis in a variety of ways.[3,16] General reactivity includes nucleophilic addition into the aryne, multi-component reactions, cycloadditions, and sigma-bond insertion reactions. Relatively few of these applications employ the C–C bond insertion transformation. The earliest example is Guyot's synthesis of melleine (**2.33**, Figure 2-3) in 1973.[17] In their strategy, the aryne was formed from an aryl bromide in the presence of sodium amide, and the corresponding bonds that were formed are shown in bold. Beginning in 2006, Stoltz and coworkers showcased their acyl-arylation of arynes through the synthesis of several natural products including amurensinine (**2.34**)[18] and curvularin (**2.35**).[19] Applications of the C–C bond insertion chemistry by Yoshida resulted in the synthesis of compounds including phomopsin C (**2.36**).[20] This transformation has yet to be showcased in the context of a complex natural product where the β-ketoester portion is more densely functionalized.

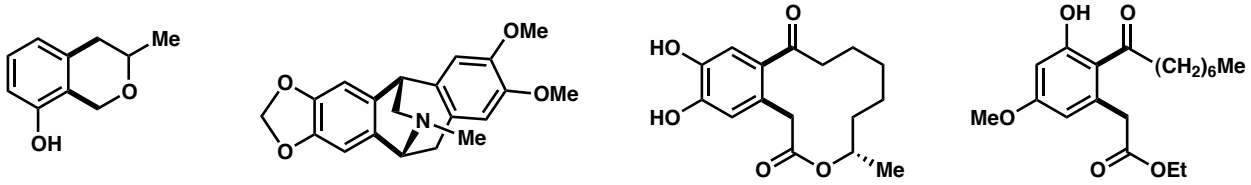

melleine (**2.33**) amurensinine (**2.34**) curvularin (**2.35**) phomopsin C (**2.36**)

Figure 2-3. Selected natural products synthesized utilizing aryne insertion into a C–C bond.

2.5 Aryne insertion model studies/preliminary results

Previous studies in our laboratory had identified hydrindanone derivative **2.7** as a viable starting point for investigations into the synthesis of diterpenoid alkaloids. **2.7** could be accessed using a Diels–Alder reaction between known diene **2.37**[21] and dienophile **2.38**.[22] This Diels–Alder reaction provided **2.7** in 75% yield and a >20:1 ratio of *endo:exo* diastereomers. Synthesis of the diene was achieved in four steps from 2-butyne-1,4-diol (Scheme 2-6). Dimethylation with dimethyl sulfate (not shown) provided alkyne **2.39**, which undergoes an elimination reaction in the presence of $NaNH_2/NH_3$ to provide enyne **2.40**. Addition into formaldehyde, followed by reduction and TBS protection of the resulting alcohol, delivered diene **2.37** in 38% yield over 3 steps. This sequence was performed routinely on a multi-gram scale to provide 70 g of diene in a

single pass. The dienophile (**2.38**) was accessed from the corresponding saturated β-ketoester via the selenide (not shown).

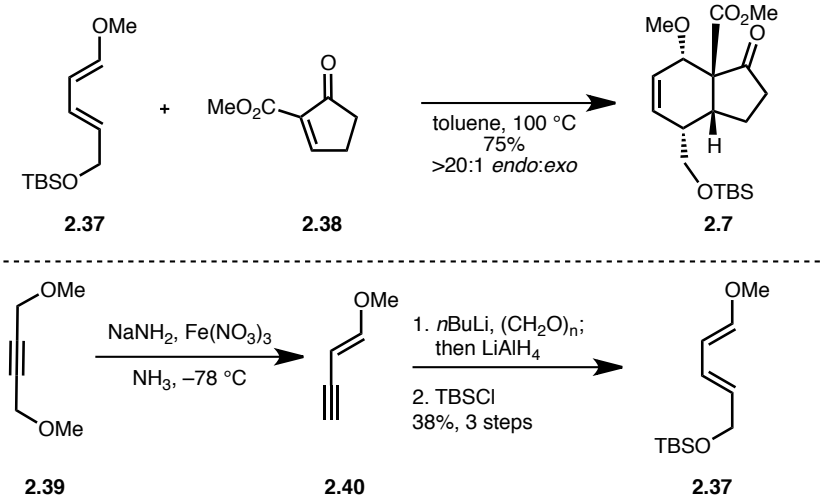

Scheme 2-6. Diels–Alder reaction and diene synthesis.

The resulting double bond in **2.7** offers an opportunity for further functionalization of C2 and C3 (see Scheme 2-7 for numbering), which is relevant for more highly oxygenated hetisine-type alkaloids. However, for the purposes of our target, the double bond was reduced using H_2 and Pd/C to arrive at **2.41**. For our initial forays into benzyne chemistry, **2.41** was acylated using Mander's reagent[23] to provide β-ketoester **2.42**. It is of note that the use of dimethyl carbonate or methyl chloroformate resulted exclusively in acylation at the oxygen. Treatment of β-ketoester **2.42** with commercial benzyne precursor **2.13** in the presence of CsF in MeCN at reflux, according to the conditions reported by Stoltz, delivered 6-7-6 tricycle **2.43** in 16% yield as a single diastereomer (the stereocenter at the carbon bearing the methyl ester group was not determined). While the efficiency of the reaction left room for optimization, we were encouraged that the general insertion strategy could be applied to our hydrindanone system. Thus, we embarked on the synthesis of appropriately substituted aryne precursors.

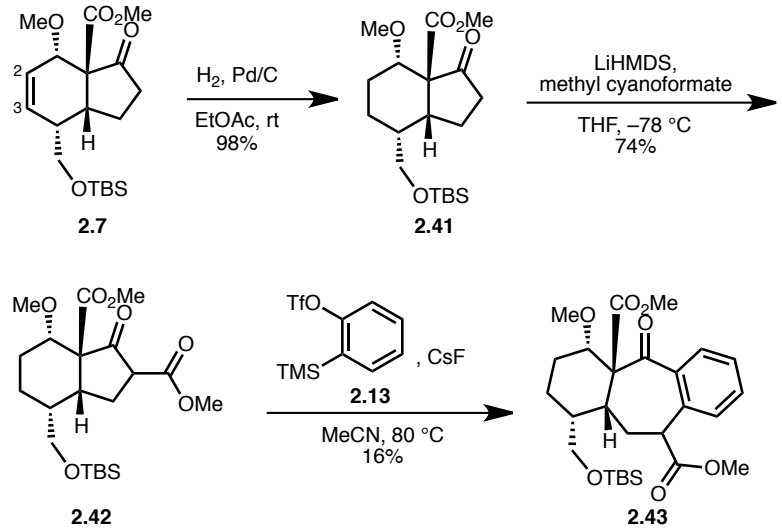

Scheme 2-7. Synthesis of β-ketoester **2.42** and proof-of-concept benzyne insertion.

In accordance with the empirical and computational studies performed by Garg and Houk (*vide supra*), we investigated the use of aryne precursors **2.44** and **2.47** (Scheme 2-8). In both cases, the substituent *ortho* to the resulting triple bond (Br or OMe) would provide the desired regioselectivity and could be removed later in the synthesis. Known[24] dimethoxy precursor **2.44** was accessed from 3,5-dimethoxyphenol in 3 steps (not shown) using a directed *ortho*-metalation (DoM)[25] sequence as employed by Garg[26] to install the trimethylsilyl group. Bromomethoxy precursor **2.47** was synthesized in 5 steps from *p*-methoxyphenol using sequential DoM steps for both trimethylsilyl and bromine atom incorporation according to a sequence developed by Garg for an indolyne precursor synthesis.[15] Cleavage of the carbamate directing group and triflation of the resulting phenol delivered **2.47**. We proceeded with our studies using **2.44** and **2.47**.

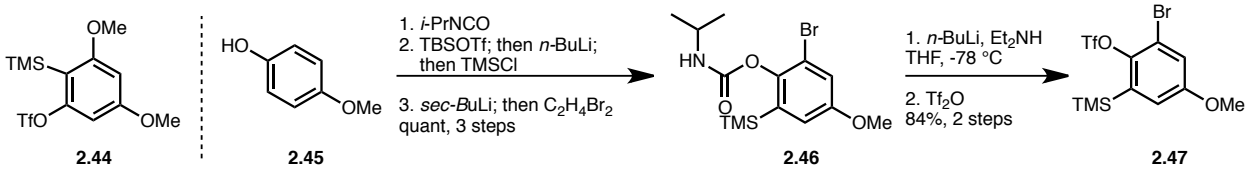

Scheme 2-8. Synthesis of aryne precursors.

Looking ahead to functional group differentiation and manipulation, an allyl ester functionality was identified as more versatile, and we therefore synthesized β-ketoester **2.48** from **2.41** and allyl cyanoformate[27] (Scheme 2-9). Subjection of **2.48** to the benzyne reaction conditions using precursor **2.44** provided 6-7-6 tricycle **2.49** in 50% yield. From this allyl ester compound, we planned to utilize palladium[28] or lead-catalyzed[29] oxidative decarboxylation chemistry to arrive at compounds such as **2.51** (see Table 2-1) in which a functional handle would be present at C6 for later C–N bond formation. Despite our efforts, a sampling of which is shown in Table 2-1, we were unable to effect decarboxylation at C7, whether in one or two steps. It is postulated that the electron-rich nature of the aromatic ring disfavors the formation of a benzylic radical or anion.

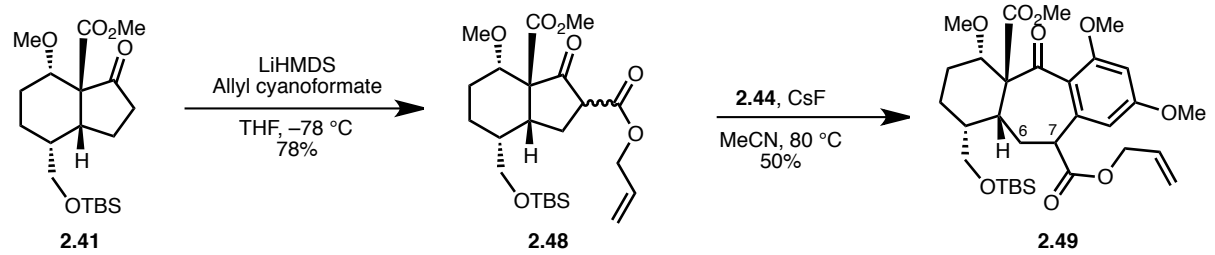

Scheme 2-9. Synthesis of **2.48** and subsequent insertion reaction.

Table 2-1. Initial investigations into oxidative decarboxylation from **2.49.**

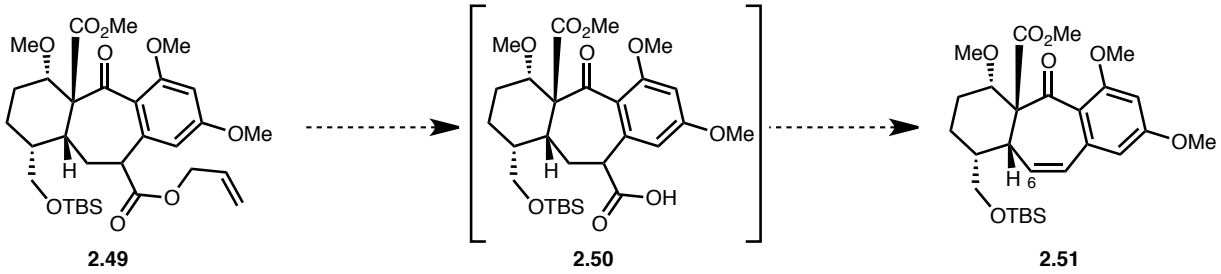

Selected Conditions	Results
*From the allyl ester (**2.49**):*	
Pd_2dba_3, MeCN, 80 °C	starting material (**2.49**)
$Pd(OAc)_2$, dppe, MeCN, 85 °C	starting material (**2.49**)
$Pd(OAc)_2$, dppe, MeCN, 110 °C, MW	starting material (**2.49**)
$Pd(OAc)_2$, PPh_3, MeCN, 90 °C	carboxylic acid (**2.50**)
*From the carboxylic acid (**2.50**):*	
$Pb(OAc)_4$, $Cu(OAc)_2$, quinoline, 125 °C	decomposition
$Pb(OAc)_4$, $Cu(OAc)_2$, C_6D_6, 150 °C MW	starting material (**2.50**)
$Pb(OAc)_4$, pyridine, C_6D_6, 80 °C	starting material (**2.50**)

To combat this potential electronic bias, we switched to the exclusive use of bromomethoxy aryne precursor **2.47**. This change would not only affect the electronics of the direct insertion product, but we anticipated that subsequent removal of the directing bromine atom would be more facile than removal of a methoxy group. Additionally, we sought to introduce the angular vinyl group, which is necessary for a later stage [2.2.2] bicycle formation via intramolecular Diels–Alder reaction, to further aid in functional group differentiation.

2.6 Construction of tricyclic intermediates

Initially, we envisioned installing the vinyl group through protection of the ketone carbonyl of **2.41** (Scheme 2-10), followed by reduction of the ester functionality and Wittig methylenation. Deprotection would then reveal the vinyl ketone. To this end, protection of the ketone as a *tert*-butyldimethylsilyl enol ether proceeded smoothly to provide **2.52** (where PG = TBS). Selective reduction of the ester to the aldehyde proved challenging, therefore it was necessary to completely reduce **2.52** to the primary alcohol, which was subsequently re-oxidized to **2.53** (where PG = TBS). Aldehyde **2.53** was treated with Ph_3PMeBr and *n*-BuLi to effect the homologation, followed by TBAF to cleave the silyl enol ether. While this route did lead to desired vinyl ketone **2.54**, there were several points that decreased its viability as a scalable route. The silyl enol ether that is introduced in the first step is sensitive to further reaction conditions and was partially cleaved during oxidation, thus requiring reprotection before further functionalization. This fact, in addition to the consistent low-yielding nature of the Wittig reaction, led us to develop a more streamlined vinyl group installation protocol.

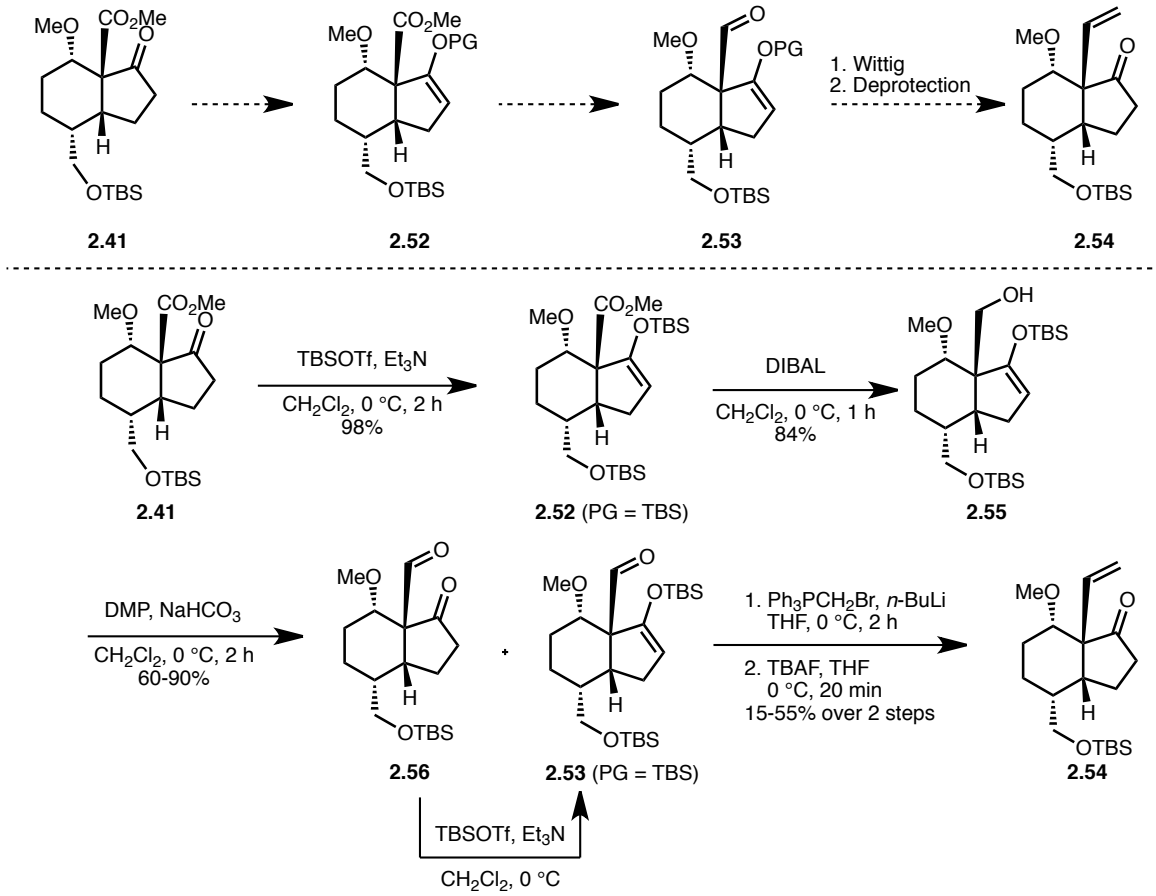

Scheme 2-10. Original methylenation proposal and execution.

In 2004, Lebel and coworkers reported a methylenation protocol which utilized $RhCl(PPh_3)_3$, $TMSCHN_2$, *i*-PrOH, and PPh_3 to form the methylene phosphonium ylide as a complement to starting from the phosphonium salt.[30] An appealing aspect of this methodology is the inherent chemoselectivity. Lebel showed that aldehyde groups reacted selectively over ketones at room temperature. Ketones could, however, be transformed in the presence of heat. This selectivity allowed us to bypass the problematic ketone protection that was previously required. Accordingly, our revised route began with the global reduction of **2.41** with $LiAlH_4$, which proceeds in 92% yield to give diol **2.57** (Scheme 2-11). Global oxidation to the ketoaldehyde (**2.56**) could be performed using the Ley protocol.[31] From this substrate, treatment with the Lebel conditions delivered the desired vinyl ketone in 51% yield over 3 steps, with the major byproduct being the decarbonylated compound (not shown).

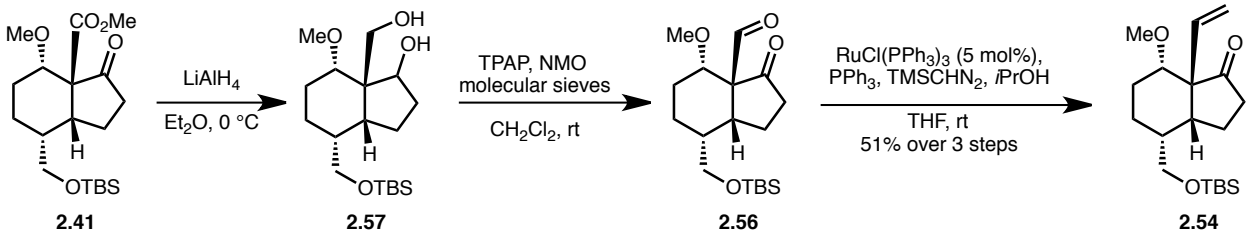

Scheme 2-11. Revised vinyl group installation sequence.

With the vinyl group installed, allyl β-ketoester **2.54** was prepared using LiHMDS and allyl cyanoformate. The desired monoacylation reaction was often difficult to control, and we routinely obtained a mixture of starting material, the desired ester, and the bisacylated compound (**2.58**) despite changing the order of addition, temperature, or equivalents of base or electrophile. To address this, the reaction was pushed to conversion of **2.54** to a mixture of the desired compound (**2.6**) and the bisacylation product (**2.58**), which was subsequently deallylated and decarboxylated in the presence of *in situ*-generated sodium allyl alkoxide to provide **2.6** in 94% over 2 steps (Scheme 2-12). Ester **2.6** was then subjected to acyl-alkylation conditions with **2.47** to provide tricycle **2.59** in 40% yield. This functionalized tricycle brought us to a position where we could again investigate the installation of a functional handle at C6 for C–N bond formation. Of note, β-ketoester **2.6** could also be used in benzyne insertion reactions with various additional precursors to give tricycles **2.61**–**2.64** (Figure 2-3).

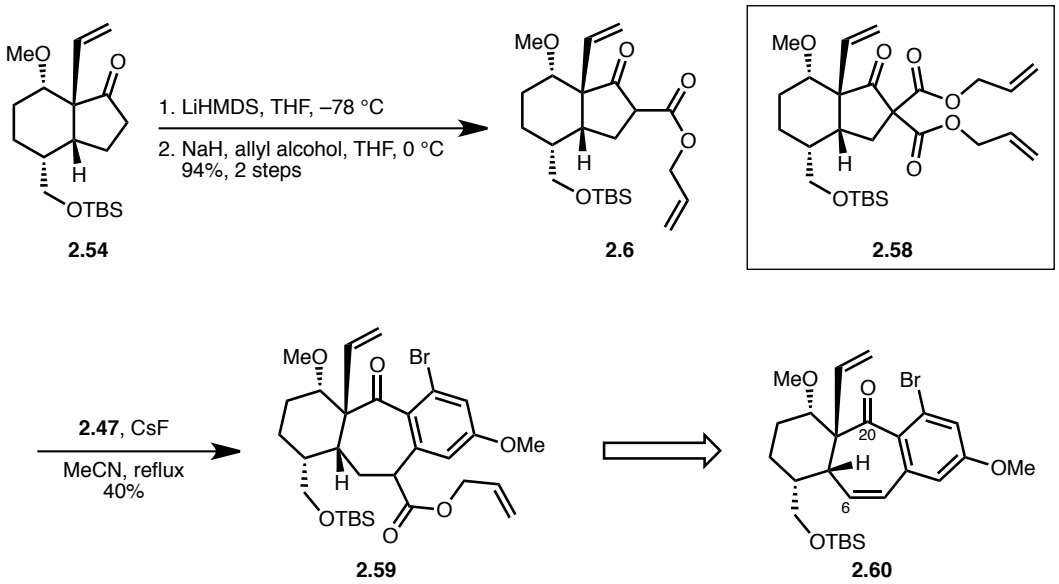

Scheme 2-12. Synthesis of vinyl-bearing tricycles **XX** and **XX**.

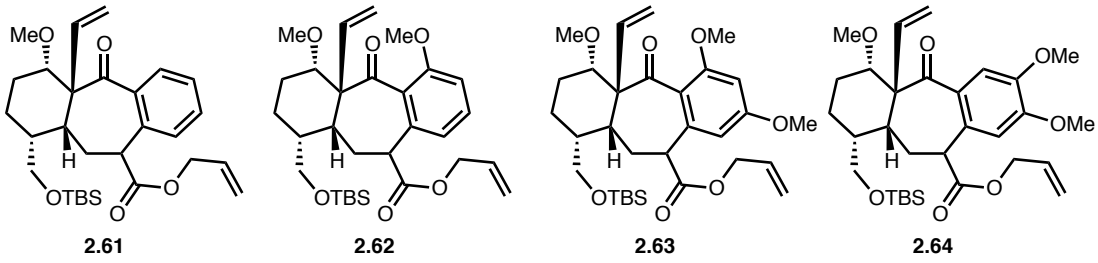

Figure 2-3. Additional aryne insertion products.

Removal of the bromine atom was explored at this stage and selected attempts to that end are shown in Table 2-2. Hydrodehalogenation via metal/halogen exchange and quenching with water (entries 1-3) provided small amounts of the desired product (**2.65**), but was not amenable to scale-up. Other transmetalation conditions tried (e.g., entries 4-6)[32,33,34] did not deliver the desired products. We were pleased to see that treatment of the aryl bromide with Bu_3SnTMS and CsF[35] gave the desired product in fair yield (entry 7), but this outcome was also challenging to reproduce and not amenable to scale-up. It was found, however, that Pd conditions reported by

Zhang and coworkers[36] succeeded in cleaving the C–Br with concomitant cleavage of the allyl ester to the carboxylic acid to provide **2.66** (entry 8). From this less electron-rich arene, we investigated anew the oxidative decarboxylation conditions, but testing a variety of conditions still returned starting material.

Table 2-2. Selected conditions for hydrodehalogenation.

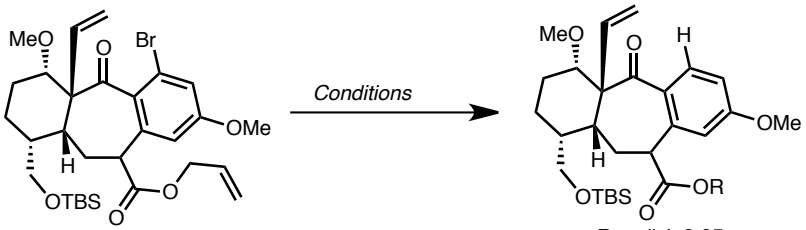

2.59

R = allyl, **2.65**
R = H, **2.66**

Entry	Conditions	Results
1	*n*-BuLi, THF, –78 °C	trace **2.65**
2	*i*-PrMgCl, THF, –20 °C	starting material (**2.59**)
3	*t*-BuLi, THF, –78 °C	dehalogenation, addition to carbonyl
4	Zn, 10% NaOH, 100 °C	deallylation
5	Bu_3SnH, AIBN, PhMe, 120 °C	complex mixture
6	$Fe(acac)_3$, EtMgBr, THF, rt	starting material (**2.59**)
7	Bu_3SnTMS, CsF, DMF, rt	**2.65** (39%)
8	$Pd(OAc)_2$, Ph_3P, K_2CO_3, *n*-BuOH, 100 °C	**2.66** (80%)

Looking to utilize a 2-step decarboxylation/elimination we applied the chemistry of Gandelman and coworkers in which they report a light-mediated radical iododecarboxylation.[37] Treatment of their acid substrates with N-iodosuccinimide (NIS) or 1,3-diiodo-5,5-dimethylhydantoin (DIH) in the presence of light (500 W tungsten filament bulb situated below the flask to additionally heat the reaction mixture) delivered the alkyl iodides in good yield. Surprisingly, subjection of **2.66** to the reaction conditions with DIH did not give us the iodo compound as the major product, but instead the oxidized alkene product (**2.67**, Scheme 2-13). It is postulated that instead of recombination of the benzylic radical with iodine, a hydrogen atom is abstracted from the alpha position to give the thermodynamically stable extended enone. Alternatively, an initially formed iodide may undergo facile elimination to give **2.67**.

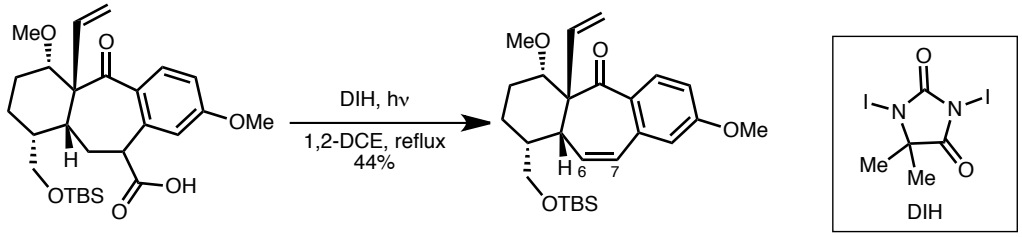

2.66 **2.67**

Scheme 2-13. Installation of the C6–C7 double bond.

Although the yields for the aryne insertion were reproducible and in line with benzyne reactions involving complex substrates, we postulated that the silyl ether present in **2.6** was

playing a part in the low yields and could lead to many of the various byproducts present in the reaction mixture. The presence of excess fluoride ions could result in silyl ether cleavage and the resulting hydroxyl group would then be available to participate in unproductive reactions with the benzyne intermediate. It has also been shown by Hoye and coworkers that silyl ethers can insert into arynes to produce silyl arenes.[38] The oxygen atom was necessary for installation of the C4 methyl group; however, in order to investigate C–N bond-forming reactions, we advanced a substrate containing a protected nitrogen atom to the benzyne insertion step.

Starting from the same vinyl hydrindanone derivative (**2.54**), the nitrogen atom was introduced in two steps via silyl group cleavage followed by a Mitsunobu reaction[39] with phthalimide, which proceeded in quantitative yield (Scheme 2-14). The analogous β-ketoester (**2.69**) was reacted with **2.70** to provide tricycle **2.70** in a slightly improved 46%. Among the byproducts isolated was chromenone **2.73** (Figure 2-4). This compound is unexpected but interesting because it indicates initial attack of the enolate on the benzyne at oxygen instead of carbon. The structure of **2.73** was confirmed by X-ray crystallography. Dehalogenation and oxidative decarboxylation of **2.70** provided enone **2.71**, but the reaction mixture was messy and difficult to purify. Excess triphenylphosphine and triphenylphosphine oxide were challenging to separate from the acid product and were, in turn, detrimental to the efficiency of the radical reaction. Electing to leave the bromine atom in place for the time being to avoid the purification difficulties, we found that the allyl group could be removed under mild conditions—$Pd(PPh_3)_4$ and phenylsilane in dichloromethane at room temperature[40]—and the Gandelman DIH protocol proceeded in a cleaner fashion to deliver **2.72** (45% yield over 2 steps).

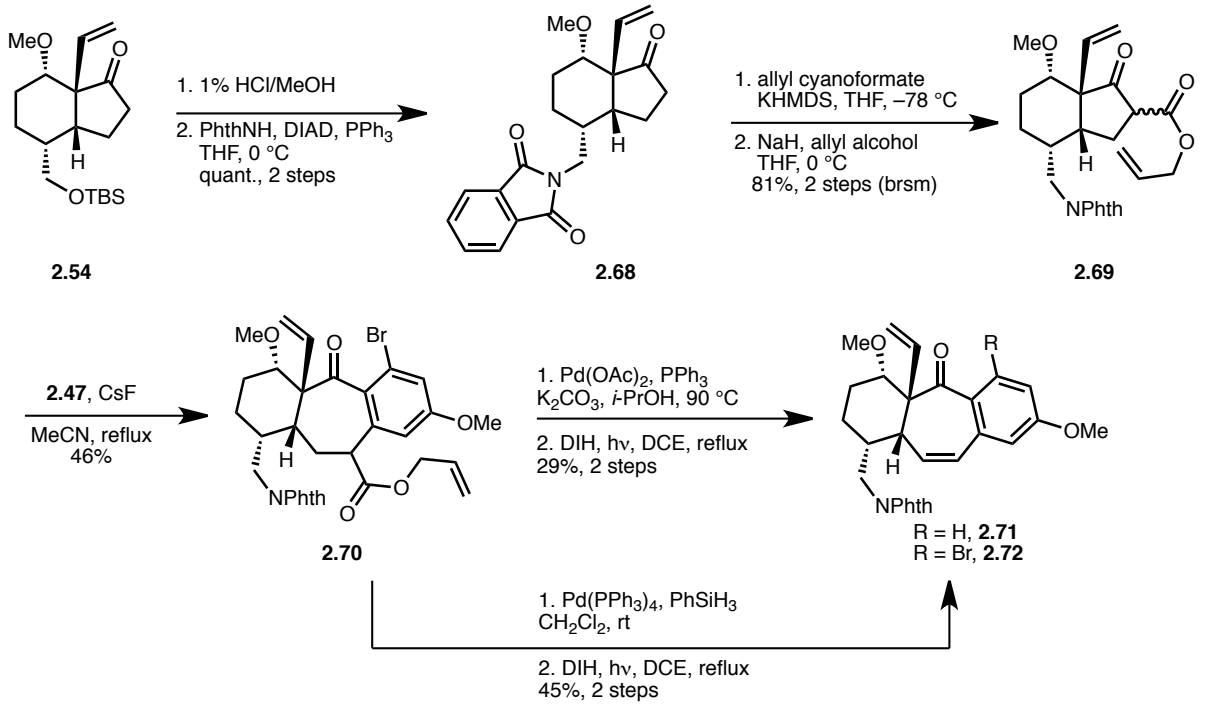

Scheme 2-14. Formation of nitrogen-containing tricycles **2.71** and **2.72**.

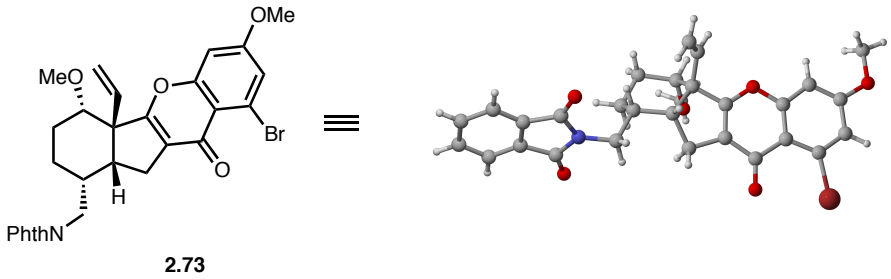

2.73

Figure 2-4. Chromenone side product **2.73** and CylView representation.

2.7 Conclusion

We have demonstrated the viability of the aryne insertion reaction to access complex 6-7-6 tricyclic intermediates that have been applied to the synthesis of the hetisine-type core. The benzyne insertion reaction was performed with several β-ketoester partners and two aryne precursors. The increased complexity of our β-ketoesters (e.g., diverse polar functional groups and adjacent quaternary center) enabled us to demonstrate the viability of aryne insertion into C–C bonds in complex natural product synthesis. An oxidative decarboxylation installed the second functional handle necessary for C–N bond formation.

2.8 Experimental Contributions

Early synthesis of the starting hydrindanone derivative was carried out by Dr. Terry Lebold. Dr. Ethan Fisher and Kyle Clagg aided in further synthesis and scale up of the hydrindanone derivative and the aryne precursors. The vinyl group installation was investigated with Christopher Marth. All other reactions were carried out by Jessica K. Kisunzu.

2.9 Experimental Methods

All reagents were obtained from commercial chemical suppliers and used without further purification unless otherwise noted. All reactions were performed in round-bottomed flasks or microwave vials sealed with rubber septa, under an atmosphere of nitrogen, and stirred with a Teflon™-coated magnetic stir bar unless otherwise noted. Temperatures above 23 °C were controlled by an IKA® temperature modulator. Pre-dried tetrahydrofuran (THF), benzene, toluene, acetonitrile (MeCN), methanol (MeOH), and triethylamine (Et_3N), were degassed with argon for 60 min and passed through activated alumina columns. Dichloromethane (CH_2Cl_2) was distilled over calcium hydride before use. Reactions were monitored by thin layer chromatography (TLC) using Silicycle Siliaplate™ glass backed TLC plates (250 μm thickness, 60 Å porosity, F- 254 indicator) and visualized using UV (254 nm) and *p*-anisaldehyde stain. Volatile solvents were removed using a rotary evaporator under reduced pressure. Silica gel chromatography was performed using Sorbent Technologies 60 Å, 230 x 400 mesh silica gel (40-63 μm). ^1H NMR and ^{13}C NMR were obtained in $CDCl_3$ on Bruker 400, 500, or 600 MHz spectrometers with ^{13}C operating frequencies of 100, 126, or 151 MHz, respectively. Chemical shifts are reported in parts per million (δ) relative to residual chloroform (7.26 ppm for ^1H and 77.00 ppm for ^{13}C). Data for ^1H NMR spectra are reported as follows: chemical shift (multiplicity, coupling constants, number of hydrogens). Multiplicity is designated as s (singlet), d (doublet), t (triplet), q (quartet), quint (quintet), or m (multiplet). IR spectra were obtained using a Nicolet MAGNA-IR 850 spectrometer as thin films on NaCl plates and reported in frequency of absorption (cm^{-1}). High-resolution mass spectral (HRMS) data was obtained from the Mass Spectral facility at the University of California, Berkeley.

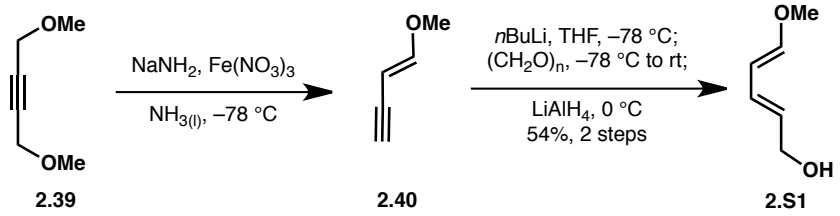

2.39 **2.40** **2.S1**

(2*E*,4*E*)-5-Methoxypenta-2,4-dien-1-ol (2.S1). NH_3 (~1 L) was condensed into a 2 L, 2-neck flask equipped with a coldfinger. $Na_{(s)}$ (2.17 g) was added slowly, resulting in a blue solution which was stirred for 10 min. $Fe(NO_3)_3$ (0.930 g, 3.85 mmol, 0.005 equiv) was then added, followed by another 20 minutes of stirring. The remainder of the Na (42.8 g, 1.96 mol total, 2.4 equiv) was added in portions over 1 h. 1,4-Dimethoxy-2-butyne (**2.39**, 94.3 g, 0.83 mmol) was added over 1 h with dry Et_2O used to ensure complete transfer. The reaction mixture was stirred for 1.5 h, at which time the coldfinger was removed and Et_2O (250 mL) was added to the flask. The flask was then placed in a room temperature water bath to assist in NH_3 evaporation. After evaporation was complete, the reaction was quenched by the slow addition of H_2O (350 mL). The layers were separated and the aqueous layer was extracted with Et_2O. The combined organic layers were washed once with brine, dried ($MgSO_4$), and filtered. The ether was then removed via short path distillation, with care taken to keep the temperature below 60 °C, until the solution was 1:1 ether to terminal alkyne product (**2.40**) by NMR analysis (approx. 43.9 g prod). The terminal alkyne (43.9 g, 0.53 mol) was taken up in THF (600 mL) and cooled to –78 °C. *n*BuLi (214.0 mL, 2.5 M in hexanes, 0.53 mol, 1 equiv) was added slowly over 45 min. The reaction mixture was then warmed to rt and allowed to stir for 30. It was then cooled back down to –78 °C, paraformaldehyde (20.24 g, 0.67 mol, 1.25 equiv) was added, and the reaction mixture was warmed to rt and stirred for 14 h. The mixture was cooled to 0 °C and $LiAlH_4$ (24.3 g, 0.64 mol, 1.2 equiv) was added slowly, followed by stirring at 0 °C for an additional 1.5 h and room temperature for 7 h. The reaction was quenched by the slow addition of 25 mL H_2O, 25 mL 10% NaOH, and 75 mL H_2O sequentially at 0 °C. The quenched mixture was then stirred at room temperature until all the solids were white, then it was filtered through Celite, washed with Et_2O, and concentrated to give a yellow oil. The oil was diluted with CH_2Cl_2 (300 mL), dried ($MgSO_4$), filtered, and solvent removed to give the diene alcohol as an orange oil (**2.S1**, 51.1 g, 0.45 mol, 54% over 2 steps). **R_f:** 0.13 (4:1 hexanes/EtOAc, anisaldehyde stain). **^{1}H NMR** (400 MHz, $CDCl_3$): δ 6.56 (d, J = 13 Hz, 1H), 6.07 (dd, J = 15, 11 Hz, 1H), 5.59 (dt, J = 12, 6.0 Hz, 1H), 5.48 (dd, J = 12, 11 Hz, 1H), 4.06 (d, J = 6.3 Hz, 2H), 3.54 (s, 3H), 2.34 (br s, 1H). **^{13}C NMR** (100 MHz, $CDCl_3$): δ 151.6, 128.4, 126.3, 104.7, 63.5, 56.3. **IR** (thin film) $\tilde{\nu}_{max}$ cm^{-1} 3355, 3001, 2936, 2836, 1657, 1461, 1213, 1162, 1144. **HRMS** could not be obtained.

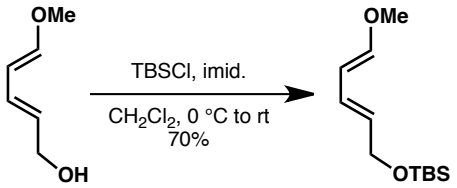

2.S1 **2.37**

***tert*-Butyl(((2*E*,4*E*)-5-methoxypenta-2,4-dien-1-yl)oxy)dimethylsilane (2.37).** Diene alcohol **S1** (51.1 g, 0.45 mol) was taken up in CH_2Cl_2 (800 mL) an a 2 L flask with a stirbar followed by imidazole (61.4 g, 0.9 mol, 2 equiv). The solution was cooled to 0 °C and *t*-butyldimethylsilyl

chloride (75.4 g, 0.50 mol, 1.1 equiv) was added in portions with vigorous stirring. When the reaction was complete by TLC analysis (approx. 3 h), the mixture was washed with $NaHCO_{3(aq)}$ then brine, dried ($MgSO_4$), and the solvent removed to give the crude TBS ether. Column chromatography (50:1 then 30:1 hexanes/EtOAc) provided diene **2.37** as a colorless oil (71.9 g, 0.31 mol, 70%). **R_f:** 0.73 (4:1 hexanes/EtOAc, anisaldehyde stain). **^{1}H NMR** (400 MHz, $CDCl_3$): δ 6.58 (d, *J* = 12 Hz, 1H), 6.09 (dd, *J* = 13, 11 Hz, 1H), 5.60 – 5.49 (m, 2H), 4.18 (dd, *J* = 5.8, 1.2 Hz, 2H), 3.58 (s, 3H), 0.91 (s, 9H), 0.07 (s, 6H). **^{13}C NMR** (100 MHz, $CDCl_3$): δ 151.0, 126.9, 126.6, 104.9, 63.9, 56.2, 25.9, 19.3, -5.3. **IR** (thin film) $\tilde{\nu}_{max}$ cm^{-1} 2962, 2929, 2893, 2856, 1659, 1622, 1458, 1262, 1238. **HRMS** could not be obtained.

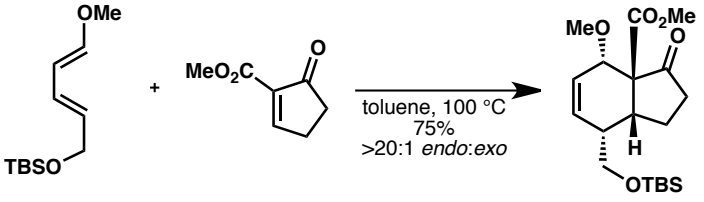

2.37 2.38 2.7

(3a*S*,4*S*,7*R*,7a*R*)-Methyl 7-(((*tert*-butyldimethylsilyl)oxy)methyl)-4-methoxy-3-oxo-2,3,3a,4,7,7a-hexahydro-1*H*-indene-3a-carboxylate (2.7). Diene **2.37** (43.6 g, 191 mmol, 1.3 equiv) and dienophile **2.38** (20.1 g, 143 mmol) were taken up in toluene (25 mL) in a round bottom flask fitted with a reflux condenser. The reaction mixture was heated to 100 °C under N_2 with vigorous stirring for 14 h, at which time the reaction was complete by NMR analysis. The solvent was removed and column chromatography (95:5 hexanes/EtOAc) provided Diels–Alder adduct **2.7** as an oil (39.5 g, >20:1 *endo*:*exo*, 75%). **R_f:** 0.43 (9:1 hexanes/EtOAc, anisaldehyde stain). **^{1}H NMR** (600 MHz, $CDCl_3$) δ 5.99 (dt, *J* = 11, 3.6 Hz, 1H), 5.71 (d, *J* = 10 Hz, 1H), 4.35 (s, 1H), 3.73 (s, 3H), 3.63 (dt, *J* = 20, 9.6 Hz, 2H), 3.31 (s, 3H), 2.99 (q, *J* = 6.6 Hz, 1H), 2.47 (d, *J* = 6.6 Hz, 1H), 2.38 (dd, *J* = 19, 8.4 Hz, 1H), 2.24 (q, *J* = 9.0 Hz, 1H), 1.96 – 1.87 (m, 2H), 0.89 (s, 9H), 0.06 (s, 6H). **^{13}C NMR** (150 MHz, $CDCl_3$) δ 211.9, 171.0, 128.0, 124.3, 73.7, 63.8, 63.3, 58.7, 52.7, 39.4, 38.6, 36.7, 25.8, 20.6, 18.2, -5.4, -5.5. **IR** (thin film) $\tilde{\nu}_{max}$ cm^{-1} 2954, 2930, 2896, 2857, 1757, 1730, 1253, 1109, 1085, 838, 777. **HRMS** (ESI) calcd for $[C_{19}H_{32}O_5{}^{23}Na^{28}Si]^+$ ($[M+H]^+$): *m/z* 391.1911, found 391.1914.

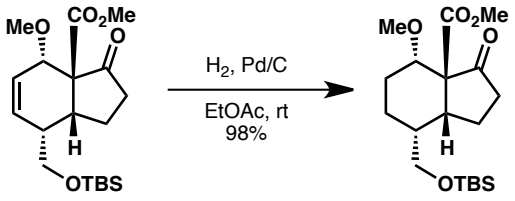

2.7 2.41

(3a*S*,4*S*,7*R*,7a*R*)-Methyl 7-(((*tert*-butyldimethylsilyl)oxy)methyl)-4-methoxy-3-oxooctahydro-1*H*-indene-3a-carboxylate (2.41). Diels–Alder adduct **2.7** (6.45 g, 17.5 mmol) was taken up in 250 mL EtOAc (250 mL) in a flame-dried round-bottom flask with a stirbar. The Pd/C was added (650 mg, 10% by mass). The reaction flask was evacuated and backfilled with H_2 3 times before being left to stir under a H_2 atmosphere. When the reaction was done complete by NMR analysis (~24 h), the suspension was filtered through Celite and eluted with EtOAc, then the solvent was removed to give the reduced product **2.41** (6.36 g, 17.2 mmol, 98%). **R_f:** 0.42 (9:1 hexanes/EtOAc, anisaldehyde stain). **mp:** 37–39 °C. **^{1}H NMR** (600 MHz, $CDCl_3$): δ 4.08 (s, 1H), 3.69 (s, 3H), 3.53 (dt, *J* = 24, 10 Hz, 2H), 3.17 (s, 3H), 3.02 (q, *J* = 6.6 Hz, 1H),

2.39 (dd, J = 19, 8.4 Hz, 1H), 2.25 (q, J = 9.0 Hz, 1H), 2.08 – 2.00 (m, 2H), 1.82 – 1.75 (m, 2H), 1.44 – 1.38 (m, 3H), 0.89 (s, 9H), 0.05 (s, 6H). **^{13}C NMR** (150 MHz, $CDCl_3$) δ 214.7, 170.9, 78.7, 65.6, 63.1, 57.2, 52.5, 41.2, 39.2, 38.2, 25.9, 25.4, 20.4, 18.3, 17.1, -5.36, -5.42. **IR** (thin film) $\tilde{\nu}_{max}$ cm^{-1} 2953, 2930, 2896, 2857, 1755, 1728, 1252, 1092, 837, 776. **HRMS** (ESI) calcd for $[C_{19}H_{34}O_5{}^{23}Na^{28}Si]^+$ ([M+Na]$^+$): *m/z* 393.2068, found 393.2070.

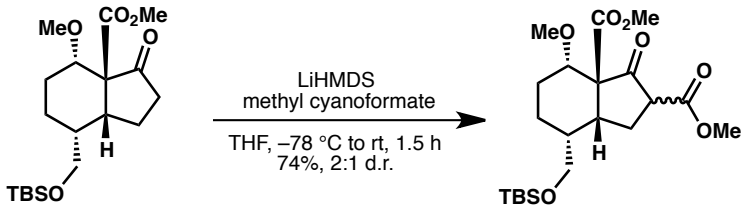

2.41 **2.42**

(3a*S*,4*S*,7*R*,7a*R*)-Dimethyl 7-(((*tert*-butyldimethylsilyl)oxy)methyl)-4-methoxy-3-oxooctahydro-1*H*-indene-2,3a-dicarboxylate (2.42). Ketone **2.41** (96.5 mg, 0.26 mmol) was dissolved in THF in an oven-dried round-bottom flask with a stir bar. The solution was cooled to –78 °C and LiHMDS (550 μL, 1 M in THF, 0.55 mmol, 2.1 equiv) was added. After stirring for 30 min at that temperature, methyl cyanoformate was added (60 μL, 0.76 mmol, 2.9 equiv). The reaction mixture was warmed to 0 °C and stirred for 1 h, at which time TLC analysis showed complete conversion. The reaction was quenched by the addition of $NH_4Cl_{(aq)}$ (3 mL) and the layers were separated. The aqueous layer was extracted with EtOAc (3 x 10 mL), and the combined organic layers were washed with brine, dried ($MgSO_4$), filtered, and the solvent removed to give a crude red oil. Column chromatography (5 → 15% EtOAc in hexanes) gave the target β-ketoester (**2.42**) as a colorless oil (82.5 mg, 0.19 mmol, 74%, 2:1 d.r.). **R_f:** 0.41 (4:1 hexanes/EtOAc, faint UV, anisaldehyde stain). **^{1}H NMR** (500 MHz, $CDCl_3$) δ 4.09 (s, 1H), 3.76 (s, 2H), 3.72 (s, 1H), 3.70 (s, 3H), 3.61 – 3.48 (m, 2H), 3.39 (d, J = 9.4 Hz, 0.5H), 3.35 – 3.26 (m, 1H), 3.18 (s, 1H), 3.10 (s, 2H), 2.95 (dt, J = 12.7, 6.0 Hz, 0.5H), 2.55 (q, J = 12.6 Hz, 1H), 2.28 (td, J = 12.7, 9.6 Hz, 0.5H), 2.16–1.97 (m, 2H), 1.90–1.78 (qd, J = 9.1, 5.8 Hz, 1H), 1.52 – 1.34 (m, 2.5H), 0.90 (s, 4H), 0.88 (s, 5H), 0.05 (s, 3H), 0.05 (s, 3H). **^{13}C NMR** (101 MHz, $CDCl_3$) δ 207.4, 206.0, 170.1, 170.0, 169.0, 167.7, 78.9, 78.5, 65.3, 65.2, 63.8, 62.8, 57.1, 56.8, 55.0, 54.9, 52.6, 52.5, 52.4, 52.2, 39.4, 38.1, 37.7, 25.77, 25.75, 25.2, 25.1, 24.7, 24.0, 18.2, 18.1, 17.0, 16.6, -5.45, -5.50. **IR** (thin film) $\tilde{\nu}_{max}$ cm^{-1} 2954, 2895, 2857, 1763, 1736, 1462, 1435, 1252, 1087, 838. **HRMS** (ESI) calcd for $[C_{21}N_{36}O_7{}^{23}Na_1Si_1]^+$ ([M+Na]$^+$): *m/z* 451.2123, found 451.2119.

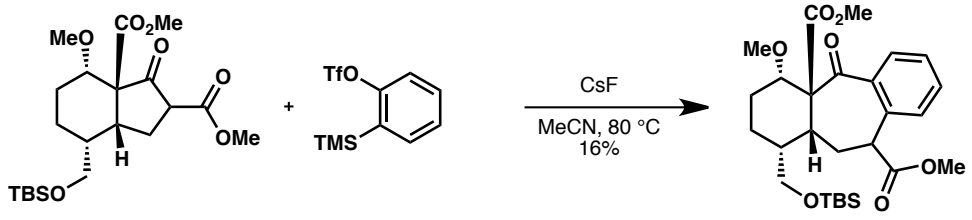

2.42 **2.13** **2.43**

(1*R*,4*S*,4a*S*,11a*R*)-Dimethyl 1-(((*tert*-butyldimethylsilyl)oxy)methyl)-4-methoxy-5-oxo-2,3,4,4a,5,10,11,11a-octahydro-1*H*-dibenzo[*a*,*d*][7]annulene-4a,10-dicarboxylate (2.43). β-Ketoester **2.42** (9.5 mg, 0.02 mmol) and commercial benzyne precursor **2.13** (7 μL, 0.03 mmol, 1.3 equiv) were taken up in MeCN (0.1 mL) in a vial with a stir bar. CsF (8.8 mg, 0.06 mmol, 3

equiv) was added, and the vial was sealed and heated to 80 °C. The reaction mixture was heated for 2 h, at which time it was cooled to rt and quenched with brine. The layers were separated and the aqueous layer was extracted with Et_2O. The combined organic layer was dried ($MgSO_4$) and solvent removed to give the crude mixture. Column chromatography (20:1 hexanes/EtOAc) delivered the title compound (**2.43**) as an oil (1.8 mg, 0.003 mmol, 16%). **R_f:** 0.43 (4:1 hexanes/EtOAc, UV, anisaldehyde stain). **^{1}H NMR** (500 MHz, $CDCl_3$) δ 7.41 (td, *J* = 7.6, 1.3 Hz, 1H), 7.31 (d, *J* = 7.5 Hz, 1H), 7.11 (dd, *J* = 7.5, 1.1 Hz, 1H), 7.05 (d, *J* = 7.7 Hz, 1H), 4.60 (s, 1H), 4.35 (dd, *J* = 11.9, 6.3 Hz, 1H), 3.76 (s, 3H), 3.63 (s, 3H), 3.45 (dd, *J* = 7.1, 3.5 Hz, 2H), 3.35 (s, 3H), 2.76 – 2.69 (m, 1H), 2.18 (td, *J* = 12.3, 6.4 Hz, 1H), 2.08 – 1.97 (m, 2H), 1.80 – 1.71 (m, 1H), 1.60 – 1.35 (m, 3H), 0.77 (s, 9H), 0.01 (s, 3H), -0.02 (s, 3H). **^{13}C NMR** (151 MHz, $CDCl_3$) δ 205.1, 174.0, 169.4, 138.5, 135.0, 131.2, 127.1, 127.0, 124.5, 78.6, 67.6, 64.6, 57.7, 52.7, 51.9, 45.6, 40.7, 34.5, 26.8, 25.7, 24.5, 18.1, 18.0, -5.4, -5.5. **IR** (thin film) $\tilde{\nu}_{max}$ cm^{-1} 2950, 2929, 2857, 1738, 1730, 1105, 1085. **HRMS (ESI)** calcd for $[C_{27}H_{40}O_7{}^{23}Na_1{}^{28}Si_1]^+$ ([M+Na]$^+$): *m/z* 527.2436, found 527.2428.

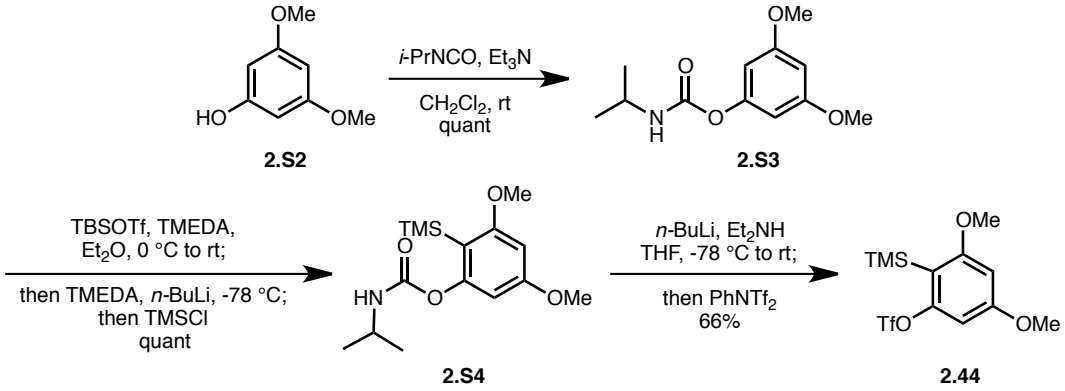

3,5-Dimethoxy-2-(trimethylsilyl)phenyl trifluoromethanesulfonate (2.44). To a flame-dried flask with a stir bar was added 3,5-dimethoxyphenol (**2.52**, 3.0 g, 19.5 mmol), followed by CH_2Cl_2 (50 mL), isopropyl isocyanate (2.9 mL, 29.5 mmol, 1.5 equiv), and Et_3N (0.540 mL, 3.9 mmol, 0.2 equiv). The solution was stirred for 24 h at which time the solvent was removed to give pure **2.S3** (4.67 g, quant). Carbamate **2.S3** (19.5 mmol) was dissolved in Et_2O (150 mL) in a flask with a stir bar. Tetramethylethylenediamine (4.2 mL, 28.2 mmol, 1.4 equiv) was added, and the solution was cooled to 0 °C. TBSOTf (6.8 mL, 29.6 mmol, 1.5 equiv) was then added, and the solution was allowed to slowly warm to rt. After 1 h, another portion of TMEDA (10.2 mL, 68.3 mmol, 3.5 equiv) was added, and the solution was cooled to –78 °C. *n*-BuLi (27.5 mL, 2.5 M in hexanes, 68.8 mmol, 3.5 equiv) was added slowly over the course of 45 min. The resulting solution was stirred at –78 °C for 3 h, at which time chlorotrimethylsilane (17.5 mL, 137.9 mmol, 7 equiv) was added over 30 min. After stirring for 1 h, the reaction was quenched by the addition of saturated $NaHSO_{4(aq)}$ (50 mL) and warmed to rt with vigorous stirring. The layers were separated and the aqueous layer was extracted with Et_2O (2x). The combined organic layer was washed with 1 M $NaHSO_4$ and brine, dried (Na_2SO_4), and the solvent removed to give clean silyl arene **2.S4** (6.17 g, quant), which was taken on directly. A portion of **2.S4** (2.00 g, 6.4 mmol) was dissolved in THF (65 mL) in a flask with a stir bar. Diethylamine (0.8 mL, 7.7 mmol, 1.2 equiv) was added, and the solution was cooled to –78 °C. *n*-BuLi (3.1 mL, 2.5 M in hexanes, 1.2 equiv) was added dropwise and the reaction mixture was stirred at –78 °C for 30 min before being warmed to rt. $PhNTf_2$ (2.76 g, 7.7 mmol, 1.2 equiv) was then added in one portion, and the mixture was stirred for 3 h, at which time the reaction was complete by TLC analysis. Column

chromatography (30:1 hexanes/EtOAc) provided **2.44** as an oil (1.52 g, 4.2 mmol, 66%). **^{1}H NMR** (600 MHz, $CDCl_3$) δ 6.50 (d, *J* = 2.0 Hz, 1H), 6.40 (d, *J* = 2.0 Hz, 1H), 3.81 (s, 3H), 3.80 (s, 3H), 0.34 (s, 9H). **^{13}C NMR** (101 MHz, $CDCl_3$) δ 166.2, 162.5, 155.3, 123.4, 120.2, 118.6 (q, *J* = 320.9), 117.0, 113.9, 112.0, 98.2, 97.3, 55.4, 55.4, 0.8. Spectra matched those previously reported.[24]

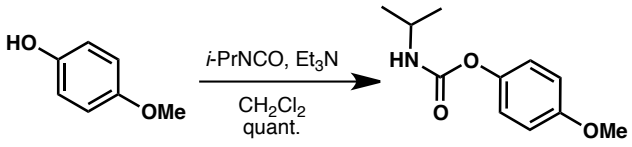

2.45 **2.S5**

4-Methoxyphenyl isopropylcarbamate (2.S5). To a round-bottom flask was added 4-methoxyphenol (10.00 g, 64.9 mmol) and CH_2Cl_2 (160 mL), followed by *iso*-propylisocyanate (9.6 mL, 97.7 mmol, 1.5 equiv) and triethylamine (1.8 mL, 12.9 mmol, 0.2 equiv). The clear reaction mixture was allowed to stir at room temperature until complete by TLC analysis. Solvent removed to provide carbamate **2.S5** as a white solid (15.50 g, quant.). **^{1}H NMR** (400 MHz, $CDCl_3$) δ 7.03 (d, *J* = 8.8 Hz, 2H), 6.85 (d, *J* = 8.7 Hz, 2H), 5.15 (bd, *J* = 8.2 Hz, 1H), 3.85 (m, 1H), 3.75 (s, 3H), 1.17 (s, 3H), 1.15 (s, 3H). **^{13}C NMR** (100 MHz, $CDCl_3$) δ 156.6, 154.0, 144.4, 122.3, 114.0, 55.3, 43.1, 22.6. **IR** (thin film) $\tilde{\nu}_{max}$ cm^{-1} 3289, 2966, 1691, 1556, 1507, 1458, 1241, 1209, 1172, 1037. **HRMS** (ESI) calcd $[C_{11}H_{16}NO_3]^+$ ($[M+H]^+$): *m/z* 210.1125, found 210.1126.

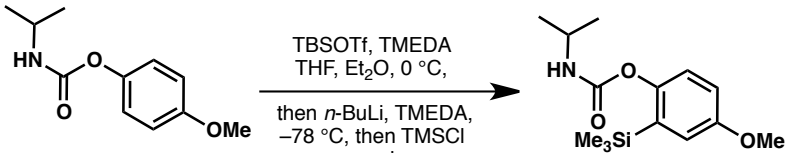

2.S5 **2.S6**

4-Methoxy-2-(trimethylsilyl)phenyl isopropylcarbamate (2.S6). Carbamate **2.S5** (17.0 g, 81.2 mmol) was taken up in Et_2O/THF (680 mL, 115 mL) and cooled to 0 °C using an ice bath. TMEDA (17.0 mL, 113.7 mmol, 1.4 equiv) added, followed by TBSOTf (22.4 mL, 97.4 mmol, 1.2 equiv) slowly. The solution was stirred at 0 °C for 5 min, then room temperature for 30 min. Another portion of TMEDA (42.6 mL, 284.2 mmol, 3.5 equiv) was added, and the reaction mixture cooled to –78 °C. *n*-BuLi (113 mL, 2.5 M in hexanes, 284.2 mmol, 3.5 equiv) was added over 1 h, then the mixture was stirred at that temperature for 3 h. TMSCl (72.1 mL, 568 mmol, 7 equiv) was added over 1 h and the mixture stirred for 1 h. The reaction was then quenched by the addition of 1N NaHSO4 (350 mL), warmed to rt, and stirred for 30 min. The aqueous layer was extracted with Et_2O and the combined organic layer was dried over $MgSO_4$, filtered, and concentrated to give the crude silyl carbamate. Column chromatography with CH_2Cl_2 gave **2.S6** as a white solid (24.34 g, quant.). **R_f:** 0.35 (CH_2Cl_2, UV, anisaldehyde stain). **^{1}H NMR** (400 MHz, $CDCl_3$) δ 7.02 (d, *J* = 8.8 Hz, 1H), 6.95 (d, *J* = 2.8 Hz, 1H), 6.88 (dd, *J* = 8.8, 3.2, 1H), 4.76 (bd, *J* = 7.9 Hz, 1H), 3.92 (m, 1H), 3.80 (s, 3H), 1.24 (s, 3H), 1.22 (s, 3H), 0.27 (s, 9H). **^{13}C NMR** (100 MHz, $CDCl_3$) δ 156.4, 154.2, 149.1, 133.0, 123.1, 120.0, 114.8, 55.5, 43.4, 23.0, -1.0. **IR** (thin film) $\tilde{\nu}_{max}$ cm^{-1} 3363, 3003, 2974, 2934, 1704 (C=O), 1569, 1531, 1474, 1405, 1270. **HRMS** (ESI) calcd $[C_{14}H_{23}NO_3NaSi]^+$ ($[M+Na]^+$): *m/z* 304.1339, found 304.1338.

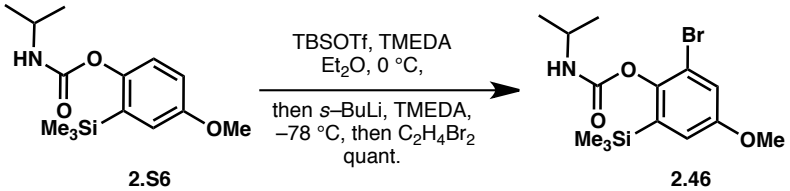

2.S6 **2.46**

2-Bromo-4-methoxy-6-(trimethylsilyl)phenyl isopropylcarbamate (2.46). Silyl carbamate **2.S6** (24.34 g, 86.5 mmol) was dissolved in Et_2O (860 mL) and cooled to 0 °C. TMEDA (14.3 mL, 95.2 mmol, 1.1 equiv) was added, followed by a slow addition of TBSOTf (20.9 mL, 90.8 mmol, 1.05 equiv). The reaction mixture was stirred at 0 °C for 5 min, then at rt for 30 min. A second portion of TMEDA (26.5 mL, 190.3 mmol, 2.2 equiv) was added and the solution was cooled to –78 °C. *s*-BuLi (136 mL, 1.2 M in cyclohexane, 190.3 mmol, 2.2 equiv) was added over 1 h, after which the solution was stirred for an additional hour. Dibromoethane (18.6 mL, 187.6 mmol, 2.5 equiv) was then added over 5 min, with continued stirring for 1 h. At this time, the reaction was quenched by the addition of MeOH (8.6 mL) and 1 N HCl (525 mL), warmed to rt, and stirred for 45 min. The aqueous layer was extracted with Et_2O and the combined organic layer was dried over $MgSO_4$ and concentrated. Column chromatography with CH_2Cl_2 then 10% EtOAc in CH_2Cl_2 provided the bromosilyl carbamate (**2.46**, 31.6 g, quant.). **R_f:** 0.55 (CH_2Cl_2, UV, anisaldehyde stain). **^{1}H NMR** (400 MHz, $CDCl_3$) δ 7.10 (d, *J* = 3.0 Hz, 1H), 6.91 (d, *J* = 3.0 Hz, 1H), 5.06 (bs, 1H), 3.90 (dt, *J* = 8.1, 6.5 Hz 1H), 3.77 (s, 3H), 1.23 (s, 3H), 1.21 (s, 3H), 0.29 (s, 9H) **^{13}C NMR** (100 MHz, $CDCl_3$) δ 156.9, 152.7, 145.8, 135.8, 119.7, 118.5, 117.9, 55.6, 43.4, 22.8, -1.0. **IR** (thin film) $\tilde{\nu}_{max}$ cm^{-1} 3342, 2966, 1744, 1720 (C=O), 1589, 1573, 1454, 1421, 1250, 1201. **HRMS** (ESI) calcd $[C_{14}H_{22}NO_3BrNaSi]^+$ ($[M+Na]^+$): *m/z* 382.0445, found 382.0446.

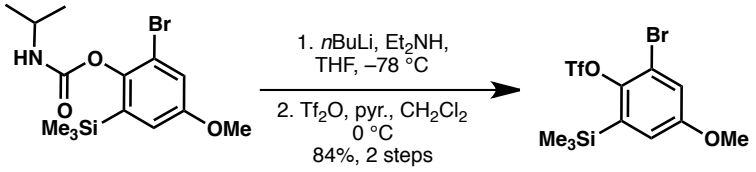

2.46 **2.47**

2-Bromo-4-methoxy-6-(trimethylsilyl)phenyl trifluoromethanesulfonate (2.47). *n*-BuLi (42 mL, 2.5 M in hexanes, 104 mmol, 1.2 equiv) was added slowly to Et_2NH (10.7 mL, 104 mmol, 1.2 equiv) in THF (130 mL) at –78 °C. After 15 min, a solution of carbamate **2.46** (31.6 g, 87 mmol) in THF (130 mL) was added slowly. The solution was stirred at that temperature for 20 min, then at room temperature for 25 min. At that time, it was quenched with sat. $NH_4Cl_{(aq)}$ and extracted with Et_2O. The combined organic layer was dried over $MgSO_4$, filtered, and concentrated. Column chromatography with 3% EtOAc in hexanes provided the known[41] phenol (20.0 g, 72.7 mmol). The phenol was then taken up in CH_2Cl_2 and cooled to 0 °C in an ice bath. Pyridine (9.5 mL, 117.5 mmol, 1.6 equiv) was added slowly followed by Tf_2O (15.0 mL, 89.2 mmol, 1.2 equiv). The reaction mixture was allowed to warm to rt and stirred for 20 h. When the reaction was complete by NMR analysis, the mixture was poured onto sat. $NaHCO_{3(aq)}$, the layers separated, and the aqueous layer extracted with CH_2Cl_2. The combined organic layer was dried over $MgSO_4$, filtered, and concentrated to give a dark red oil. Flash chromatography (9:1 hexanes/EtOAc then 4:1 hexanes/EtOAc) provided the *o*-silyl triflate **2.47** as a pale yellow oil (29.6 g, 84% over 2 steps). **R_f:** 0.51 (9:1 hexanes/EtOAc, UV). **^{1}H NMR** (500 MHz, $CDCl_3$) δ 7.15 (d, *J* = 3.1 Hz, 1H), 6.98 (d, *J* = 3.0 Hz, 1H), 3.82 (s, 3H), 0.39 (s, 9H). **^{13}C NMR** (151

MHz, $CDCl_3$) δ 158.6, 142.2, 138.2, 121.3, 119.8, 118.6 (q, *J* = 320.7 Hz), 116.9, 55.8, -0.1. **IR** (thin film) $\tilde{\nu}_{max}$ cm^{-1} 3078, 3008, 2959, 2905, 2842, 1580, 1560, 1406, 1213, 845. **HRMS** (EI) calcd for $[^{12}C_{11}H_{14}O_4F_3SiS^{79}Br]^+$ ([M]$^+$): *m/z* 405.9518, found 405.9518.

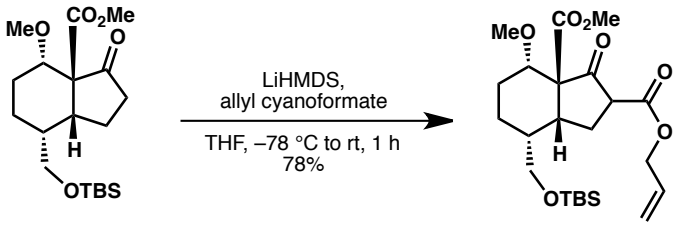

2.41 **2.48**

(3a*S*,4*S*,7*R*,7a*R*)-2-Allyl 3a-methyl 7-(((*tert*-butyldimethylsilyl)oxy)methyl)-4-methoxy-3-oxooctahydro-1*H*-indene-2,3a-dicarboxylate (2.48). Ketone **2.41** (113.3 mg, 0.31 mmol) was dissolved in THF in an oven-dried round-bottom flask with a stir bar. The solution was cooled to –78 °C and LiHMDS (620 μL, 1 M in THF, 0.62 mmol, 2.0 equiv) was added. After stirring for 30 min at that temperature, allyl cyanoformate was added (90 μL, 0.81 mmol, 2.6 equiv). The reaction mixture was warmed to 0 °C and stirred for 1 h, at which time TLC analysis showed complete conversion. The reaction was quenched by the addition of $NH_4Cl_{(aq)}$ (3 mL) and the layers were separated. The aqueous layer was extracted with EtOAc (3 x 10 mL), and the combined organic layers were washed with brine, dried ($MgSO_4$), filtered, and the solvent removed to give a crude red oil. Column chromatography (0 → 21% EtOAc in hexanes) gave the target β-ketoester (**2.48**) as a colorless oil (109.0 mg, 0.24 mmol, 78%). **R_f:** 0.53 (4:1 hexanes/EtOAc, UV, anisaldehyde stain) **^{1}H NMR** (500 MHz, $CDCl_3$) δ 5.98 – 5.84 (m, 1H), 5.35 (ddd, *J* = 28.2, 17.2, 1.5 Hz, 1H), 5.23 (ddd, *J* = 10.5, 5.2, 1.3 Hz, 1H), 4.75 – 4.58 (m, 2H), 4.10 (s, 1H), 3.70 (s, 2H), 3.69 (s, 1H), 3.60 – 3.49 (m, 2H), 3.42 (d, *J* = 9.3 Hz, 0.5H), 3.37 – 3.29 (m, 1H), 3.18 (s, 1H), 3.09 (s, 2H), 2.99 – 2.93 (m, 0.5H), 2.57 (dd, *J* = 25.0, 11.8 Hz, 0.5H), 2.29 (td, *J* = 12.8, 9.6 Hz, 0.5H), 2.06 (tdd, *J* = 13.1, 9.4, 5.4 Hz, 2H), 1.84 (s, 1H), 1.52 – 1.36 (m, 3H), 0.89 (s, 4H), 0.89 (s, 5H), 0.05 (s, 3H), 0.04 (s, 3H). **^{13}C NMR** (151 MHz, $CDCl_3$) δ 207.4, 206.0, 170.2, 170.1, 168.5, 167.0, 131.9, 131.7, 118.2, 118.1, 78.96, 78.5, 65.8, 65.6, 65.4, 65.3, 63.8, 62.9, 57.2, 56.9, 55.2, 55.2, 52.6, 52.6, 39.6, 38.2, 37.9, 37.8, 25.9, 25.3, 25.2, 24.9, 24.1, 18.2, 18.2, 17.1, 16.7, -5.37, -5.42. **IR** (thin film) $\tilde{\nu}_{max}$ cm^{-1} 2953, 2930, 2894, 2857, 1762, 1733, 1253, 1088, 838. **HRMS** (ESI) calcd for $[C_{23}H_{39}O_7{}^{28}Si_1]^+$ ([M+H]$^+$): *m/z* 455.2460, found 455.2456.

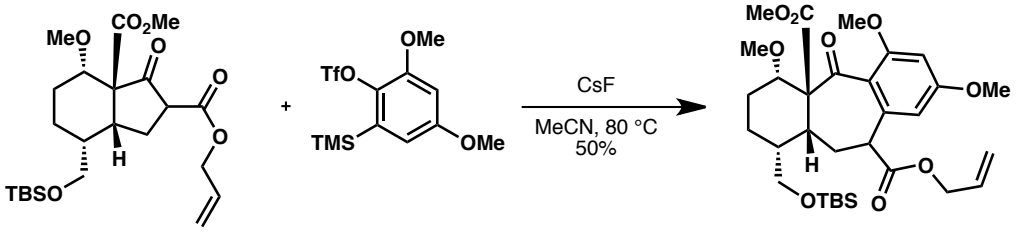

2.48 **2.44** **2.49**

(1*R*,4*S*,4a*S*,11a*R*)-10-Allyl 4a-methyl 1-(((*tert*-butyldimethylsilyl)oxy)methyl)-4,6,8-trimethoxy-5-oxo-2,3,4,4a,5,10,11,11a-octahydro-1*H*-dibenzo[*a*,*d*][7]annulene-4a,10-dicarboxylate (2.49). A flame-dried vial was charged with dry CsF (155 mg, 1.02 mmol, 2.6 equiv). Allyl ester **2.48** (182 mg, 0.40 mmol) and dimethoxy aryne precursor **2.44** (177 mg, 0.49 mmol, 1.2 equiv) were added sequentially in MeCN (2.5 mL total) The vial was sealed and

heated to 80 °C for 1.5 h, at which time it was cooled to rt and quenched with brine. The layers were separated and the aqueous layer was extracted with EtOAc. The combined organic layer was dried ($MgSO_4$) and solvent removed to give the crude mixture. Column chromatography (9:1 hexanes/EtOAc) delivered the title compound (**2.49**) as an oil (120.4 mg, 0.20 mmol, 50%). **R_f:** 0.26 (9:1 hexanes/EtOAc, UV, anisaldehyde stain). **^{1}H NMR** (500 MHz, $CDCl_3$) δ 6.34 (d, *J* = 2.1 Hz, 1H), 6.23 (d, *J* = 2.0 Hz, 1H), 5.90 (ddt, *J* = 17.2, 10.5, 5.7 Hz, 1H), 5.29 (dq, *J* = 17.2, 1.5 Hz, 1H), 5.21 (dq, *J* = 10.5, 1.3 Hz, 1H), 4.74 – 4.57 (m, 3H), 4.15 (dd, *J* = 12.0, 6.3 Hz, 1H), 3.77 (s, 3H), 3.71 (s, 3H), 3.59 (s, 3H), 3.48 – 3.38 (m, 2H), 3.35 (s, 3H), 2.78 – 2.69 (m, 1H), 2.10 (td, *J* = 12.4, 6.3 Hz, 1H), 2.05 – 1.95 (m, 1H), 1.89 (td, *J* = 12.4, 6.8 Hz, 1H), 1.66 – 1.29 (m, 4H), 0.78 (s, 9H), -0.00 (s, 3H), -0.03 (s, 3H). **^{13}C NMR** (126 MHz, $CDCl_3$) δ 200.0, 173.1, 168.5, 162.3, 156.8, 137.6, 132.0, 119.5, 118.3, 101.4, 97.2, 78.0, 68.3, 65.3, 64.8, 57.9, 55.8, 55.3, 52.6, 45.5, 40.7, 34.7, 26.9, 25.7, 24.7, 18.1, 18.0, -5.4, -5.5. **IR** could not be obtained. **HRMS** (ESI) calcd for $[C_{31}H_{46}O_9{}^7Li_1{}^{28}Si_1]^+$ ($[M+Li]^+$): *m/z* 597.3066, found 597.3066.

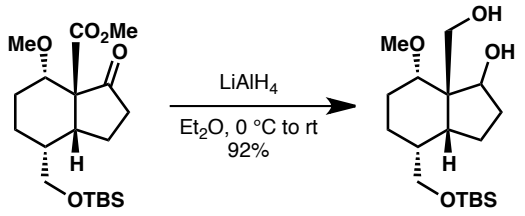

2.41 **2.57**

(3a*R*,4*R*,7*S*,7a*R*)-4-(((*tert*-Butyldimethylsilyl)oxy)methyl)-7a-(hydroxymethyl)-7-methoxyoctahydro-1*H*-inden-1-ol (2.57). To a cooled (0 °C) solution of ketoester **2.41** (7.0435 g, 19.0 mmol) in dry Et_2O (200 ml) was added $LiAlH_4$ (2.8935 g, 76.2 mmol, 4 equiv) with vigorous stirring. The ice bath was allowed to gradually expire. After the reaction was complete by TLC analysis (approx. 3 h), the mixture was cooled to 0 °C and quenched by sequential addition of H_2O (2.9 mL), 10% NaOH (2.9 mL), and H_2O (8.7 mL). The resulting mixture was stirred vigorously and allowed to warm to room temperature. After the resulting solids had turned white, the mixture was filtered and the solid washed with Et_2O. The organic layer was dried ($NaSO_4$) and concentrated to give diol **2.57** a white solid (6.0555 g, 92%). **R_f:** 0.19 (2:1 hexanes/EtOAc, anisaldehyde stain). **mp:** 67.1–67.7 °C. **^{1}H NMR** (400 MHz, $CDCl_3$) δ 4.15 (td, *J* = 10.8, 6.7 Hz, 1H), 3.81 (t, *J* = 3.0 Hz, 1H), 3.72 (t, *J* = 9.1 Hz, 1H), 3.44 – 3.37 (m, 3H), 3.31 (s, 3H), 2.77 (d, *J* = 11.4 Hz, 1H), 2.40 (d, *J* = 7.7 Hz, 1H), 2.20 – 2.05 (m, 2H), 1.86 – 1.29 (m, 8H), 0.88 (s, 9H), 0.02 (s, 6H). **^{13}C NMR** (101 MHz, $CDCl_3$) δ 81.8, 76.8, 68.9, 66.3, 55.5, 50.6, 39.9, 37.9, 34.0, 25.8, 23.0, 22.0, 18.2, 17.6, -5.47, -5.50. **IR** (thin film) $\tilde{\nu}_{max}$ cm^{-1} 3418.1 (broad, O–H), 2929.2, 2890.6, 2854.7, 1470.9, 1254.6, 1084.5, 835.8, 774.7. **HRMS** (ESI) calcd for $[C_{18}H_{37}O_4Si]^+$ ($[M+H]^+$): *m/z* 345.2456, found 345.2454.

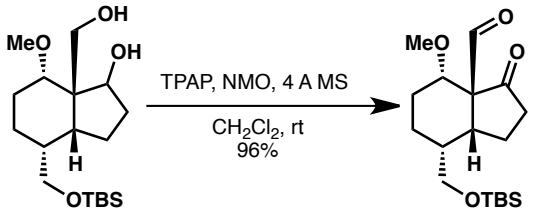

2.57 **2.56**

(3a*R*,4*S*,7*R*,7a*R*)-7-(((*tert*-Butyldimethylsilyl)oxy)methyl)-4-methoxy-3-oxooctahydro-1*H*-indene-3a-carbaldehyde (2.56). To a flame-dried flask equipped with a stir bar was added diol **2.57** (6.0555 g, 17.6 mmol) in dry CH_2Cl_2 (300 mL), followed by *N*-methylmorpholine oxide (7.3140 g, 62.4 mmol, 3.5 equiv) and molecular sieves (4 Å, 8.9357 g, 0.5 g/mmol). This mixture was stirred at room temperature for 15 min. TPAP was then added (310 mg, 0.05 equiv) and the mixture was stirred for 2 h. The reaction mixture was passed through SiO_2 and eluted with EtOAc. The resulting solution was concentrated to give a ketoaldehyde **2.56** as a yellow oil (5.7700 g, 96%). **R_f:** 0.61 (2:1 hexanes/EtOAc, anisaldehyde stain). **^{1}H NMR** (400 MHz, $CDCl_3$) δ 9.45 (s, 1H), 4.02 (t, *J* = 2.7 Hz, 1H), 3.61 – 3.50 (m, 2H), 3.21 (s, 3H), 2.86 (dt, *J* = 12.4, 6.1 Hz, 1H), 2.46 – 2.36 (m, 1H), 2.17 (ddd, *J* = 18.9, 10.7, 8.7 Hz, 1H), 2.10 – 1.98 (m, 1H), 1.91 – 1.77 (m, 2H), 1.48 – 1.31 (m, 2H), 1.31 – 1.22 (m, 1H), 1.22 – 1.11 (m, 1H), 0.90 (s, 9H), 0.06 (s, 6H). **^{13}C NMR** (101 MHz, $CDCl_3$) δ 214.5, 198.4, 77.0, 68.5, 65.3, 57.1, 39.4, 38.1, 38.0, 25.8, 25.1, 20.2, 18.2, 16.8, -5.4, -5.5. **IR** (thin film) $\tilde{\nu}_{max}$ cm^{-1} 2930 (broad), 2712 (aldehyde C-H), 1751, 1716, 1463, 1093 (broad), 838, 776. **HRMS** (ESI) calcd for $[C_{18}H_{32}O_4SiNa]^+$ ($[M+Na]^+$): *m/z* 363.1962, found 363.1964.

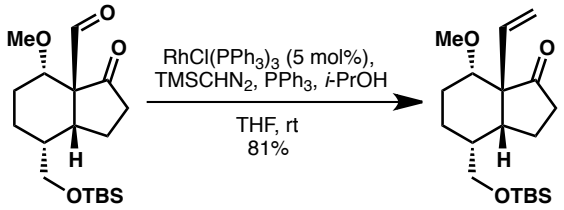

2.56 **2.54**

(3a*R*,4*R*,7*S*,7a*R*)-4-(((*tert*-Butyldimethylsilyl)oxy)methyl)-7-methoxy-7a-vinyloctahydro-1*H*-inden-1-one (2.54). To ketoaldehyde **2.56** (3.5 g, 10.3 mmol) in dry THF (120 mL) was added sequentially PPh_3 (4.15 g, 15.8 mmol, 1.5 equiv), dry *iso*-propanol (1.2 mL, 15.5 mmol, 1.5 equiv), trimethylsilyldiazomethane (10.3 mL, 20.6 mmol, 2 equiv), and $RhCl(PPh_3)_3$ (0.515 g, 0.54 mmol, 0.05 equiv). The reaction was stirred at room temperature. When the reaction was complete by TLC analysis (approx. 6 h), it was quenched by the addition of 10% H_2O_2 (10 mL). The mixture was then extracted with CH_2Cl_2 and the combined organic layer was washed with water, then brine, and concentrated to give a white-orange solid. Purification by flash chromatography (30:1 hexanes/EtOAc) provided vinyl ketone **2.54** as a white solid (3.49 g, 81%). **R_f:** 0.49 (9:1 hexanes/EtOAc, anisaldehyde stain). **mp:** 34.6 – 35.1 °C. **^{1}H NMR** (500 MHz, $CDCl_3$) δ 5.81 (dd, *J* = 17.6, 11.0 Hz, 1H), 5.22 – 5.13 (m, 2H), 3.54 (ddd, *J* = 25.9, 9.6, 7.0 Hz, 2H), 3.47 (s, 1H), 3.15 (s, 3H), 2.51 (dt, *J* = 12.2, 6.1 Hz, 1H), 2.38 – 2.28 (m, 1H), 2.13 – 1.84 (m, 4H), 1.73 (dt, *J* = 10.5, 7.0 Hz, 1H), 1.48 – 1.28 (m, 3H), 0.89 (s, 9H), 0.05 (s, 6H). **^{13}C NMR** (126 MHz, $CDCl_3$) δ 220.3, 138.4, 115.8, 82.0, 65.8, 57.5, 57.0, 40.4, 38.7, 37.7, 25.9, 23.7, 20.1, 18.3, 17.5, -5.35, -5.44. **IR** (thin film) $\tilde{\nu}_{max}$ cm^{-1} 2953, 2930, 2893, 2857, 1743 (carbonyl), 1636 (C=C), 1093, 838. **HRMS** (ESI) calcd for $[C_{19}H_{35}O_3Si]^+$ ($[M+H]^+$): *m/z* 339.2350, found 339.2355.

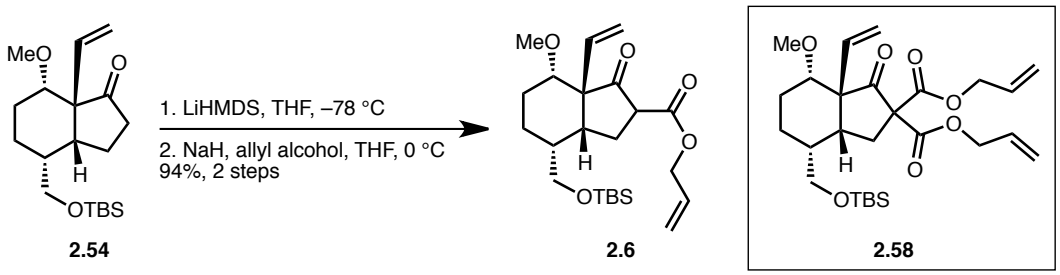

2.54 **2.6** **2.58**

(3a*R*,4*R*,7*S*,7a*R*)-Allyl 4-(((*tert*-butyldimethylsilyl)oxy)methyl)-7-methoxy-1-oxo-7a-vinyloctahydro-1*H*-indene-2-carboxylate (2.6). A solution of **2.54** (3.69 g, 10.9 mmol) in THF (36 mL) was cooled to –78 °C. KHMDS (22.5 mL, 1 M in THF, 2.1 equiv) was added slowly, and the resulting solution was stirred for 1 h. Allyl cyanoformate (3.4 mL, 33.0 mmol, 3 equiv) was added and the reaction mixture was stirred at –78 °C for 3 h. The reaction was quenched by the addition of saturated $NH_4Cl_{(aq)}$, and the aqueous layer was extracted with EtOAc. The combined organic layer was washed with brine, dried (Na_2SO_4), and solvent removed to give a mixture of the mono and diester products. Column chromatography (20:1 hexanes/EtOAc) gave **2.54** (2.37 g) and **2.58** (2.39 g). A solution of sodium allyl alkoxide was prepared by the addition of NaH (229 mg, 5.7 mmol, 1.2 equiv) to a solution of allyl alcohol (0.385 mL, 5.7 mmol, 1.2 equiv) in THF (14 mL) at 0 °C. Diester **2.58** (2.39 g, 4.7 mmol) in THF (10 mL) was added to the alkoxide solution at 0 °C. The reaction mixture was stirred for 30 min, at which time it was complete by TLC analysis. The reaction was quenched with $NH_4Cl_{(aq)}$ and the aqueous layer was extracted with EtOAc. The combined organic layer was washed with brine, dried (Na_2SO_4), and the solvent removed. The crude β-ketoester was filtered through SiO_2 and combined with the previous material to give pure **2.54** as a colorless oil (4.36 g, 10.3 mmol, 94%, 2 steps). **R_f:** 0.37 (9:1 hexanes/EtOAc, UV, anisaldehyde stain). **^{1}H NMR** (500 MHz, $CDCl_3$) δ 5.99 – 5.74 (m, 2H), 5.42 – 5.16 (m, 4H), 4.75 – 4.60 (m, 1H), 4.60 – 4.54 (m, 1H), 3.63 – 3.48 (m, 3H), 3.36 (dt, *J* = 9.6, 1.0 Hz, 0.5H), 3.15 (s, 2H), 3.08 (s, 1H), 2.84 (dt, *J* = 12.8, 6.4 Hz, 0.5H), 2.61 – 2.44 (m, 1H), 2.29 (td, *J* = 12.7, 9.6 Hz, 0.5H), 2.07 – 1.85 (m, 3H), 1.53 – 1.31 (m, 3H), 0.90 (s, 3.5H), 0.89 (s, 5H), 0.06 (s, 6H). **^{13}C NMR** (101 MHz, $CDCl_3$) δ 213.0, 211.1, 169.4, 167.6, 137.6, 137.5, 132.1, 131.7, 118.2, 117.1, 116.6, 116.4, 82.4, 81.6, 65.7, 65.6, 65.50, 65.46, 58.2, 57.5, 57.0, 56.8, 54.8, 39.2, 37.51, 37.45, 25.9, 25.0, 23.9, 23.7, 23.6, 18.22, 18.20, 17.4, 17.0, -5.37, -5.43, -5.45. **IR** (thin film) $\tilde{\nu}_{max}$ cm^{-1} 3086, 2891, 2859, 2739, 1755, 1736, 1649, 1638. **HRMS** (ESI) calcd for $[C_{23}H_{39}O_5Si]^+$ ($[M+H]^+$): *m/z* 423.2561, found 423.2558.

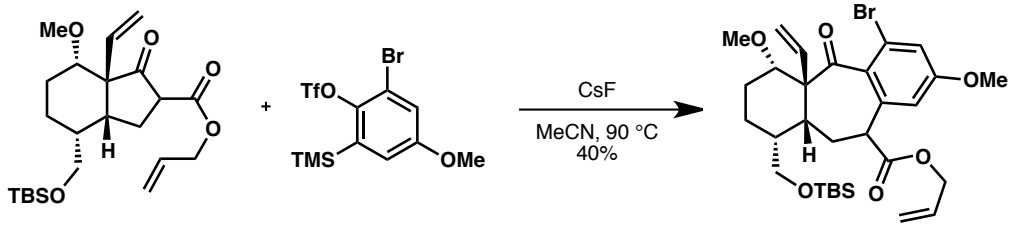

2.6 **2.47** **2.59**

(1*R*,4*S*,4a*R*,11a*R*)-Allyl 6-bromo-1-(((*tert*-butyldimethylsilyl)oxy)methyl)-4,8-dimethoxy-5-oxo-4a-vinyl-2,3,4,4a,5,10,11,11a-octahydro-1*H*-dibenzo[*a*,*d*][7]annulene-10-carboxylate (2.59). To a flame dried Schlenk flask with a stir bar was added CsF (820.0 mg, 5.40 mmol, 3 equiv), followed by β-ketoester **2.6** (778.3 mg, 1.84 mmol) in MeCN (5 mL) then aryne precursor **2.47** (1.5004 g, 3.68 mmol, 2 equiv) in MeCN (5 mL). The flask was sealed and the

reaction mixture heated to 80 °C. Over time the mixture turned brown. After the reaction was complete by NMR analysis (approx. 2 h) the mixture was cooled to room temperature and quenched by the addition of brine (30 mL). Upon separation of the layers, the aqueous layer was extracted with EtOAc, washed one time with brine, dried, and concentrated to give a brown foam. Purification by column chromatography (9:1 hexanes/EtOAc) yielded tricycle **2.59** as a white foam (502.0 mg, 40%). **R_f:** 0.60 (4:1 hexanes/EtOAc, UV, anisaldehyde stain). **mp:** 128-130 °C. **^{1}H NMR** (500 MHz, $CDCl_3$) δ 6.97 (d, *J* = 2.3 Hz, 1H), 6.61 (d, *J* = 2.4 Hz, 1H), 5.89 (ddt, *J* = 17.2, 10.4, 5.7 Hz, 1H), 5.38 (dd, *J* = 8.9, 3.1 Hz, 2H), 5.29 (dd, *J* = 17.2, 1.5 Hz, 1H), 5.22 (dd, *J* = 10.4, 1.3 Hz, 1H), 5.15 – 5.06 (m, 1H), 4.71 – 4.58 (m, 2H), 4.27 – 4.19 (m, 2H), 3.77 (s, 3H), 3.41 (d, *J* = 7.0 Hz, 2H), 3.37 (s, 3H), 2.21 – 2.13 (m, 2H), 2.01 (dq, *J* = 11.5, 4.0 Hz, 1H), 1.98 – 1.88 (m, 2H), 1.54 – 1.35 (m, 2H), 1.30 – 1.23 (m, 1H), 0.77 (s, 9H), 0.02 (s, 3H), -0.02 (s, 3H). **^{13}C NMR** (151 MHz, $CDCl_3$) δ 202.2, 172.8, 160.8, 138.6, 136.60, 131.8, 130.6, 120.0, 119.7, 118.4, 116.7, 110.1, 80.3, 65.3, 64.4, 61.1, 57.7, 55.4, 45.9, 37.6, 34.6, 27.6, 25.7, 23.4, 18.2, 18.0, -5.5, -5.6. **IR** (thin film) $\tilde{\nu}_{max}$ cm^{-1} 2930, 2856, 1738, 1697, 1599, 1090, 836, 776. **HRMS** (ESI) calcd for $[C_{30}H_{44}BrO_6Si]^+$ ($[M+H]^+$): *m/z* 607.2085, found 607.2090.

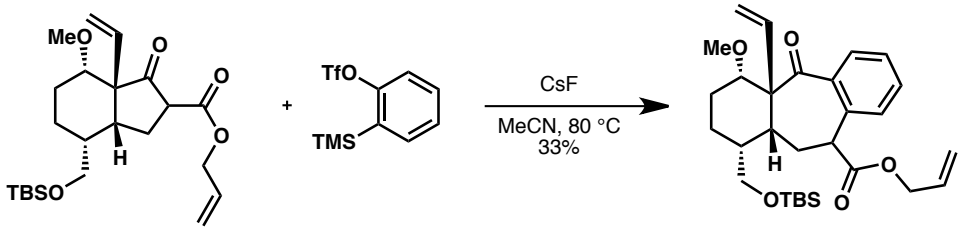

2.6 **2.13** **2.61**

General procedure for aryne insertion with 2.6.

(1*R*,4*S*,4a*R*,11a*R*)-Allyl 1-(((*tert*-butyldimethylsilyl)oxy)methyl)-4-methoxy-5-oxo-4a-vinyl-2,3,4,4a,5,10,11,11a-octahydro-1*H*-dibenzo[*a*,*d*][7]annulene-10-carboxylate (2.61). Ketoester **2.6** (50 mg, 0.12 mmol) was taken up in MeCN (0.6 mL). CsF (46 mg, 0.30 mmol, 2.5 equiv) was added, followed by triflate **2.13** (0.036 mL, 0.15 mmol, 1.25 equiv). The vial was sealed and heated to 80 °C overnight. The reaction was quenched with brine, extracted with EtOAc, dried (Mg_2SO_4), and the solvent removed. Column chromatography (3 → 5% EtOAc in hexanes) gave the title compound (**2.61**) as a foam (20 mg, 0.04 mmol, 33%). **^{1}H NMR** (400 MHz, $CDCl_3$) δ 7.39 – 6.98 (m, 4H), 5.91 (ddt, *J* = 16.3, 10.7, 5.6 Hz, 1H), 5.48 (dd, *J* = 17.5, 10.9 Hz, 1H), 5.35 – 5.17 (m, 3H), 5.01 (d, *J* = 17.5 Hz, 1H), 4.74 – 4.59 (m, 1H), 4.27 (dd, *J* = 12.0, 6.3 Hz, 1H), 4.22 (s, 1H), 3.46 – 3.39 (m, 2H), 3.37 (s, 3H), 2.28 – 2.16 (m, 1H), 2.15 – 1.89 (m, 4H), 1.53 – 1.23 (m, 4H), 0.75 (s, 9H), 0.00 (s, 3H), -0.03 (s, 3H). **^{13}C NMR** (126 MHz, $CDCl_3$) δ 208.5, 173.3, 138.8, 138.6, 134.8, 132.0, 130.3, 128.4, 126.8, 124.2, 118.4, 118.3, 80.7, 65.3, 64.6, 60.4, 57.5, 45.5, 37.6, 34.8, 27.6, 25.8, 23.5, 18.2, 18.0, -5.4, -5.6. **IR** (thin film) $\tilde{\nu}_{max}$ cm^{-1} 2954, 2925, 2852, 1740, 1691, 1250, 1099. **HRMS** (ESI) calcd for $[C_{29}H_{43}O_5{}^{28}Si_1]^+$ ($[M+H]^+$): *m/z* 499.2874, found 499.2883.

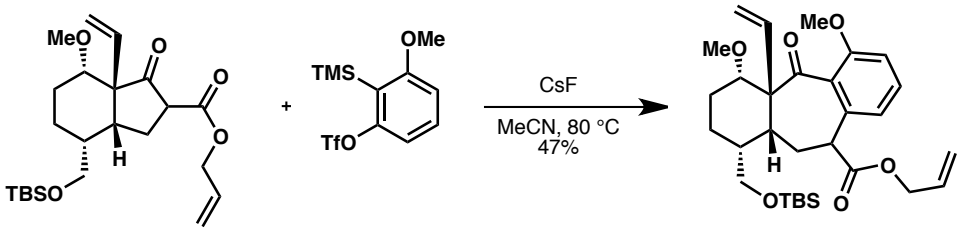

2.6 2.S7 2.62

(1*R*,4*S*,4a*R*,11a*R*)-Allyl 1-(((*tert*-butyldimethylsilyl)oxy)methyl)-4,6-dimethoxy-5-oxo-4a-vinyl-2,3,4,4a,5,10,11,11a-octahydro-1*H*-dibenzo[*a*,*d*][7]annulene-10-carboxylate (2.62). Prepared according to the above general procedure to give **2.62** as a foam (30 mg, 0.06 mmol, 47%). **^{1}H NMR** (500 MHz, $CDCl_3$) δ 7.26 (d, *J* = 16.0 Hz, 1H), 6.82 (d, *J* = 8.9 Hz, 1H), 6.77 (d, *J* = 7.7 Hz, 1H), 5.83 (ddt, *J* = 17.3, 10.5, 5.3 Hz, 1H), 5.41 (dd, *J* = 17.6, 10.8 Hz, 1H), 5.25 – 5.10 (m, 3H), 4.99 (d, *J* = 17.6 Hz, 1H), 4.59 – 4.42 (m, 2H), 4.01 (s, 1H), 3.97 (t, *J* = 8.8 Hz, 1H), 3.71 (s, 3H), 3.55 – 3.45 (m, 2H), 3.38 (s, 3H), 2.87 (ddd, *J* = 14.8, 10.0, 8.2 Hz, 1H), 2.34 – 2.26 (m, 1H), 2.10 – 2.01 (m, 1H), 1.98 – 1.83 (m, 2H), 1.45 – 1.30 (m, 2H), 1.23 – 1.15 (m, 1H), 0.81 (s, 9H), 0.03 (s, 3H), -0.01 (s, 3H). **^{13}C NMR** (126 MHz, $CDCl_3$) δ 199.6, 173.0, 157.0, 136.8, 136.2, 132.1, 130.3, 128.4, 122.6, 118.2, 117.2, 110.4, 80.1, 65.2, 64.7, 62.7, 57.9, 56.2, 51.1, 37.6, 35.0, 25.9, 24.4, 23.5, 18.8, 18.1, -5.46, -5.48. **IR** (thin film) $\tilde{\nu}_{max}$ cm^{-1} 2925, 2860, 1724, 1699, 1601, 1589, 1474, 1254, 1221, 1099. **HRMS** (ESI) calcd for $[C_{30}H_{45}O_6{}^{28}Si_1]^+$ ($[M+H]^+$): *m/z* 529.2980, found 529.2983.

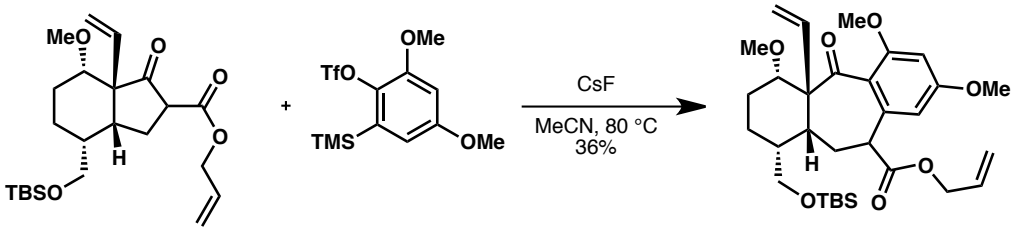

2.6 2.44 2.63

(1*R*,4*S*,4a*R*,11a*R*)-Allyl 1-(((*tert*-butyldimethylsilyl)oxy)methyl)-4,6,8-trimethoxy-5-oxo-4a-vinyl-2,3,4,4a,5,10,11,11a-octahydro-1*H*-dibenzo[*a*,*d*][7]annulene-10-carboxylate (2.63). A flame-dried vial was charged with dry CsF (20.4 mg, 0.13 mmol, 2.2 equiv). Allyl ester **2.6** (27.4 mg, 0.06 mmol) and dimethoxy aryne precursor **2.44** (31.3, 0.09 mmol, 1.5 equiv) were added sequentially in MeCN (0.3 mL total) The vial was sealed and heated to 80 °C for 2 h, at which time it was cooled to rt and quenched with brine. The layers were separated and the aqueous layer was extracted with EtOAc. The combined organic layer was dried ($MgSO_4$) and solvent removed to give the crude mixture. Column chromatography (20:1 hexanes/EtOAc) delivered the title compound (**2.63**) as an oil (12.9 mg, 0.023 mmol, 36%). **R_f:** 0.42 (9:1 hexanes/EtOAc, UV, anisaldehyde stain). **^{1}H NMR** (600 MHz, $CDCl_3$) δ 6.34 (d, *J* = 2.1 Hz, 1H), 6.23 (d, *J* = 2.1 Hz, 1H), 5.90 (ddt, *J* = 16.5, 10.9, 5.7 Hz, 1H), 5.40 (dd, *J* = 17.6, 10.8 Hz, 1H), 5.33 – 5.18 (m, 3H), 4.98 (d, *J* = 17.6 Hz, 1H), 4.65 (ddd, *J* = 53.7, 13.3, 5.5 Hz, 2H), 4.22 – 4.16 (m, 2H), 3.76 (s, 3H), 3.68 (s, 3H), 3.41 (d, *J* = 7.7 Hz, 2H), 3.36 (s, 3H), 2.18 – 2.09 (m, 2H), 2.03 – 1.87 (m, 3H), 1.51 – 1.35 (m, 2H), 1.31 – 1.23 (m, 1H), 0.78 (s, 9H), 0.01 (s, 3H), -0.02 (s, 3H). **^{13}C NMR** (151 MHz, $CDCl_3$) δ 202.9, 173.4, 161.9, 156.7, 137.8, 137.5, 132.1, 119.7, 118.2, 118.0, 101.4, 97.4, 80.4, 65.2, 64.8, 61.0, 57.7, 55.9, 55.3, 45.6, 37.8, 34.9, 27.5, 25.8, 23.7, 18.4, 18.1, -5.4, -5.5. **IR** (thin film) $\tilde{\nu}_{max}$ cm^{-1} 2931, 2856, 1736, 1697, 1603, 1586, 1462, 1157, 1091, 836. **HRMS** (ESI) calcd for $[C_{31}H_{47}O_7{}^{28}Si_1]^+$ ($[M+H]^+$): *m/z* 559.3086, found 559.3091.

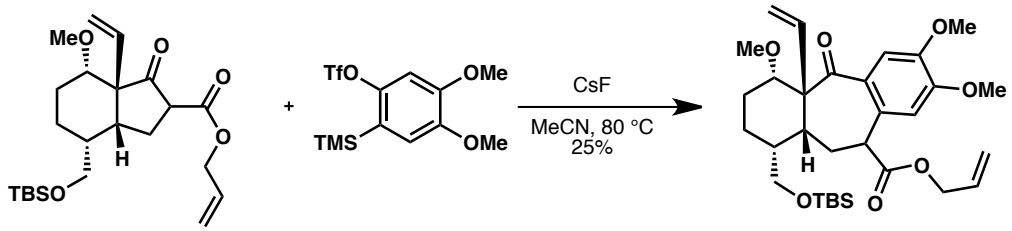

2.6 2.S8 2.64

(1*R*,4*S*,4a*R*,11a*R*)-Allyl 1-(((*tert*-butyldimethylsilyl)oxy)methyl)-4,7,8-trimethoxy-5-oxo-4a-vinyl-2,3,4,4a,5,10,11,11a-octahydro-1*H*-dibenzo[*a*,*d*][7]annulene-10-carboxylate (2.64). Prepared according to the above general procedure to give **2.64** as a foam (20 mg, 0.04 mmol, 25%). **^{1}H NMR** (400 MHz, $CDCl_3$) δ 6.62 (s, 1H), 6.58 (s, 1H), 5.92 (ddt, *J* = 16.2, 10.8, 5.5 Hz, 1H), 5.49 (dd, *J* = 17.6, 10.8 Hz, 1H), 5.36 – 5.18 (m, 3H), 5.01 (d, *J* = 17.6 Hz, 1H), 4.80 – 4.55 (m, 2H), 4.32 – 4.20 (m, 2H), 3.83 (s, 3H), 3.83 (s, 3H), 3.42 (d, *J* = 7.6 Hz, 2H), 3.36 (s, 3H), 2.22 – 2.12 (m, 2H), 2.07 – 1.91 (m, 3H), 1.50 – 1.37 (m, 3H), 0.78 (s, 9H), 0.02 (s, 3H), -0.02 (s, 3H). **^{13}C NMR** (126 MHz, $CDCl_3$) δ 208.2, 173.7, 150.3, 147.4, 139.5, 132.0, 130.8, 127.8, 118.4, 118.0, 110.6, 107.7, 80.8, 65.2, 64.7, 60.6, 57.5, 56.1, 55.8, 45.1, 37.6, 34.9, 27.7, 25.8, 23.5, 18.3, 18.1, -5.4, -5.6. **IR** (thin film) $\tilde{\nu}_{max}$ cm^{-1} 2925, 2847, 1737, 1729, 1691, 1605, 1507, 1462, 1286, 1204. **HRMS** (ESI) calcd for $[C_{31}H_{47}O_7{}^{28}Si_1]^+$ ($[M+H]^+$): *m/z* 559.3086, found 559.3091.

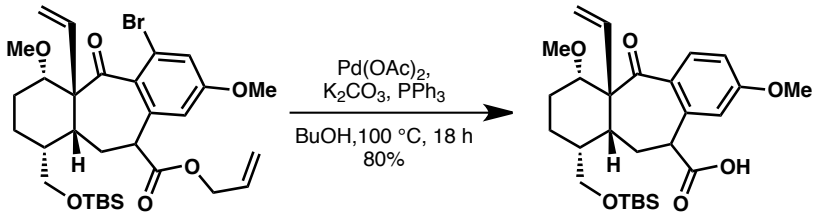

2.59 2.66

(1*R*,4*S*,4a*R*,11a*R*)-1-(((*tert*-Butyldimethylsilyl)oxy)methyl)-4,8-dimethoxy-5-oxo-4a-vinyl-2,3,4,4a,5,10,11,11a-octahydro-1*H*-dibenzo[*a*,*d*][7]annulene-10-carboxylic acid (2.66). *n*-BuOH (2 mL) was added to aryl bromide **2.59** (105.5 mg, 0.17 mmol) in a vial with a stir bar. The solution was warmed slightly with stirring to dissolve **2.59**. K_2CO_3 (45.0 mg, 0.33 mmol, 1.9 equiv), $Pd(OAc)_2$ (3.5 mg, 0.02 mmol, 0.1 equiv), and PPh_3 (16.0 mg, 0.06 mmol, 0.4 equiv) were added sequentially. The reaction mixture was then sealed under N_2 heated to 100 °C. After 18 h, the reaction mixture was cooled to rt, diluted with EtOAc (10 mL), filtered through Celite, and the solvent removed to give the crude product. Column chromatography (2:1 EtOAc, then 9:1 CH_2Cl_2/MeOH) provided the title compound (**2.66**) as a powder (68.2 mg, 0.14 mmol, 80%). **R_f:** 0.40 (2:1 hexanes/EtOAc, UV, anisaldehyde stain). **^{1}H NMR** (500 MHz, $CDCl_3$) δ 6.99 (d, *J* = 8.9 Hz, 1H), 6.79 – 6.71 (m, 2H), 5.48 (dd, *J* = 17.6, 10.8 Hz, 1H), 5.23 (d, *J* = 10.8 Hz, 1H), 4.99 (d, *J* = 17.6 Hz, 1H), 4.32 (dd, *J* = 11.9, 6.2 Hz, 1H), 4.22 (s, 1H), 3.80 (s, 3H), 3.42 (d, *J* = 7.5 Hz, 2H), 3.37 (s, 3H), 2.25 (td, *J* = 12.1, 6.4 Hz, 1H), 2.16 – 2.08 (m, 1H), 2.06 – 1.90 (m, 3H), 1.53 – 1.37 (m, 2H), 1.31 – 1.23 (m, 1H), 0.76 (s, 9H), 0.00 (s, 3H), -0.03 (s, 3H), carboxylic acid H not observed. **^{13}C NMR** (151 MHz, $CDCl_3$) δ 208.2, 178.5, 161.3, 139.3, 136.2, 131.5, 128.5, 117.9, 111.4, 110.8, 80.8, 64.6, 60.6, 57.5, 55.3, 45.5, 37.6, 34.8, 27.7, 25.7, 23.5, 18.2, 18.0, -5.4, -5.6. **IR** (thin film) $\tilde{\nu}_{max}$ cm^{-1} 3100 (br), 2930, 2856, 1710, 1692, 1604, 1254, 1089, 837. **HRMS** (ESI) calcd for $[C_{27}H_{41}O_6{}^{28}Si_1]^+$ ($[M+H]^+$): *m/z* 489.2667, found 489.2680.

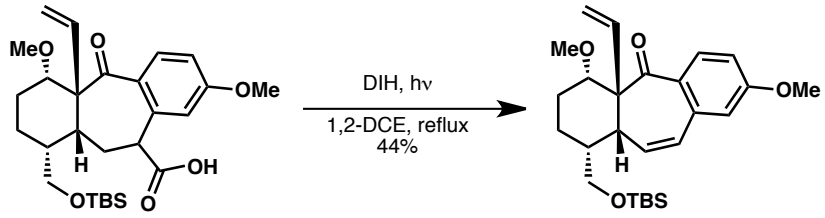

2.66 **2.67**

(1*R*,4*S*,4a*R*,11a*R*)-1-(((*tert*-Butyldimethylsilyl)oxy)methyl)-4,8-dimethoxy-4a-vinyl-2,3,4,4a-tetrahydro-1*H*-dibenzo[*a*,*d*][7]annulen-5(11a*H*)-one (2.67). Acid **2.66** (14.7 mg, 0.03 mmol) was taken up in 1,2-dichloroethane (0.70 mL) in a reaction tube with a stir bar. 1,3-Diiodo-5,5-dimethylhydantoin (18.3 mg, 0.08 mmol, 2.7 equiv) was added, and the tube was evacuated and backfilled with nitrogen (2x). The reaction mixture was then placed in front of a 600 W tungsten-filament lamp at a distance of ~0.2 m such that the reaction mixture was also heated by the lamp to reflux. After stirring for 3 h, the reaction mixture was removed from in front of the light, cooled to rt, and quenched by the addition of 1 M $NaHSO_{3(aq)}$. The layers were separated and the organic layer was extracted with CH_2Cl_2 (3 x 3 mL). The combined organic layer was washed with brine, dried (Na_2SO_4), and solvent removed to give the crude enone. Column chromatography (9:1 hexanes/EtOAc) provided title compound (**2.67**) as a yellow oil (5.2 mg, 0.012 mmol, 44%). **R_f:** 0.30 (9:1 hexanes/EtOAc, UV, and anisaldehyde stain). **^{1}H NMR** (600 MHz, $CDCl_3$) δ 7.23 (d, *J* = 8.5 Hz, 1H), 6.74 (dd, *J* = 8.5, 2.4 Hz, 1H), 6.54 (d, *J* = 2.4 Hz, 1H), 6.33 (d, *J* = 10.7 Hz, 1H), 6.09 (dd, *J* = 10.7, 6.0 Hz, 1H), 5.60 (dd, *J* = 17.7, 10.8 Hz, 1H), 5.27 (d, *J* = 10.8 Hz, 1H), 5.23 (d, *J* = 17.4 Hz, 1H), 4.07 (s, 1H), 3.81 (s, 3H), 3.51 (q, *J* = 8.1 Hz, 2H), 3.27 (s, 3H), 3.26 – 3.23 (m, 1H), 2.07 – 1.99 (m, 1H), 1.95 (d, *J* = 12.7 Hz, 1H), 1.54 – 1.40 (m, 3H), 0.82 (s, 9H), 0.01 (s, 3H), -0.01 (s, 3H). **^{13}C NMR** could not be obtained. **IR** could not be obtained. **HRMS** (ESI) calcd for $[C_{26}H_{38}O_4Si_1]^+$ ($[M+H]^+$): *m/z* 443.2612, found 443.2619.

2.54 **2.68**

2-(((3a*R*,4*R*,7*S*,7a*R*)-7-Methoxy-1-oxo-7a-vinyloctahydro-1*H*-inden-4-yl)methyl)isoindoline-1,3-dione (2.68). Vinyl ketone **2.54** (1.0048 g, 2.95 mmol) was taken up in 1% HCl/MeOH (15 mL) at room temperature in a 25 mL round bottom flask with a stir bar. After 20 min, the reaction mixture was poured onto 10 mL saturated $NaHCO_{3(aq)}$, and diluted with EtOAc (30 mL). The layers were separated, and the aqueous layer was extracted with EtOAc (3x, 30 mL). The combined organic layer was washed once with brine, dried (Na_2SO_4), filtered, and concentrated to give the primary alcohol as a colorless oil, which was taken forward directly. The alcohol was dissolved in THF (150 mL) in a 250 mL round bottom flask equipped with a stir bar and cooled to 0 °C. PPh_3 (1.56 g, 5.90 mmol, 2 equiv), diisopropylazodicarboxylate (1.16 mL, 5.90 mmol, 2 equiv), and phthalimide (870.1 mg, 5.91 mmol, 2 equiv) were added sequentially, and the yellow reaction mixture was stirred at that

temperature. After 1 h, the reaction mixture was poured onto 100 mL saturated $NaHCO_{3(aq)}$. The layers were separated, and the aqueous layer was extracted with EtOAc (2x, 50 mL). The combined organic layer was washed with brine, dried ($MgSO_4$), filtered, and concentrated to give a yellow oil with a white solid. Column chromatography (9:1 hexanes/EtOAc to 4:1 hexanes/EtOAc) resulted in the product contaminated with phthalimide. These fractions were washed with 1M NaOH once, dried, and concentrated to give the desired hydrindanone product (**2.68**) as a white solid (quant., 2 steps). **R_f:** 0.41 (2:1 hexanes/EtOAc, UV and anisaldehyde stain). **mp:** 159–163 °C. **^{1}H NMR** (500 MHz, $CDCl_3$) δ 7.86 (dd, *J* = 5.4, 3.1 Hz, 2H), 7.73 (dd, *J* = 5.4, 3.0 Hz, 2H), 5.79 (dd, *J* = 17.7, 11.0 Hz, 1H), 5.18 (d, *J* = 11.0 Hz, 1 H), 5.14 (d, *J* = 17.7 Hz, 1 H), 3.75 (dd, *J* = 13.5, 6.4 Hz, 1H), 3.66 (dd, *J* = 13.5, 8.3 Hz, 1H), 3.45 (t, *J* = 2.5 Hz, 1H), 3.16 (s, 3H), 2.45 –2.31 (m, 2H), 2.25 – 2.03 (m, 2H), 1.98 – 1.84 (m, 2H), 1.71 – 1.57 (m, 2H), 1.37 – 1.26 (m, 2H). **^{13}C NMR** (126 MHz, $CDCl_3$) δ 219.6, 168.6, 137.7, 134.0, 131.9, 123.2, 116.2, 81.3, 57.6, 56.9, 41.8, 41.3, 38.6, 34.4, 23.5, 20.2, 18.7. **IR** (thin film) $\tilde{\nu}_{max}$ cm^{-1} 2937, 1771, 1739, 1713, 1399, 1368. **HRMS** (ESI) calcd for $[C_{21}H_{24}NO_4]^+$ ($[M+H]^+$): *m/z* 354.1700, found 354.1699.

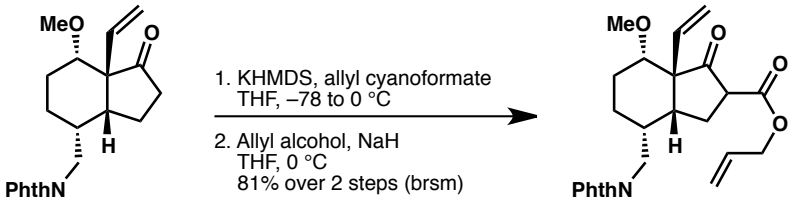

2.68 **2.69**

(3a*R*,4*R*,7*S*,7a*R*)-Allyl 4-((1,3-dioxoisoindolin-2-yl)methyl)-7-methoxy-1-oxo-7a-vinyloctahydro-1*H*-indene-2-carboxylate (2.69). Phthalimide **2.68** (600. mg, 1.70 mmol) was dissolved in THF (10 mL) in a round-bottom flask equipped with a stir bar and cooled to –78 °C. KHMDS (2.60 mL, 1 M in hexanes, 2.60 mmol, 1.5 equiv) was added slowly, and the reaction mixture was stirred at that temperature for 30 min. Neat allyl cyanoformate (0.60 mL, 5.10 mmol, 3 equiv) was then added slowly and the reaction mixture was stirred for 1 h at –78 °C and 1 h at 0 °C. When complete, the reaction was quenched by the addition of saturated $NH_4Cl_{(aq)}$. The layers were separated and the aqueous layer was extracted with EtOAc (3x). The combined organic layer was washed with brine, dried ($MgSO_4$), and solvent removed to give the crude diester as an orange oil (598.2 mg). Column chromatography (25 to 46% EtOAc in hexanes) was used to separate the diester from the starting ketone. To a separate flame-dried round-bottom flask was added a stir bar, THF (25 mL), and allyl alcohol (0.120 mL, 1.73 mmol, 1.5 equiv). The solution was cooled to 0 °C and NaH (73.5 mg, 1.84 mmol, 1.6 equiv) was added. After 10 min, the diester in THF (5 mL) was added slowly to the allyl alkoxide solution at 0 °C, which resulted in vigorous bubbling. After the bubbling had ceased and the reaction was complete by TLC and LCMS analysis, the reaction mixture was quenched with saturated $NH_4Cl_{(aq)}$ and extracted with EtOAc (3x). The organic layer was washed with brine, dried ($MgSO_4$), filtered, and concentrated to give the mono ester product (**2.69**, 523.5 mg, 1.20 mmol, 81% over 2 steps, based on recovered starting material). **R_f:** 0.12 (4:1 hexanes/EtOAc, UV and anisaldehyde stain). **mp:** 110–111°C. **^{1}H NMR** (500 MHz, $CDCl_3$) δ 7.86 (dd, *J* = 5.4, 3.1 Hz, 2H), 7.73 (dd, *J* = 5.5, 3.0 Hz, 2H), 5.95 (dd, *J* = 17.2, 10.5 Hz, 1H), 5.78 (dd, *J* = 17.7, 11.0 Hz, 1H), 5.39 (dd, *J* = 17.2, 1.5 Hz, 1H), 5.24 (dd, *J* = 10.5, 1.4 Hz, 1H), 5.20 (d, *J* = 11.0 Hz, 1H), 5.16 (d, *J* = 17.7 Hz, 1H), 4.68 (dd, *J* = 18.2, 5.6 Hz, 2H), 3.76 (d, *J* = 6.7 Hz, 1H), 3.70 (d, *J* = 7.6 Hz, 1H), 3.49

(t, *J* = 2.6 Hz, 1H), 3.16 (dd, *J* = 11.4, 8.4 Hz, 1H), 3.08 (s, 3H), 2.74 (q, *J* = 11.9 Hz, 1H), 2.36 (dt, *J* = 12.4, 5.2 Hz, 2H), 2.28 – 2.20 (m, 1H), 1.89 (dd, *J* = 14.5, 3.3 Hz, 1H), 1.80 – 1.68 (m, 1H), 1.34 (d, *J* = 12.2 Hz, 2H). **^{13}C NMR** (126 MHz, $CDCl_3$) 210.5, 168.5, 167.2, 137.0, 134.0, 132.0, 131.9, 123.3, 118.1, 116.8, 81.8, 65.5, 57.7, 56.7, 54.7, 41.7, 38.5, 34.2, 23.9, 23.6, 18.7. **IR** (thin film) $\tilde{\nu}_{max}$ cm^{-1} 3085, 2984, 2934, 2886, 1771, 1754, 1731, 1713. **HRMS** (ESI) calcd for $[C_{25}H_{28}NO_6]^+$ ($[M+H]^+$): *m/z* 438.1911, found 438.1914.

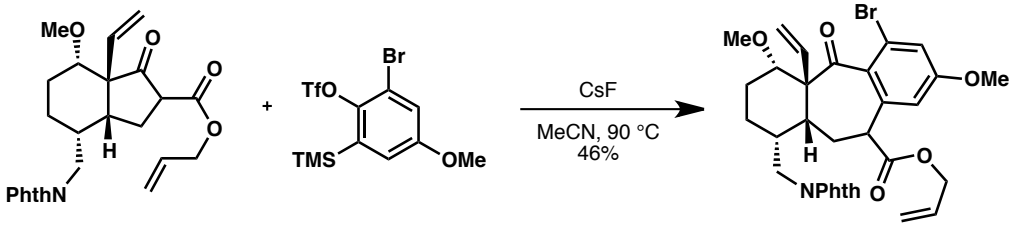

2.69 **2.47** **2.70**

(1*R*,4*S*,4a*R*,11a*R*)-Allyl 6-bromo-1-((1,3-dioxoisoindolin-2-yl)methyl)-4,8-dimethoxy-5-oxo-4a-vinyl-2,3,4,4a,5,10,11,11a-octahydro-1*H*-dibenzo[*a*,*d*][7]annulene-10-carboxylate (2.70). To dry CsF (1.8660 g, 12.3 mmol, 2.5 equiv) in a Schlenk flask equipped with a stir bar was added β-ketoester **2.69** (2.1370 g, 4.9 mmol) in MeCN (38 mL). The reaction mixture was heated to 85 °C, then a solution of aryne precursor **2.47** (3.6750 g, 9.0 mmol, 1.8 equiv) in MeCN (8 mL) was added at once. The dark brown solution was stirred at that temperature under nitrogen until consumption of the starting materials was observed by NMR analysis (approximately 2 h). After being cooled to room temperature, the reaction mixture was poured onto brine (75 mL). The layers were separated and the aqueous layer was extracted with EtOAc (3x, 50 mL). The combined organic layer was dried and concentrated to give a red-brown oil. Column chromatography (9:1 hexanes/EtOAc → 4:1 hexanes/EtOAc) provided tricycle **2.70** as a white foam (1.3894 g, 46%). **R_f:** 0.19 (4:1 hexanes/EtOAc, UV and anisaldehyde stain). **^{1}H NMR** (500 MHz, $CDCl_3$) δ 7.82 (dd, *J* = 5.4, 3.1 Hz, 2H), 7.70 (dd, *J* = 5.5, 3.0 Hz, 2H), 6.99 (d, *J* = 2.3 Hz, 1H), 6.65 (d, *J* = 2.3 Hz, 1H), 5.98 – 5.86 (m, 1H), 5.46 – 5.14 (m, 5H), 4.76 – 4.60 (m, 2H), 4.30 (dd, *J* = 11.9, 6.2 Hz, 1H), 4.20 (d, *J* = 2.7 Hz, 1H), 3.80 (s, 3H), 3.71 (dd, *J* = 13.4, 10.4 Hz, 1H), 3.42 (dd, *J* = 13.4, 3.5 Hz, 1H), 3.36 (s, 3H), 2.40 (td, *J* = 12.2, 6.3 Hz, 1H), 2.30 – 2.20 (m, 1H), 2.21 – 2.11 (m, 1H), 2.06 (td, *J* = 12.2, 6.5 Hz, 1H), 1.92 – 1.84 (m, 1H), 1.73 – 1.60 (m, 1H), 1.43 – 1.32 (m, 1H), 1.24 (d, *J* = 12.3 Hz, 1H).**^{13}C NMR** (126 MHz, $CDCl_3$) δ 201.7, 172.6, 168.4, 161.0, 138.3, 136.2, 133.9, 131.9, 131.7, 130.6, 123.2, 120.5, 119.9, 118.6, 116.8, 110.4, 79.6, 65.5, 61.3, 57.6, 55.5, 45.8, 42.0, 37.1, 35.2, 28.3, 23.1, 19.5. **IR** (thin film) $\tilde{\nu}_{max}$ cm^{-1} 3086, 2936, 2835, 2255, 1771, 1716, 1600, 1557, 912, 727, 648. **HRMS** (ESI) calcd for $[C_{32}H_{33}O_7N_1Br]^+$ ($[M+H]^+$): *m/z* 622.1435, found 622.1437.

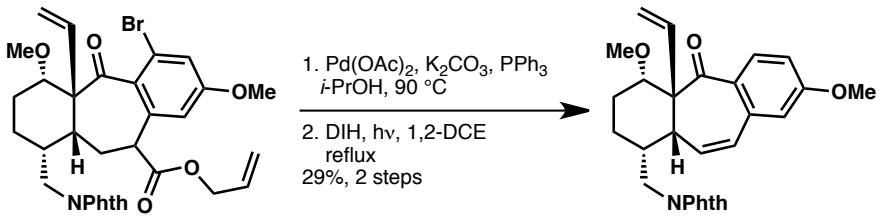

2.70 **2.71**

2-(((1*R*,4*S*,4a*R*,11a*R*)-4,8-Dimethoxy-5-oxo-4a-vinyl-2,3,4,4a,5,11a-hexahydro-1*H*-dibenzo[*a*,*d*][7]annulen-1-yl)methyl)isoindoline-1,3-dione (2.71). Tricycle **2.70** (466.2 mg,

0.75 mmol) was taken up in *i*-PrOH in an oven-dried vial w/ a stir bar. K_2CO_3 (209.3 mg, 1.50 mmol, 2.0 equiv), PPh_3 (120.1 mg, 0.46 mmol, 0.6 equiv), and $Pd(OAc)_2$ (17.0 mg, 0.08 mmol, 0.10 equiv) were added. The vial was evacuated and backfilled with N_2 twice, then sealed and heated to 90 °C. When complete by NMR analysis (approx.12 h), the reaction mixture was filtered through Celite and eluted with EtOAc. Column chromatography (2:1 hexanes/EtOAc then 9:1 CH_2Cl_2/MeOH) provided the acid as an orange-brown foam. The acid was then taken up in 1,2-dichloroethane (DCE, 8 mL). 1,3-Diiodo-5,5-dimethylhydantoin (544.0 mg, 2.4 mmol, 3.2 equiv) was added and the reaction tube was evacuated and backfilled with N_2. The tube was then placed in front of a 600 W tungsten-filament lamp at a distance of ~0.2 m such that the reaction mixture was also heated by the lamp to reflux. After 4 h, the light was turned off and the reaction was quenched by the addition of saturated 1 M $NaHSO_{3(aq)}$. Column chromatography (4:1 CH_2Cl_2/EtOAc) delivered the title compound (**2.71**) as a brown-white foam (101.0 mg, 0.22 mmol, 29%, 2 steps). **R_f:** 0.45 (2:1 hexanes/EtOAc, UV, anisaldehyde stain). **^{1}H NMR** (600 MHz, $CDCl_3$) δ 7.82 (dd, *J* = 5.5, 3.1 Hz, 2H), 7.70 (dd, *J* = 5.5, 3.0 Hz, 2H), 7.23 (d, *J* = 8.5 Hz, 1H), 6.74 (dd, *J* = 8.5, 2.5 Hz, 1H), 6.57 (d, *J* = 2.5 Hz, 1H), 6.41 (dd, *J* = 10.8, 2.2 Hz, 1H), 6.25 (dd, *J* = 10.7, 6.0 Hz, 1H), 5.58 (dd, *J* = 17.6, 10.9 Hz, 1H), 5.29 (d, *J* = 11.0 Hz, 1H), 5.26 (d, *J* = 17.5 Hz, 1H), 4.05 (s, 1H), 3.81 (s, 3H), 3.74 (dd, *J* = 13.7, 9.7 Hz, 1H), 3.52 (dd, *J* = 13.7, 4.9 Hz, 1H), 3.26 (s, 3H), 3.24 (s, 1H), 2.34 (ddq, *J* = 13.1, 8.5, 4.6 Hz, 1H), 1.96 – 1.88 (m, 1H), 1.76 (qd, *J* = 13.0, 3.6 Hz, 1H), 1.44 – 1.32 (m, 2H). **^{13}C NMR** (151 MHz, $CDCl_3$) δ 205.4, 168.4, 161.5, 137.5, 137.2, 133.9, 133.0, 132.5, 132.0, 131.6, 127.2, 123.2, 118.5, 113.0, 112.4, 80.5, 70.7, 57.3, 55.3, 41.9, 38.6, 33.9, 23.6, 19.9. **IR** (thin film) $\tilde{\nu}_{max}$ cm^{-1} 2933, 2835, 2253, 1772, 1713, 1675, 1597, 723. **HRMS** (ESI) calcd for $[C_{28}H_{28}O_5N_1]^+$ ($[M+H]^+$): *m/z* 458.1962, found 458.1954.

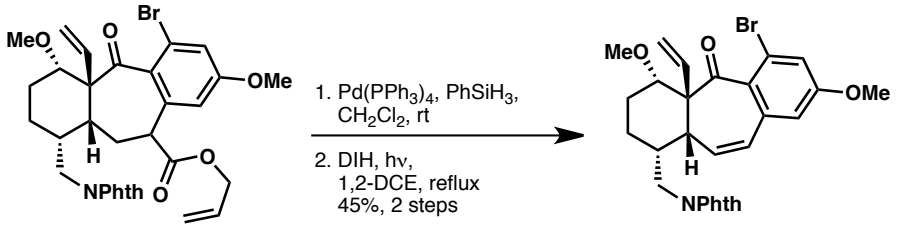

2.70 **2.72**

2-(((1*R*,4*S*,4a*R*,11a*R*)-6-Bromo-4,8-dimethoxy-5-oxo-4a-vinyl-2,3,4,4a,5,11a-hexahydro-1*H*-dibenzo[*a*,*d*][7]annulen-1-yl)methyl)isoindoline-1,3-dione (2.72). Bromomethoxy tricycle **2.70** (415.5 mg, 0.67 mmol) was taken up in CH_2Cl_2 (20 mL) in a flame-dried round-bottom flask. $Pd(PPh_3)_4$ (40.1 mg, 0.03 mmol, 0.04 equiv) was added to the reaction mixture and the flask was covered in foil. Phenylsilane (0.180 mL, 1.46 mmol, 2.2 equiv) was added slowly and the solution was stirred at room temperature. When the reaction was complete according to NMR analysis the solvent was removed. The crude residue was run through a silica column (Gradient: 2 → 7% MeOH in CH_2Cl_2) to give the acid as a brown/white foam (240.2 mg). The acid (240.2 mg, 0.41 mmol) was added to a long reaction tube in 1,2-dichloroethane (4.5 mL), followed by 1,3-diiodo-5,5-dimethylhydantoin (389.2 mg, 1.03 mmol, 2.5 equiv). The reaction tube was evacuated and backfilled with nitrogen (3x), then set 1 foot in front of a 600 W tungsten lamp such that the solution was brought to reflux. When the reaction was deemed complete by TLC analysis it was quenched by the addition of 1 M $NaHSO_3$ (4 mL), and the aqueous layer was extracted with dichloromethane. The combined organic layer was washed once with brine, dried ($MgSO_4$), and concentrated. Purification via column chromatography (20 → 41% EtOAc in

hexanes) provided styrene **2.72** as a white foam. (161.2 mg, 45%, 2 steps). **R_f:** 0.38 (2:1 hexanes/EtOAc, UV and anisaldehyde stain). **^{1}H NMR** (500 MHz, $CDCl_3$) δ 7.82 (dd, *J* = 5.5, 3.1 Hz, 2H), 7.70 (dd, *J* = 5.5, 3.0 Hz, 2H), 6.99 (d, *J* = 2.4 Hz, 1H), 6.53 (d, *J* = 2.4 Hz, 1H), 6.39 – 6.31 (m, 1H), 6.28 (dd, *J* = 10.6, 6.1 Hz, 1H), 5.54 – 5.42 (m, 2H), 5.42 – 5.28 (m, 1H), 4.01 (t, *J* = 2.5 Hz, 1H), 3.79 (s, 3H), 3.70 (dd, *J* = 13.7, 9.6 Hz, 1H), 3.50 (dd, *J* = 13.7, 5.1 Hz, 1H), 3.30 (s, 3H), 3.22 (t, *J* = 4.9 Hz, 1H), 2.32 (ddq, *J* = 12.6, 8.5, 4.1 Hz, 1H), 1.96 – 1.84 (m, 1H), 1.82 – 1.68 (m, 1H), 1.47 – 1.30 (m, 2H). **^{13}C NMR** (126 MHz, $CDCl_3$) δ 200.0, 168.4, 160.4, 138.9, 134.4, 133.9, 133.7, 132.3, 131.9, 126.2, 123.2, 122.3, 120.9, 118.0, 112.1, 79.3, 71.7, 57.5, 55.6, 41.8, 38.4, 33.6, 23.4, 20.0. **IR** (thin film) $\tilde{\nu}_{max}$ cm^{-1} 2934, 2830, 1772, 1713,1590. **HRMS** (ESI) calcd for $[C_{28}H_{27}O_5N_1Br]^+$ ($[M+H]^+$): *m/z* 536.1067, found 536.1060.

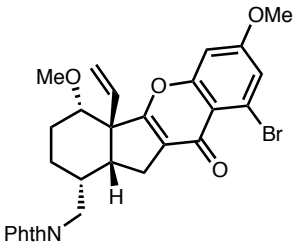

2.73

2-(((1*R*,4*S*,4a*R*,11a*R*)-9-bromo-4,7-dimethoxy-10-oxo-4a-vinyl-1,2,3,4,4a,10,11,11a-octahydroindeno[1,2-*b*]chromen-1-yl)methyl)isoindoline-1,3-dione (2.73). R_f: 0.52 (1:1 hexanes/EtOAc, UV, anisaldehyde stain). **^{1}H NMR** (500 MHz, $CDCl_3$) δ 7.85 (dd, *J* = 5.4, 3.1 Hz, 2H), 7.72 (dd, *J* = 5.5, 3.1 Hz, 2H), 7.21 (d, *J* = 2.5 Hz, 1H), 6.85 (d, *J* = 2.5 Hz, 1H), 5.99 (dd, *J* = 17.7, 11.0 Hz, 1H), 5.37 – 5.30 (m, 2H), 3.87 (s, 3H), 3.74 – 3.65 (m, 2H), 3.54 (dd, *J* = 3.9, 1.9 Hz, 1H), 3.05 (s, 3H), 2.76 – 2.64 (m, 2H), 2.61 – 2.54 (m, 1H), 2.29 (qt, *J* = 9.4, 5.2 Hz, 1H), 1.95 (dq, *J* = 14.2, 3.4 Hz, 1H), 1.65 – 1.54 (m, 1H), 1.46 – 1.36 (m, 1H), 1.35 – 1.23 (m, 1H). **^{13}C NMR** (126 MHz, $CDCl_3$) δ 174.5, 168.3, 167.0, 161.6, 159.5, 137.4, 133.9, 131.8, 123.1, 122.5, 121.1, 120.2, 117.5, 115.8, 101.1, 79.0, 56.8, 56.6, 55.8, 43.2, 41.6, 34.1, 25.3, 23.6, 18.4. **IR** (thin film) $\tilde{\nu}_{max}$ cm^{-1} 3085, 3058, 2935, 2891, 2861, 2828, 1771, 1713, 1651, 1605, 1551. **HRMS** (ESI) calcd for $[C_{29}H_{27}O_6N_1Br]^+$ ($[M+H]^+$): *m/z* 564.1016, found 564.1014.

X-Ray Data and Crystal Refinement for Chromenone 2.73.

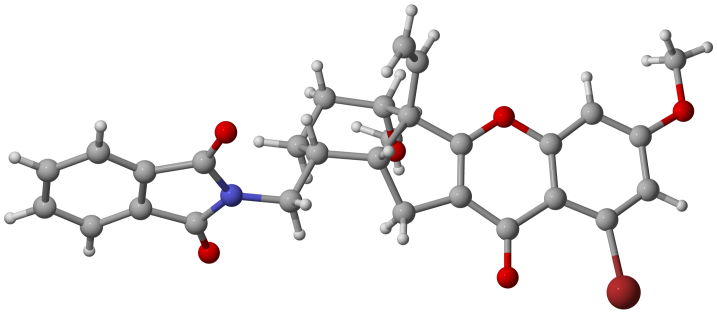

A colorless plate 0.120 x 0.060 x 0.020 mm in size was mounted on a Cryoloop with Paratone oil. Data were collected in a nitrogen gas stream at 100(2) K using phi and omega scans. Crystal-to-detector distance was 50 mm and exposure time was 10 seconds per frame using a scan width of 0.5°. Data collection was 100.0% complete to 25.000° in θ. A total of 69602 reflections were

collected covering the indices, -11<=*h*<=11, -12<=*k*<=12, -28<=*l*<=29. 4514 reflections were found to be symmetry independent, with an R_{int} of 0.0555. Indexing and unit cell refinement indicated a primitive, monoclinic lattice. The space group was found to be P 21/n (No. 14). The data were integrated using the Bruker SAINT software program and scaled using the SADABS software program. Solution by iterative methods (SHELXT) produced a complete heavy-atom phasing model consistent with the proposed structure. All non-hydrogen atoms were refined anisotropically by full-matrix least-squares (SHELXL-2013). All hydrogen atoms were placed using a riding model. Their positions were constrained relative to their parent atom using the appropriate HFIX command in SHELXL-2013.

Empirical formula	C29 H26 Br N O6	
Formula weight	564.42	
Temperature	100(2) K	
Wavelength	0.71073 Å	
Crystal system	Monoclinic	
Space group	P 21/n	
Unit cell dimensions	a = 9.4680(3) Å	α= 90°.
	b = 10.6674(4) Å	β= 91.1620(10)°.
	c = 24.3414(9) Å	γ = 90°.
Volume	2457.95(15) $Å^3$	
Z	4	
Density (calculated)	1.525 Mg/m^3	
Absorption coefficient	1.719 mm^{-1}	
F(000)	1160	
Crystal size	0.120 x 0.060 x 0.020 mm^3	
Crystal color/habit	colorless plate	
Theta range for data collection	1.674 to 25.391°.	
Index ranges	-11<=h<=11, -12<=k<=12, -28<=l<=29	
Reflections collected	69602	
Independent reflections	4514 [R(int) = 0.0555]	
Completeness to theta = 25.000°	100.0 %	
Absorption correction	Semi-empirical from equivalents	
Max. and min. transmission	0.928 and 0.820	
Refinement method	Full-matrix least-squares on F^2	
Data / restraints / parameters	4514 / 0 / 336	
Goodness-of-fit on F^2	1.067	
Final R indices [I>2sigma(I)]	R1 = 0.0292, wR2 = 0.0613	
R indices (all data)	R1 = 0.0401, wR2 = 0.0669	
Extinction coefficient	n/a	
Largest diff. peak and hole	0.505 and -0.353 e.$Å^{-3}$	

2.10 References and Notes

[1] (a) Matias, R.; Gavin, J. A.; Madinaveitia, A.; Acosta, R. D.; de la Fuente, G. *J. Nat. Prod.* **1996**, *59*, 145. (b) Desai, H.; Srivastava, S. K.; Hart, B. P.; Park, J.-C.; Joshi, B. S.; Pelletier, S. W. *J. Nat. Prod.* **1996**, *59*, 360.
[2] Wenk, H. H.; Winkler, M.; Sander, W. *Angew. Chem. Int. Ed. Engl.* **2003**, *42*, 502.
[3] Tadross, P. M.; Stoltz, B. M. *Chem. Rev.*, **2012**, *112*, 3550.
[4] Himeshima, Y.; Sonoda, T.; Kobayashi, H. *Chem. Lett.* **1983**, 1211.
[5] For selected recent examples of mild benzyne formation, see: (a) Sumida, Y.; Kato, T.; Hosoya, T. *Org. Lett.* **2013**, *15,* 2806. (b) Ikawa, T.; Nishiyama, T.; Nosaki, T.; Takagi, A.; Akai, S. *Org. Lett.* **2011**, *13,* 1730. (c) Kitamura, T. *Aust. J. Chem.* **2010**, *63,* 987 (Review).
[6] Tambar, U. K.; Stoltz, B. M. *J. Am. Chem. Soc.* **2005**, *127*, 5340.
[7] Yoshida, H.; Takaki, K. *Synlett* **2012**, *23*, 1725.
[8] Yoshida, H.; Watanabe, M.; Ohshita, J.; Kunai, A. *Chem. Commun.* **2005**, 3292.
[9] Tadross, P. M.; Gilmore, C. D.; Bugga, P.; Virgil, S. C.; Stoltz, B. M. *Org. Lett.* **2010**, *12,* 1224.
[10] Ikawa, T.; Nishiyama, T.; Shigeta, T.; Mohri, S.; Morita, S.; Takayanagi, S.; Terauchi, Y.; Morikawa, Y.; Takagi, A.; Ishikawa, Y.; Fujii, S.; Kita, Y.; Akai, S. *Angew. Che. Int. Ed.* **2011**, *50,* 5674.
[11] Bronner, S. M.; Bahnck, K. B.; Garg, N. K. *Org. Lett.* **2009**, *11,* 1007.
[12] Cheong, P. H.-Y.; Paton, R. S.; Bronner, S. M.; Im, G.-Y. J.; Garg, N. K.; Houk, K. N. *J. Am. Chem. Soc.* **2010**, *132,* 1267.
[13] (a) Hamura, T.; Ibusuki, Y.; Sato, K.; Matsumoto, T.; Osamura, Y.; Suzuki, K. *Org. Lett.* **2003**, *5,* 3551. (b) Ikawa, T.; Tokiwa, H.; Akai, S. *J. Synth. Org. Chem., Jpn.* **2012**, *11,* 1123.
[14] Im, G.-Y. J.; Bronner, S. M.; Goets, A. E.; Paton, R. S.; Cheong, P. H.-Y.; Houk, K. N.; Garg, N. K. *J. Am. Chem. Soc.* **2010**, *132,* 17933.
[15] Bronner, S. M.; Goetz, A. E.; Garg, N. K. *J. Am. Chem. Soc.* **2011**, *133*, 3832.
[16] Gampe, C. M.; Carreira, E. M. *Angew. Chem. Int. Ed.* **2012**, *51,* 3766.
[17] Guyot, M.; Molho, D. *Tetrahedron Lett.* **1973**, *14,* 3433.
[18] Tambar, U. K.; Ebner, D. C.; Stoltz, B. M. *J. Am. Chem. Soc.* **2006**, *128,* 11752.
[19] Tadross, P. M.; Virgil, S. C.; Stoltz, B. M. *Org. Lett.* **2010**, *12,* 1612.
[20] Yoshida, H.; Morishita, T.; Ohshita, J. *Chem. Lett.* **2010**, *39,* 508.
[21] Prabhakaran, J.; Lhermitte, H.; Das, J.; Sasi-Kumar, T. K.; Grierson, D. S. *Synlett* **2000**, *5,* 658.
[22] Wang, C.; Gu, X.; Yu, M. S.; Curran, D. P. *Tetrahedron*, **1998**, *54*, 8355.
[23] Mander, L. N.; Sethi, S. P. *Tetrahedron Lett.* **1983**, *24,* 5425.
[24] Allan, K. M.; Hong, B. D.; Stoltz, B. M. *Org. Biomol. Chem.* **2009**, *7,* 4960.
[25] (a) Kauch, M.; Snieckus, V. Hoppe, D. *J. Org. Chem.* **2005**, *70,* 7149. (b) Kauch, M.; Hoppe, D. *Synthesis* **2006**, 1578.
[26] Bronner, S. M.; Garg, N. K. *J. Org. Chem* **2009**, *74,* 8842.
[27] Donnelly, D. M. X.; Finet, J.-P.; Rattigan, B. A. *J. Chem. Soc., Perkin Trans. 1* **1993**, 1729.
[28] Tsuji, J. *Tetrahedron* **1986**, *42,* 4361.
[29] For a review of oxidative decarboxylation of acids using lead, see: Sheldon, R. A.; Kochi, J. K. *Organic Reactions* **1972**, *19,* 279.
[30] Lebel, H.; Paquet, V. *J. Am. Chem. Soc.* **2004,** *126*, 320.

[31] Griffith, W.P.; Ley, S. V.; Whitcombe, G. P.; White, A. D. *J. Chem. Soc. Chem. Commun.* **1987**, 1625.
[32] Fukata, G.; Kubota, Y.; Mataka, S.; Thiemann, T.; Tashiro, M. *Bull. Chem. Soc. Jpn.,* **1994**, *67*, 592.
[33] For a discussion on the use of tin in hydrodehalogenations, see: Alonso, F.; Beletskaya, I. P.; Yus, M.. *Chem. Rev.* **2002**, *102,* 4009.
[34] Czaplik, W. M.; Grupe, S.; Mayer, M.; von Wangelin, A. J. *Chem. Commun.* **2010**, *46*, 6350.
[35] Mori, M.; Isono, N.; Kaneta, N.; Shibasaki, M. *J. Org. Chem.*, **1993**, *58*, 2972.
[36] Chen, J.; Zhang, Y.; Yang, L.; Zhang, X.; Liu, J.; Li, L.; Zhang, H. *Tetrahedron*. **2007**, *63*, 4266.
[37] Kulbitski, K.; Nisnevich, G.; Gandelman, M. *Adv. Synth. Catal.* **2011**, *353*, 1438.
[38] Hoye, T. R.; Baire, B.; Niu, D.; Willoughby, P. H.; Woods, B. P. *Nature* **2012**, *490,* 202.
[39] Hughes, D. L. *Org. React.* **1992**, *42,* 335.
[40] Dessolin, M.; Guillerez, M.-J.; Thieriet, N.; Guibé, F.; Loffet, A. *Tetrahedron Lett.* **1995**, *36,* 5741.
[41] Ikawa, T.; Nishiyama, T.; Shigeta, T.; Mohri, S.; Morita, S.; Takayanagi, S.; Terauchi, Y.; Morikawa, Y.; Takagi, A.; Ishikawa, Y.; Fujii, S.; Kita, Y.; Akai, S. *Angew. Chem. Int. Ed.* **2011**, *50,* 5674.

Appendix 1. Spectra Relevant to Chapter 2

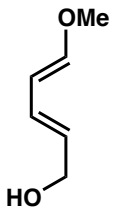
OMe
HO

2.S1

6.58
6.54
6.11
6.08
6.06
6.03
5.64
5.62
5.59
5.59
5.57
5.54
5.53
5.48
5.48
5.44
4.07
4.05
3.54
2.37
1.00
1.04
1.03
1.04
2.16
3.28
1.10
f1 (ppm)

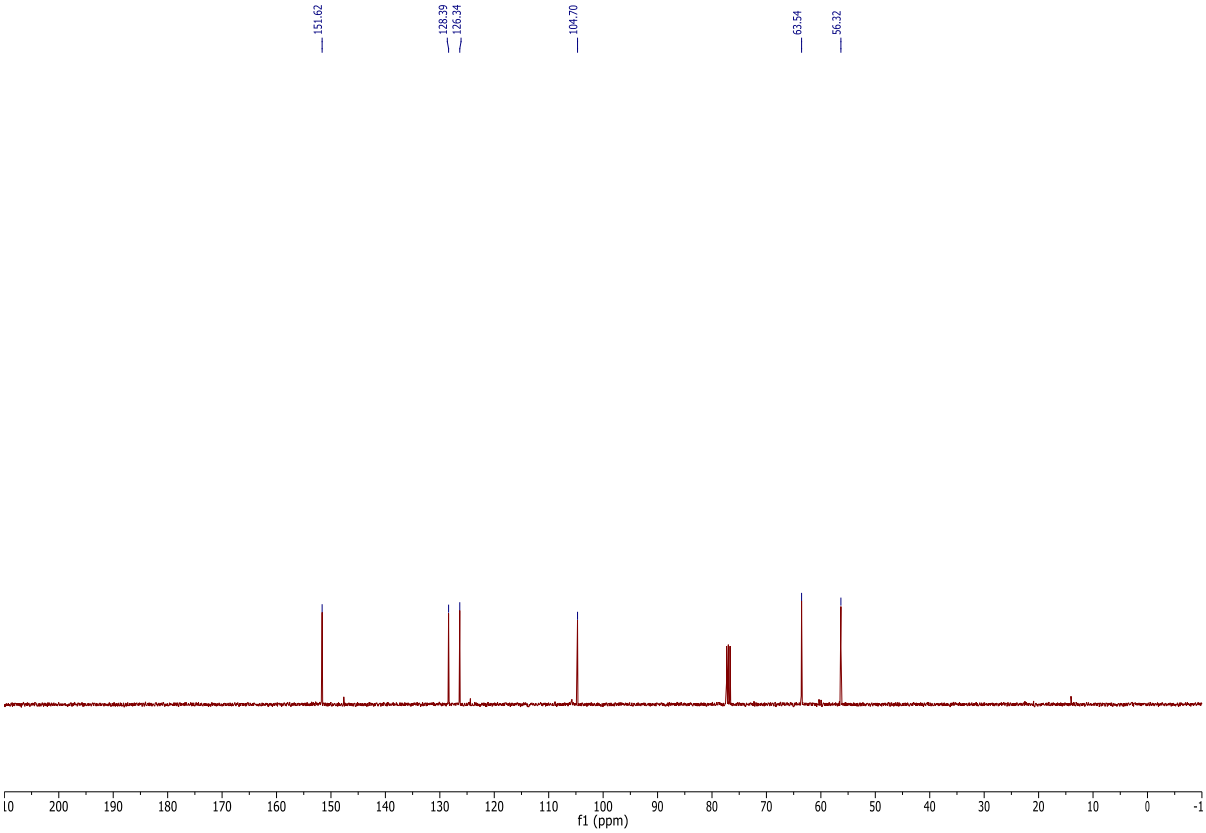
151.62
128.39
126.34
104.70
63.54
56.32
f1 (ppm)

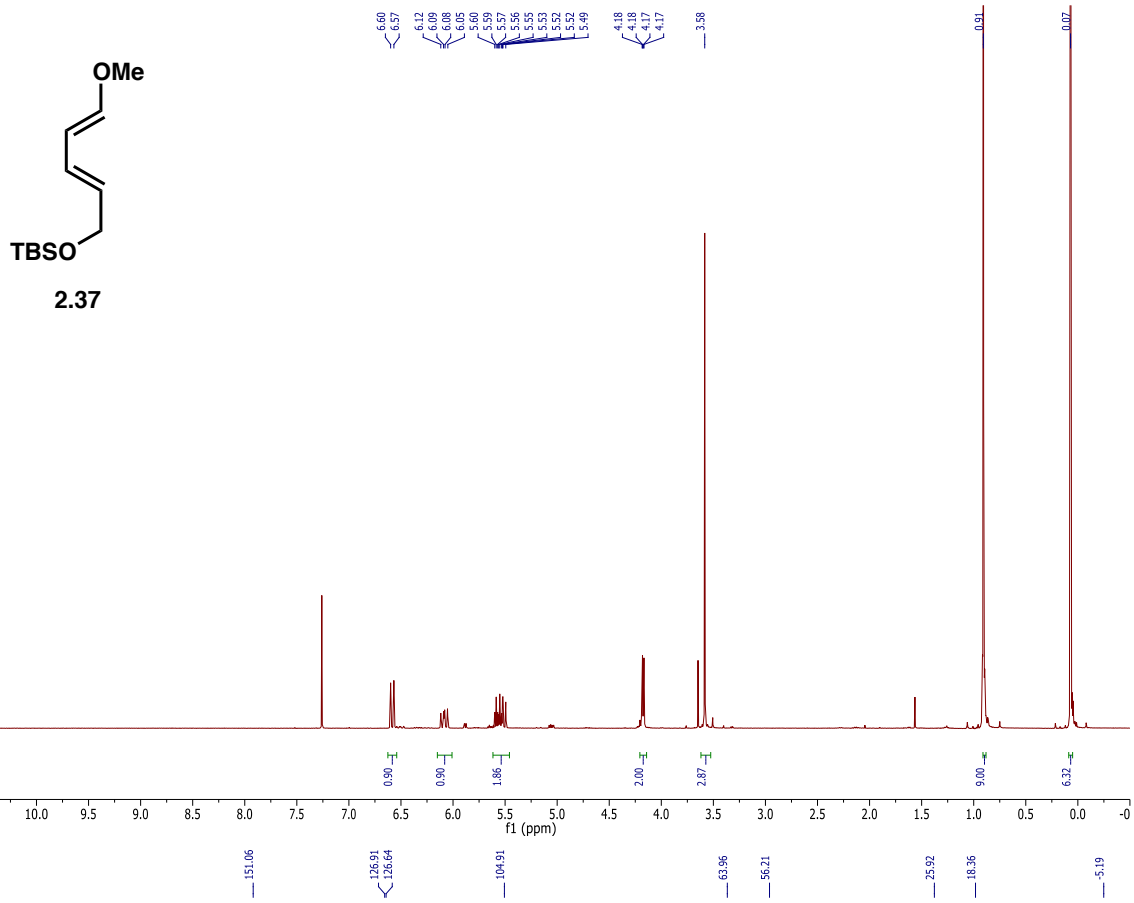
OMe
TBSO
2.37
6.60
6.57
6.12
6.09
6.08
6.05
5.60
5.59
5.57
5.56
5.55
5.53
5.52
5.52
5.49
4.18
4.18
4.17
4.17
3.58
0.91
0.07
0.90
0.90
1.86
2.00
2.87
9.00
6.32
f1 (ppm)

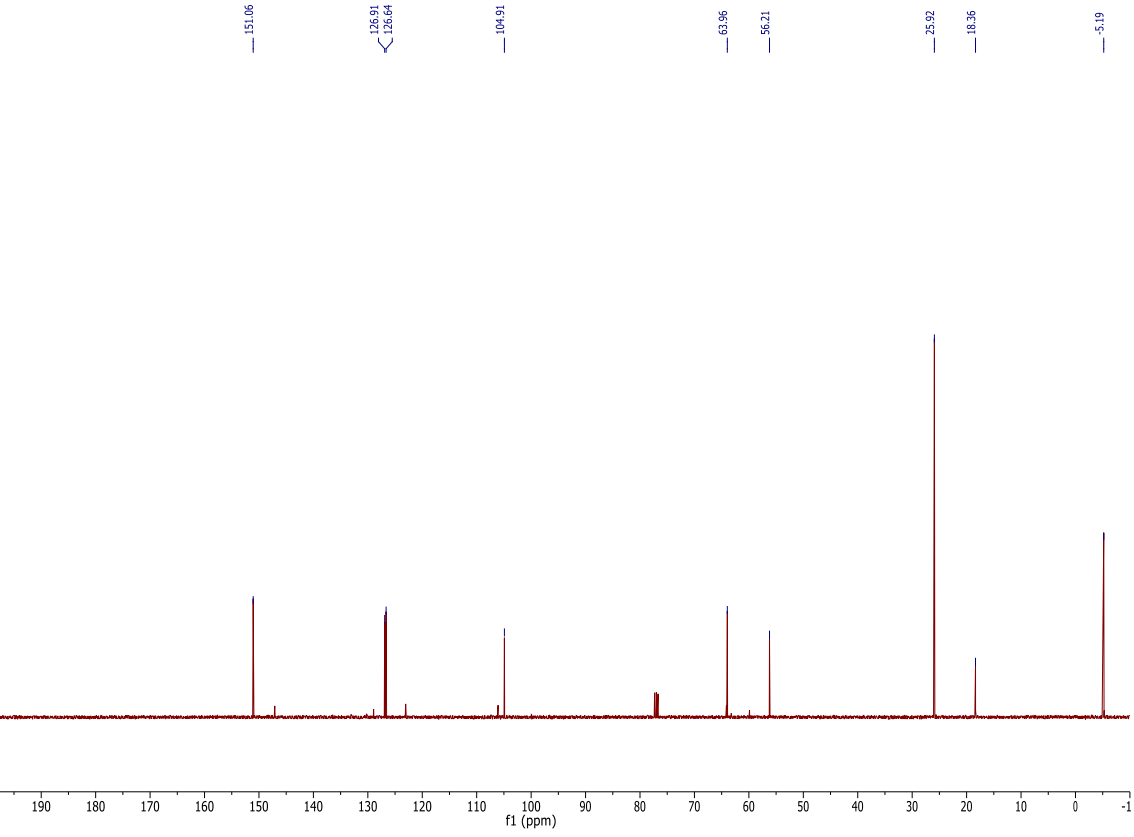
151.06
126.91
126.64
104.91
63.96
56.21
25.92
18.36
-5.19
f1 (ppm)

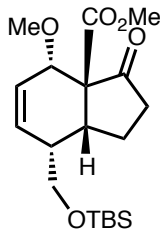

2.7

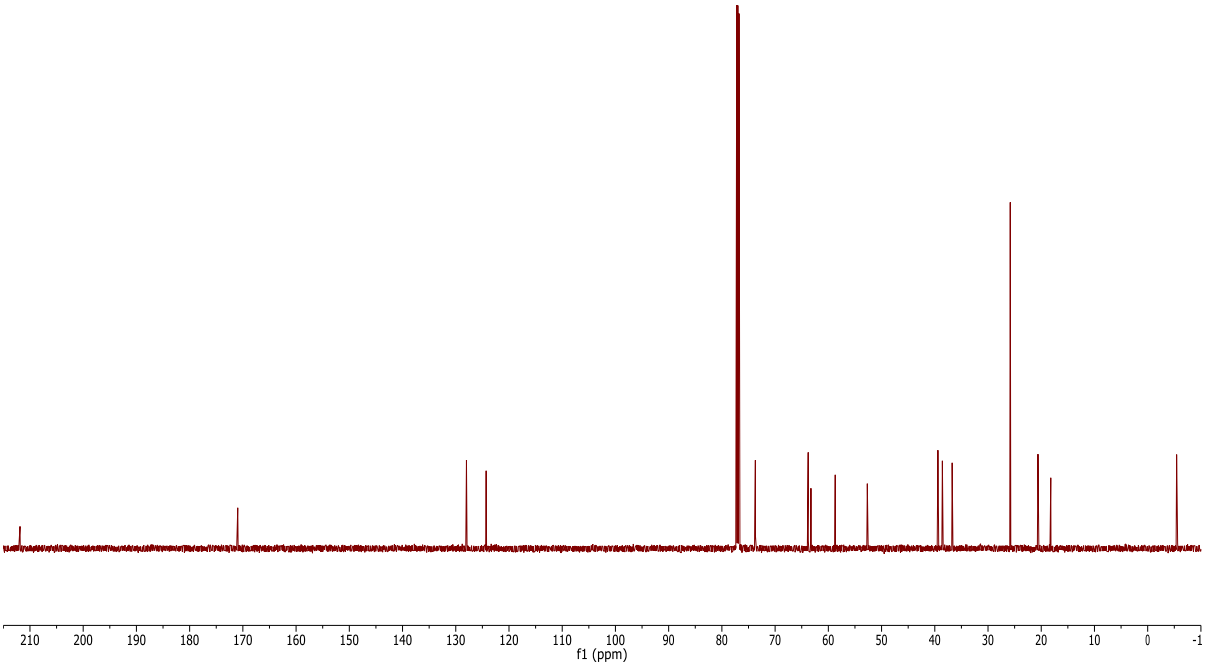

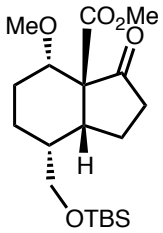

2.41

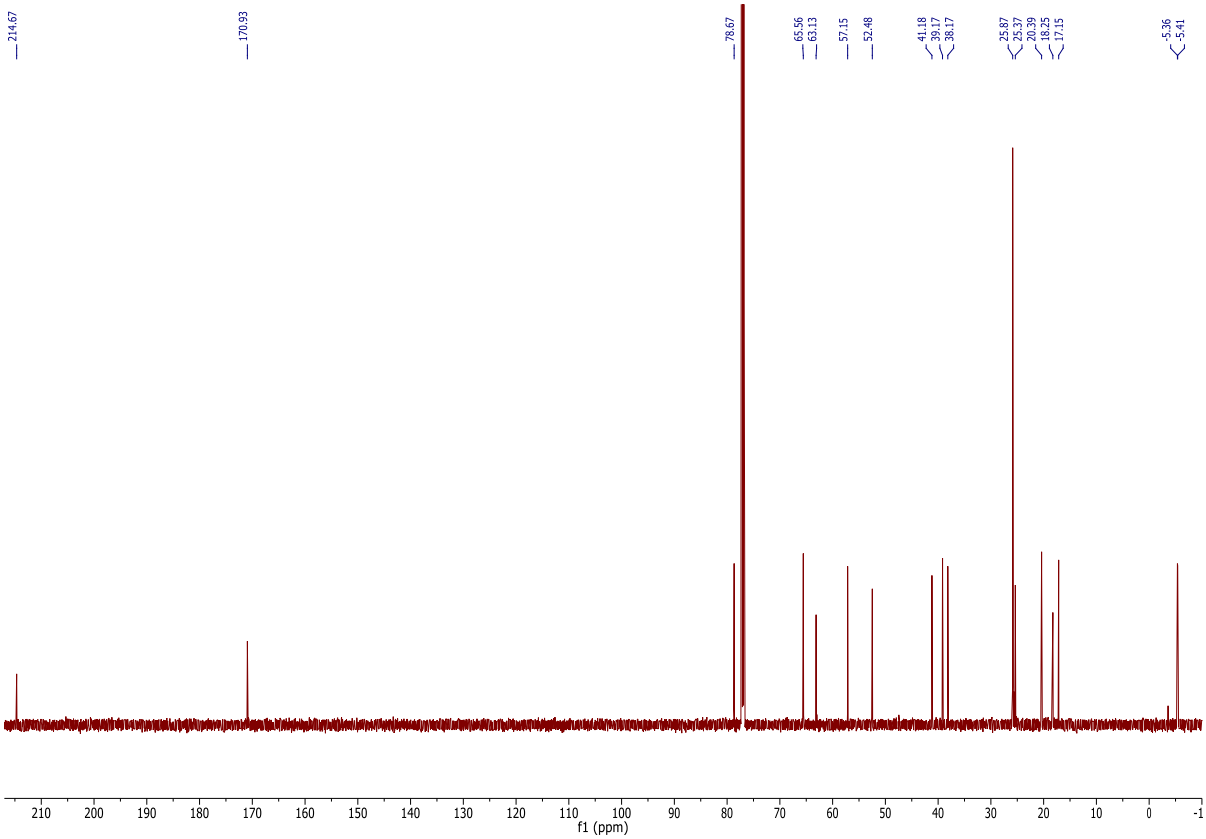

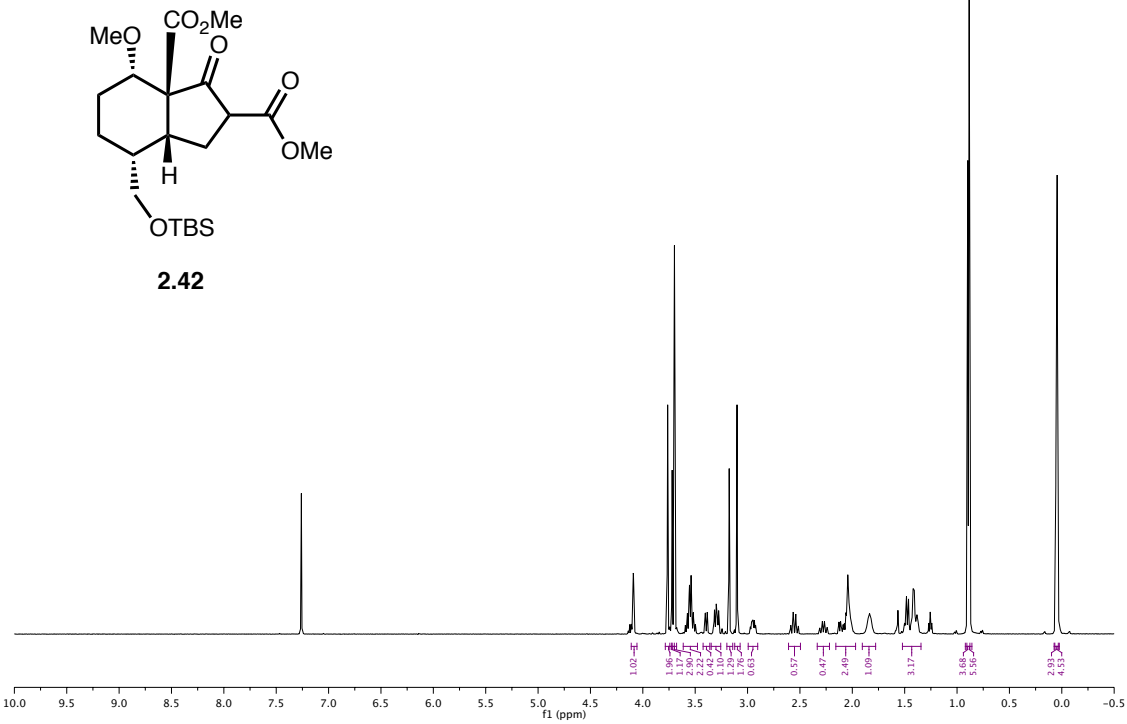

2.42

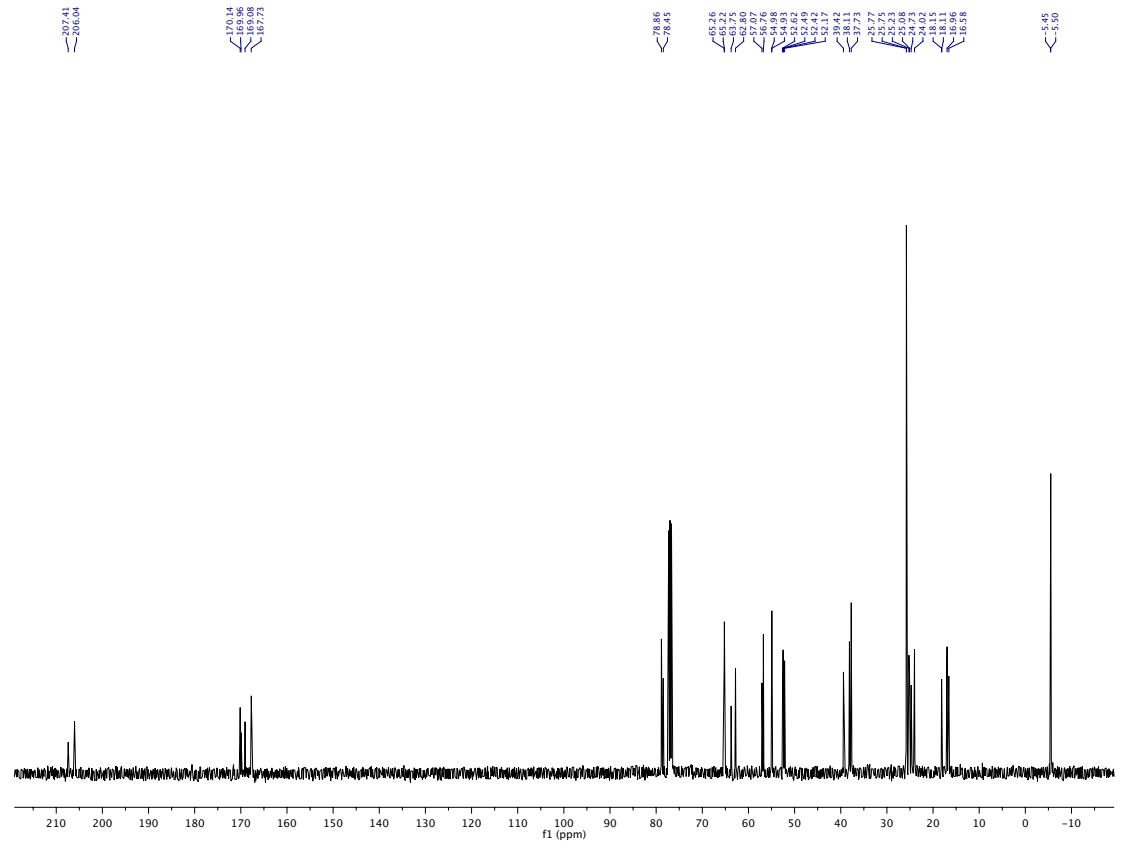

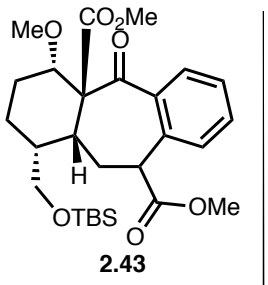

2.43

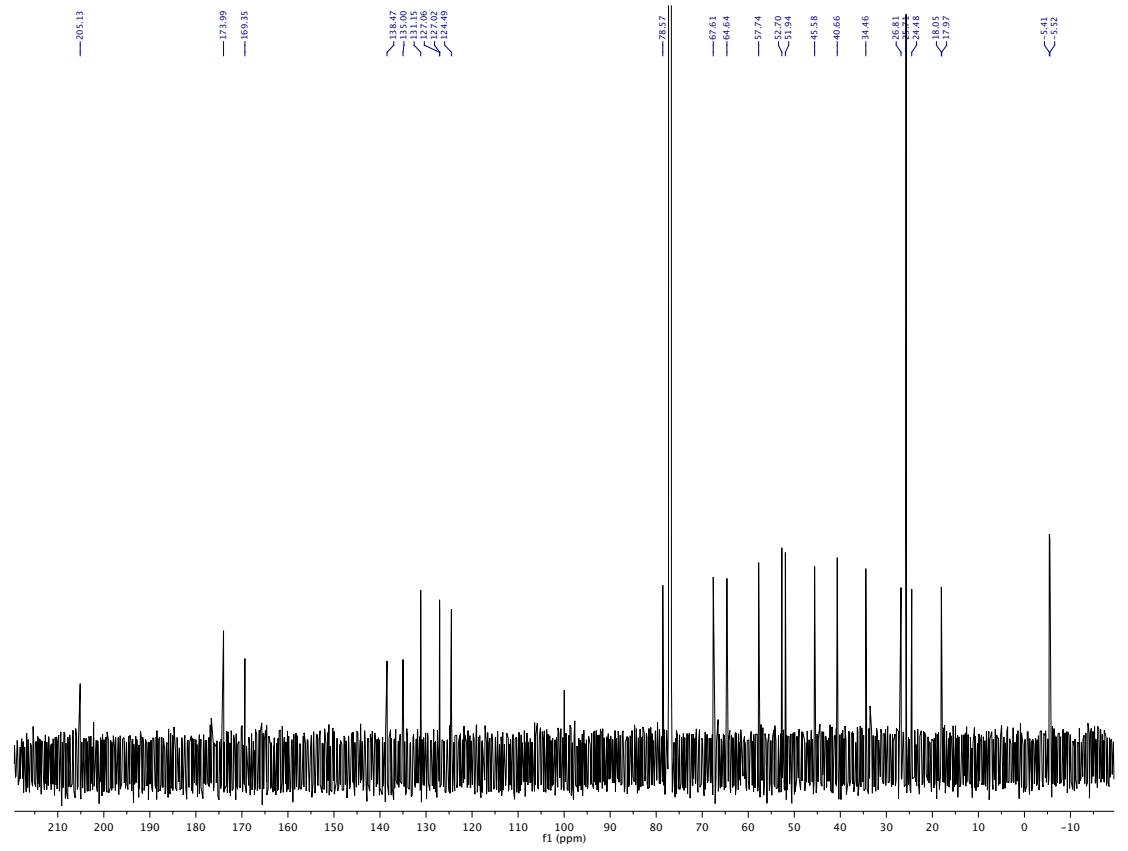

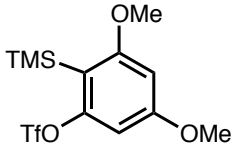
OMe
TMS
TfO
OMe

2.44

6.53
6.52
6.50
6.50
6.40
6.40
3.83
3.82
3.81
3.80
0.37
0.37
0.36
0.35
0.34
0.34
1.00
1.02
3.45
2.04
9.18
f1 (ppm)

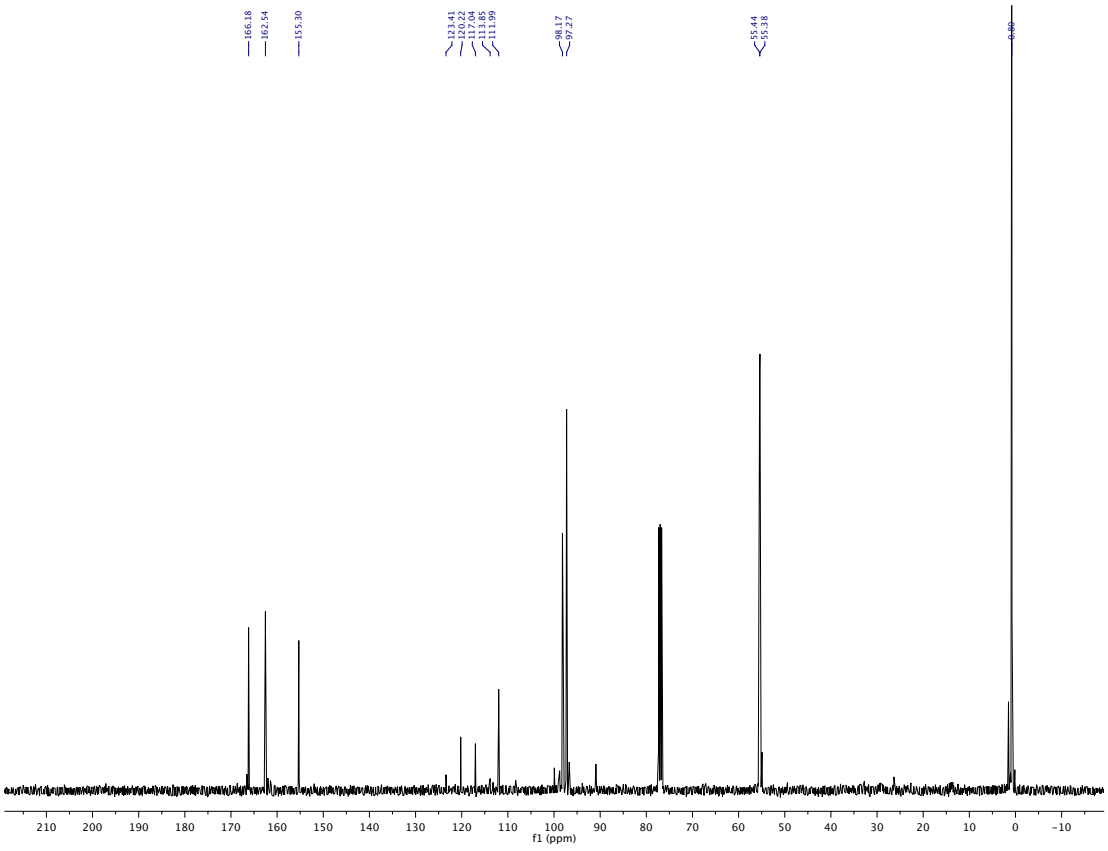
166.18
162.54
155.30
123.41
120.22
117.04
113.95
111.99
98.17
97.27
55.44
55.38
0.00
f1 (ppm)

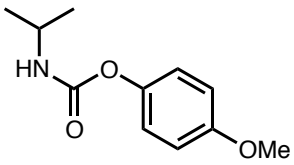
HN
O
O
OMe

2.S5

7.04
7.02
6.86
6.84
5.16
5.14
3.87
3.86
3.84
3.82
3.75
1.17
1.15
2.00
2.00
0.82
1.07
2.98
3.32
2.73
f1 (ppm)

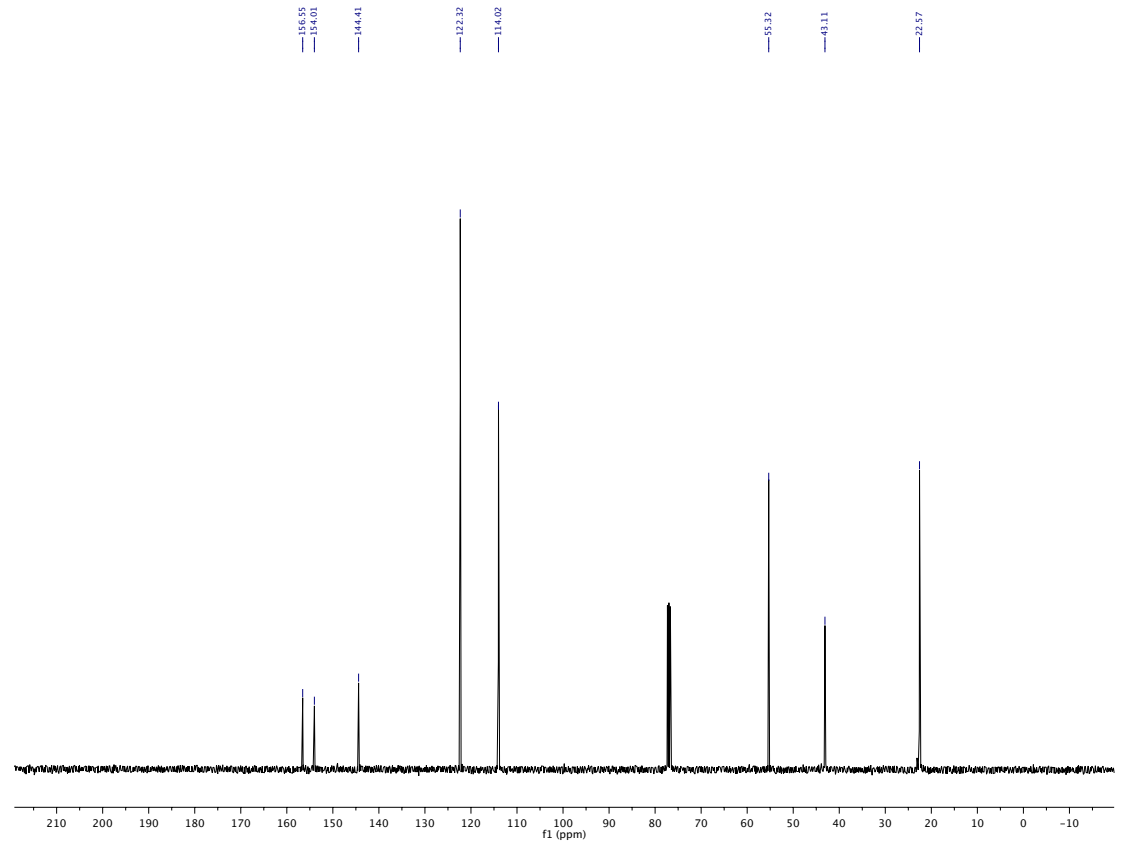
156.55
154.01
144.41
122.32
114.02
55.32
43.11
22.57
f1 (ppm)

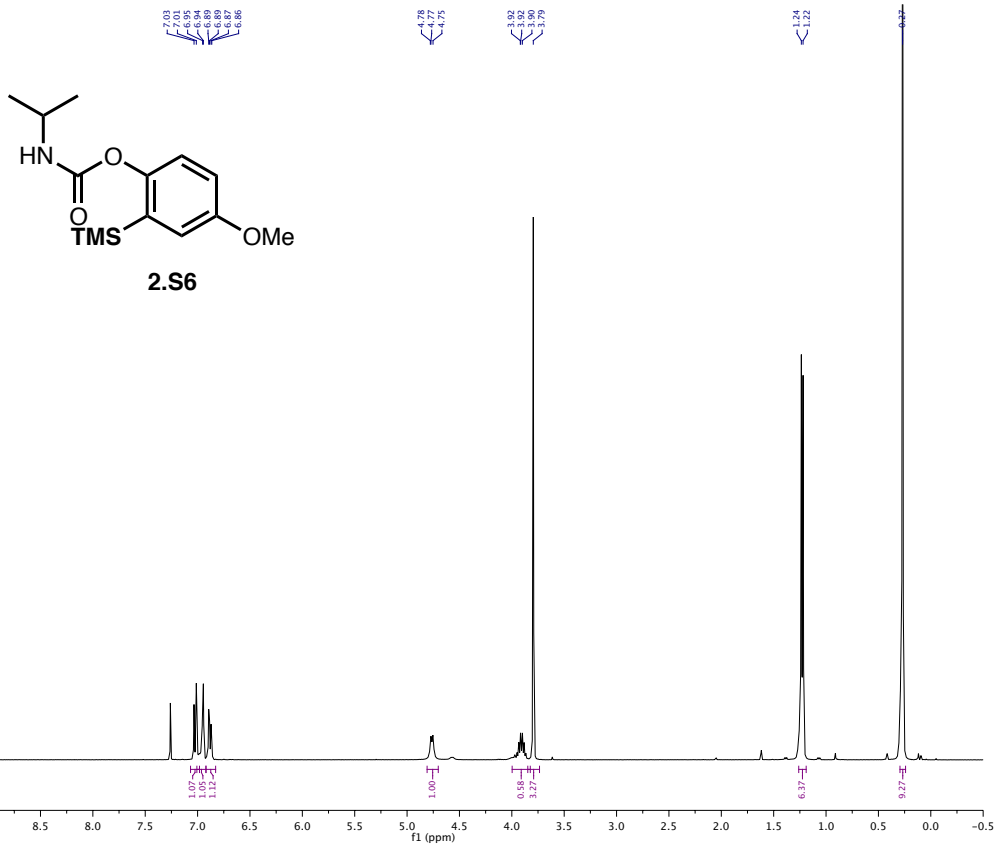

2.S6

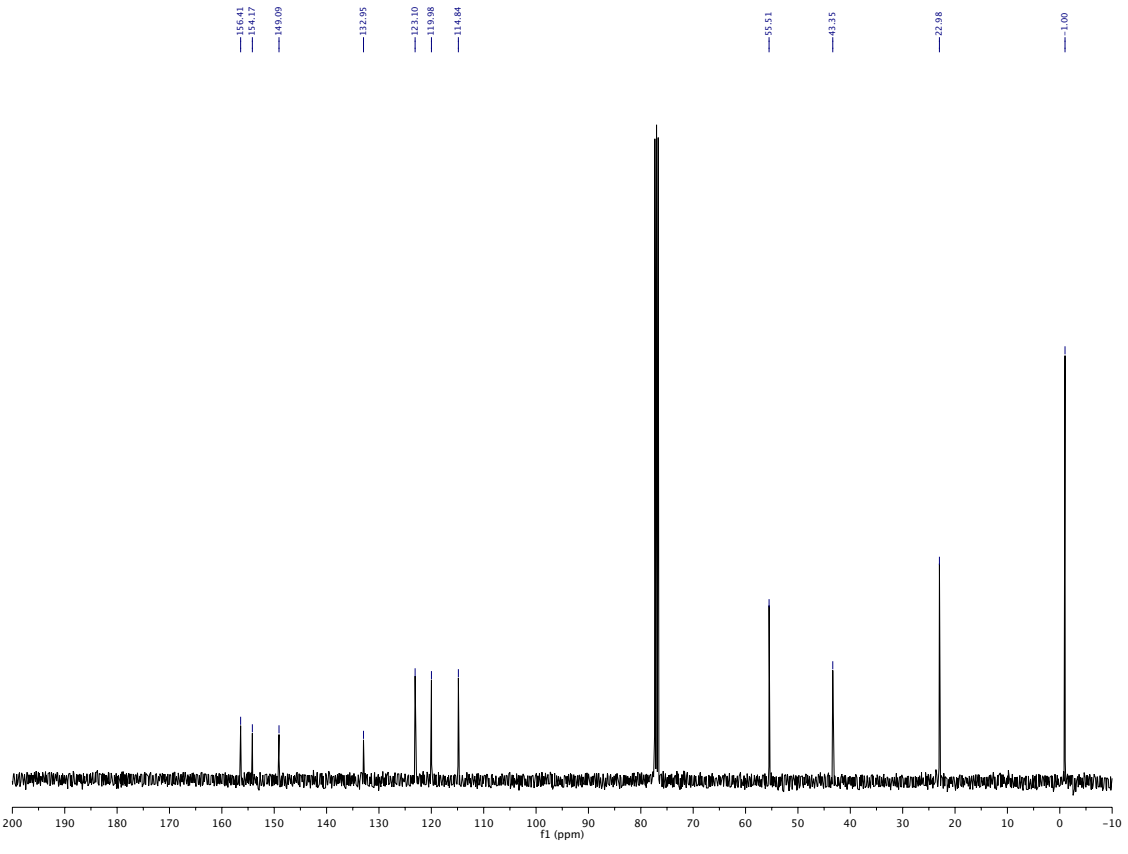

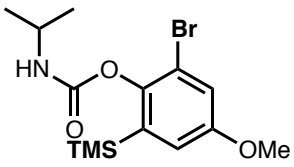
Br
HN
O
O
TMS
OMe

2.46

7.11
7.10
6.92
6.91
5.08
5.07
5.06
3.93
3.91
3.91
3.90
3.89
3.88
3.78
3.77
1.23
1.21
0.27
1.00
0.97
0.95
0.80
3.24
6.11
8.18
f1 (ppm)

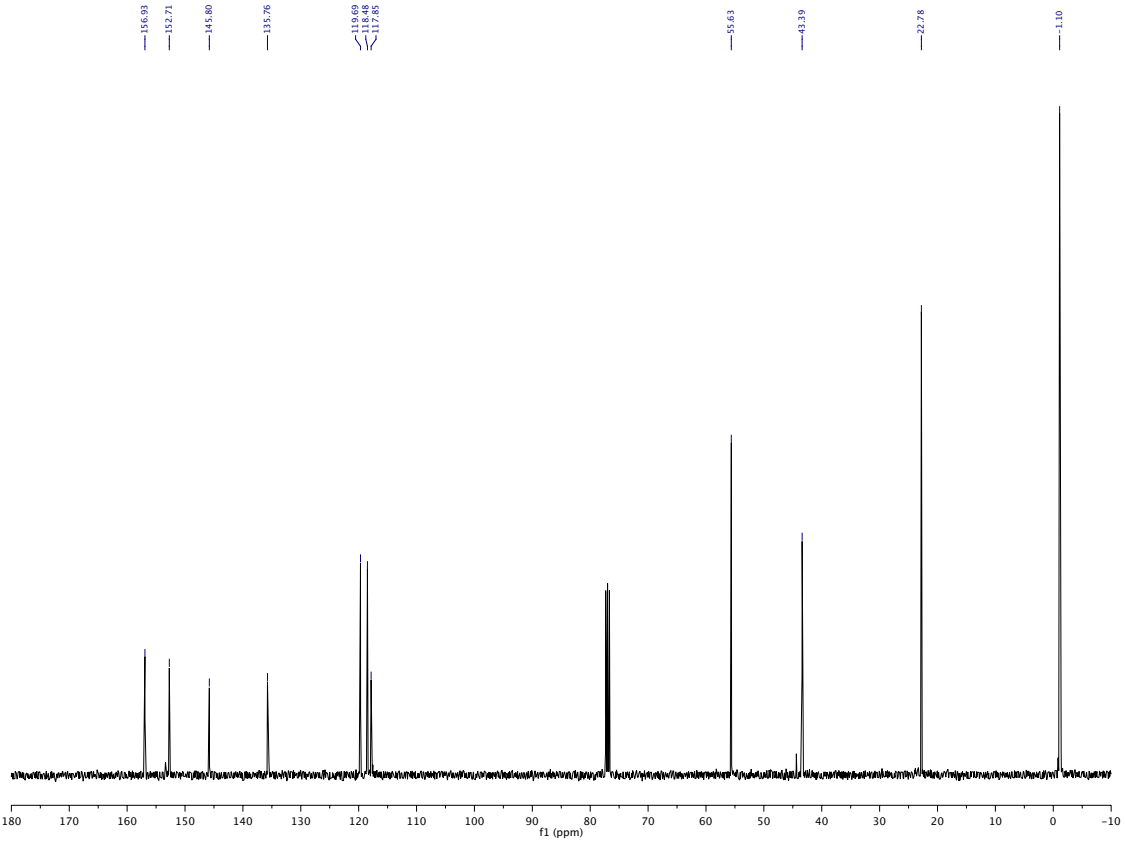
156.93
152.71
145.80
135.76
119.69
118.48
117.85
55.63
43.39
22.78
1.10
f1 (ppm)

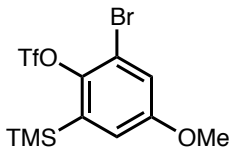
Br
TfO
TMS
OMe

2.47

7.16
7.15
6.99
6.98
3.82
0.39
0.99
1.00
3.62
10.82
f1 (ppm)

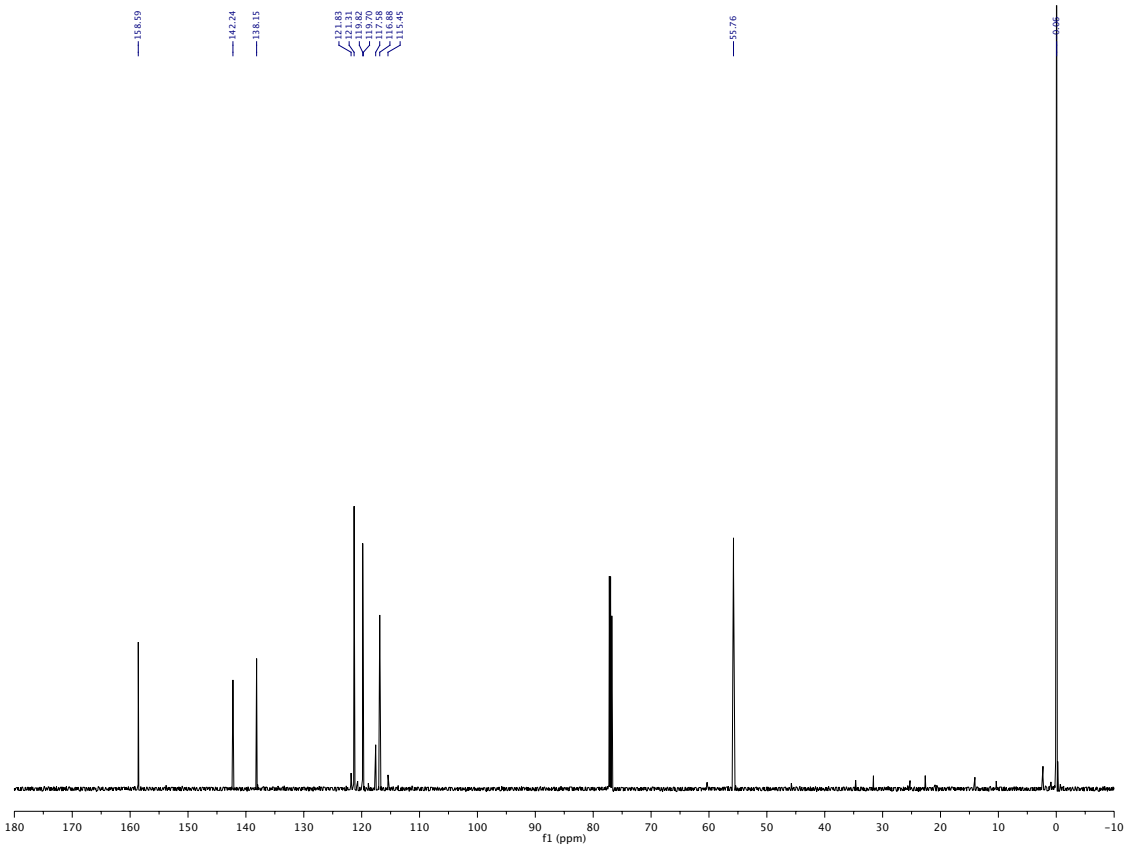
158.59
142.24
138.15
121.83
121.31
119.82
119.70
117.58
116.68
115.45
55.76
0.00
f1 (ppm)

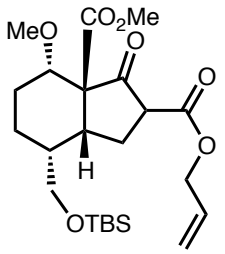

2.48

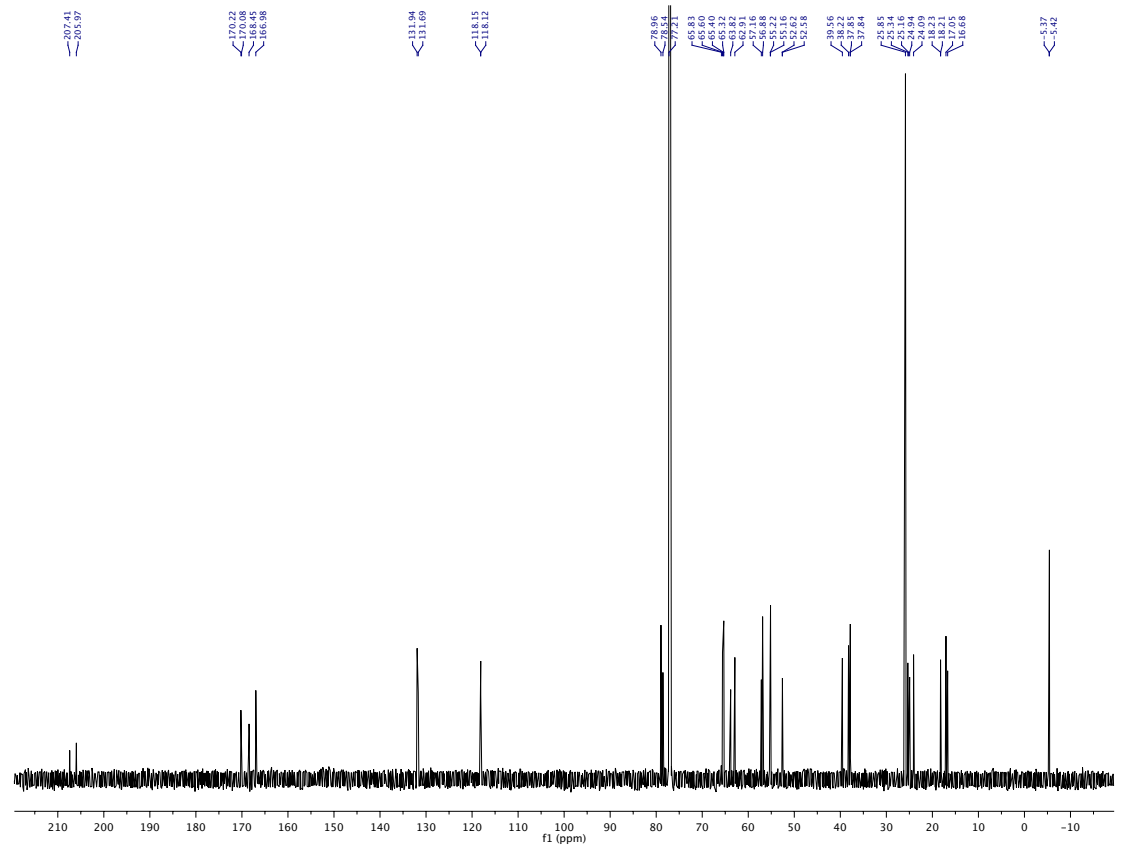

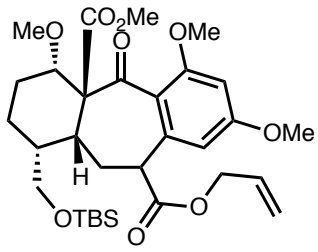
MeO
CO2Me
O
OMe
OMe
H
OTBS
O
O

2.49

f1 (ppm)

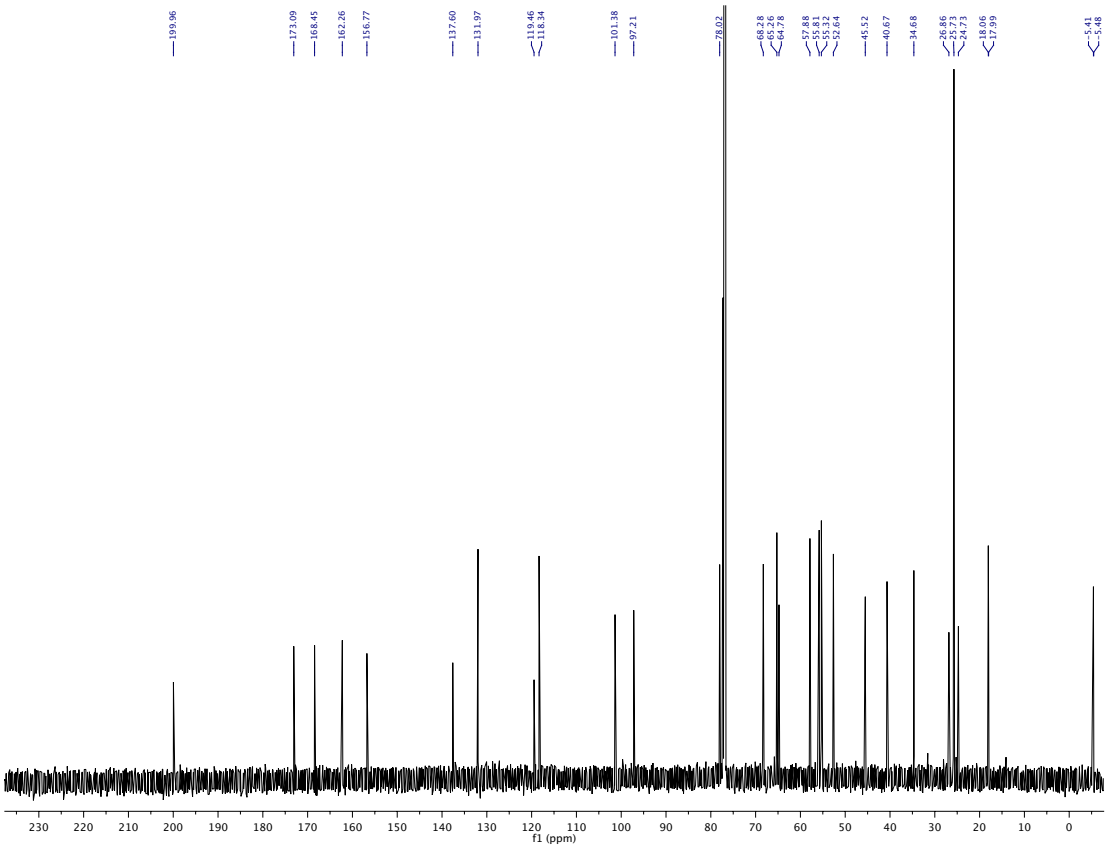
199.96
173.09
168.45
162.26
156.77
137.60
131.97
119.46
118.34
101.38
97.21
78.02
68.28
65.26
64.78
57.88
56.81
55.32
52.64
45.52
40.67
34.68
26.86
25.73
24.73
18.06
17.99
-5.41
-5.48
f1 (ppm)

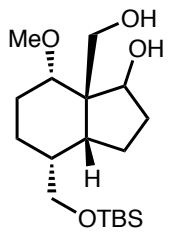
MeO
OH
OH
H
OTBS

2.57

1.04
1.00
1.09
3.28
2.93
0.99
0.93
2.10
9.39
9.61
6.11
10.0 9.5 9.0 8.5 8.0 7.5 7.0 6.5 6.0 5.5 5.0 4.5 4.0 3.5 3.0 2.5 2.0 1.5 1.0 0.5 0.0 -0.5
f1 (ppm)

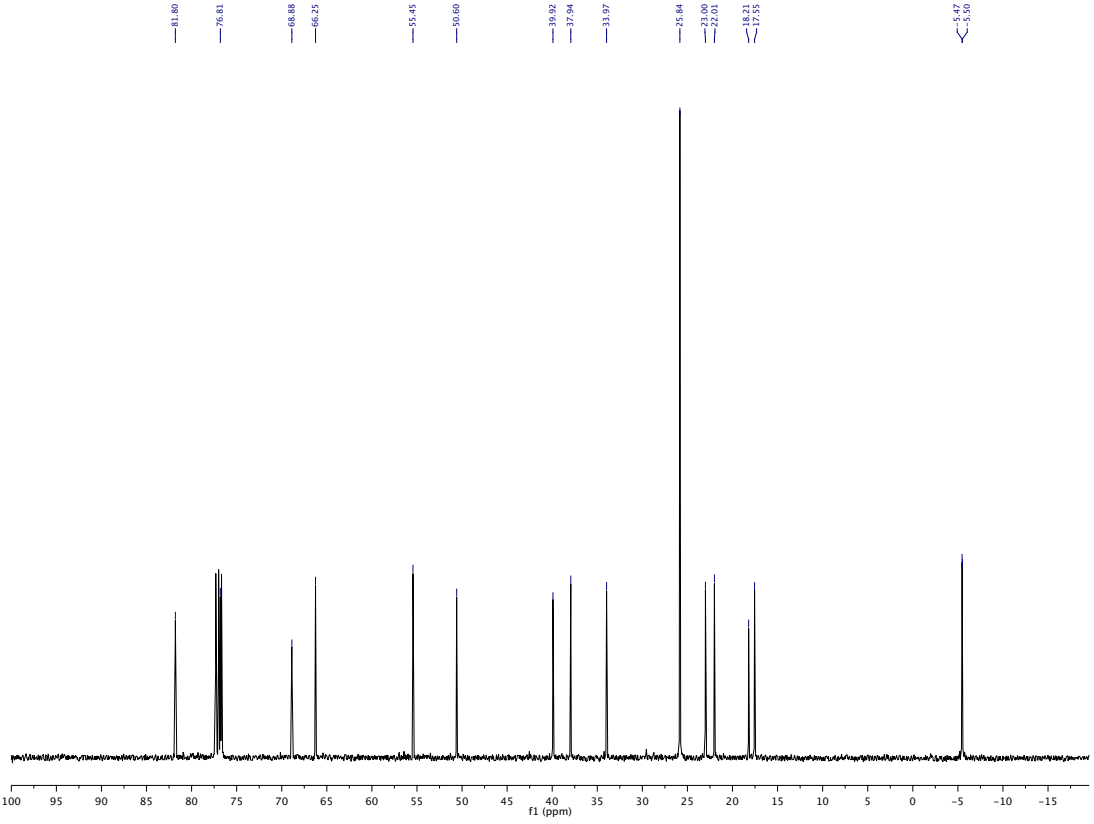
81.80
76.81
68.88
66.25
55.45
50.60
39.92
37.94
33.97
25.84
23.00
22.01
18.21
17.55
-5.47
-5.50
100 95 90 85 80 75 70 65 60 55 50 45 40 35 30 25 20 15 10 5 0 -5 -10 -15
f1 (ppm)

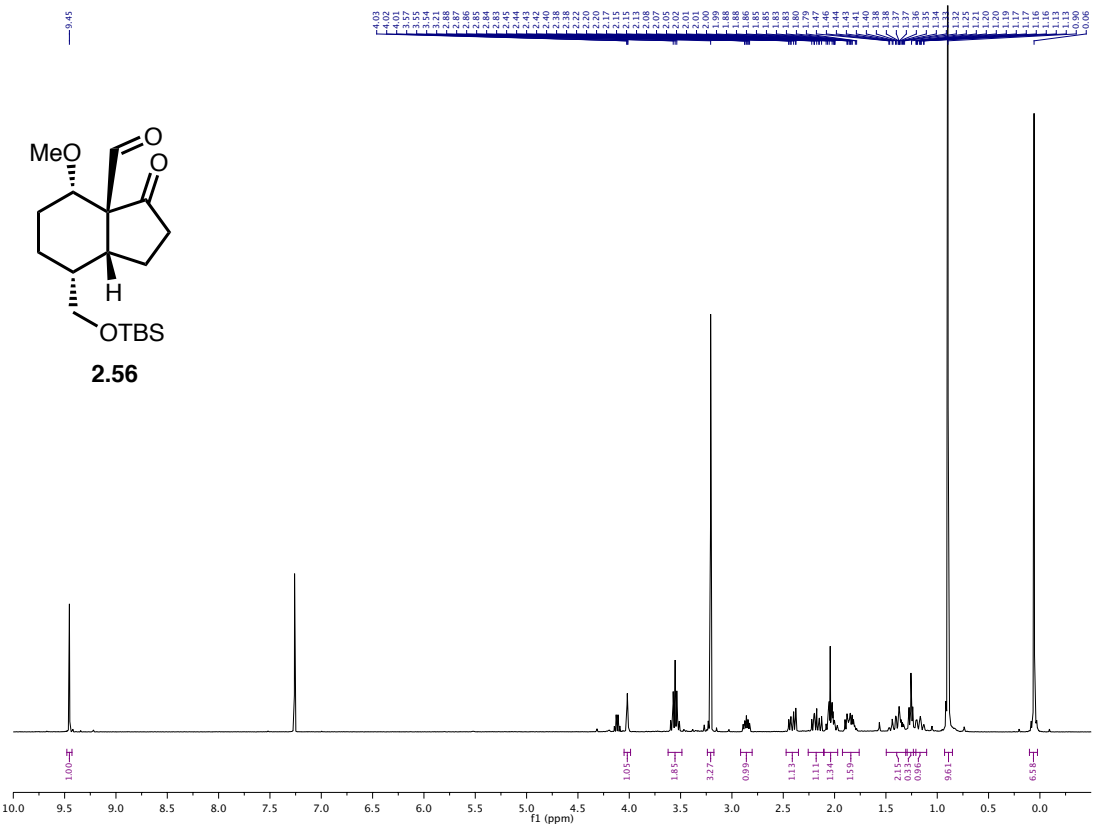
MeO
O
O
H
OTBS
2.56
f1 (ppm)

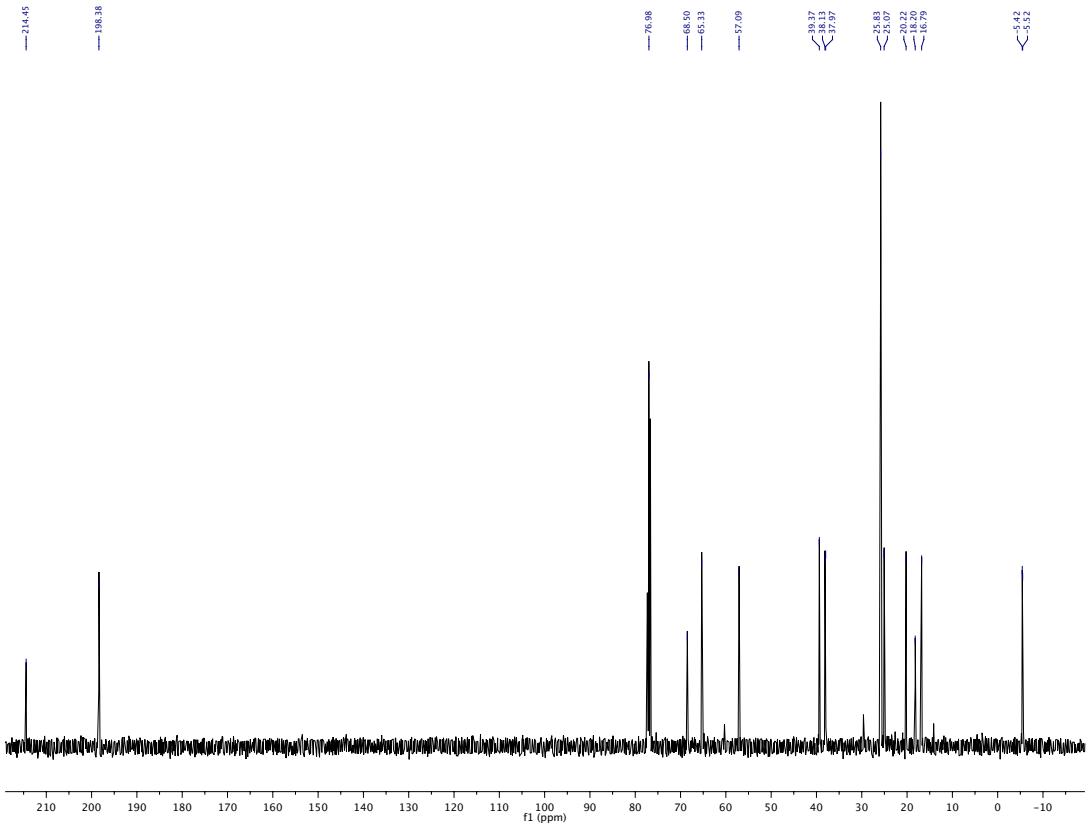
f1 (ppm)

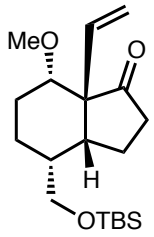

2.54

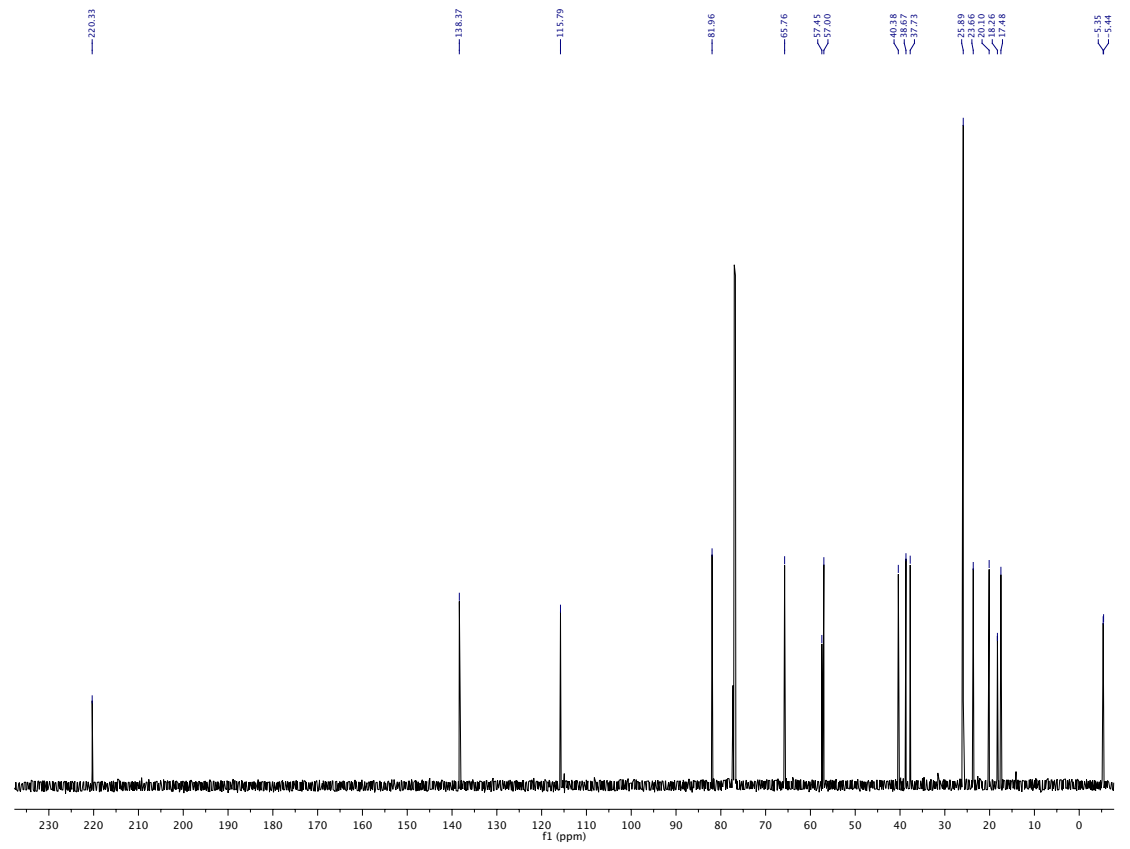

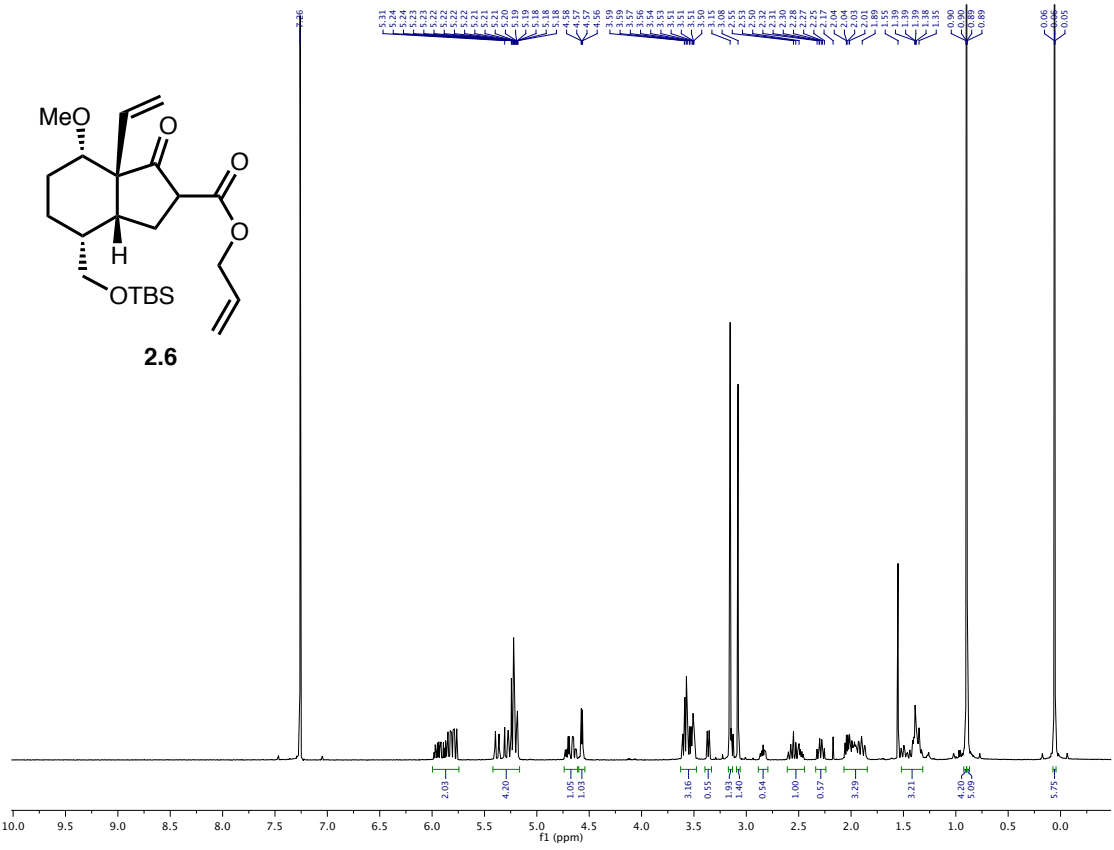

2.6

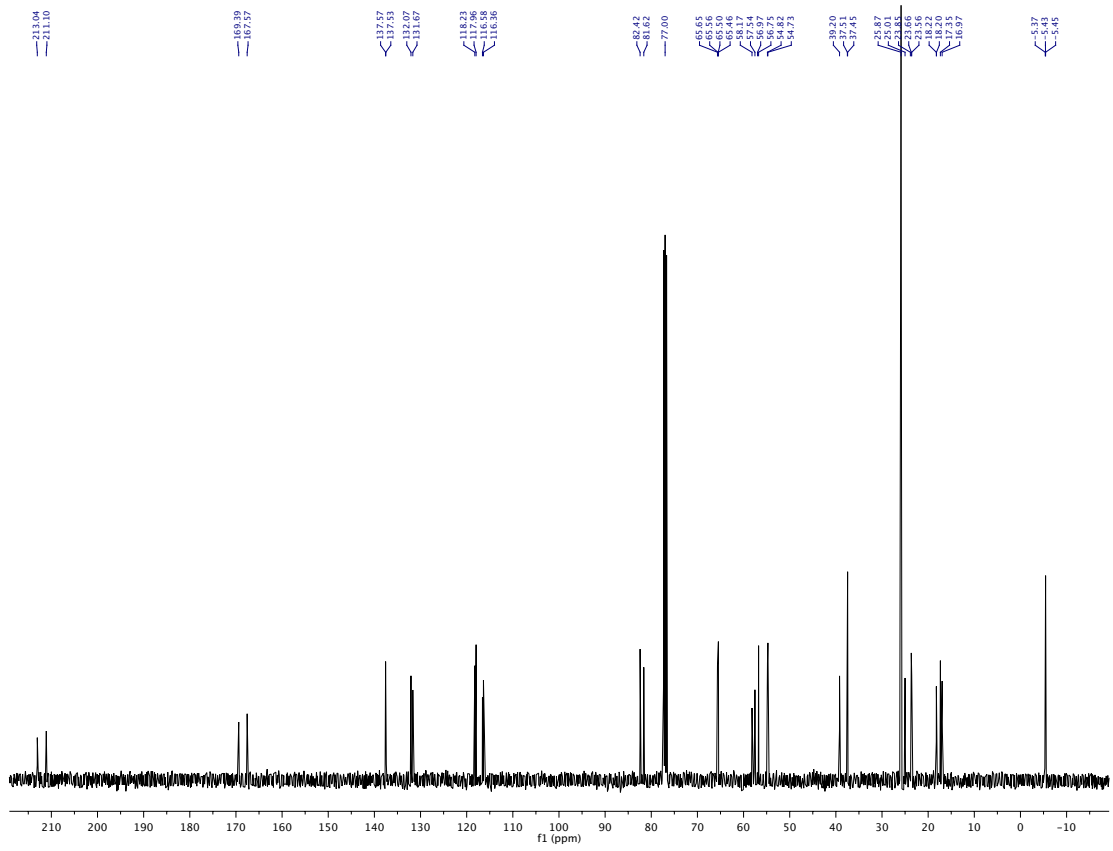

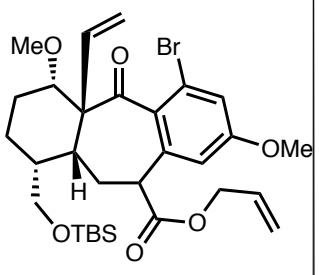

2.59

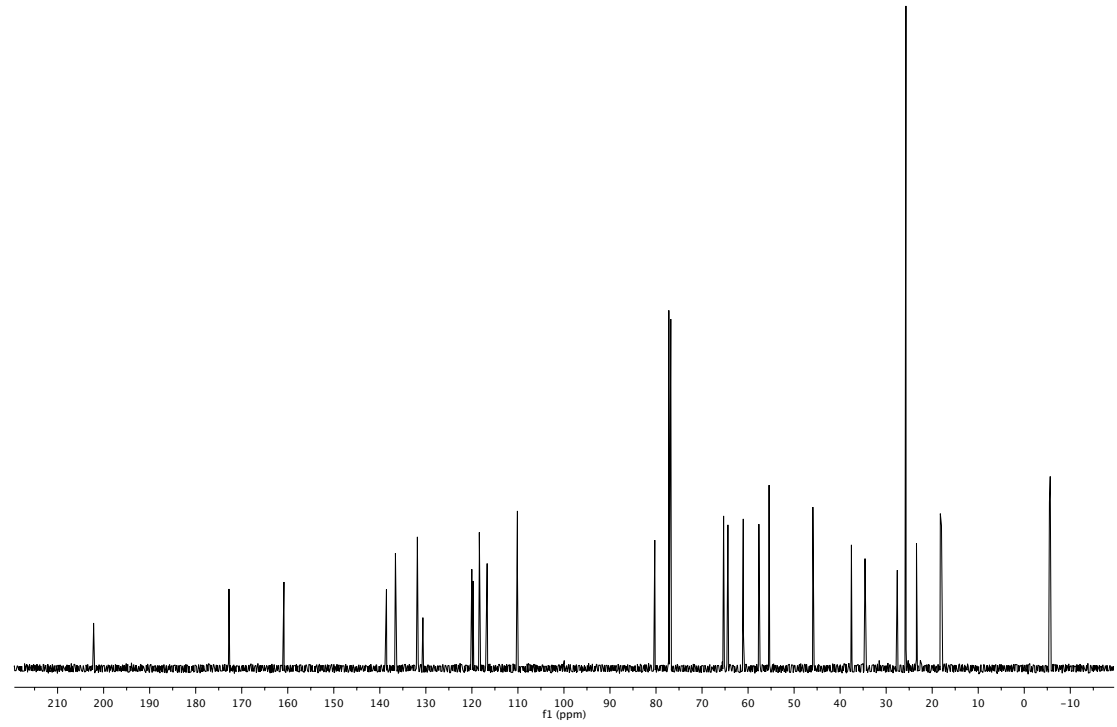

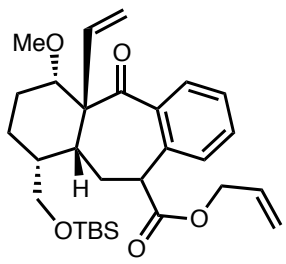
MeO
O
H
OTBS
O
O

2.61

5.34
0.76
0.90
3.02
0.83
1.44
0.86
0.71
2.06
3.06
5.26
4.03
8.94
2.96
2.80
10.0 9.5 9.0 8.5 8.0 7.5 7.0 6.5 6.0 5.5 5.0 4.5 4.0 3.5 3.0 2.5 2.0 1.5 1.0 0.5 0.0 -0.5
f1 (ppm)

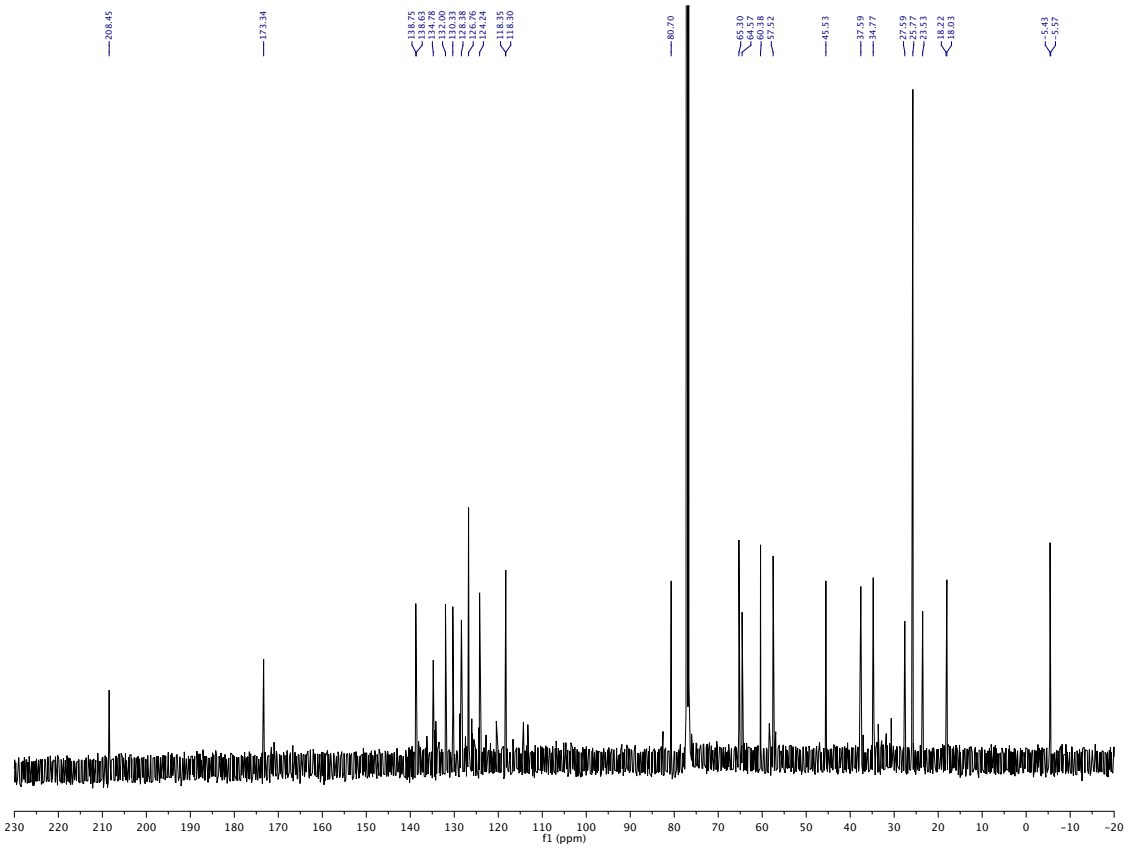
208.45
173.34
138.75
138.63
134.78
132.00
130.33
128.38
126.76
124.24
118.35
118.30
80.70
65.30
64.57
60.38
57.52
45.53
37.59
34.77
27.59
25.77
25.53
18.22
18.03
-5.43
-5.57
230 220 210 200 190 180 170 160 150 140 130 120 110 100 90 80 70 60 50 40 30 20 10 0 -10 -20
f1 (ppm)

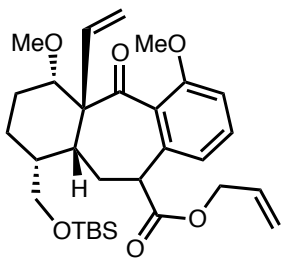
MeO
O
MeO
H
OTBS
O
O
O

2.62

1.78
1.00
1.03
1.01
1.07
2.60
1.03
2.04
0.83
0.54
3.05
2.01
3.09
1.04
0.96
1.04
2.13
2.18
1.07
9.17
3.00
9.5 9.0 8.5 8.0 7.5 7.0 6.5 6.0 5.5 5.0 4.5 4.0 3.5 3.0 2.5 2.0 1.5 1.0 0.5 0.0 -0.5
f1 (ppm)

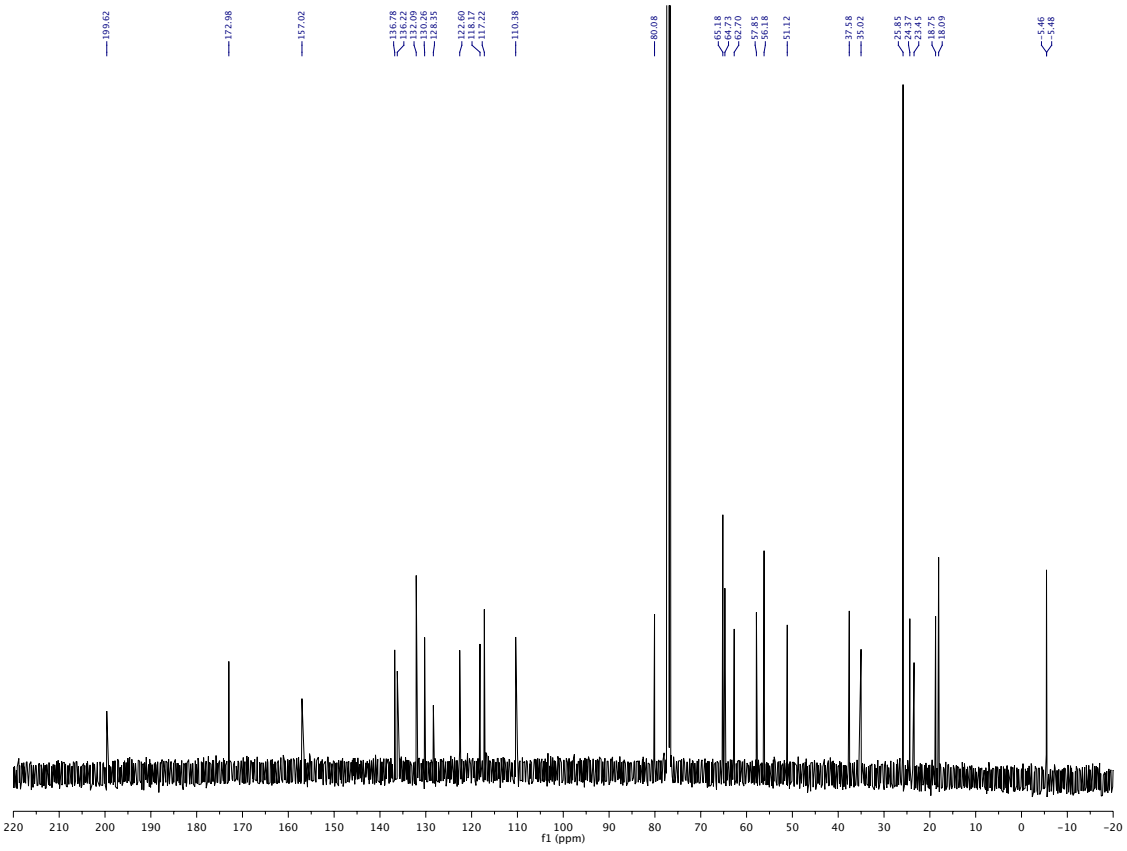
199.62
172.98
157.02
136.78
136.22
132.09
130.26
128.35
122.60
118.17
117.22
110.38
80.08
66.18
62.73
62.70
57.85
56.18
51.12
37.58
35.02
25.85
24.37
23.45
18.75
18.09
-5.46
-5.48
220 210 200 190 180 170 160 150 140 130 120 110 100 90 80 70 60 50 40 30 20 10 0 -10 -20
f1 (ppm)

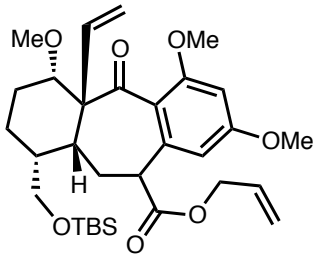
MeO
O
OMe
OMe
H
OTBS
O
O

2.63

0.96
1.00
0.94
1.04
2.75
1.00
2.24
1.92
2.83
2.09
2.72
1.69
3.41
2.25
1.34
8.94
2.87
2.93
10.0 9.5 9.0 8.5 8.0 7.5 7.0 6.5 6.0 5.5 5.0 4.5 4.0 3.5 3.0 2.5 2.0 1.5 1.0 0.5 0.0 -0.5
f1 (ppm)

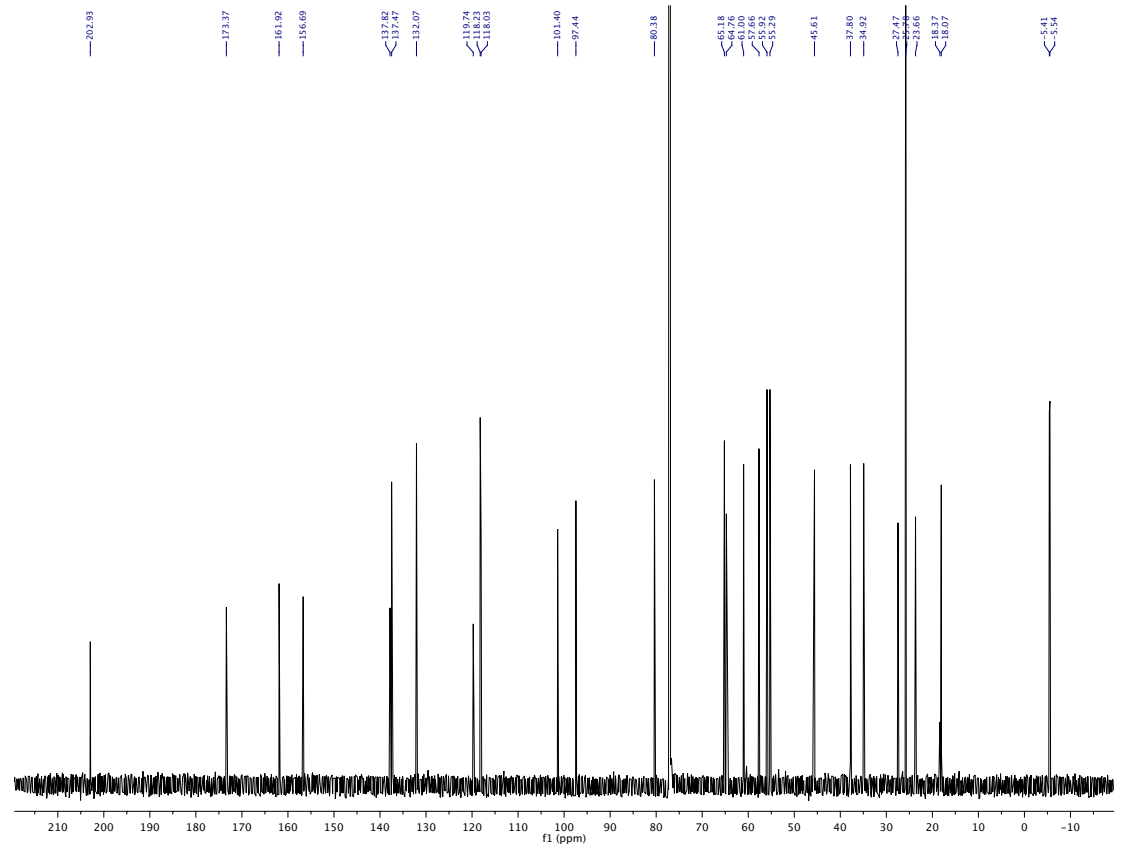
202.93
173.37
161.92
156.69
137.82
137.47
132.07
119.74
118.23
118.03
101.40
97.44
80.38
65.18
64.76
60.00
57.66
55.92
55.29
45.61
37.80
34.92
27.47
26.78
23.66
18.37
18.07
-5.41
-5.54
210 200 190 180 170 160 150 140 130 120 110 100 90 80 70 60 50 40 30 20 10 0 -10
f1 (ppm)

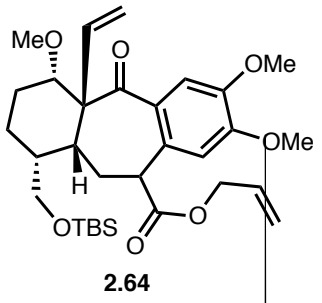
MeO
O
OMe
OMe
H
OTBS
O
O

2.64

0.96
0.94
1.00
0.96
3.93
0.97
2.36
1.76
5.86
2.01
2.81
1.99
3.35
3.21
8.63
3.73
2.85
10.0 9.5 9.0 8.5 8.0 7.5 7.0 6.5 6.0 5.5 5.0 4.5 4.0 3.5 3.0 2.5 2.0 1.5 1.0 0.5 0.0 -0.5
f1 (ppm)

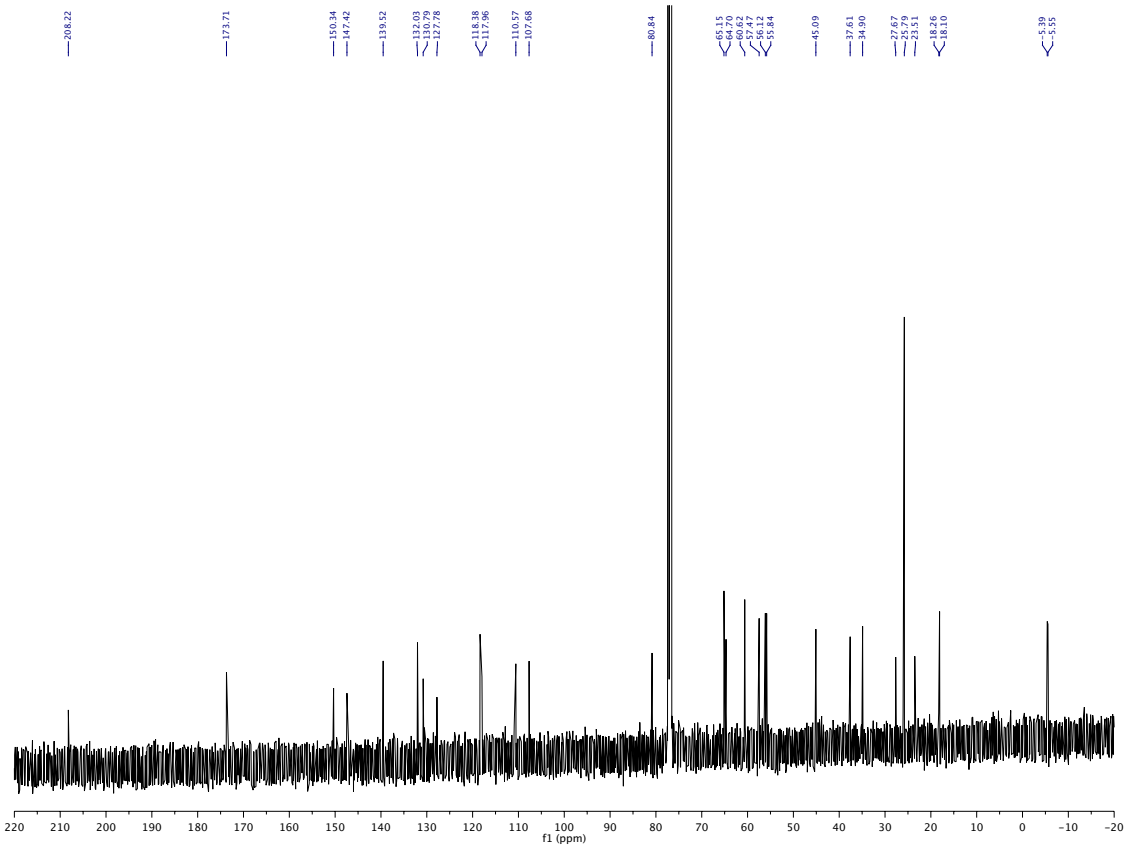
208.22
173.71
150.34
147.42
139.52
132.03
130.79
127.78
118.38
117.96
110.57
107.68
80.84
65.15
64.70
60.62
57.47
56.12
55.84
45.09
37.61
34.90
27.67
25.79
23.51
18.26
18.10
-5.39
-5.55
220 210 200 190 180 170 160 150 140 130 120 110 100 90 80 70 60 50 40 30 20 10 0 -10 -20
f1 (ppm)

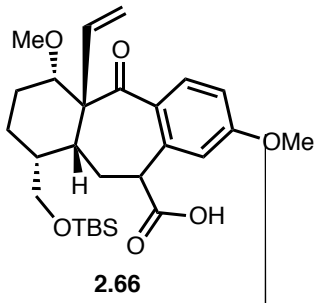
MeO
O
OMe
H
OTBS
OH
O

2.66

0.82
2.01
0.99
0.99
0.99
1.04
0.97
3.08
2.13
3.06
1.05
1.11
3.19
2.08
2.41
9.69
3.10
3.13
10.0 9.5 9.0 8.5 8.0 7.5 7.0 6.5 6.0 5.5 5.0 4.5 4.0 3.5 3.0 2.5 2.0 1.5 1.0 0.5 0.0
f1 (ppm)

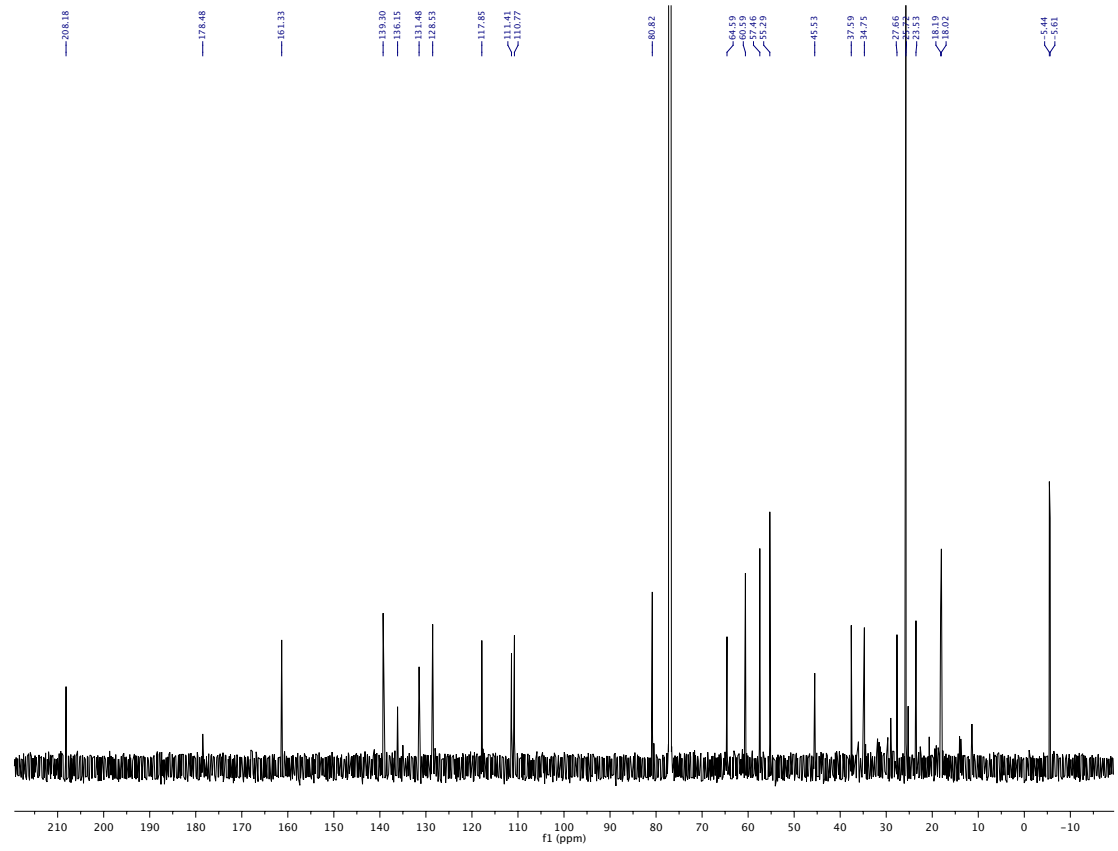
208.18
178.48
161.33
139.30
136.15
131.48
128.53
117.85
111.41
110.77
80.82
64.59
60.50
57.46
55.29
45.53
37.59
34.75
27.66
26.72
23.53
18.19
18.02
-5.44
-5.61
210 200 190 180 170 160 150 140 130 120 110 100 90 80 70 60 50 40 30 20 10 0 -10
f1 (ppm)

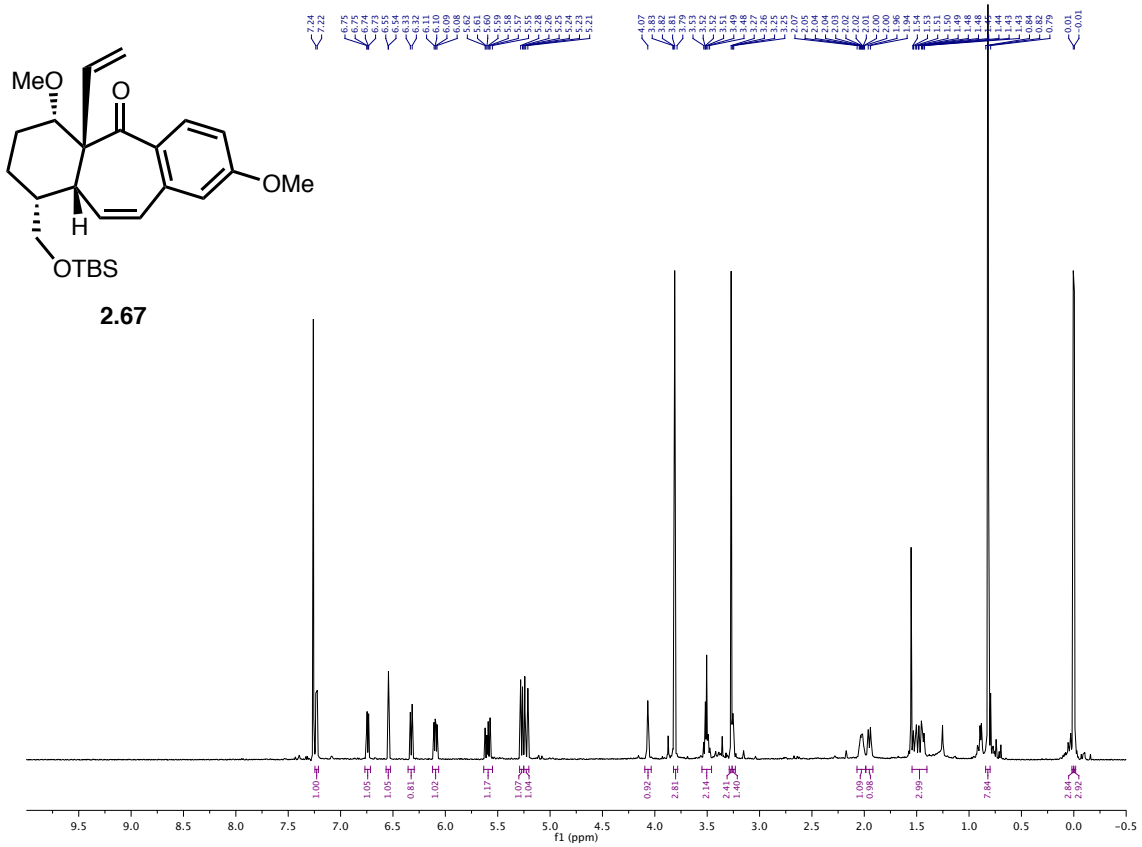

2.67

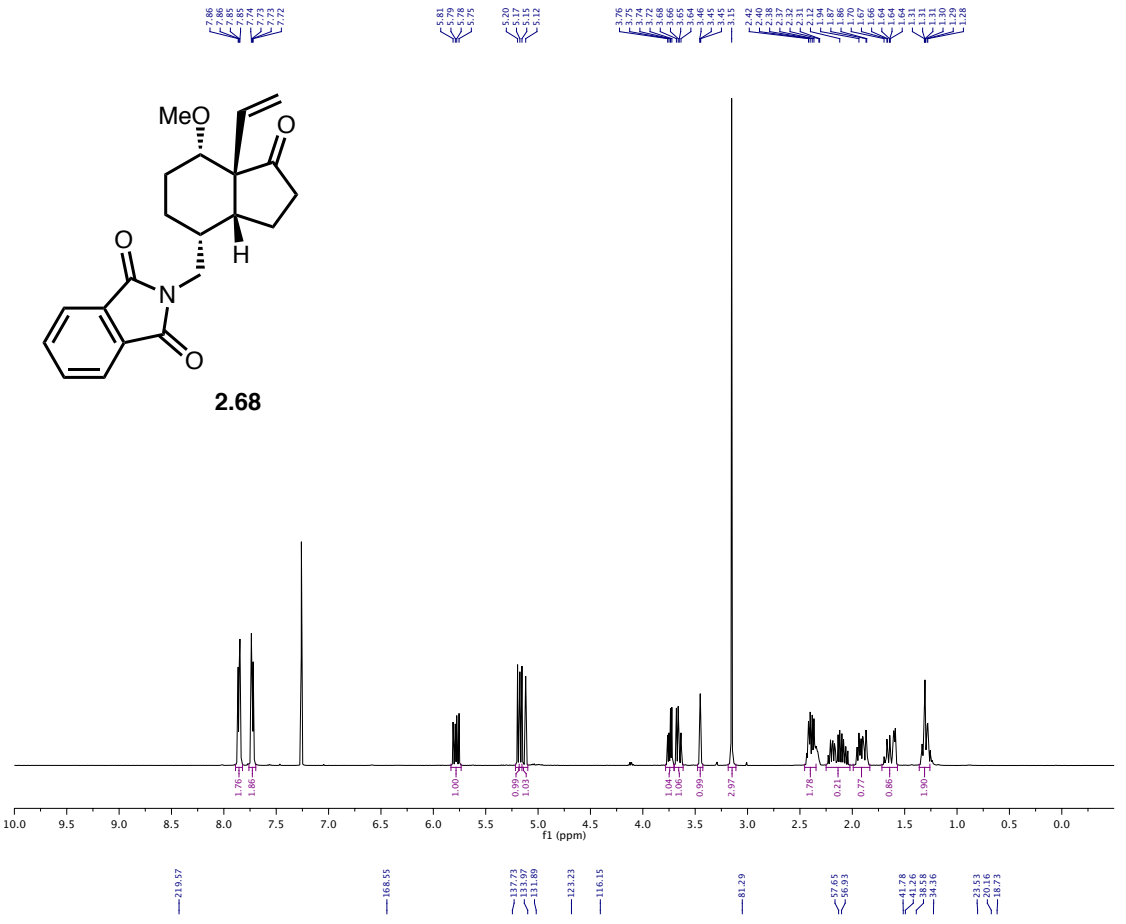
MeO
O
O
N
O
H
7.86
7.86
7.85
7.85
7.74
7.73
7.73
7.72
5.81
5.79
5.78
5.75
5.20
5.17
5.15
5.12
3.76
3.75
3.74
3.72
3.68
3.66
3.65
3.64
3.46
3.45
3.45
3.15
2.42
2.40
2.38
2.37
2.32
2.31
2.12
1.94
1.87
1.86
1.70
1.67
1.66
1.64
1.64
1.64
1.31
1.31
1.30
1.29
1.28
1.76
1.86
1.00
0.99
1.03
1.04
1.06
0.99
2.97
1.78
0.21
0.77
0.86
1.90
f1 (ppm)

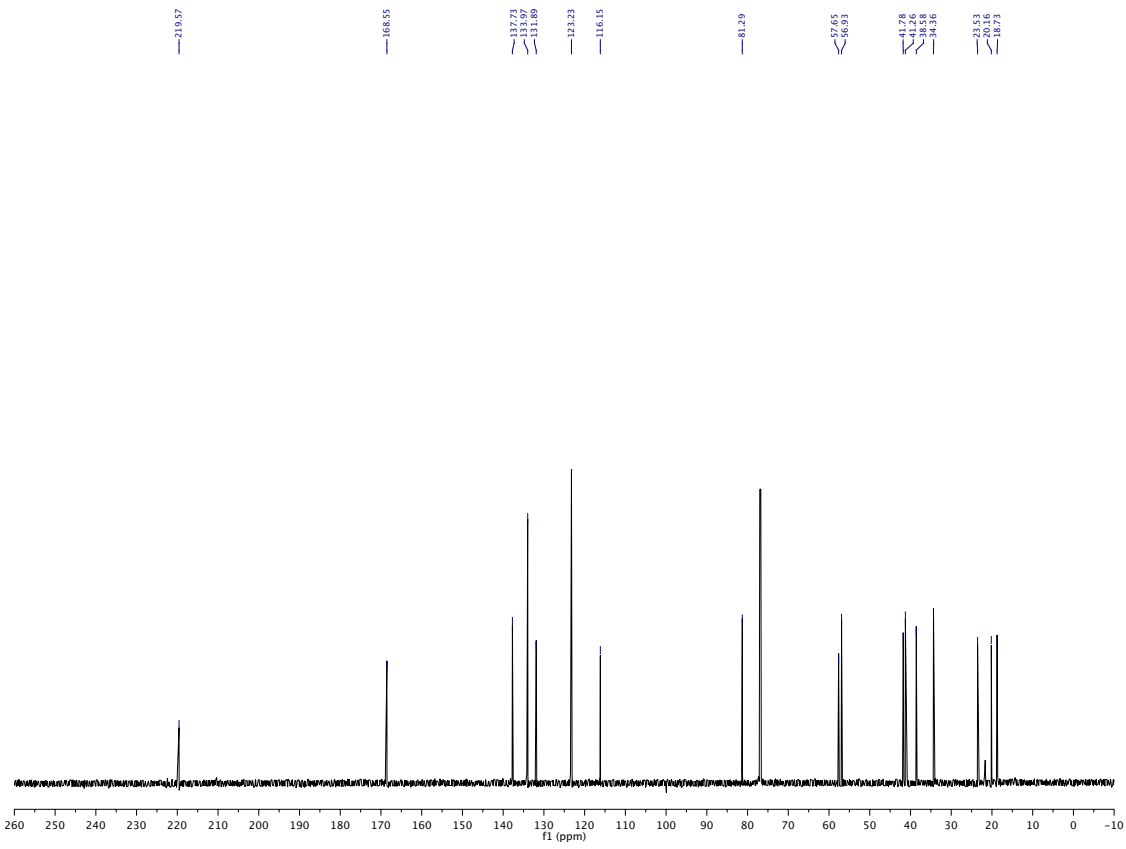
219.57
168.55
137.73
133.97
131.89
123.23
116.15
81.29
57.65
56.93
41.78
41.26
38.56
34.36
23.53
20.16
18.73
f1 (ppm)

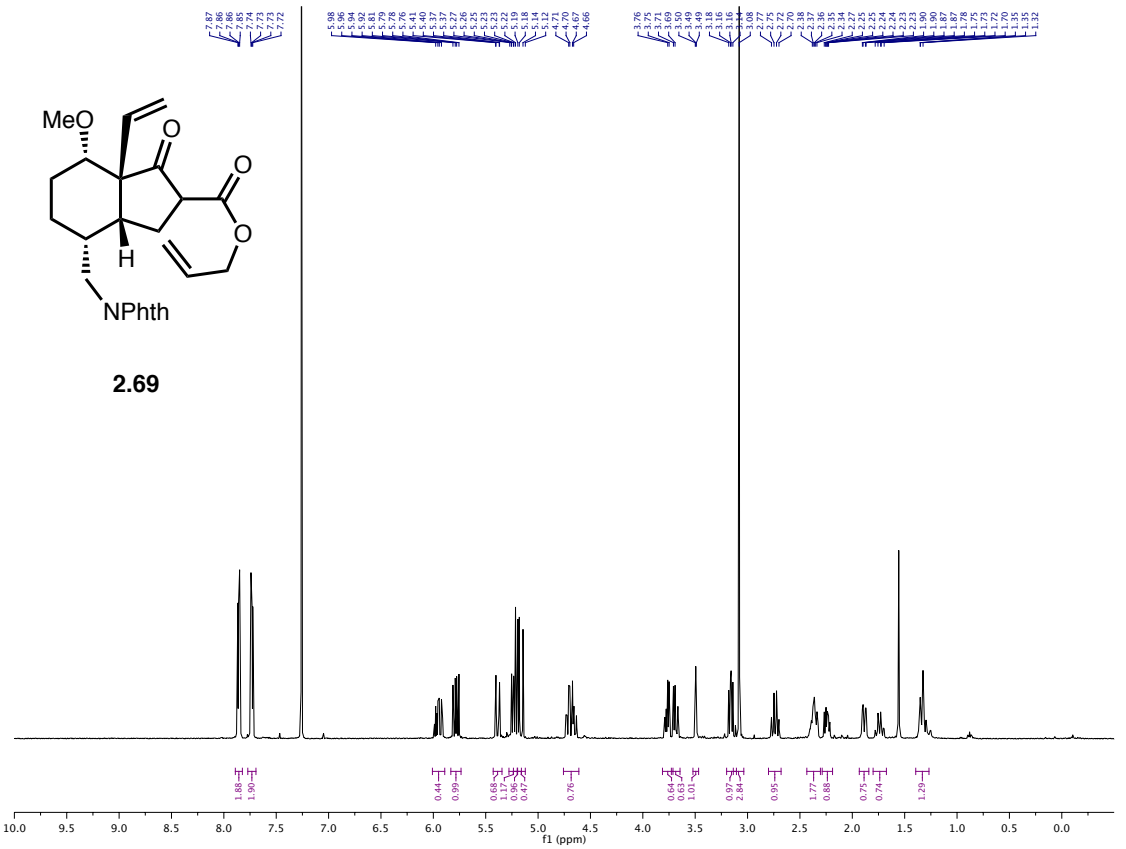

2.69

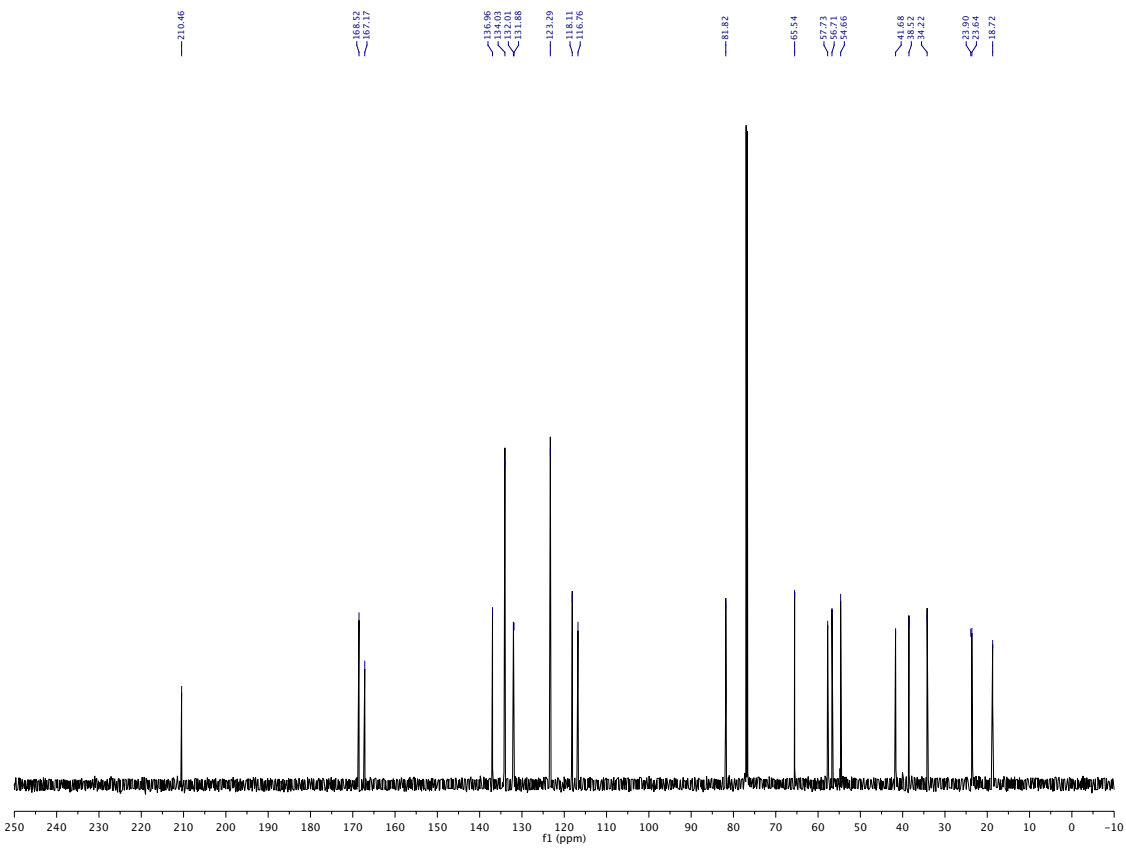

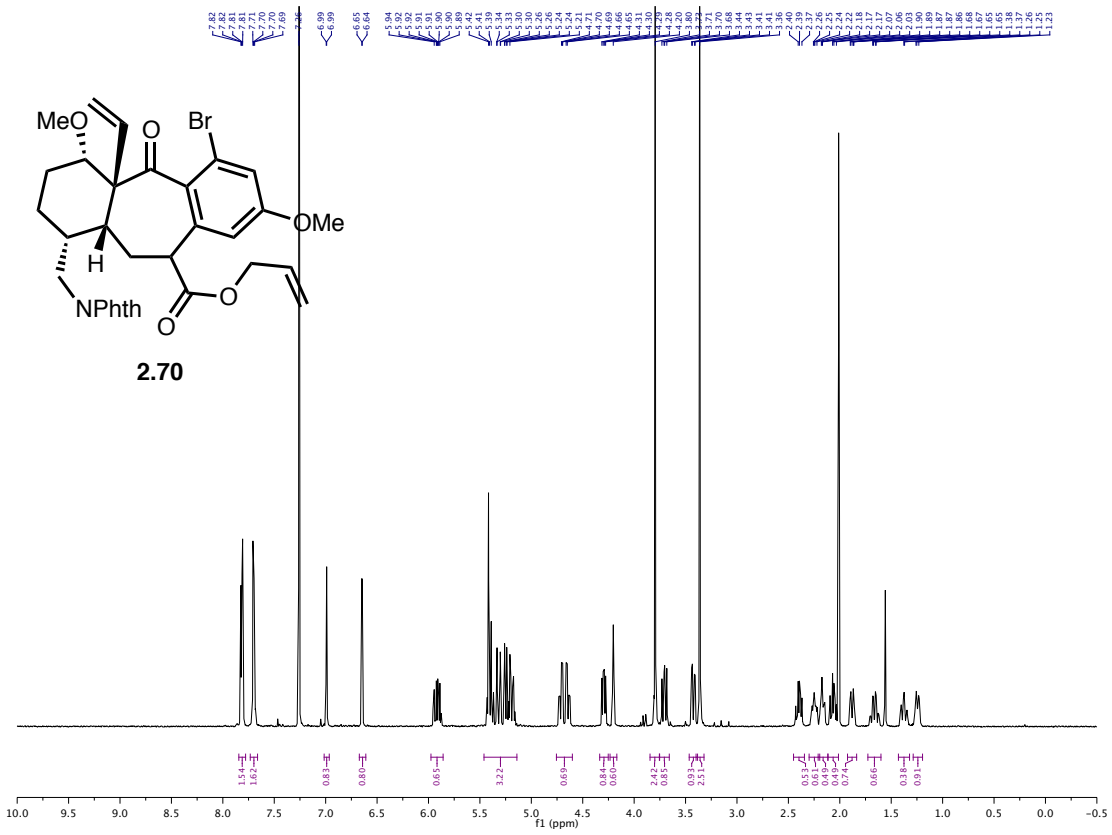
MeO
O
Br
OMe
H
NPhth
O
O
2.70
f1 (ppm)

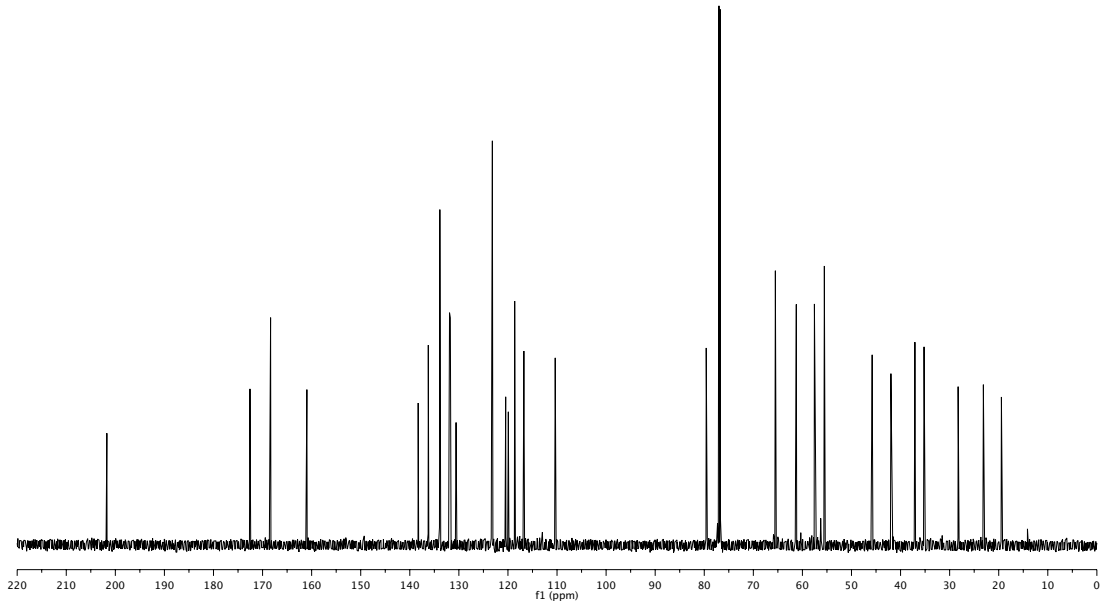
f1 (ppm)

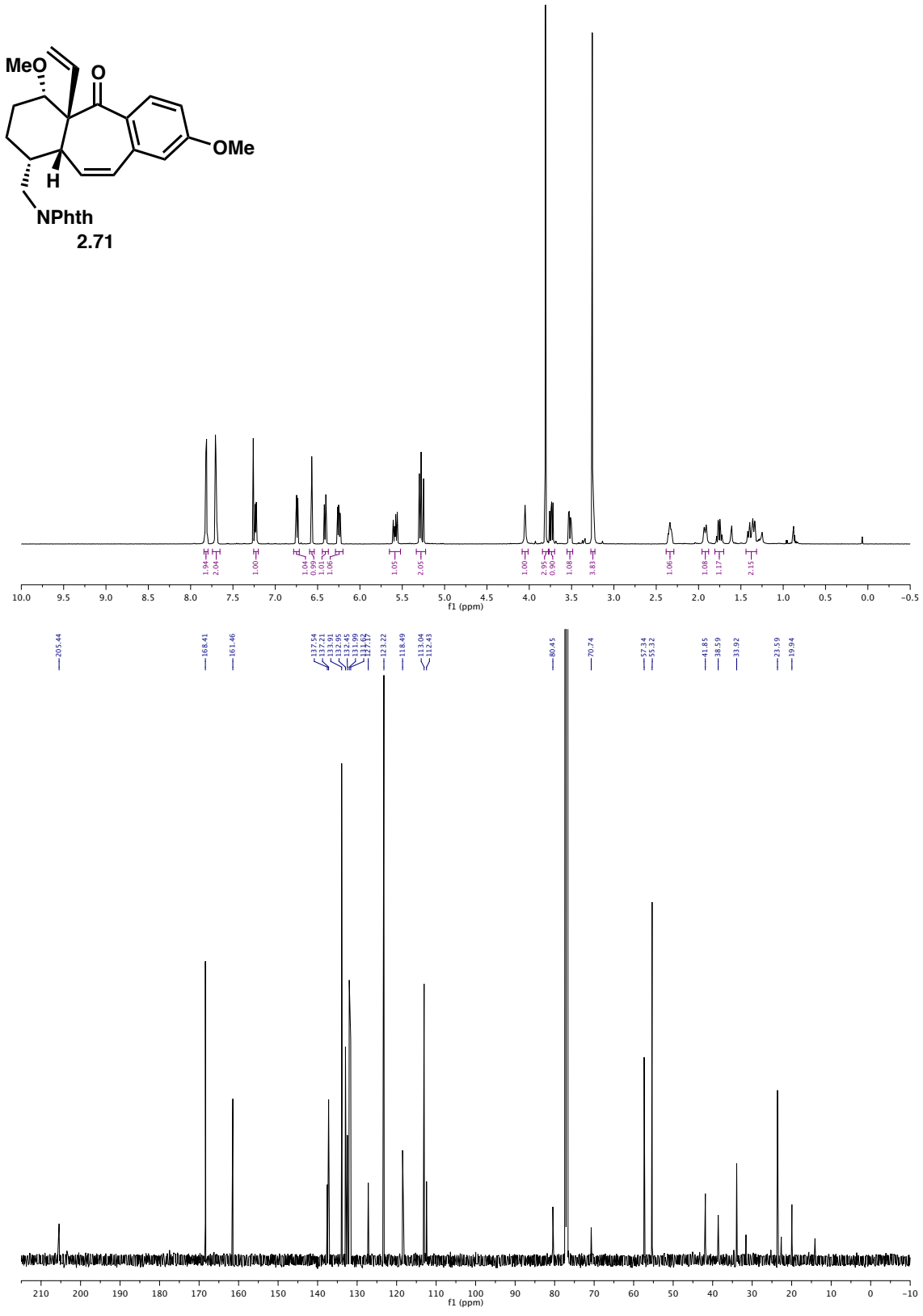
MeO
O
OMe
H
NPhth
2.71
f1 (ppm)
205.44
168.41
161.46
137.54
137.21
133.91
132.86
132.45
131.99
123.22
118.49
113.04
112.43
80.45
70.74
57.34
55.32
41.85
38.59
33.92
23.59
19.94

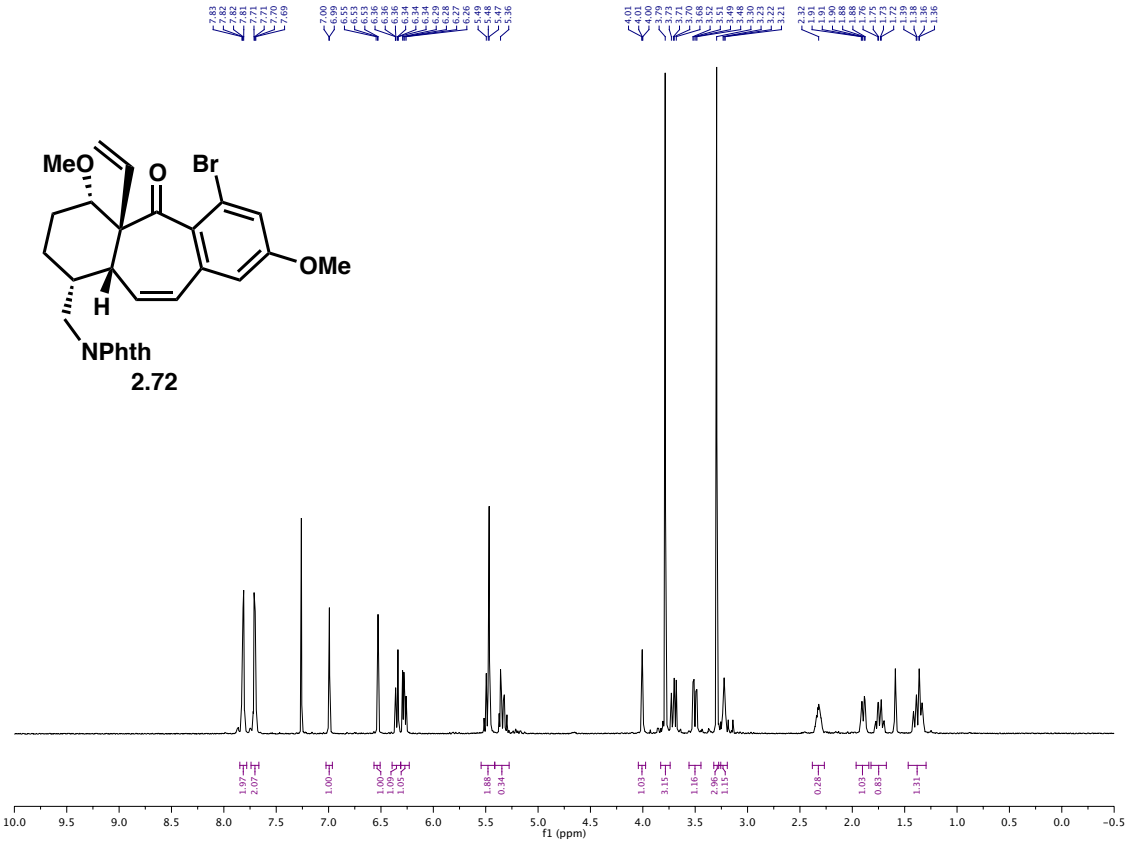
MeO
O
Br
OMe
H
NPhth
2.72
f1 (ppm)

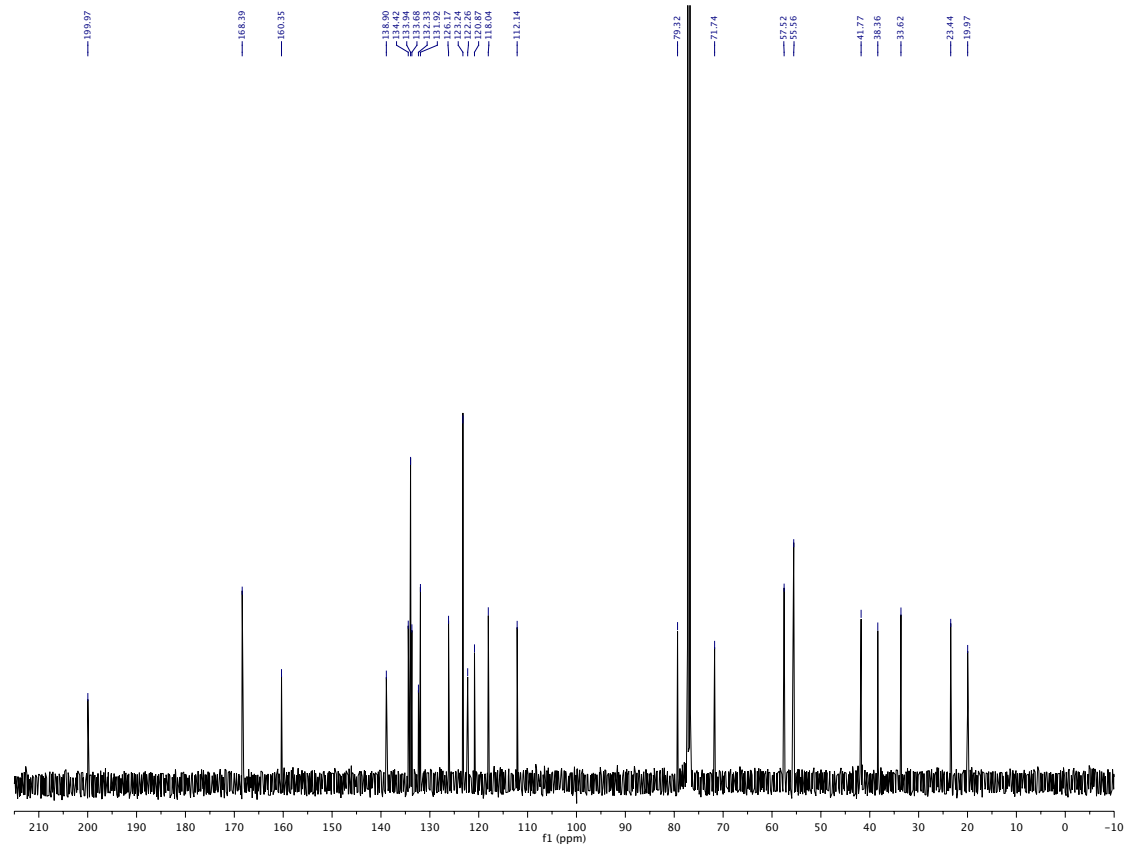
f1 (ppm)

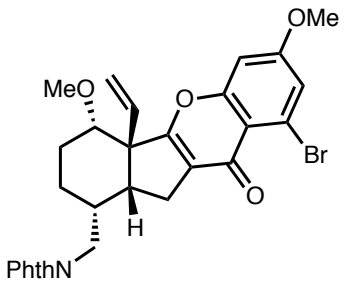
OMe
MeO
O
Br
O
H
PhthN

2.73

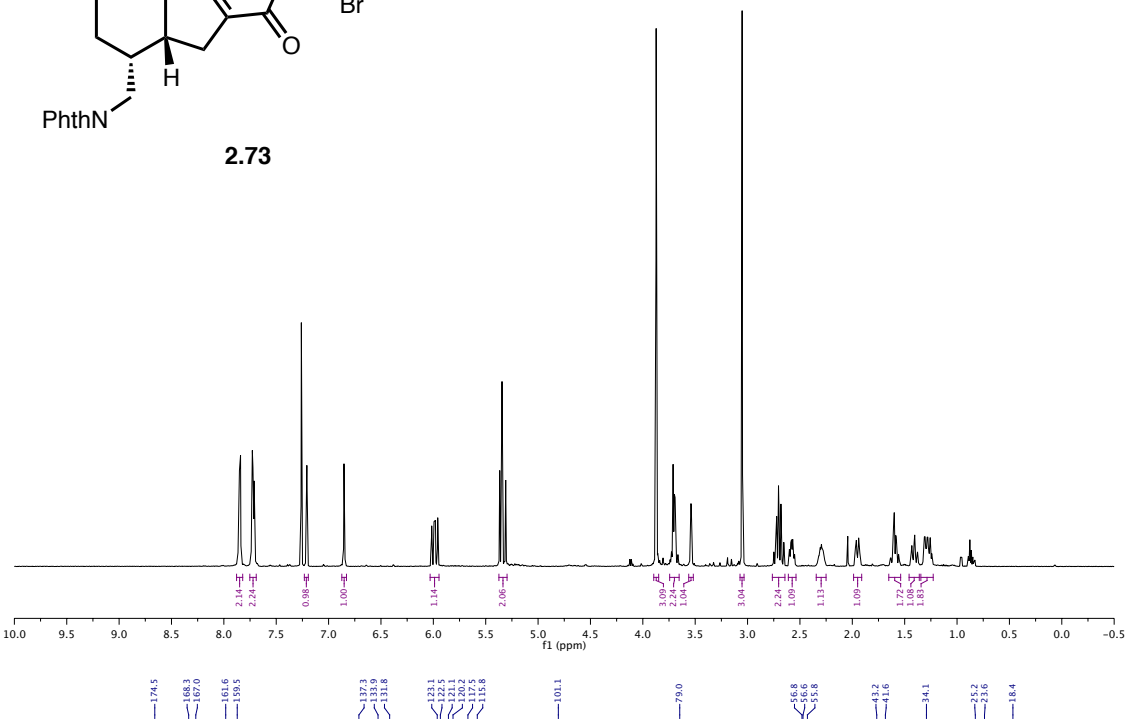
2.14
2.24
0.98
1.00
1.14
2.06
3.09
2.24
1.04
3.04
2.24
1.09
1.13
1.09
1.72
1.08
1.83
10.0 9.5 9.0 8.5 8.0 7.5 7.0 6.5 6.0 5.5 5.0 4.5 4.0 3.5 3.0 2.5 2.0 1.5 1.0 0.5 0.0 -0.5
f1 (ppm)

174.5
168.3
167.0
161.6
159.5
137.3
133.9
131.8
123.1
122.5
121.1
120.2
117.5
115.8
101.1
79.0
56.8
56.6
55.8
43.2
41.6
34.1
25.2
23.6
18.4

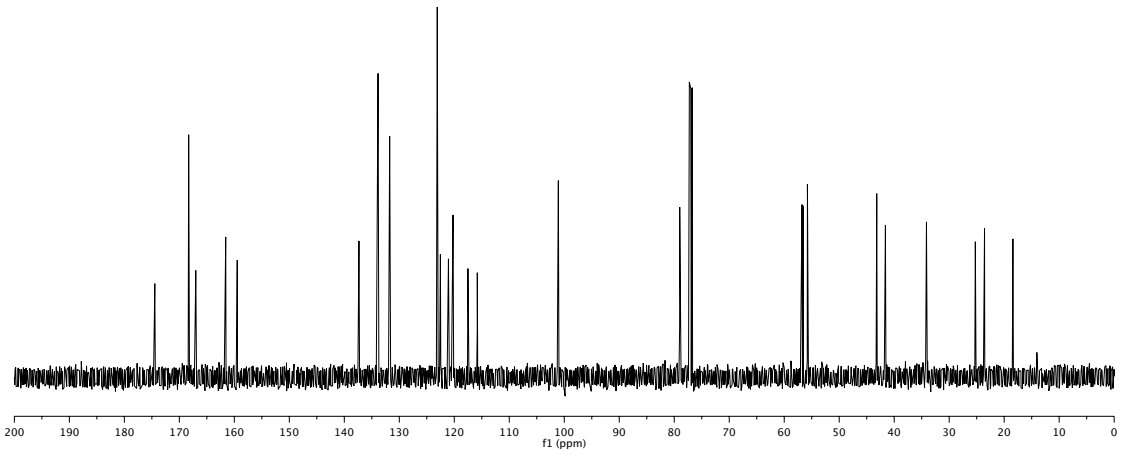
200 190 180 170 160 150 140 130 120 110 100 90 80 70 60 50 40 30 20 10 0
f1 (ppm)

Chapter 3. Azabicycle Completion and Progress toward the Synthesis of Cossonidine

3.1 Introduction

After utilizing an aryne insertion reaction to access variously substituted 6-7-6 tricyclic frameworks, our focus turned to forming the key C–N bonds present in the hetisine diterpenoid alkaloid skeleton. This chapter will discuss our studies toward completion of the azabicycle. Additionally, installation of the methyl group at C4 and subsequent advancement of these methylated compounds will be detailed.

3.2 Initial investigations into C–N bond formation

As described in Chapter 2, we were able to advance hydrindanone derivative **2.41** (Figure 3-1) to three tricyclic compounds. With functional handles at C6 and C20 in place (see **2.67**, **2.71**, and **2.72**), we focused on C–N bond formation to complete the synthesis of the azabicycle core of the hetisine framework.

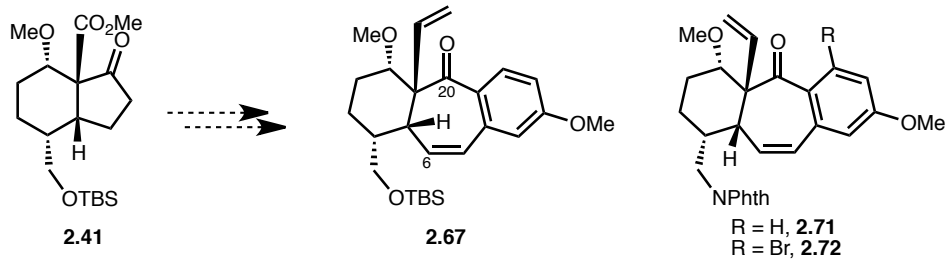

Figure 3-1. Tricyclic substrates for C–N bond formation.

From silyl ether **2.67**, we were able to access **3.1** (Scheme 3-1), in which the nitrogen atom had been incorporated as an azide. Unfortunately, attempts to effect an aza-Wittig/reduction transformation (for C20–N bond formation)[1] or an aziridination/reduction[2] were unsuccessful, returning starting material or the primary amine following reduction of the azide. In the case of phthalimide substrates **2.71** and **2.72**, cleavage of the protecting group proceeded smoothly with hydrazine hydrate in ethanol at room temperature to give primary amines **3.4** and **3.5**. From these substrates, a variety of metal-free and transition metal-catalyzed hydroaminations were attempted (Table 3-1). We investigated both alkene activation conditions, to give iodoamination or aminohydroxylation products (entries 1-2),[3,4] and metal-catalyzed conditions (entries 3-6).[5,6,7] Each was met, however, with the return of starting material.

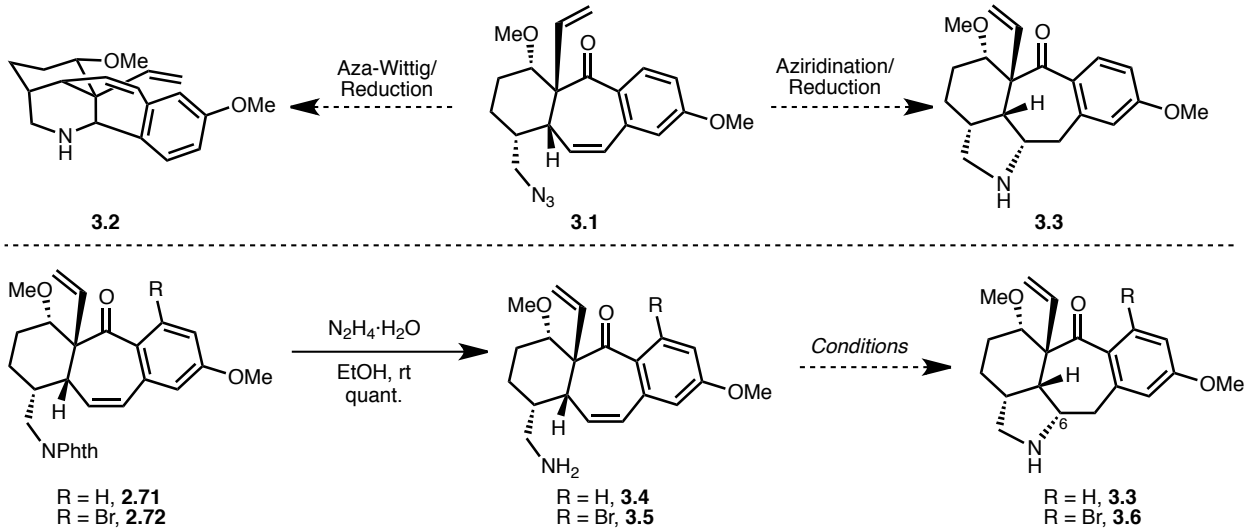

Scheme 3-1. Attempted C–N bond-forming pathways.

Table 3-1. Hydroamination studies on **3.4** and **3.5**.

Entry	Selected Conditions
1	I_2, CH_2Cl_2/$NaHCO_{3(aq)}$
2	BH_3·DMS, I_2, NaOMe, then H_2O_2
3	$Ti(NMe_2)_4$, PhMe, 110 °C
4	Zr ureate complex, PhMe, 110 °C
5	$[Ir(COD)Cl]_2$, Et_3NHCl, 1,4-dioxane, 110 °C
6	BnCl, Ca_2CO_3; $[Ir(COD)Cl]_2$, 1,4-dioxane, 110 °C

In an alternative sequence, the C6–C7 double bond of **2.72** could be epoxidized to give **3.7** (Scheme 3-2). Epoxide **3.7** was in turn subjected to epoxide opening[8] and Meinwald rearrangement[9] conditions to provide the amino alcohol (**3.8**) or diketone (**3.9**), respectively. While attempts to open the epoxide via intramolecular nucleophilic attack of the primary or Boc amine did not proceed and returned starting material, treatment of **3.7** with Lewis acids (e.g. $Cu(OTf)_2$, $Sc(OTf)_3$) did provide the rearranged product (**3.9**). This transformation did not proceed to completion, however, because of the facile and rapid engagement of the C1 methoxy group with the activated epoxide to give **3.10** in an approximately 1:1 ratio (**3.9**:**3.10**).

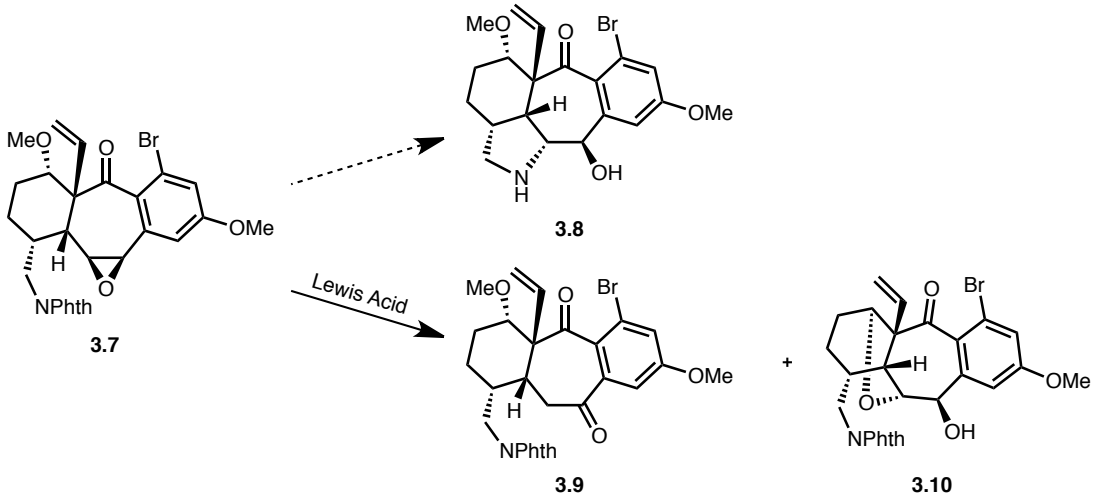

Scheme 3-2. Manipulation of epoxide **3.7**.

Faced with the lack of productive reactivity of the amine with either the double bond or the epoxide in the tricyclic framework, we theorized that the lowest-energy conformation of **3.7** may be such that the methylene amine functionality resided in the equatorial position, therefore pointing it directly away from the C6 position (Figure 3-2). This is supported by the facile reaction of the C1 methoxy group with the epoxide ring in the presence of Lewis and Brønsted acids to provide cyclic ether **3.10**.

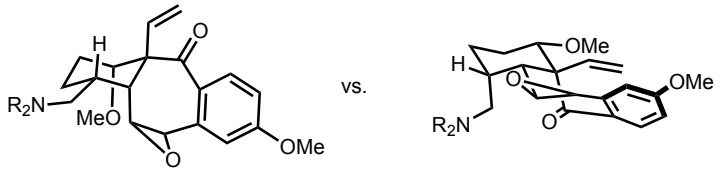

3.7A
Favored conformation

3.7B

Figure 3-2. Conformational challenges to C6–N bond formation from **3.7** (R_2 = phthalimide).

To disfavor conformer **3.7A**, and cognizant of other work in our laboratory in which C–N bonds had been formed from a hydrindanone system,[10] we postulated that the C6–N bond could be formed prior to the benzyne insertion and a β-ketoester such as **3.12** could be accessed (Scheme 3-3). Starting from **2.54**, the diprotected nitrogen was introduced using a Mitsunobu reaction with BocNHNs,[11] which proceeded smoothly in 85% yield over 2 steps to provide **3.14**. Saegusa-Ito oxidation[12] delivered the enone (**3.15**), which, upon treatment with trifluoroacetic acid, underwent Boc group cleavage and subsequent 1,4-addition in the same pot to arrive at tricycle **3.16** in 89% yield. Excited to have formed one of the requisite C–N bonds, we needed to now form the β-ketoester. Thus, **3.16** was subjected to a variety of acylation conditions (different bases, temperatures, etc.), but only a trace amount of **3.17** was observed, with the majority of material accounted for by elimination back to the enone and acylation of the resulting sulfonamide. We also investigated the installation of the allyl ester before cyclization on enone **3.15**, but those attempts were unfruitful. Finally, with the knowledge that silyl enol ethers could undergo formal [2+2] cycloadditions with benzynes to form cyclobutenols,[13] we examined the use of **3.18** in that context. In the end, we were unable to advance **3.16**, prompting us to turn to C20–N bond formation as the initial C–N bond forming step.

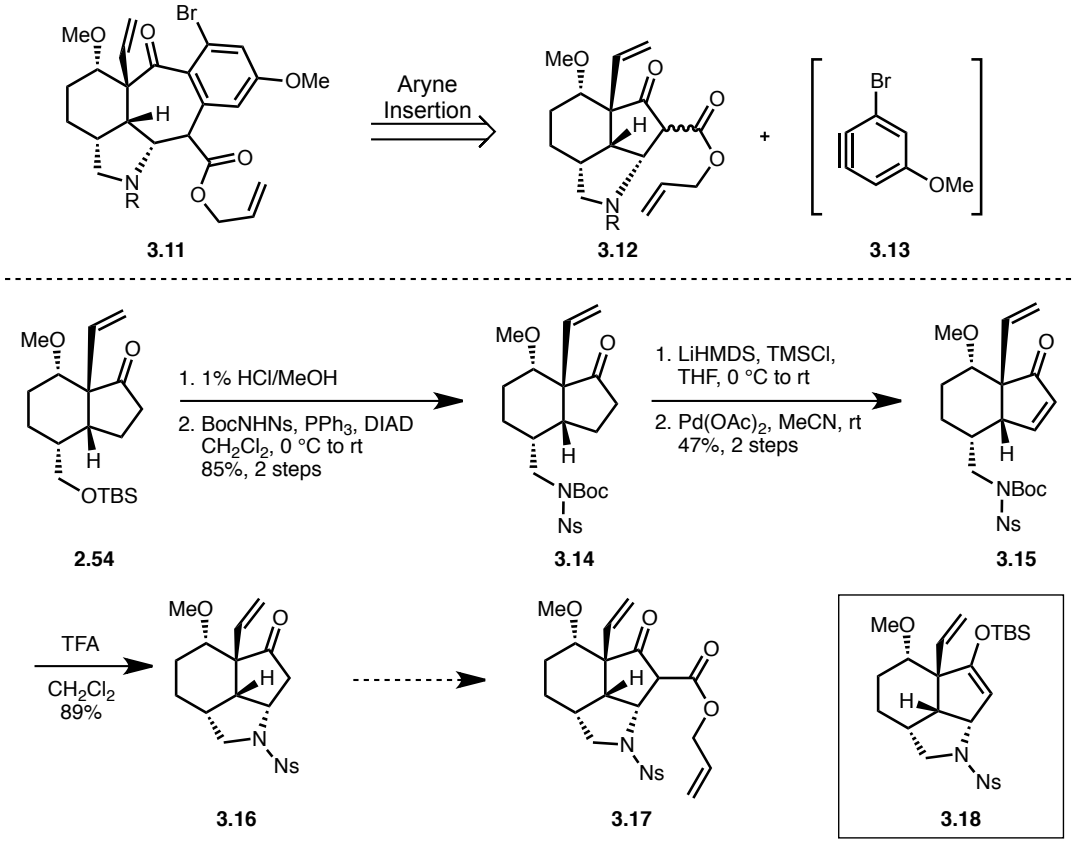

Scheme 3-3. Alternative retrosynthesis and synthesis of 6-5-5 tricycle **3.16**.

3.3 Construction of the hetisine azabicycle

Previous work in our group has shown that the C20–N bond could be formed effectively using a mild set of conditions. In studies toward navirine and other hetisine-type diterpenoid alkaloids (see Chapter 1.4),[14] it was shown that **3.19** (Scheme 3-4), a similar tricyclic substrate to the one accessed using the benzyne insertion chemistry, could be reduced with lithium aluminum hydride to provide the corresponding amino alcohol, which could then be protected as the *tert*-butyl carbamate to give **3.20**. Activation of the hydroxyl group in **3.20** with thionyl chloride at room temperature led to ring closure to give **3.21** in good yield.

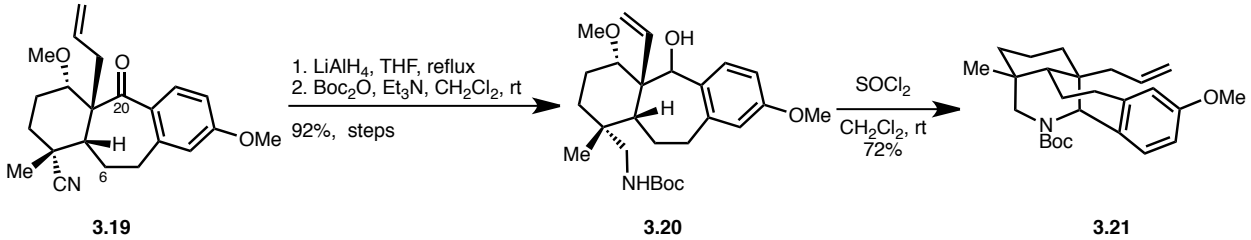

Scheme 3-4. Sarpong group precedent for C20–N bond formation.

To evaluate this transformation for our tricycle, we began with primary amine **3.5** (Scheme 3-5), obtained from the deprotection of **2.72** with hydrazine hydrate. The crude amine was then treated with excess $LiAlH_4$ in THF at 70 °C for 4 h and it was anticipated that we

would arrive at the analogous amino alcohol (not shown). The same conditions resulted in loss of the bromine atom that had served as an aryne directing group.[15] Several mechanisms have been proposed for the reduction of aryl halides with $LiAlH_4$, including S_NAr or sigma-bond metathesis, but radical trap[16] experiments have shown that a single electron mechanism may be at play. EPR experiments with alkyl halides have also shown the presence of radical intermediates in that pathway as well.[17] Taking what we expected to be the secondary alcohol, we subjected it to the protection/cyclization sequence. When it appeared that the corresponding alkyl chloride had been isolated after treatment with thionyl chloride, that intermediate was subjected to AgOTf to induce ionization. To our delight, we were able to confirm the cyclization product (**3.23**) through X-ray crystallography of the *p*-nitrobenzoyl derivative (**3.24**).

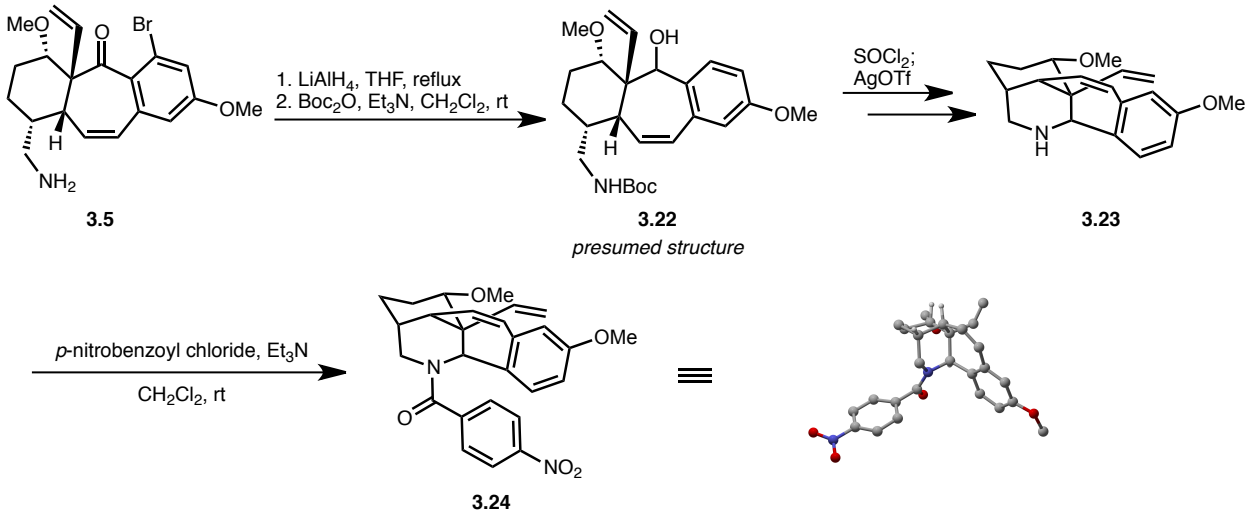

3.5 **3.22** *presumed structure* **3.23**

3.24

Scheme 3-5. Reduction and cyclization of **3.5** and CylView representation of **3.24** (most hydrogen atoms removed for clarity).

However, in the process of reproducing the ring closure sequence and characterizing **3.22**, it became clear that the product of reduction of **3.5** was not, in fact, the amino alcohol. Instead, NMR studies (COSY, DEPT, HSQC, and HMBC) coupled with direct acylation of the reduction product for comparison to **3.24** confirmed that the actual product following reduction of **3.5** was **3.23**, in which the C6–N bond had already been formed. It has been shown by Baik and coworkers that benzylic hydroxyl groups can be reduced to the methylene in the presence of $LiAlH_4$ at reflux when there is an electron-donating group in the *para* position on the arene (e.g., **3.25**, Scheme 3-6).[18] This reduction presumably proceeds through a *p*-quinone methide intermediate such as **3.26**. In our case, rather than the quinone methide being reduced, the primary amine is likely situated close enough that it can immediately engage to form the C–N bond (see **3.28** → **3.23**, bolded bond). This unanticipated, but effective, direct bond formation, rendered the chlorination unnecessary.

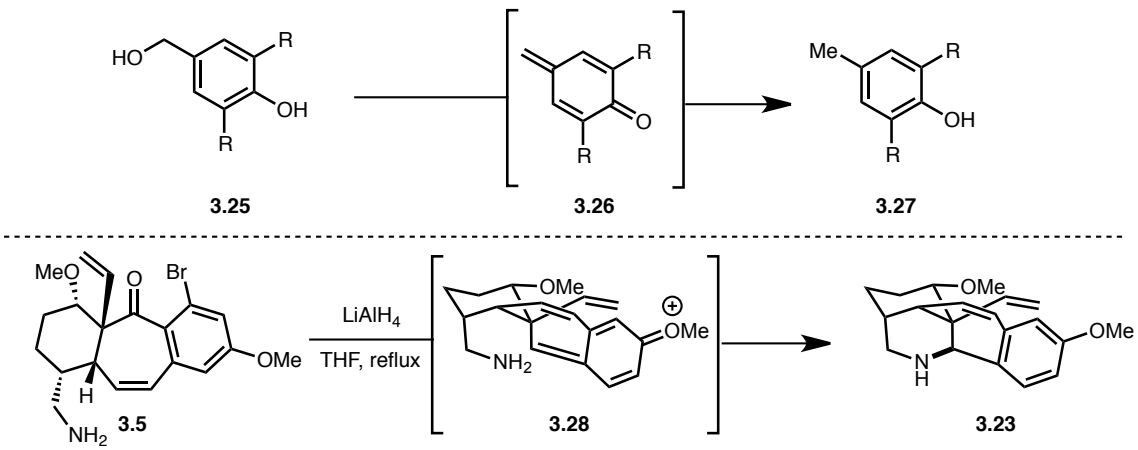

Scheme 3-6. Baik reduction of benzylic hydroxyl groups with LAH and application to **3.5**.

With the C20–N bond in place, we were encouraged by the degradation studies of Okamoto (see Chapter 1.3) that formation of the C6–N bond would be energetically favorable. To pursue this bond formation, our first attempts to effect a hydroamination from **3.23** with Schafer's tethered (bis)ureate Zr complex[19] or activation with NIS[20] did not deliver the desired product. At this time, we were intrigued by a light-mediated hydroamination employed by Trost in syntheses of morphine and codeine[21] (Scheme 3-7). Nitrogen-centered radicals are often used to effect cyclization and can be generated from a variety of precursors.[22] Additionally, it has been shown that lithium amides can react with alkenes to achieve hydroamination, albeit in low yields over long periods of time.[23] These transformations have been shown to proceed through a single electron transfer (SET) mechanism. Newcomb and coworkers have studied the generation and reactivity of nitrogen-centered radicals from lithium amides.[24] In their studies, the lithium amides were oxidized either electrochemically or through the use of organic oxidants (e.g., *(E)*-2-*tert*-butyl-3-phenyloxaziridine (**3.31**) and thianthrene radical cation (**3.32**), Scheme 3-7). Several years later, Tokuda and Suginome showed that anodic oxidation of lithium dialkylamides to the nitrogen-centered radical could also by executed and applied to synthesis.[25] With this reactivity in mind, Trost and coworkers treated secondary amine (**3.33**) with *in situ*-generated LDA in the presence of light (150 W tungsten lamp at a distance of 0.5m) and obtained codeine as the clean hydroamination product (**3.34**).

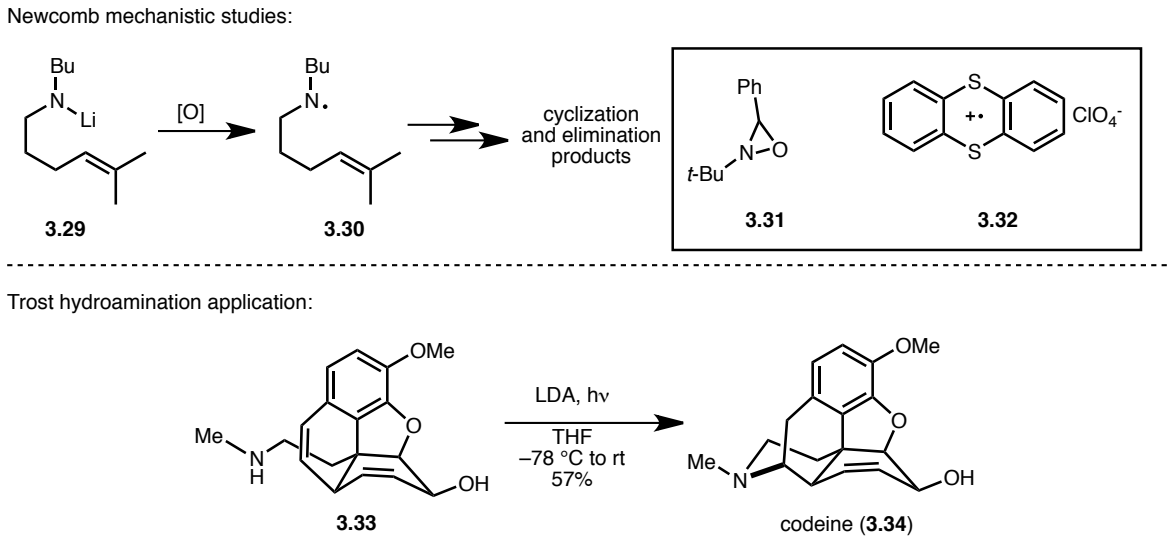

Scheme 3-7. Study of nitrogen–centered radicals from lithium amides; Light-mediated hydroamination.

Gratifyingly, these hydroamination conditions easily translated to our system, and subjection of **3.23** to these conditions delivered **3.35** in 88% yield (Scheme 3-8). With this second C–N bond formed, we were able to secure the azabicyclic portion of the hetisine framework (see Figure 1-3, Chapter 1.4). With **3.35** in hand, we had arrived at a substrate analogous to the late-stage intermediate utilized by Gin in the synthesis of nominine (Scheme 1-28, Chapter 1.4). In accordance with Gin's synthesis endgame, **3.35** was reduced using a Birch reduction (dissolving metal conditions) to give enone **3.36** after hydrolysis of the resulting enol ether (Scheme 3-8). Treatment of **3.36** with pyrrolidine in methanol at 90 °C delivered [2.2.2] bicycle **3.37** in 75% yield through an intramolecular Diels–Alder reaction, thereby completing the hetisine framework. In order to avoid decomposition and rearomatization under the reaction conditions, it was necessary to redistill the pyrrolidine and degas the reaction mixture using freeze-pump-thaw cycles.

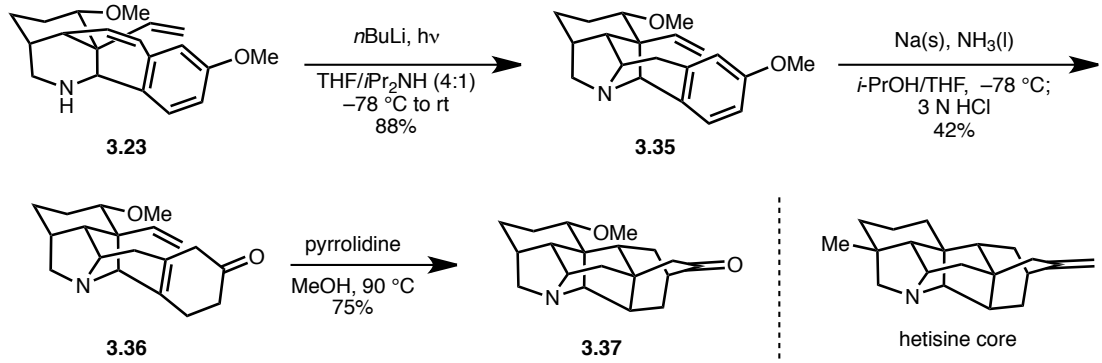

Scheme 3-8. Formation of the C6–N bond and the [2.2.2] bicycle.

3.4 Progress toward the synthesis of cossonidine

Although our approach provided us with access to the main hetisine core, the synthesis of cossonidine and other C_{20}-diterpenoid alkaloids necessitated the challenging installation of a methyl group at C4 (see atisane type, Figure 1-2). Concurrent with the studies discussed in Sections 2.5, 2.6, and 3.3, we investigated various compounds (Figure 3-3) along the different

synthetic pathways where a methyl group could potentially be incorporated using a methylation. Each of the methylation attempts was conducted using potassium *tert*-butoxide as the base with iodomethane in THF at temperatures ranging from –78 °C to room temperature. For compounds such as **3.38**–**342**, the reactions led to various products and were low yielding, and we observed poor diastereoselectivity. Alternatively, we looked at the methylation of substrates after the ring expansion (e.g., **3.43**). These reactions also resulted in a complex mixture and poor diastereoselectivity. In all cases, methylation of the aldehyde oxygen atom to give the methyl enol ether was also observed in varying amounts as a side product.

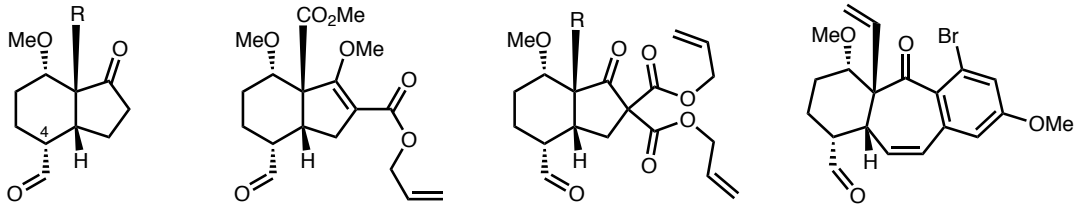

Figure 3-3. Substrates for C4 methylation studies.

At this point, we envisioned that we could effect the methylation after incorporation of the requisite nitrogen atom in the form of a nitrile, akin to the methylation employed by Mander and coworkers in their studies toward the hetisine core (see Scheme 1-7, Chapter 1.4). Benzyne insertion product **2.59** could be advanced to enone **3.44** in 55% yield over 2 steps. The silyl ether of **3.44** was cleaved with tetrabutylammonium fluoride and oxidized to the aldehyde using Dess–Martin periodinane (Scheme 3-9).[26] Formation of the oxime (not shown) was accomplished with hydroxylamine hydrochloride in pyridine. Subsequent dehydration mediated by acetic anhydride provided nitrile **3.45** in 88% yield over 2 steps.

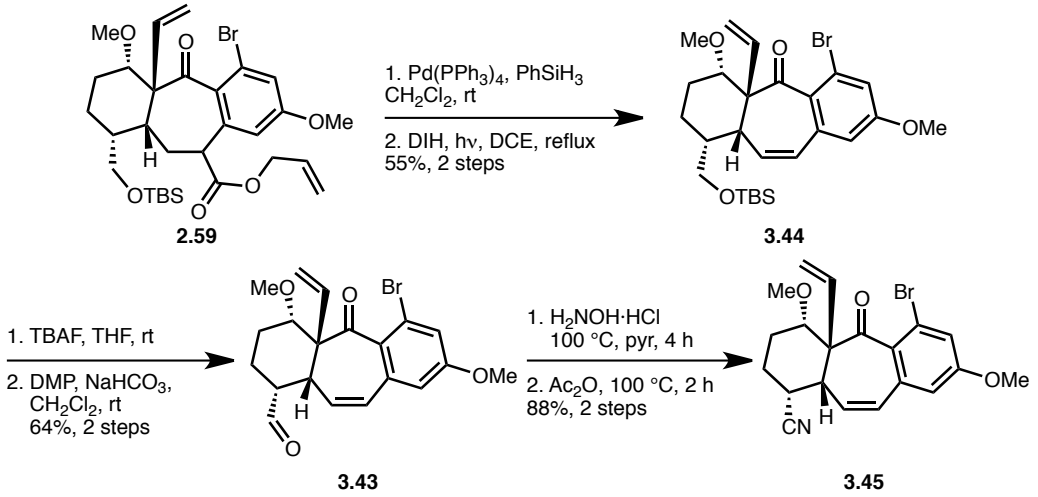

Scheme 3-9. Formation of the cyano group.

α-Alkylation of nitriles has been studied and reviewed extensively by Fleming and coworkers[27] using lithium amide bases. In their studies, lithium diethylamide was an ideal base for the reaction. However, using these conditions, we did not see appreciable reactivity. Instead, LiHMDS effectively deprotonates the nitrile in our hands, resulting in epimerization at C4 in the absence of an electrophile (entry 1, Table 3-2). A large excess of iodomethane was necessary for the alkylation to occur (compare entries 2 and 3). We found that the order of addition proved to

be very important for diastereoselectivity. While addition of iodomethane after stirring **3.45** with base gave the desired diastereomer (**3.46**), the inverse addition provided the epimeric alkylated compound (compare entries 3 and 4). The starting nitrile and methylated product were inseparable by column chromatography, but we found that by increasing the amount of base, we could push the reaction to complete conversion and obtain good yields of the methylated product (entries 5-8).

Table 3-2. Optimization of **3.45** methylation.

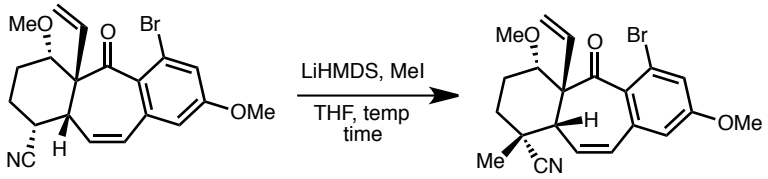

3.45 **3.46**

Entry	Added First	Temp (°C)	Time (h)	Equiv Base	Equiv MeI	Results
1[a]	–	0	1.5	3.0	–	**3.45** + epi-**3.45** (1.0:1.0)
2	base	0 to rt	3.5	1.2	10	**3.45** + *epi*-**3.45** (1.0:0.2)
3	base	0 to rt	12	1.5	30	**3.45** + **3.46** + epi-**3.45** (1.0:0.8:0.1)
4	MeI	0 to rt	18	4.0	100	**3.45** + *epi*-**3.46** (1.0:1.0)
5	base	rt	3	3.0	50	**3.45** + **3.46** (1.0:4.0)
6	base	rt	12	2.5	50	60% **3.46**
7	base	rt	4.5	3.0	50	71% **3.46**
8	base	rt to 40	2	4.0	50	63% **3.46**

[a]*Performed in the absence of iodomethane*

With **3.46** in hand, we attempted the cyclization sequence that had been developed for the des-methyl compound (i.e., **3.5**). Unfortunately, treatment of **3.46** with $LiAlH_4$ did not give clean conversion to the ring-closed product. Instead, the reaction mixture contained the amino alcohol (not shown) as the major product, which could be protected as the carbamate (**3.47**, Scheme 3-10). Additionally, we observed a small amount of the desired piperidine and a third compound that could not be cleanly isolated, but appeared to have the ketone carbonyl group fully reduced to the corresponding methylene. In keeping with our proposed intermediates (e.g., **3.28**, Scheme 3-6), we considered that reduction of the cyano group to reveal the primary amine may not be occurring fast enough to allow for cyclization. Alternatively, coordination to $LiAlH_4$ may force a different conformation that is no longer conducive to ring closure. The presence of the methyl group at C4 could significantly affect the conformation of **3.46** as compared to the des-methyl compound (**3.5**). Unable to cyclize, the likelihood of complete reduction of the benzylic position would increase. Despite the fact that cyclization during the reduction step was no longer facile, it could be carried out in a stepwise manner using the previously described protection/chlorination sequence (see Scheme 3-4) to arrive at piperidine **3.48** (Scheme 3-10). The carbamate could be cleaved by the addition of trifluoroacetic acid (TFA) after cyclization. Efforts to cyclize from the free amine instead resulted in an undesired product, necessitating the use of a protecting group. Reinvestigating the reduction, we found that the nitrile could be reduced under mild conditions

by $NaBH_4/CoCl_2$,[28] giving a mixture of the aminoketone and aminoalcohol. Treatment of this crude mixture with the previous cyclization/dehalogenation conditions ($LiAlH_4$, THF, reflux) provided piperidine **3.48** in an unoptimized 37% yield over 2 steps.

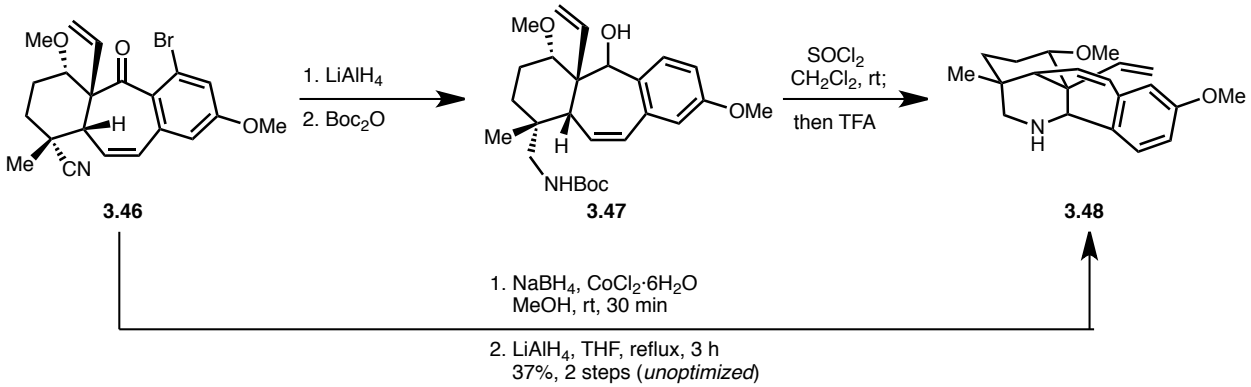

Scheme 3-10. Reduction of **3.46** and formation of the C20–N bond.

We were pleased to see that, in contrast to the reduction step (i.e., **3.46→3.48**), the hydroamination, Birch reduction, and intramolecular Diels–Alder reactions all proceeded analogously to the des-methyl case (see Scheme 3-8) to arrive at caged structure **3.50** (Scheme 3-11).

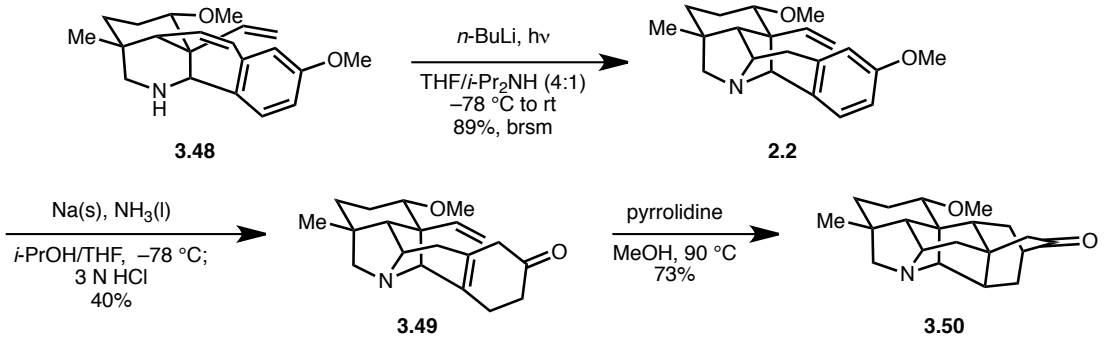

Scheme 3-11. Completion of the methylated hetisine core.

What remains in order to complete the synthesis of cossonidine (**2.1**) is methyl ether cleavage and inversion of the C1 stereocenter, installation of the exomethylene on the [2.2.2] bicycle using a Wittig homologation, and allylic oxidation to introduce the final hydroxyl group (Scheme 3-12). Both the Wittig reaction and allylic oxidation have been previously executed as the final steps in the Gin nominine synthesis. Studies are ongoing to investigate the methyl ether cleavage and hydroxyl inversion to provide **3.51**.

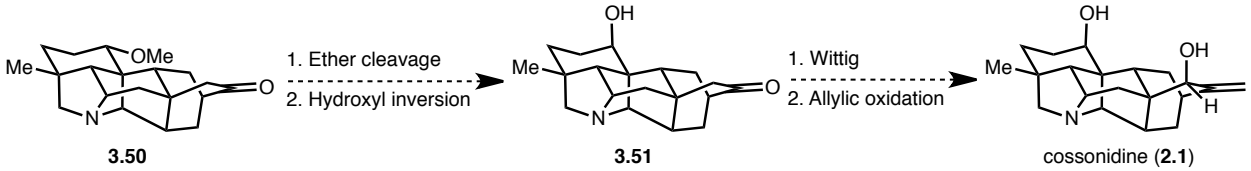

Scheme 3-12. Final sequence required for completion of cossonidine.

3.5 Conclusion

Starting from a functionalized 6-7-6 tricyclic compound, we were able to sequentially form the C20–N and C6–N bonds to stitch together the azabicycle present in the hetisine

framework. Starting from the des-methyl primary amine, $LiAlH_4$ reduction and light-mediated LDA hydroamination produced the azabicyclic product. A required methylation could be achieved from the corresponding tricyclic nitrile to give the single, desired diastereomer in good yield. Cyclization from the methylated compound proceeded through $LiAlH_4$ reduction, $SOCl_2$ cyclization, and LDA/hν hydroamination. Birch reduction and intramolecular Diels–Alder cycloaddition forms the [2.2.2] bicycle to complete the hetisine core. Work is underway to complete the synthesis of cossonidine and then apply our optimized synthetic sequence to the synthesis of additional hetisine-type diterpenoid alkaloids and analogs in order to investigate their biological activity.

3.6 Experimental Contributions

Methylation optimization studies and large-scale β-ketoester synthesis for scale-up were carried out by Dr. Toshihiro Kiho. Jessica K. Kisunzu performed the rest of the experiments described in this chapter.

3.7 Experimental Methods

All reagents were obtained from commercial chemical suppliers and used without further purification unless otherwise noted. All reactions were performed in round-bottomed flasks or microwave vials sealed with rubber septa, under an atmosphere of nitrogen, and stirred with a Teflon™-coated magnetic stir bar unless otherwise noted. Temperatures above 23 °C were controlled by an IKA® temperature modulator. Pre-dried tetrahydrofuran (THF), benzene, toluene, acetonitrile (MeCN), methanol (MeOH), and triethylamine (Et_3N), were degassed with argon for 60 min and passed through activated alumina columns. Dichloromethane (CH_2Cl_2) was distilled over calcium hydride before use. Reactions were monitored by thin layer chromatography (TLC) using Silicycle Siliaplate™ glass backed TLC plates (250 μm thickness, 60 Å porosity, F- 254 indicator) and visualized using UV (254 nm) and *p*-anisaldehyde stain. Volatile solvents were removed using a rotary evaporator under reduced pressure. Silica gel chromatography was performed using Sorbent Technologies 60 Å, 230 x 400 mesh silica gel (40-63 μm). ^1H NMR and ^{13}C NMR were obtained in $CDCl_3$ on Bruker 400, 500, or 600 MHz spectrometers with ^{13}C operating frequencies of 100, 126, or 151 MHz, respectively. Chemical shifts are reported in parts per million (δ) relative to residual chloroform (7.26 ppm for ^1H and 77.00 ppm for ^{13}C). Data for ^1H NMR spectra are reported as follows: chemical shift (multiplicity, coupling constants, number of hydrogens). Multiplicity is designated as s (singlet), d (doublet), t (triplet), q (quartet), quint (quintet), or m (multiplet). IR spectra were obtained using a Nicolet MAGNA-IR 850 spectrometer as thin films on NaCl plates and reported in frequency of absorption (cm^{-1}). High-resolution mass spectral (HRMS) data was obtained from the Mass Spectral facility at the University of California, Berkeley.

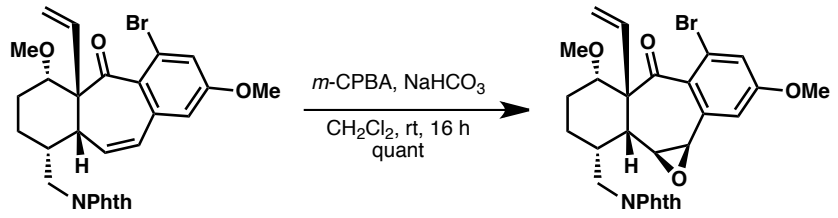

2.72 **3.7**

2-(((1a*S*,1b*R*,2*R*,5*S*,5a*R*,10b*R*)-7-Bromo-5,9-dimethoxy-6-oxo-5a-vinyl-1b,2,3,4,5,5a,6,10b-octahydro-1a*H*-dibenzo[3,4:6,7]cyclohepta[1,2-*b*]oxiren-2-yl)methyl)isoindoline-1,3-dione (3.7). Enone **2.72** (21.8 mg, 0.04 mmol) was dissolved in CH_2Cl_2 (0.80 mL) in an oven-dried vial with a stir bar. $NaHCO_{3(s)}$(12.0 mg, 0.14 mmol, 3.5 equiv) was added, followed by *m*-chloroperbenzoic acid (22.0 mg, 0.13 mmol, 3.25 equiv) at rt. The reaction mixture was stirred at rt for 16 h, at which time it was diluted with EtOAc (3 mL) and washed with $Na_2CO_{3(aq)}$ (2 x 2 mL). The aqueous layer was extracted with EtOAc (3 x 5 mL), and the combined organic layer was washed once with brine, dried ($MgSO_4$), and the solvent removed to give the epoxide (**3.7**) as a white foam (quant.). **R_f:** 0.32 (2:1 hexanes/EtOAc, UV, anisaldehyde stain).**^{1}H NMR** (500 MHz, $CDCl_3$) δ 7.83 (dd, *J* = 5.4, 3.1 Hz, 2H), 7.71 (dd, *J* = 5.5, 3.1 Hz, 2H), 7.14 (d, *J* = 2.4 Hz, 1H), 7.05 (d, *J* = 2.5 Hz, 1H), 5.49 – 5.38 (m, 2H), 5.21 – 5.10 (m, 1H), 4.11 (s, 1H), 3.98 (d, *J* = 4.5 Hz, 1H), 3.94 – 3.87 (m, 2H), 3.84 (s, 5H), 3.71 (dd, *J* = 13.9, 3.5 Hz, 1H), 3.38 (s, 3H), 2.32 (td, *J* = 11.3, 3.9 Hz, 1H), 2.07 – 1.99 (m, 1H), 1.99 – 1.89 (m, 1H), 1.80 – 1.67 (m, 1H). **^{13}C NMR** (151 MHz, $CDCl_3$) δ 199.3, 168.5, 161.1, 136.1, 134.4, 133.9, 132.0, 129.2, 123.2, 121.92, 120.8, 120.4, 113.5, 78.1, 63.1, 57.4, 55.7, 55.0, 52.6, 42.5, 41.9, 34.0, 23.0, 20.0. **IR** (thin film) $\tilde{\nu}_{max}$ cm^{-1} 2932, 1772, 1712, 1596, 1400, 1370, 725. **HRMS** (ESI) calcd for $[C_{28}H_{27}O_6N_1{}^{79}Br_1]^+$ ($[M+H]^+$): *m/z* 552.1016, found 552.1021.

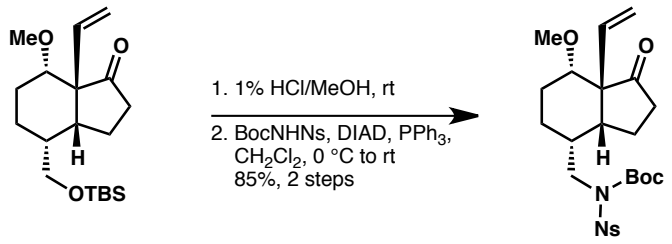

2.54 **3.14**

***tert*-Butyl (((3a*R*,4*R*,7*S*,7a*R*)-7-methoxy-1-oxo-7a-vinyloctahydro-1*H*-inden-4-yl)methyl)(2-nitrophenyl)carbamate (3.14).** Vinyl ketone **2.54** (0.913 g, 4.1 mmol) was taken up in 1% HCl/MeOH (40 mL) at room temperature in a 100 mL round bottom flask with a stir bar. After the reaction was deemed complete by TLC analysis, the reaction mixture was poured onto 40 mL saturated $NaHCO_{3(aq)}$, and extracted with EtOAc (3 x 50 mL). The combined organic layer was washed once with brine, dried ($MgSO_4$), filtered, and concentrated to give the primary alcohol as a colorless oil, which was taken forward directly. The alcohol was taken up in CH_2Cl_2 (40 mL) in a flame-dried round-bottom flask with a stir bar. PPh_3 (1.62 g, 6.2 mmol, 1.5 equiv) and N-(*tert*-butoxycarbonyl)-2-nitrobenzenesulfonamide[11] (1.91 g, 6.3 mmol, 1.6 equiv) added, and the resulting solution was cooled to 0 °C. DIAD (1.20 mL, 6.1 mmol, 1.5 equiv) was added slowly, and the reaction mixture was stirred and allowed to warm to room temperature. After the reaction was complete by TLC, the reaction was quenched with $NaHCO_{3(aq)}$ (40 mL), extracted with CH_2Cl_2 (3 x 50 mL). The combined organic layer was washed once with brine, dried ($MgSO_4$), filtered, and the solvent removed to give an orange oil. Purification by sequential flash

chromatography (sequential purifications with 4:1 hexanes:EtOAc, then 4:1 CH_2Cl_2:EtOAc) delivered the sulfonamide (**3.14**) as a white foam (1.75 g, 3.5 mmol, 85%). **R_f:** 0.58 (1:1 hexanes/EtOAc, UV, anisaldehyde stain).**^{1}H NMR** (500 MHz, $CDCl_3$) δ 8.37 – 8.30 (m, 1H), 7.83 – 7.70 (m, 3H), 5.82 (dd, J = 17.7, 11.0 Hz, 1H), 5.21 (d, J = 11.0 Hz, 1H), 5.18 (d, J = 17.7 Hz, 1H), 3.86 – 3.75 (m, 2H), 3.47 (t, J = 2.5, 2.5 Hz, 1H), 3.16 (s, 3H), 2.50 – 2.33 (m, 2H), 2.28 – 2.17 (m, 1H), 2.17 – 2.06 (m, 2H), 2.00 – 1.84 (m, 2H), 1.71 – 1.53 (m, 3H), 1.36 (s, 9H). **^{13}C NMR** (125 MHz, $CDCl_3$) δ 219.7, 150.4, 147.5, 138.0, 134.2, 133.7, 133.5, 131.8, 124.4, 116.0, 85.0, 81.4, 57.8, 57.0, 51.8, 41.5, 38.6, 36.0, 27.9, 23.8, 20.0, 18.3. **IR** (thin film) $\tilde{\nu}_{max}$ cm^{-1} 3088, 2982, 2936, 2827, 1755, 1732, 1544, 1368, 1152. **HRMS** (ESI) calcd for $[C_{24}H_{32}O_8N_2S_1Na_1]^+$ ($[M+Na]^+$): *m/z* 531.1772, found 531.1771.

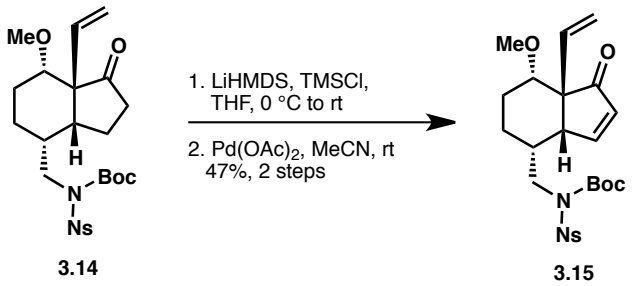

3.14 **3.15**

***tert*-Butyl (((3a*R*,4*R*,7*S*,7a*R*)-7-methoxy-1-oxo-7a-vinyl-3a,4,5,6,7,7a-hexahydro-1*H*-inden-4-yl)methyl)(2-nitrophenyl)carbamate (3.15).** Sulfonamide **3.14** (217.0 mg, 0.53 mmol) was taken up in THF (15 mL) under N_2 in a round-bottom flask with a stir bar and was cooled to 0 °C. LiHMDS (0.80 mL, 1 M in THF, 0.80 mmol, 1.5 equiv) was added slowly and the solution was stirred at that temperature for 10 min. TMSCl (0.110 mL, 0.87 mmol, 1.6 equiv) was then added, and the solution was allowed to warm to rt. When the reaction was complete by TLC, it was quenched with saturated $NaHCO_{3(aq)}$ (5 mL) and extracted with EtOAc (3 x 10 mL). The combined organic layer was washed with brine, dried ($MgSO_4$), filtered, and the solvent removed. The resulting oil was directly dissolved in acetonitrile (15 mL). $Pd(OAc)_2$ (155.7 mg, 0.69 mmol, 1.3 equiv) was added and the flask was sealed under N_2. The reaction mixture was stirred at rt. When the reaction was complete by TLC analysis (approx. 2 h), the mixture was filtered through Celite and eluted with EtOAc. The solvent was then removed to give a crude oil. Column chromatography (gradient: 28 → 49% EtOAc in hexanes) gave the enone (**3.15**) as a white foam (124.4 mg, 0.25 mmol, 47%). **R_f:** 0.36 (1:1 hexanes/EtOAc, UV, anisaldehyde stain)**. ^{1}H NMR** (500 MHz, $CDCl_3$) δ 8.36 – 8.30 (m, 1H), 7.82 – 7.72 (m, 4H), 6.25 (dd, J = 6.0, 2.8 Hz, 1H), 6.16 (dd, J = 17.7, 11.0 Hz, 1H), 5.23 (d, J = 11.0 Hz, 1H), 5.20 (d, J = 17.8 Hz, 1H), 4.02 – 3.87 (m, 2H), 3.51 (dd, J = 6.5, 2.8 Hz, 1H), 3.29 – 3.25 (m, 1H), 3.22 (s, 3H), 2.33 (dquint, J = 12.5, 5.9 Hz, 1H), 1.80 – 1.65 (m, 2H), 1.61 – 1.53 (m, 1H), 1.49 – 1.41 (m, 1H), 1.35 (s, 9H). **^{13}C NMR** (126 MHz, $CDCl_3$) δ 208.9, 164.5, 160.0, 150.2, 147.4, 138.3, 134.8, 134.3, 133.7, 133.4, 131.8, 124.5, 115.5, 85.5, 81.6, 57.8, 51.1, 47.0, 36.0, 27.9, 23.1, 20.6. **IR** (thin film) $\tilde{\nu}_{max}$ cm^{-1} 3081, 2981, 2935, 2826, 1731, 1712, 1543, 1367, 1153. **HRMS** (ESI) calcd $[C_{24}H_{31}O_8N_2S_1]^+$ ($[M+1]^+$): *m/z* 507.1796, found 507.1789.

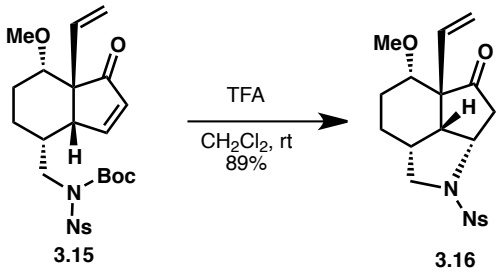

3.15 3.16

(2a*R*,2a^1*R*,5*S*,5a*R*,7a*S*)-5-Methoxy-1-(2-nitrophenyl)-5a-vinyloctahydro-1*H*-cyclopenta[*cd*]isoindol-6(2a^1*H*)-one (3.16). A solution of enone **3.15** (445.6 mg, 0.89 mmol) in CH_2Cl_2 (3 mL) was added slowly to a solution of trifluoroacetic acid (3 mL) and CH_2Cl_2 (7 mL) in a flame-dried round bottom flask with a stir bar. The pale yellow solution was stirred at room temperature. When the reaction was complete by LCMS analysis (approx. 13 h), the reaction mixture was neutralized by the addition of 10% NaOH, then extracted with EtOAc. The combined organic layer was washed with brine, dried ($MgSO_4$), filtered, and the solvent removed to give tricyclic nosylamide **3.16** as a brown powder (323.6 mg, 0.80 mmol, 89% yield). **R_f:** 0.29 (1:1 hexanes/EtOAc, UV, anisaldehyde stain). **^{1}H NMR** (500 MHz, $CDCl_3$) δ 8.00 (dd, J = 7.7, 1.6 Hz, 1H), 7.77 – 7.67 (m, 2H), 7.62 (dd, J = 7.6, 1.6 Hz, 1H), 6.08 (dd, J = 17.6, 10.7 Hz, 1H), 5.21 (d, J = 10.7 Hz, 1H), 5.09 (d, J = 17.6 Hz, 1H), 4.28 (ddd, J = 10.2, 9.0, 5.8 Hz, 1H), 3.51 – 3.43 (m, 2H), 3.31 (dd, J = 6.0, 3.2 Hz, 1H), 3.24 (s, 3H), 3.06 (t, J = 9.8 Hz, 1H), 2.78 (dd, J = 19.1, 8.9 Hz, 1H), 2.68 (dd, J = 19.1, 5.8 Hz, 1H), 2.46 – 2.36 (m, 1H), 1.78 – 1.55 (m, 4H). **^{13}C NMR** (125 MHz, $CDCl_3$) δ 214.8, 138.7, 133.9, 131.4, 131.1, 130.9, 124.1, 115.7, 78.9, 77.2, 58.3, 57.4, 57.4, 55.4, 45.8, 45.5, 33.8, 21.0, 20.8. **IR** (thin film) $\tilde{\nu}_{max}$ cm^{-1} 3084, 2937, 1742, 1545, 1374, 1358, 1171. **HRMS** (ESI) calcd for [$C_{19}H_{22}O_6N_2S_1Na_1$] ([M+Na]$^+$): *m/z* 429.1091, found 429.1091.

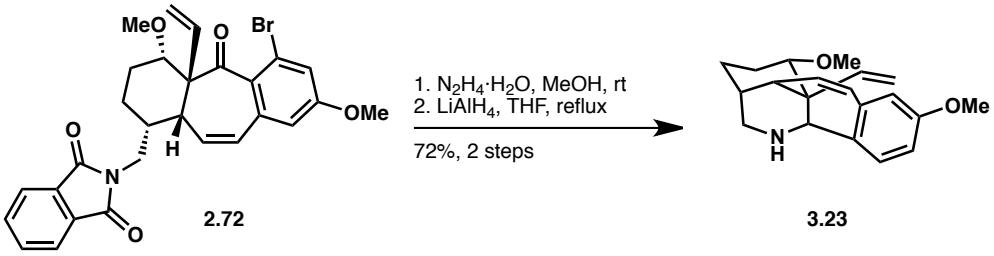

2.72 3.23

(1*R*,4*S*,4a*S*,11a*S*)-4,8-Dimethoxy-4a-vinyl-2,3,4,4a,5,11a-hexahydro-1*H*-5,1-(epiminomethano)dibenzo[*a*,*d*][7]annulene (3.23). Phthalimide **2.72** (640.0 mg, 1.19 mmol) was taken up in MeOH (40 mL) in a round-bottom flask with a stir bar. Hydrazine hydrate (0.60 mL, 11.9 mmol, 10 equiv) was added and the reaction mixture was stirred at room temperature until the reaction was complete by TLC and LCMS analysis. Solvent removed under reduced pressure to give the 1° amine which was passed through silica gel (eluted with 9:1 CH_2Cl_2/MeOH with 1% NH_4OH) to remove the excess hydrazine and deliver the amine as a white foam (347.2 mg). The amine was then taken up in THF and transferred to an oven-dried pressure reaction tube with a stir bar. The reaction mixture was cooled to 0 °C and $LiAlH_4$ (165.5 mg, 4.36 mmol, 5 equiv) was added slowly. When the vigorous bubbling had ceased, the mixture was warmed to rt, then sealed and heated to 70 °C. After 1.5 h, the reaction was cooled to 0 °C and quenched by the sequential addition of H_2O (0.17 mL), 10% NaOH (0.17 mL), and H_2O (0.51 mL). The reaction mixture was then allowed to warm to rt and stir until all the solids turned white, at which time it was filtered through Celite, eluted with EtOAc, and the solvent was then

removed to give piperidine **3.23** as a white foam (266.3 mg, 0.86 mmol, 72% over 2 steps). **R_f:** 0.55 (9:1 CH_2Cl_2/MeOH with 1% NH_4OH, faint UV, Dragendorff-Munier stain). **^{1}H NMR** (500 MHz, $CDCl_3$) δ 7.18 (d, *J* = 8.3 Hz, 1H), 6.72 (dd, *J* = 8.3, 2.7 Hz, 1H), 6.65 (d, *J* = 2.7 Hz, 1H), 6.32 (d, *J* = 12.3 Hz, 1H), 5.78 (dd, *J* = 12.2, 7.2 Hz, 1H), 5.73 (dd, *J* = 17.6, 10.9 Hz, 1H), 4.91 (dd, *J* = 17.7, 1.2 Hz, 1H), 4.76 (dd, *J* = 11.0, 1.2 Hz, 1H), 4.45 – 4.41 (m, 1H), 3.78 (s, 3H), 3.38 (s, 3H), 3.20 (dd, *J* = 11.2, 6.4 Hz, 1H), 3.08 (dt, *J* = 11.8, 2.6 Hz, 1H), 2.67 – 2.53 (m, 3H), 2.52 (dt, *J* = 7.4, 1.8 Hz, 1H), 2.20 – 2.10 (m, 1H), 1.97 (ddt, *J* = 13.7, 6.6, 1.8 Hz, 1H), 1.83 – 1.72 (m, 1H), 1.72 – 1.67 (m, 1H). **^{13}C NMR** (125 MHz, $CDCl_3$) δ 158.1, 142.3, 136.90, 135.7, 132.4, 132.3, 132.1, 117.0, 112.8, 111.2, 87.7, 59.9, 58.0, 55.1, 44.2, 43.3, 42.8, 32.1, 29.8, 28.4. **IR** (thin film) $\tilde{\nu}_{max}$ cm^{-1} 3076, 3008, 2908 (br), 2850, 1602. **HRMS** (ESI) calcd for $[C_{20}H_{26}NO_2]^+$ ($[M+H]^+$): *m/z* 312.1958, found 312.1953.

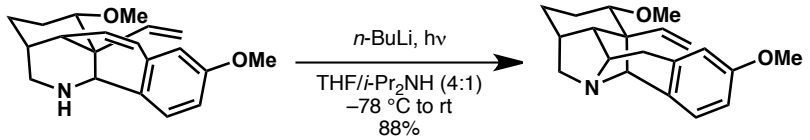

3.23 **3.35**

(9*R*,12*S*,13*S*,14*R*)-3,12-Dimethoxy-13-vinyl-6,8,9,10,11,12,13,13a-octahydro-5*H*-6,9,13-(epimethanetriyl)azocino[2,1-*a*]isoquinoline (3.35). The starting material was azetroped with benzene (1 x 2 mL). To an oven-dried Schlenk tube was added a stir bar and *i*-Pr_2NH (0.80 mL) followed by amine **3.23** (25.2 mg, 0.08 mmol) in THF (3.5 mL). The solution was cooled to –78 °C under N_2 and *n*-BuLi (0.30 mL, 1.6 M in hexanes, 6 equiv) was added slowly down the side with rapid mixing. The solution turned dark red then yellow and was warmed to rt. The Schlenk tube was then set up in front of a tungsten filament lamp (EIKO ELH 300 W, 120 V) at a distance of 2.1 ft for 5 h. At this time, the light was turned off and the reaction quenched by the addition of sat. $NaHCO_{3(aq)}$ (5 mL), extracted with EtOAc (3 x 5 mL), dried (Na_2SO_4), filtered, and concentrated to give a yellow oil. Column chromatography (EtOAc flush, then 20:1 CH_2Cl_2/MeOH with 1% NH_4OH → 9:1 CH_2Cl_2/MeOH with 1% NH_4OH) provided tertiary amine **3.35** as an orange oil (21.2 mg, 0.07 mmol, 88%). **R_f:** 0.18 (20:1 CH_2Cl_2/MeOH with 1% NH_4OH, Dragendorff-Munier stain). **^{1}H NMR** (500 MHz, $CDCl_3$) δ 6.94 (d, *J* = 8.2 Hz, 1H), 6.59 (dd, *J* = 8.2, 2.6 Hz, 1H), 6.50 (d, *J* = 2.5 Hz, 1H), 5.63 (dd, *J* = 17.8, 11.0 Hz, 1H), 4.96 (dd, *J* = 18.0, 1.3 Hz, 1H), 4.55 (dd, *J* = 11.0, 1.3 Hz, 1H), 3.88 (d, *J* = 2.0 Hz, 1H), 3.74 (s, 3H), 3.28 (s, 3H), 3.17 (d, *J* = 8.3 Hz, 1H), 3.07 (dd, *J* = 17.7, 8.4 Hz, 1H), 3.03 – 2.97 (m, 2H), 2.82 (d, *J* = 17.6 Hz, 1H), 2.60 (dd, *J* = 12.1, 4.8 Hz, 2H), 2.36 – 2.27 (m, 1H), 1.95 – 1.85 (m, 1H), 1.73 – 1.63 (m, 1H), 1.59 – 1.48 (m, 2H). **^{13}C NMR** (126 MHz, $CDCl_3$) δ 158.6, 144.3, 135.0, 133.5, 126.3, 113.3, 110.1, 108.6, 86.8, 67.8, 67.6, 57.5, 55.2, 54.7, 53.1, 48.4, 34.8, 30.3, 23.0, 20.9. **IR** (thin film) $\tilde{\nu}_{max}$ cm^{-1} cm^{-1} 3075 (broad), 2933, 2831, 1609, 1501. **HRMS** (ESI) calcd for $[C_{20}H_{26}O_2N_1]^+$ ($[M+H]^+$): *m/z* 312.1958, found 312.1961.

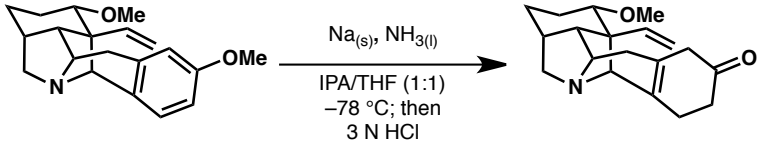

3.35 **3.36**

(9*R*,12*S*,13*S*,14*R*)-12-Methoxy-13-vinyl-4,5,6,8,9,10,11,12,13,13a-decahydro-1*H*-6,9,13-(epimethanetriyl)azocino[2,1-*a*]isoquinolin-3(2*H*)-one (3.36). NH_3 (~1.5 mL) was condensed into an oven-dried Schlenk tube at –78 °C under Ar. A solution of arene **3.35** (25.5 mg, 0.08

mmol) in 1:1 IPA/THF (1.0 mL) was added, and the solution was stirred for 20 min. $Na_{(s)}$ (68.0 mg, 2.96 mmol, 37 equiv) was then added. Within 30 min, the solution had turned dark blue. After stirring for 1.5 h, the reaction mixture had turned from blue to cloudy white. NH_4Cl (225.2 mg, 4.2 mmol, 51 equiv) was added to quench the reaction and the cooling bath was removed. After 30 min, 3 N HCl (2 mL) was added and the reaction mixture was stirred for 20 min. The mixture was then poured onto $NaHCO_{3(aq)}$ (8 mL), basified with 10% NaOH (0.5 mL), extracted with CH_2Cl_2, dried (Na_2SO_4), and the solvent was removed to give the crude ketone. Column chromatography (20:1 CH_2Cl_2/MeOH with 1% NH_4OH → 9:1 CH_2Cl_2/MeOH with 1% NH_4OH) provided ketone **3.36** as a yellow oil (10.2 mg, 0.03 mmol, 42%). **R_f:** 0.21(9:1 CH_2Cl_2/MeOH with 1% NH_4OH, Dragendorff-Munier stain). **^{1}H NMR** (500 MHz, $CDCl_3$) δ 6.09 (dd, *J* = 17.7, 11.0 Hz, 1H), 5.00 (d, *J* = 17.6 Hz, 1H), 4.69 (d, *J* = 11.0 Hz, 1H), 3.30 (s, 3H), 3.21 – 3.17 (m, 1H), 3.02 (dd, *J* = 7.4, 1.7 Hz, 1H), 2.96 (dd, *J* = 11.3, 5.7 Hz, 1H), 2.92 (dd, *J* = 12.7, 10.6 Hz, 1H), 2.67 – 2.56 (m, 3H), 2.55 – 2.43 (m, 5H), 2.34 – 2.20 (m, 2H), 1.92 (d, *J* = 17.8 Hz, 1H), 1.89 – 1.83 (m, 1H), 1.66 – 1.58 (m, 1H), 1.52 – 1.35 (m, 2H). **^{13}C NMR** (126 MHz, $CDCl_3$) δ 210.3, 143.9, 135.3, 124.9, 106.6, 85.4, 67.4, 66.6, 57.3, 55.9, 53.1, 48.1, 42.3, 38.3, 34.9, 32.5, 29.4, 23.00, 20.8. **IR** (thin film) $\tilde{\nu}_{max}$ cm^{-1} 2921, 2851, 1722, 1711, 1096. **HRMS** (ESI) calcd for $[C_{19}H_{26}NO_2]^+$ ($[M+H]^+$): *m/z* 300.1958, found 300.1956.

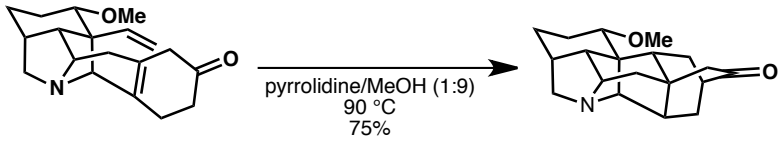

3.36 **3.37**

(1*S*,3a*R*,3a^1*R*,5a*S*,6a*S*,10a*R*,10b*S*)-1-Methoxydodecahydro-1*H*-5,7,10b-(epimethanetriyl)-6a,9-ethanodibenzo[*cd*,*f*]indol-12-one (3.37). Enone **3.36** (10.2 mg, 0.034 mmol) was taken up in MeOH (1.6 mL) in a Schlenk tube. Pyrrolidine (redistilled, 0.18 mL) was added and the resulting reaction mixture was then sealed and heated to 90 °C. After 6 h, the solution was cooled to room temperature and the solvent removed to give the crude cycloaddition product. Column chromatography (20:1 CH_2Cl_2/MeOH with 1% NH_4OH → 9:1 CH_2Cl_2/MeOH with 1% NH_4OH) gave the pure ketone (**3.37**) as an orange oil (7.7 mg, 0.026 mmol, 75%). **R_f:** 0.09 (9:1 CH_2Cl_2/MeOH with 1% NH_4OH, Dragendorff-Munier stain). **^{1}H NMR** (600 MHz, $CDCl_3$) δ 3.36 (dd, J = 10.7, 5.5 Hz, 1H), 3.31 (s, 3H), 3.00 – 2.90 (m, 3H), 2.69 (dd, J = 14.3, 5.0 Hz, 1H), 2.33 – 2.24 (m, 2H), 2.14 – 2.05 (m, 4H), 2.01 – 1.93 (m, 3H), 1.88 (ddt, J = 14.0, 11.4, 2.5 Hz, 1H), 1.79 (dd, J = 13.3, 3.0 Hz, 1H), 1.75 (dd, J = 9.7, 2.0 Hz, 1H), 1.67 – 1.49 (m, 4H), 1.39 – 1.27 (m, 1H). **^{13}C NMR** (151 MHz, $CDCl_3$) δ 216.6, 77.9, 73.2, 67.1, 56.3, 54.8, 54.7, 54.6, 49.7, 45.2, 43.5, 42.4, 41.3, 36.0, 35.2, 27.7, 24.8, 23.1, 22.8. **IR** (thin film) $\tilde{\nu}_{max}$ cm^{-1} 2933, 2819, 1720, 1440, 1350, 1078. **HRMS** (ESI) calcd for $[C_{19}H_{26}O_2N_1]^+$ ($[M+H]^+$): *m/z* 300.1958, found 300.1956.

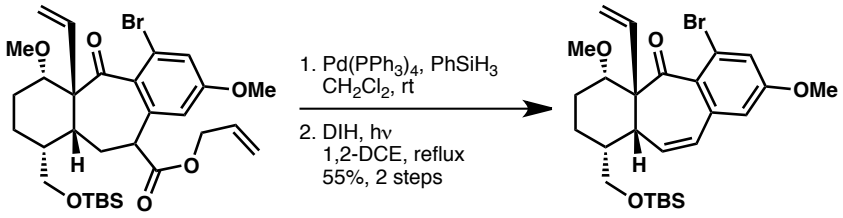

2.59 **3.44**

(1*R*,4*S*,4a*R*,11a*R*)-6-Bromo-1-(((*tert*-butyldimethylsilyl)oxy)methyl)-4,8-dimethoxy-4a-vinyl-2,3,4,4a-tetrahydro-1*H*-dibenzo[*a*,*d*][7]annulen-5(11a*H*)-one (3.44). Allyl ester **2.59** (486.8 mg, 0.80 mmol) was dissolved in CH_2Cl_2 (7 mL) in a flask with a stir bar. The flask was covered in foil, then $Pd(PPh_3)_4$ (19.0 mg, 0.016 mmol, 0.02 equiv) was added, followed by phenylsilane (0.212 mL, 1.7 mmol, 2.1 equiv). The reaction mixture was stirred at rt for 6 h. The solvent was removed and the crude material was filtered through SiO_2 (eluted with 1:1 hexanes/EtOAc) to remove the Pd residue. The white residue was then taken up in 1,2-DCE (8 mL) in a Schlenk tube. DIH (608 mg, 1.6 mmol, 2 equiv), and the reaction vessel was sealed and placed in front of a 600 W tungsten-filament lamp at a distance of ~0.2 m such that the reaction mixture was also heated by the lamp to reflux. After 2 h, the tube was taken from in front of the lamp, cooled to rt, and the reaction was quenched by the addition of 1 M $NaHSO_3$. The mixture was extracted with CH_2Cl_2, and the combined organic layer was washed with brine, dried (Na_2SO_4), and the solvent removed to give the crude enone. Column chromatography (20:1 hexanes/EtOAc, then 2:1 hexanes/EtOAc) provided **3.44** was a yellow oil (232.0 mg, 0.44 mmol, 55%). The corresponding primary alcohol was also isolated (85.2 mg, 0.21 mmol, 26%). **R_f:** 0.69 (2:1 hexanes/EtOAc, UV, anisaldehyde). **^{1}H NMR** (400 MHz, $CDCl_3$) δ 6.99 (d, *J* = 2.4 Hz, 1H), 6.51 (d, *J* = 2.4 Hz, 1H), 6.26 (dd, *J* = 10.6, 1.8 Hz, 1H), 6.13 (dd, *J* = 10.7, 6.2 Hz, 1H), 5.54 – 5.41 (m, 2H), 5.31 (dd, *J* = 15.6, 2.5 Hz, 1H), 4.04 – 3.99 (m, 1H), 3.78 (s, 3H), 3.47 (qd, *J* = 10.0, 10.0, 10.0, 7.3 Hz, 2H), 3.31 (s, 3H), 3.29 – 3.23 (m, 1H), 2.08 – 1.96 (m, 1H), 1.92 (dt, *J* = 10.9, 2.9, 2.9 Hz, 1H), 1.56 – 1.36 (m, 3H), 0.80 (s, 9H), -0.01 (s, 3H), -0.02 (s, 3H). **^{13}C NMR** (101 MHz, $CDCl_3$) δ 200.5, 160.2, 139.2, 135.2, 134.0, 132.4, 125.5, 122.1, 120.5, 117.8, 112.1, 80.0, 71.5, 65.3, 57.6, 55.5, 36.7, 36.6, 25.8, 23.7, 18.7, 18.2, -5.4, -5.5. **IR** (thin film) $\tilde{\nu}_{max}$ cm^{-1} 3084, 3038, 2925, 1703, 1692, 1628, 1588, 1092. **HRMS** (ESI) calcd for $[C_{26}H_{38}O_4BrSi]^+$ ($[M+H]^+$): *m/z* 521.1717, found 521.1724.

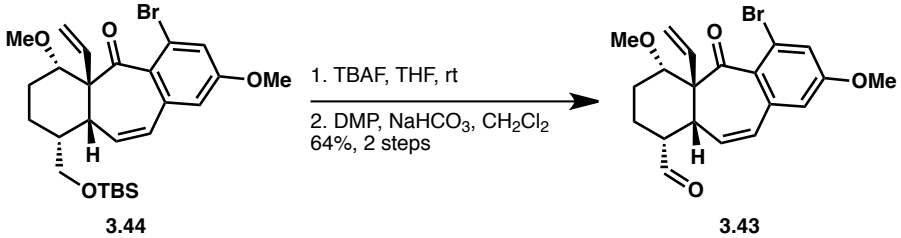

3.44 **3.43**

(1*R*,4*S*,4a*R*,11a*R*)-6-Bromo-4,8-dimethoxy-5-oxo-4a-vinyl-2,3,4,4a,5,11a-hexahydro-1*H*-dibenzo[*a*,*d*][7]annulene-1-carbaldehyde (3.43). TBAF (0.3 mL, 1 M in THF, 0.3 mmol, 2.1 equiv) was added to a solution of silyl ether **3.44** (71.0 mg, 0.14 mmol) in THF (1.5 mL) at 0 °C. The solution was warmed to rt and stirred for 15 h. When the reaction was complete by TLC analysis, the solution was diluted with EtOAc and washed sequentially with 1 N HCl and brine. The organic layer was dried (Na_2SO_4), filtered, and solvent removed to give the crude alcohol. The alcohol was purified via column chromatography (2:1 hexanes/EtOAc) to give a colorless solid (39.5 mg, 0.10 mmol). The alcohol was dissolved in CH_2Cl_2 (2.5 mL) and cooled to 0 °C.

$NaHCO_3$ (100.2 mg, 1.2 mmol, 12.0 equiv) and Dess-Martin Periodinane (134.0 mg, 0.32 mmol, 3.2 equiv) were added sequentially. When the reaction was complete by TLC analysis, the reaction mixture was diluted with EtOAc, washed with sat. $NaHCO_{3(aq)}$ and brine, dried (Na_2SO_4) and solvent was removed to give the crude aldehyde. Column chromatography (6:1 hexanes/EtOAc) provided **3.43** as a white foam (36.3 mg, 0.09 mmol, 64%, 2 steps). **R_f:** 0.44 (2:1 hexanes/EtOAc, UV, anisaldehyde stain) **mp:** 116-118 °C. **^{1}H NMR** (400 MHz, $CDCl_3$) δ 9.59 (s, 1H), 6.98 (d, *J* = 3.0 Hz, 1H), 6.52 (d, *J* = 2.4 Hz, 1H), 6.25 (dd, *J* = 10.5, 2.1 Hz, 1H), 5.87 (dd, *J* = 10.7, 6.0 Hz, 1H), 5.54 – 5.41 (m, 2H), 5.41 – 5.28 (m, 1H), 4.03 – 3.98 (m, 1H), 3.75 (s, 3H), 3.64 (t, *J* = 4.7 Hz, 1H), 3.25 (s, 3H), 2.63 (dt, *J* = 12.7, 3.8 Hz, 1H), 2.04 – 1.94 (m, 1H), 1.86 (qd, *J* = 13.2, 13.2, 3.7 Hz, 1H), 1.78 – 1.67 (m, 1H), 1.52 – 1.38 (m, 1H). **^{13}C NMR** (101 MHz, $CDCl_3$) δ 203.6, 199.1, 160.3, 138.4, 134.2, 133.4, 131.8, 126.1, 122.3, 120.6, 118.2, 112.1, 79.2, 71.0, 57.5, 55.4, 47.6, 35.4, 22.7, 15.8. **IR** (thin film) $\tilde{\nu}_{max}$ cm^{-1} 2938, 2826, 2722, 1721, 1693, 1590. **HRMS** (ESI) calcd for $[C_{20}H_{21}O_4BrNa]^+$ ($[M+Na]^+$): *m/z* 427.0515, found 427.0515.

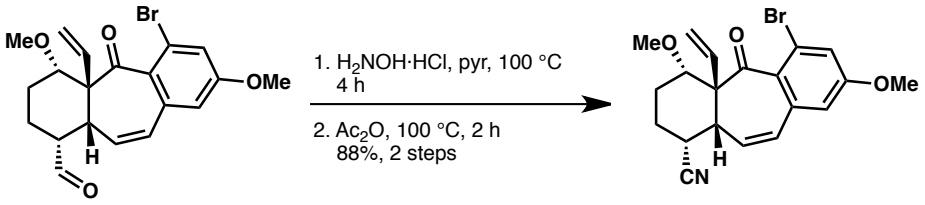

3.43 **3.45**

(1*R*,4*S*,4a*R*,11a*R*)-6-Bromo-4,8-dimethoxy-5-oxo-4a-vinyl-2,3,4,4a,5,11a-hexahydro-1*H*-dibenzo[*a*,*d*][7]annulene-1-carbonitrile (3.45). Aldehyde **3.43** (13.8 mg, 0.034 mmol) was taken up with hydroxylamine hydrochloride (12.9 mg, 0.19 mmol, 6.3 equiv) in pyridine (0.5 mL) in an oven-dried vial with a stir bar. The reaction mixture was heated to 100 °C for 4 h, then cooled to rt. The mixture was diluted with EtOAc (3 mL) and acidified with 1 N HCl (2 mL). The layers were separated and the aqueous layer was extracted with EtOAc. The combined organic layer was washed sequentially with H_2O, $NH_4Cl_{(aq)}$, and brine, then dried (Na_2SO_4), filtered, and the solvents removed to give the oxime. The crude oxime was dissolved in Ac_2O (0.5 mL) and heated to 100 °C for 2 h. After cooling to rt, the reaction was quenched by the addition of 10% NaOH, then stirred at rt for 1 h. The aqueous layer was extracted with EtOAc and washed with 1 M NaOH, H_2O, and brine. The layer was then dried (Na_2SO_4) and solvent removed to give the crude nitrile. Column chromatography (18 → 39% EtOAc in hexanes) provided nitrile **3.45** (10.6 mg, 0.026 mmol, 88%) as a white solid. **R_f:** 0.43 (2:1 hexanes/EtOAc, UV, anisaldehyde stain) **mp:** 205-207 °C. **^{1}H NMR** (500 MHz, $CDCl_3$) δ 7.03 (d, *J* = 2.4 Hz, 1H), 6.59 (d, *J* = 2.4 Hz, 1H), 6.42 (dd, *J* = 10.7, 2.0 Hz, 1H), 6.25 (dd, *J* = 10.6, 6.0 Hz, 1H), 5.53 (d, *J* = 10.5 Hz, 1H), 5.45 (dd, *J* = 17.4, 10.5 Hz, 1H), 5.35 (d, *J* = 17.3 Hz, 1H), 4.03 (dd, *J* = 3.8, 2.0 Hz, 1H), 3.81 (s, 3H), 3.51 (t, *J* = 5.3 Hz, 1H), 3.31 (s, 3H), 2.98 (dt, *J* = 13.1, 4.0 Hz, 1H), 2.16 (qd, *J* = 13.4, 3.7 Hz, 1H), 1.97 (dq, *J* = 14.4, 3.4 Hz, 1H), 1.87 – 1.77 (m, 1H), 1.47 (tdd, *J* = 13.9, 4.1, 2.0 Hz, 1H). **^{13}C NMR** (151 MHz, $CDCl_3$) δ 198.3, 160.7, 138.4, 133.1, 133.1, 131.6, 127.1, 122.6, 121.3, 120.9, 118.7, 112.4, 78.0, 70.1, 57.9, 55.6, 36.85, 27.0, 22.9, 19.9. **IR** (thin film) $\tilde{\nu}_{max}$ cm^{-1} 2931, 2239, 1695, 1590, 1544, 1459. **HRMS** (ESI) calcd for $[C_{20}H_{21}O_3NBr]^+$ ($[M+H]^+$): *m/z* 402.0699, found 402.0705.

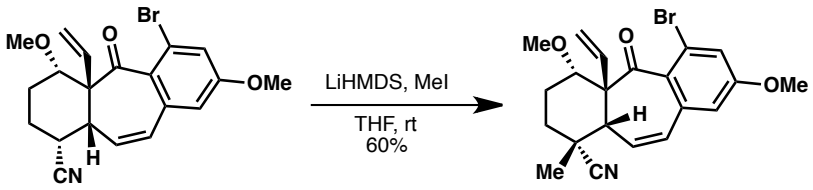

3.45 3.46

(1*R*,4*S*,4a*R*,11a*R*)-6-Bromo-4,8-dimethoxy-1-methyl-5-oxo-4a-vinyl-2,3,4,4a,5,11a-hexahydro-1*H*-dibenzo[*a*,*d*][7]annulene-1-carbonitrile (3.46). Nitrile **3.45** (19.9 mg, 0.049 mmol) was taken up in THF (0.7 mL) in a flame-dried round-bottom flask with a stir bar. LiHMDS (0.124 mL, 1 M in THF, 2.5 equiv) was added at rt, and the solution was stirred for 1 h. Iodomethane (0.154 mL, 2.5 mmol, 51 equiv) was added and the reaction mixture was stirred at that temp for 16 h. $NH_4Cl_{(aq)}$ was added, and the aqueous layer was extracted with EtOAc. The combined organic layer was washed with brine, dried (Na_2SO_4), and the solvent removed. Column chromatography (6:1 hexanes/EtOAc) provided **3.46** as a yellow residue (12.3 mg, 0.030 mmol, 60%). **R_f:** 0.21 (4:1 hexanes/EtOAc, UV, anisaldehyde stain). **^{1}H NMR** (400 MHz, $CDCl_3$) δ 7.04 (d, *J* = 2.4 Hz, 1H), 6.60 (d, *J* = 2.4 Hz, 1H), 6.35 (d, *J* = 10.1 Hz, 1H), 6.25 (dd, *J* = 11.0, 6.4 Hz, 1H), 5.69 (dd, *J* = 17.8, 11.0 Hz, 1H), 5.43 (d, *J* = 10.8 Hz, 1H), 5.30 (d, *J* = 17.8 Hz, 1H), 4.17 (d, *J* = 3.7 Hz, 1H), 3.81 (s, 3H), 3.35 (s, 3H), 3.18 (d, *J* = 5.9 Hz, 1H), 2.42 (t, *J* = 13.9 Hz, 1H), 1.92 (d, *J* = 14.6 Hz, 1H), 1.78 – 1.54 (m, 2H), 1.52 (s, 3H). **^{13}C NMR** could not be obtained. **IR** (thin film) $\tilde{\nu}_{max}$ cm^{-1} 3056, 2932, 2833, 2232, 1710, 1692, 1587. **HRMS** (ESI) calcd for $[C_{21}H_{23}O_3N_1{}^{79}Br]^+$ ($[M+H]^+$): *m/z* 416.0856, found 416.0856.

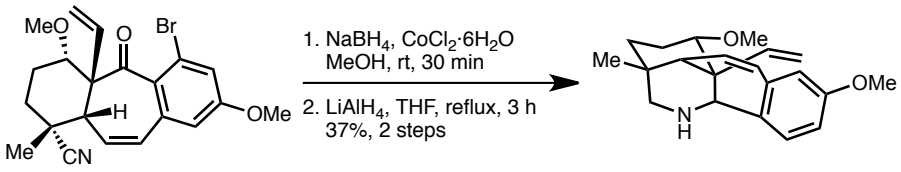

3.46 3.48

(1*R*,4*S*,4a*S*,11a*S*)-4,8-Dimethoxy-1-methyl-4a-vinyl-2,3,4,4a,5,11a-hexahydro-1*H*-5,1-(epiminomethano)dibenzo[*a*,*d*][7]annulene (3.48). Nitrile **3.46** (19.6 mg, 0.05 mmol) was taken up in dry MeOH (2.5 mL) in a flask with a stir bar. $CoCl_2 \cdot 6H_2O$ (27.2 mg, 0.11 mmol, 2.2 equiv) was added, followed by $NaBH_4$ (23.1 mg, 0.61 mmol, 12 equiv) in portions. The reaction mixture was stirred at rt until complete by TLC analysis (approx. 1 h). 3 N HCl was added dropwise until the black precipitate dissolved (approx. 2 mL), then the MeOH was removed under reduced pressure. The residue was diluted with 1 N NaOH and extracted with EtOAc. The combined organic layer was washed with brine, dried (Na_2SO_4), and the solvent removed to give the primary amine as a yellow-white residue. The amino alcohol was taken up in THF (2.5 mL) in an oven-dried vial with a stir bar. $LiAlH_4$ (8.9 mg, 0.23 mmol, 4.6 equiv) was added. The vial was sealed and the reaction mixture heated to 70 °C. After 3 h, the solution was cooled to 0 °C and quenched by the sequential addition of H_2O (0.01 mL), 10% NaOH (0.01 mL), and H_2O (0.03 mL). The mixture was stirred until the solids turned white, at which time it was filtered through Celite, eluted with EtOAc, and the solvent removed to give the crude piperidine. Column chromatography (20:1 CH_2Cl_2/MeOH with 1% NH_4OH, then 9:1 CH_2Cl_2/MeOH with 1% NH_4OH) provided **3.48** as a yellow oil (6.1 mg, 0.02 mmol, 37%, 2 steps). **R_f:** 0.31 (20:1 CH_2Cl_2/MeOH with 1% NH_4OH, UV, Dragendorff-Munier stain). **^{1}H NMR** (500 MHz, $CDCl_3$) δ 7.22 (d, *J* = 8.3 Hz, 1H), 6.74 (dd, *J* = 8.3, 2.8 Hz, 1H), 6.66 (d, *J* = 2.7 Hz, 1H), 6.35 (d, *J* =

12.4 Hz, 1H), 5.81 (dd, *J* = 12.4, 7.5 Hz, 1H), 5.72 (dd, *J* = 17.7, 11.0 Hz, 1H), 4.86 (dd, *J* = 17.7, 1.2 Hz, 1H), 4.77 (dd, *J* = 11.1, 1.2 Hz, 1H), 4.47 (s, 1H), 3.78 (s, 3H), 3.37 (s, 3H), 3.19 (dd, *J* = 11.3, 6.5 Hz, 1H), 2.70 – 2.56 (m, 2H), 2.43 (d, *J* = 11.9 Hz, 1H), 2.25 (d, *J* = 7.5 Hz, 1H), 2.15 – 2.06 (m, 1H), 1.78 (dd, *J* = 13.4, 6.9 Hz, 1H), 1.53 (tdd, *J* = 13.7, 6.6, 2.6 Hz, 1H), 0.85 (s, 3H), N*H* not observed. **^{13}C NMR** (151 MHz, $CDCl_3$) δ 158.2, 142.2, 137.0, 132.8, 132.5, 130.2, 117.1, 113.1, 111.7, 87.5, 59.2, 58.0, 55.2, 49.1, 48.9, 43.9, 38.1, 34.0, 28.0, 27.0. **IR** (thin film) $\tilde{\nu}_{max}$ cm^{-1} 2926, 2850, 1603, 1463, 1101. **HRMS** (ESI) calcd for $[C_{21}H_{28}O_2N_1]^+$ ($[M+H]^+$): *m/z* 326.2115, found 326.2113.

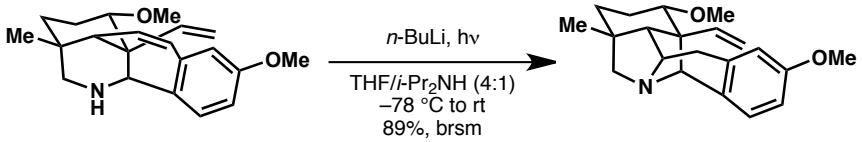

3.48 2.2

(9*R*,12*S*,13*S*,14*R*)-3,12-Dimethoxy-9-methyl-13-vinyl-6,8,9,10,11,12,13,13a-octahydro-5*H*-6,9,13-(epimethanetriyl)azocino[2,1-*a*]isoquinoline (2.2). The starting amine (**3.48**) was dried by azeotrope with benzene (1 x 2 mL). To an oven-dried Schlenk tube was added a stir bar and *i*-Pr_2NH (0.440 mL) followed by amine **3.48** (14.4 mg, 0.044 mmol) in THF (2.0 mL). The solution was cooled to –78 °C under N_2 and *n*-BuLi (0.180 mL, 1.6 M in hexanes, 6 equiv) was added slowly with rapid mixing. The solution turned dark red and was warmed to rt. The Schlenk tube was then set up in front of a tungsten filament lamp (EIKO ELH 300 W, 120 V) at a distance of 2.1 ft for 5 h. At this time, the light was turned off and the reaction was quenched by the addition of sat. $NaHCO_{3(aq)}$ and extracted with EtOAc (3 x 5 mL). The combined organic layer was washed once with brine, dried (Na_2SO_4), filtered, and concentrated to give a yellow oil. Column chromatography (EtOAc flush, then 20:1 CH_2Cl_2/MeOH with 1% NH_4OH → 9:1 CH_2Cl_2/MeOH with 1% NH_4OH) provided tertiary amine **2.2** as an orange oil (8.5 mg, 0.26 mmol, 59%, 89% based on recovered starting material). **R_f:** 0.16 (20:1 CH_2Cl_2/MeOH with 1% NH_4OH, Dragendorff-Munier stain). **^{1}H NMR** (600 MHz, $CDCl_3$) δ 6.95 (d, *J* = 8.2 Hz, 1H), 6.60 (dd, *J* = 8.2, 2.6 Hz, 1H), 6.50 (d, *J* = 2.5 Hz, 1H), 5.61 (dd, *J* = 17.8, 11.0 Hz, 1H), 4.95 (dd, *J* = 17.8, 1.3 Hz, 1H), 4.57 (dd, *J* = 11.0, 1.2 Hz, 1H), 3.88 (d, *J* = 2.0 Hz, 1H), 3.74 (s, 3H), 3.48 (dd, *J* = 8.5, 2.2 Hz, 1H), 3.26 (s, 3H), 3.10 (dd, *J* = 17.8, 8.4 Hz, 1H), 3.01 (dd, *J* = 11.3, 5.4 Hz, 1H), 2.81 (d, *J* = 17.9 Hz, 1H), 2.78 (d, *J* = 12.8 Hz, 1H), 2.60 (d, *J* = 12.6 Hz, 1H), 2.24 (s, 1H), 1.95 (ddt, *J* = 12.4, 5.2, 2.9 Hz, 1H), 1.59 – 1.36 (m, 3H), 1.13 (s, 3H). **^{13}C NMR** (151 MHz, $CDCl_3$) δ 158.5, 144.8, 135.2, 134.3, 126.3, 113.3, 110.0, 108.7, 87.3, 66.9, 65.3, 60.8, 57.4, 55.4, 55.2, 54.9, 38.0, 32.6, 30.3, 28.6, 23.0. **IR** (thin film) $\tilde{\nu}_{max}$ cm^{-1} 3073, 2936, 1611, 1502, 1096, 1036**.** **HRMS** (ESI) calcd for $[C_{21}H_{28}O_2N_1]^+$ ($[M+H]^+$): *m/z* 326.2115, found 326.2112.

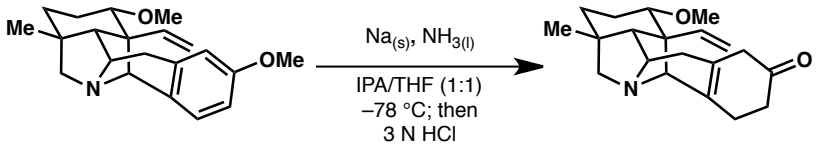

2.2 3.49

(9*R*,12*S*,13*S*,14*R*)-12-Methoxy-9-methyl-13-vinyl-4,5,6,8,9,10,11,12,13,13a-decahydro-1*H*-6,9,13-(epimethanetriyl)azocino[2,1-*a*]isoquinolin-3(2*H*)-one (3.49). NH_3 (~0.5 mL) was condensed into an oven-dried Schlenk tube at –78 °C under Ar. A solution of arene **2.2** (9.7 mg,

0.03 mmol) in 1:1 IPA/THF (0.340 mL) was added, and the solution was stirred for 20 min. $Na_{(s)}$ (25.3 mg, 1.1 mmol, 37 equiv) was then added. After stirring for 3.5 h, NH_4Cl (75.0 mg, 1.4 mmol, 47 equiv) was added to quench the reaction and the cooling bath was removed. After 20 min, 3 N HCl (3 mL) was added and the reaction mixture was stirred for 30 min. The mixture was then basified with 10% NaOH (8 mL) and extracted with EtOAc (3 x 5 mL). The combined organic layer was dried (Na_2SO_4) and the solvent was removed to give the crude ketone. Column chromatography (20:1 CH_2Cl_2/MeOH with 1% NH_4OH → 9:1 CH_2Cl_2/MeOH with 1% NH_4OH) provided ketone **3.49** as a yellow oil (3.8 mg, 0.012 mmol, 40%). **R_f:** 0.16 (9:1 CH_2Cl_2/MeOH with 1% NH_4OH, Dragendorff-Munier stain). **^{1}H NMR** (500 MHz, $CDCl_3$) δ 6.08 (dd, *J* = 17.7, 11.0 Hz, 1H), 4.98 (dd, *J* = 17.8, 1.2 Hz, 1H), 4.69 (dd, *J* = 11.0, 1.2 Hz, 1H), 3.34 – 3.27 (m, 5H), 3.17 (d, *J* = 2.1 Hz, 1H), 3.01 – 2.90 (m, 1H), 2.71 – 2.58 (m, 2H), 2.54 – 2.43 (m, 5H), 2.34 – 2.26 (m, 1H), 2.23 (s, 1H), 1.97 – 1.88 (m, 2H), 1.54 – 1.46 (m, 1H), 1.41 – 1.32 (m, 2H), 1.09 (s, 3H). **^{13}C NMR** (151 MHz, $CDCl_3$) δ 210.1, 143.8, 135.4, 124.9, 106.8, 85.6, 65.6, 65.1, 60.6, 57.1, 56.1, 54.8, 42.3, 38.3, 37.7, 32.4, 32.4, 29.4, 28.6, 22.7. **IR** (thin film) $\tilde{\nu}_{max}$ cm^{-1} 2935, 2846, 1717, 1665, 1095. **HRMS** (ESI) calcd for $[C_{20}H_{28}O_2N_1]^+$ ($[M+H]^+$): *m/z* 314.2115, found 314.2114.

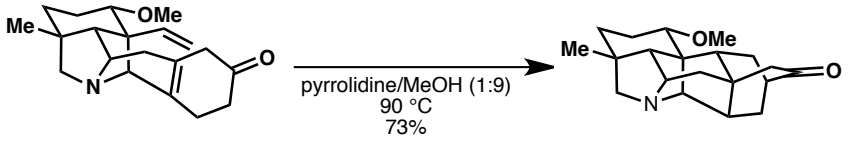

3.49 **3.50**

(1*S*,3a*R*,3a^1*R*,5a*S*,6a*S*,10a*R*,10b*S*)-1-Methoxy-3a-methyldodecahydro-1*H*-5,7,10b-(epimethanetriyl)-6a,9-ethanodibenzo[*cd*,*f*]indol-12-one (3.50). Enone **3.49** (3.4 mg, 0.11 mmol) was taken up in MeOH (0.80 mL) in a Schlenk tube. Pyrrolidine (redistilled, 60 μL) was added and the resulting reaction mixture was degassed via 3 freeze-pump-thaw cycles. The Schlenk tube was then sealed under N_2 and heated to 90 °C. After 8.5 h, the solution was cooled to room temperature and the solvent removed to give the crude cycloaddition product. Column chromatography (20:1 CH_2Cl_2/MeOH with 1% NH_4OH → 9:1 CH_2Cl_2/MeOH with 1% NH_4OH) gave the pure ketone (**3.50**) as an orange-white foam (2.5 mg, 0.008 mmol, 73%). **R_f:** 0.13 (9:1 CH_2Cl_2/MeOH with 1% NH_4OH, Dragendorff-Munier stain). **^{1}H NMR** (500 MHz, $CDCl_3$) δ 3.36 (dd, *J* = 10.2, 5.4 Hz, 1H), 3.31 (s, 3H), 3.22 (s, 1H), 2.95 (s, 1H), 2.70 (dd, *J* = 14.3, 5.0 Hz, 1H), 2.53 (d, *J* = 12.5 Hz, 1H), 2.44 (d, *J* = 12.5 Hz, 1H), 2.27 (d, *J* = 19.3 Hz, 1H), 2.18 – 2.12 (m, 1H), 2.11 – 2.03 (m, 2H), 2.03 – 1.92 (m, 2H), 1.92 – 1.83 (m, 1H), 1.80 (dd, *J* = 13.3, 2.9 Hz, 1H), 1.75 – 1.68 (m, 1H), 1.63 – 1.49 (m, 3H), 1.41 – 1.23 (m, 3H), 0.98 (s, 3H). **^{13}C NMR** (151 MHz, $CDCl_3$) δ 216.6, 78.0, 72.4, 64.7, 62.5, 62.1, 54.8, 54.5, 49.6, 44.9, 43.3, 42.31, 41.3, 37.7, 36.0, 31.9, 28.5, 27.6, 24.9, 24.7. **IR** (thin film) $\tilde{\nu}_{max}$ cm^{-1} 2931, 2872, 2848, 2820, 1723, 1088. **HRMS** (ESI) calcd for $[C_{20}H_{28}O_2N_1]^+$ ($[M+H]^+$): *m/z* 314.2115, found 314.2114.

X-Ray Data and Crystal Refinement for the *p*-Nitrobenzoyl Derivative of 3.24.

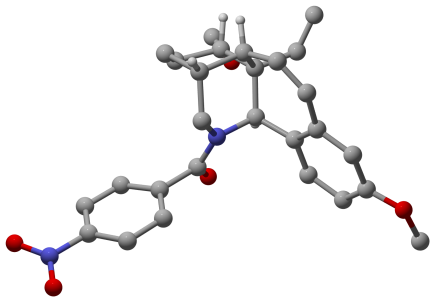

A colorless rod 0.060 x 0.030 x 0.030 mm in size was mounted on a Cryoloop with Paratone oil. Data were collected in a nitrogen gas stream at 100(2) K using phi and omega scans. Crystal-to-detector distance was 60 mm and exposure time was 5 seconds per frame using a scan width of 1.0°. Data collection was 100.0% complete to 67.000° in θ. A total of 42642 reflections were collected covering the indices, -8<=*h*<=9, -19<=*k*<=19, -22<=*l*<=22. 4220 reflections were found to be symmetry independent, with an R_{int} of 0.0195. Indexing and unit cell refinement indicated a primitive, monoclinic lattice. The space group was found to be P 21/n (No. 14). The data were integrated using the Bruker SAINT software program and scaled using the SADABS software program. Solution by iterative methods (SHELXT) produced a complete heavy-atom phasing model consistent with the proposed structure. All non-hydrogen atoms were refined anisotropically by full-matrix least-squares (SHELXL-2013). All hydrogen atoms were placed using a riding model. Their positions were constrained relative to their parent atom using the appropriate HFIX command in SHELXL-2013.

Empirical formula	C27 H28 N2 O5	
Formula weight	460.51	
Temperature	100(2) K	
Wavelength	1.54178 Å	
Crystal system	Monoclinic	
Space group	P 21/n	
Unit cell dimensions	a = 7.9803(6) Å	α= 90°.
	b = 15.8783(12) Å	β= 102.128(3)°.
	c = 18.5446(15) Å	γ = 90°.
Volume	2297.4(3) $Å^3$	
Z	4	
Density (calculated)	1.331 Mg/m^3	
Absorption coefficient	0.751 mm^{-1}	
F(000)	976	
Crystal size	0.060 x 0.030 x 0.030 mm^3	
Crystal color/habit	colorless rod	
Theta range for data collection	3.700 to 68.317°.	
Index ranges	-8<=h<=9, -19<=k<=19, -22<=l<=22	
Reflections collected	42642	
Independent reflections	4220 [R(int) = 0.0195]	

Completeness to theta = 67.000°	100.0 %
Absorption correction	Semi-empirical from equivalents
Max. and min. transmission	0.929 and 0.877
Refinement method	Full-matrix least-squares on F^2
Data / restraints / parameters	4220 / 0 / 309
Goodness-of-fit on F^2	1.014
Final R indices [I>2sigma(I)]	R1 = 0.0416, wR2 = 0.1082
R indices (all data)	R1 = 0.0434, wR2 = 0.1099
Extinction coefficient	n/a
Largest diff. peak and hole	0.687 and -0.226 e.$Å^{-3}$

3.8 References and Notes

[1] (a) For a review of the aza-Wittig transformation, see: Palacios, F.; Alonso, C.; Aparicio, D.; Rubiales, G.; de los Santos, J. M. *Tetrahedron* **2007**, *63,* 523. (b) For an example involving bridgehead imines: Sasaki, T.; Eguchi, S.; Okano, T. *Heterocycles* **1984**, *21,* 576.
[2] Fu, Y.; Lee, S. K.; Min, H.-Y.; Lee, T.; Lee, J.; Cheng, M.; Kim, S. *Bioorg. Med. Chem. Lett.* **2007**, *17,* 97.
[3] Mai, W.; Green, S. A.; Bates, D. K.; Fang, S. *Synth. Commun.* **2010**, *40,* 2571.
[4] Pronin, S. V.; Tabor, M. G.; Jansen, D. J.; Shenvi, R. A. *J. Am. Chem. Soc.* **2012**, *134,* 2012.
[5] Bexrud, J. A.; Beard, J. D.; Leitch, D. C.; Schafer, L. L. *Org. Lett.* **2005**, *7,* 1959.
[6] Leitch, D. C.; Payne, P. R.; Dunbar, C. R.; Schafer, L. L. *J. Am. Chem. Soc.* **2009**, *131,* 18246.
[7] Hesp, K. D.; Tobisch, S.; Stradiotto, M. *J. Am.Chem. Soc.* **2010**, *132,* 413.
[8] Attempted conditions included heating the primary amine-bearing epoxide compound both in the presence and absence of acid.
[9] (a) Meinwald, J.; Labama, S. S.; Chadha, M. S. *J. Am Chem. Soc.* **1963**, *85,* 582. (b) Jones, D. W.; Nongrum, F. M. *J. Chem. Soc., Perkin Trans 1,* **1996,** *7,* 705. (c) Kulasegaram, S.; Kulawiec, R. J. *J. Org. Chem.* **1997**, *62,* 6547.
[10] Lebold, T. P.; Gallego, G. M.; Marth, C. J.; Sarpong, R. *Org. Lett.* **2012**, *14,* 2110.
[11] Fukuyama, T.; Cheung, M.; Kan, T. *Synlett* **1999**, *8,* 1301.
[12] Ito, Y.; Hirao, T.; Saegusa, T. *J. Org. Chem.,* **1978**, *43,* 1011.
[13] (a) Bhunia, A.; Yetra, S. R.; Biju, A. T. *Chem. Soc. Rev.* **2012**, *41,* 3140. (b) Zhang, W.; Gorny, R.; Dowd, P. *Synth. Commun.* **1999**, *29,* 2903.
[14] Hamlin, A. M.; Cortez, F. de J.; Lapointe, D.; Sarpong, R. *Angew. Chem. Int. Ed.* **2013**, *52,* 4854.
[15] Karabatsos, G. J.; Shone, R. L. *J. Org. Chem.* **1968**, *33,* 619.
[16] Beckwith, A. L. J.; Goh, S. H. *J. Chem. Soc., Chem. Commun.,* **1983**, 905.
[17] For a discussion on the single electron transfer mechanism for alkyl halide reduction, see: Alonso, F.; Beletskaya, I. P.; Yus, M.. *Chem. Rev.* **2002**, *102,* 4009.
[18] Baik, W.; Lee, H. J.; Koo, S.; Kim, B. H. *Tetrahedron Lett.* **1998**, *39,* 8125.
[19] (a) Leitch, D. C.; Payne, P. R.; Dunbar, C. R.; Schafer, L. L. *J. Am. Chem. Soc.* **2009**, *131,* 18246. (b) Leitch, D. C.; Platel, R. H. ; Schafer, L. L. *J. Am. Chem. Soc.* **2011**, *133,* 15453.
[20] For an example of the use of an NIS-mediated iodoamination in natural product synthesis, see: Beshore, D. C.; Smith, A. B. *J. Am. Chem. Soc.* **2008**, *130,* 13778.
[21] (a) Trost, B. M.; Tang, W. *J. Am. Chem. Soc.* **2002**, *124,* 14542. (b) Trost, B. M.; Tang, W.; Toste, F. D. *J. Am. Chem. Soc.* **2005**, *127,* 14785.

[22] For a review on nitrogen-centered radicals, see: Zard, S. Z. *Chem. Soc. Rev.,* **2008**, *37,* 1603.
[23] (a) Ashby, E. C.; Goel, A. B.; DePriest, R. N. *J. Org. Chem.* **1981**, *46,* 2429. (b) Ashby, E. C.; Goel, A. B.; DePriest, R. N. *Tetrahedron Lett.* **1981**, *22,* 4355.
[24] Newcomb, M.; Burchill, M.T.; Deeb, T. M. *J. Am. Chem. Soc.* **1988**, *110,* 6528.
[25] Tokuda, M.; Fujita, H.; Miyamoto, T.; Suginome, H. Anodic Cyclization. *Tetrahedron* **1993**, *49,* 2412.
[26] Dess, D. B.; Martin, J. C. *J. Org. Chem.* **1983**, *48,* 4155.
[27] For reviews on alkylation of nitriles and their use in synthesis, see: (a) Fleming, F. F.: Gudipati, S. G.; Zhang, Z.; Liu, W.; Steward, O. W. *J. Org. Chem.* **2005**, *70,* 3845. (b) Fleming, F. F.; Zhang, Z. *Tetrahedron* **2005**, *61,* 747.
[28] Satoh, T.; Suzuki, S. *Tetrahedron Lett.* **1969**, *52,* 4555.

Appendix 2. Spectra Relevant to Chapter 3

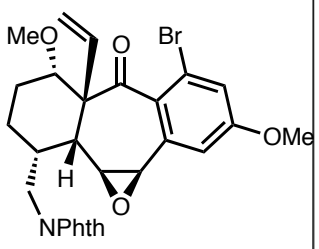
MeO
O
Br
OMe
H
O
NPhth

3.7

2.38
2.62
1.00
1.17
2.24
1.19
1.19
1.10
2.45
5.38
1.14
3.19
1.21
1.30
1.17
1.29
10.0 9.5 9.0 8.5 8.0 7.5 7.0 6.5 6.0 5.5 5.0 4.5 4.0 3.5 3.0 2.5 2.0 1.5 1.0 0.5 0.0 -0.5
f1 (ppm)

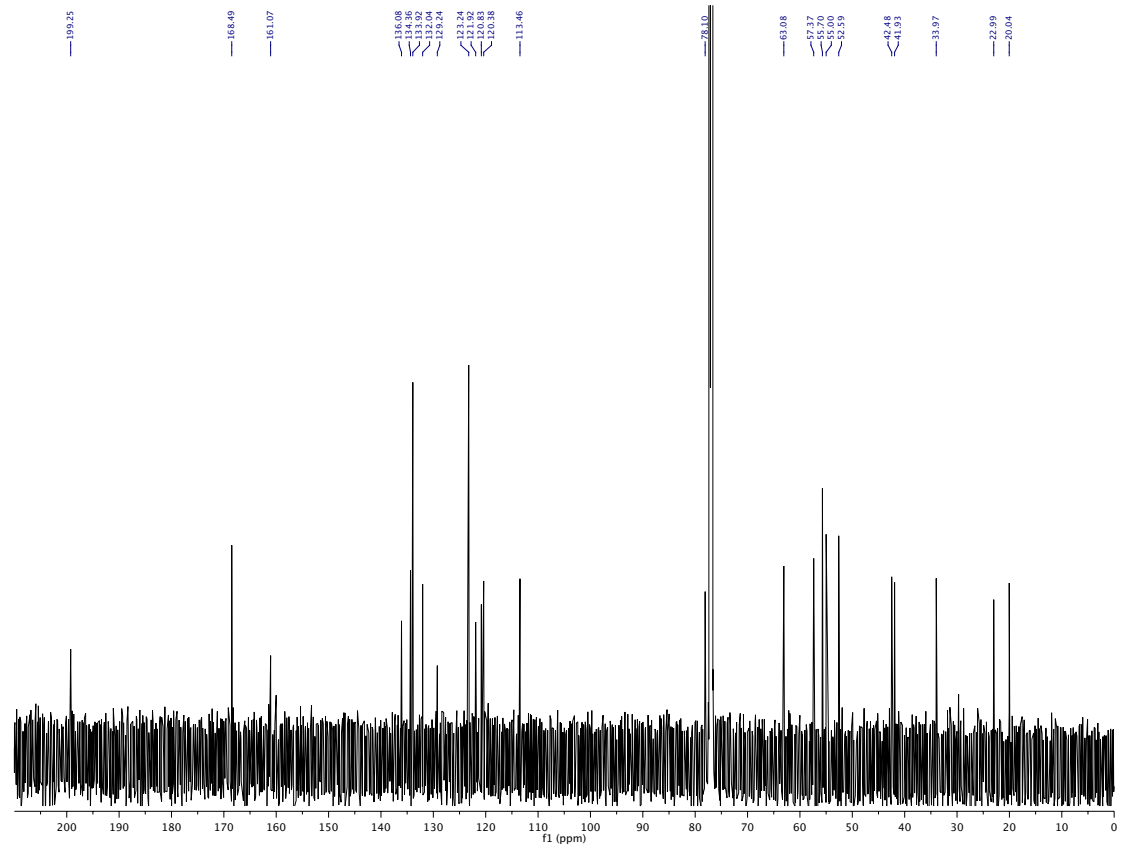
199.25
168.49
161.07
136.08
134.36
133.92
132.04
129.24
123.24
121.92
120.83
120.38
113.46
28.10
63.08
57.37
55.70
55.00
52.59
42.48
41.93
33.97
22.99
20.04
200 190 180 170 160 150 140 130 120 110 100 90 80 70 60 50 40 30 20 10 0
f1 (ppm)

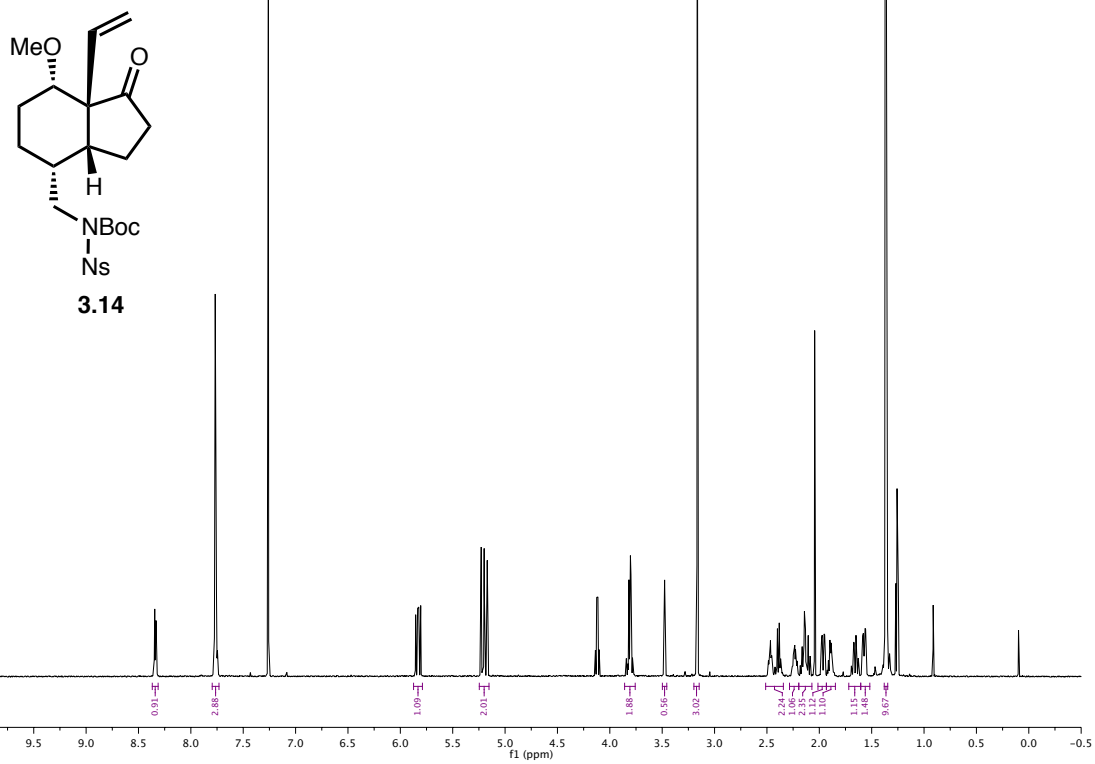
MeO
O
H
NBoc
Ns
3.14
f1 (ppm)

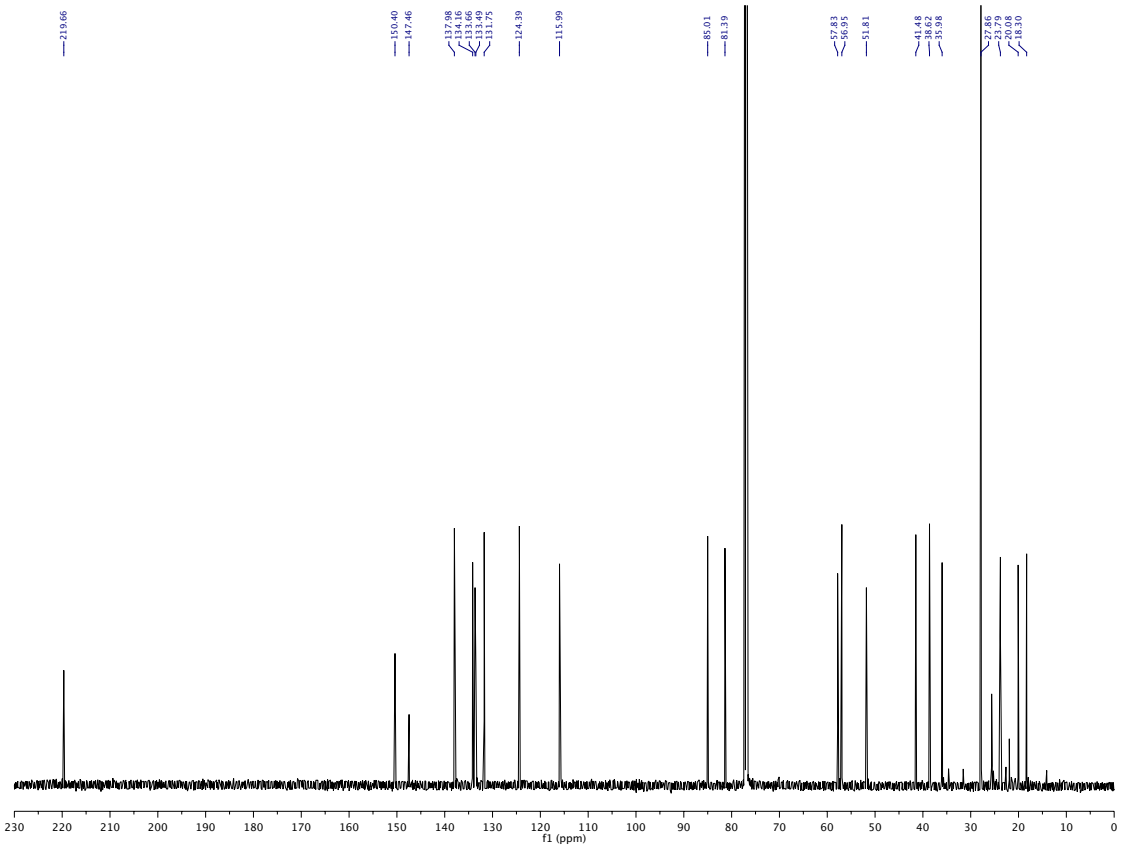
219.66
150.40
147.46
137.98
134.16
133.66
133.49
131.75
124.39
115.99
85.01
81.39
57.83
56.95
51.81
41.48
38.62
35.98
27.86
23.79
20.68
18.30
f1 (ppm)

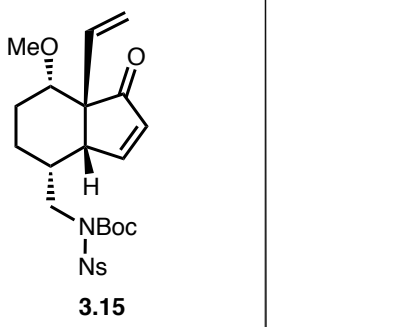
MeO
O
H
NBoc
Ns

3.15

0.92
3.96
0.96
1.00
0.96
1.00
1.36
0.83
1.07
2.74
1.06
3.43
3.95
1.23
9.12
10.0 9.5 9.0 8.5 8.0 7.5 7.0 6.5 6.0 5.5 5.0 4.5 4.0 3.5 3.0 2.5 2.0 1.5 1.0 0.5 0.0 -0.5
f1 (ppm)

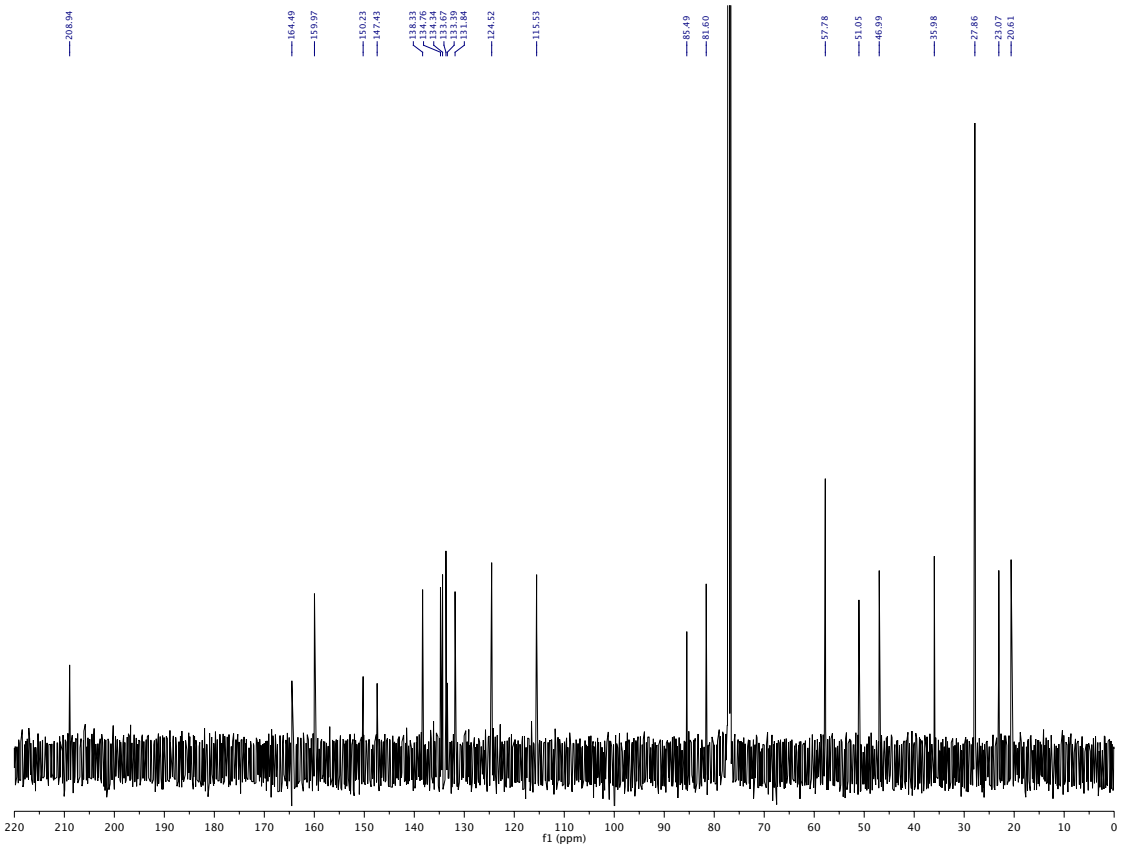
208.94
164.49
159.97
150.23
147.43
138.33
134.76
134.34
133.67
133.39
131.84
124.52
115.53
85.49
81.60
57.78
51.05
46.99
35.98
27.86
23.07
20.61
220 210 200 190 180 170 160 150 140 130 120 110 100 90 80 70 60 50 40 30 20 10 0
f1 (ppm)

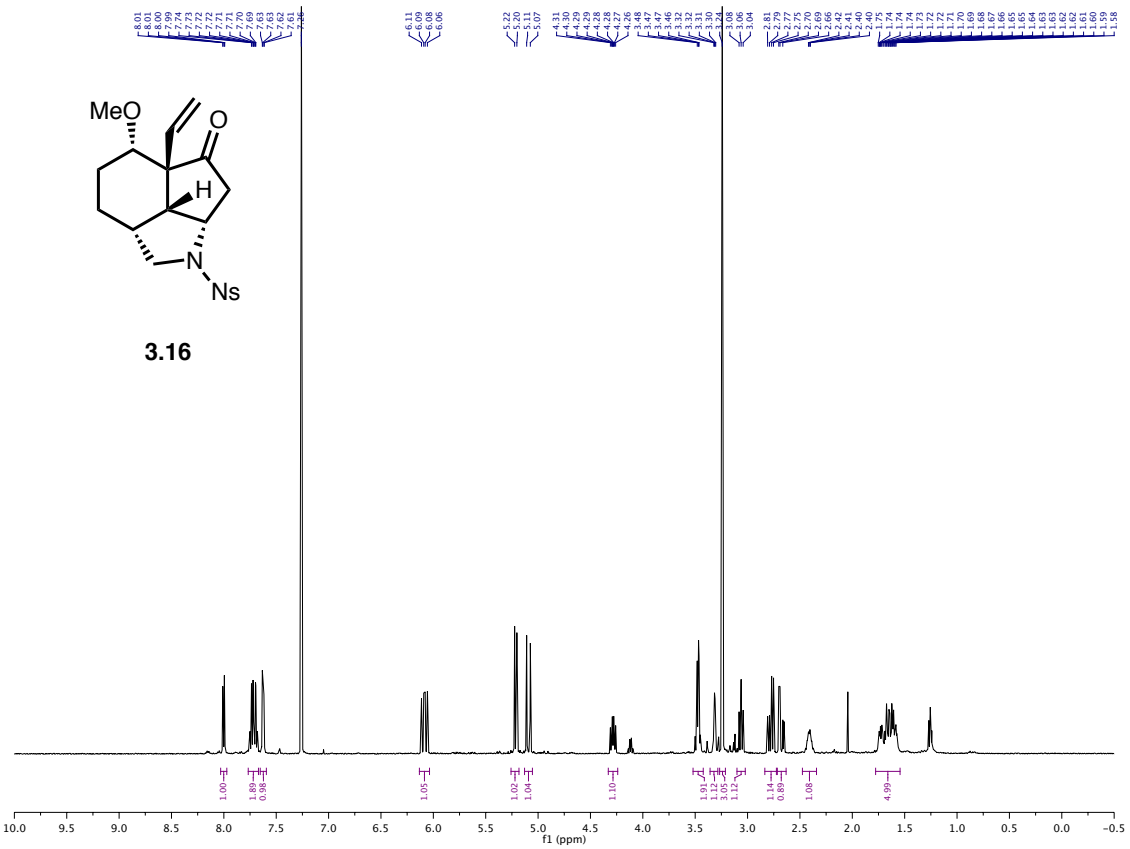

3.16

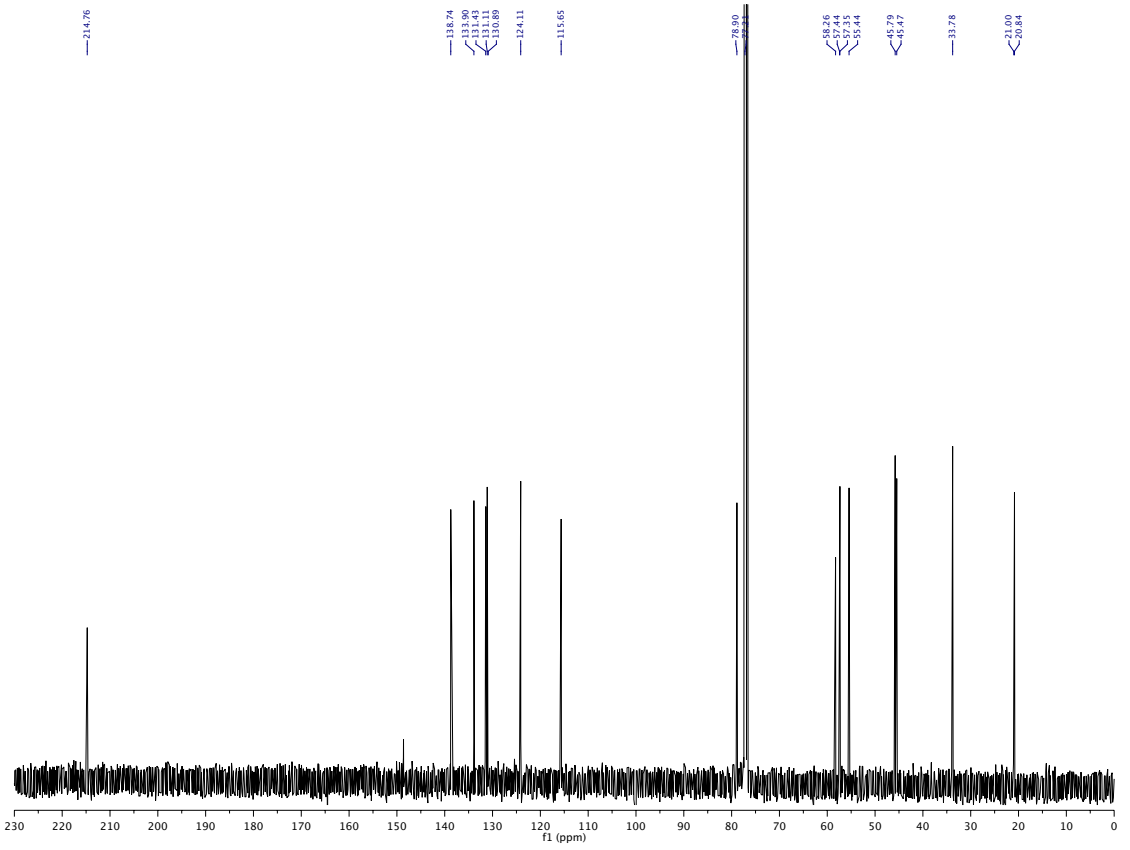

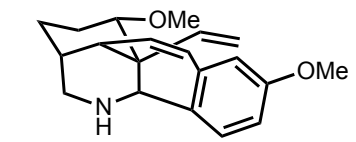

3.23

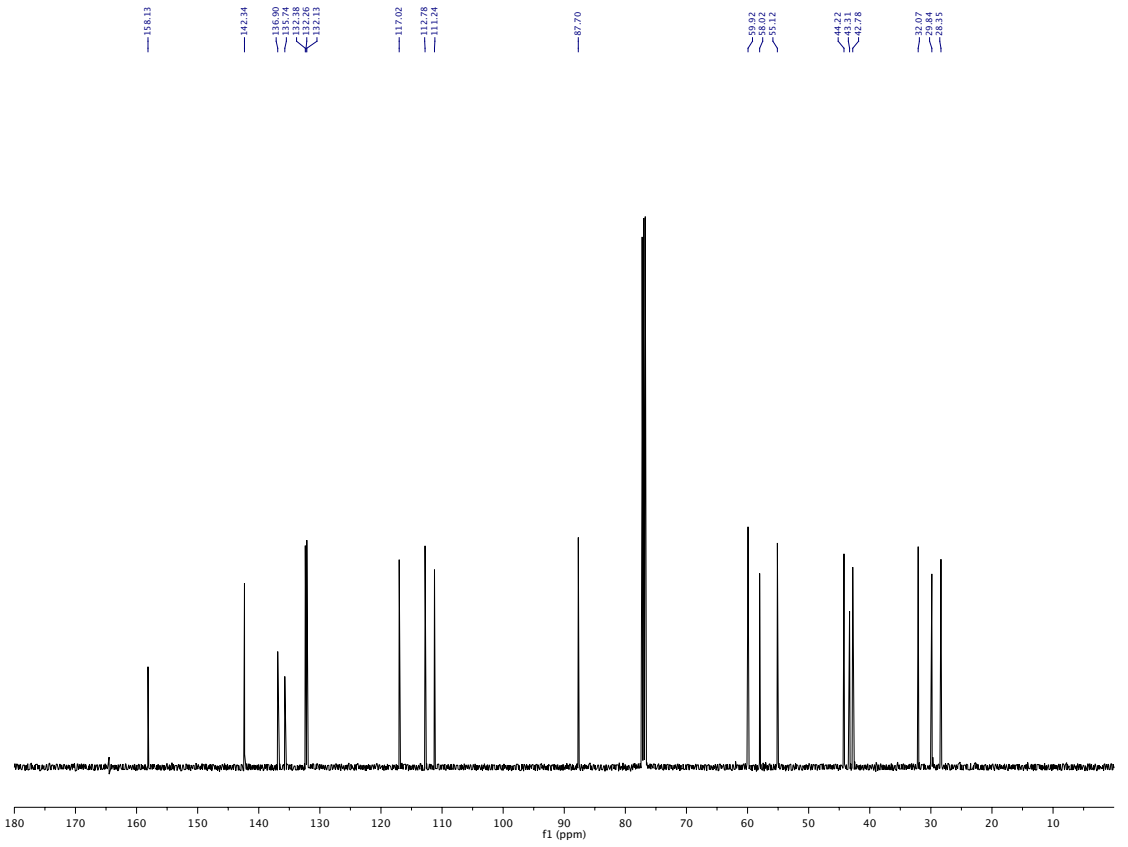

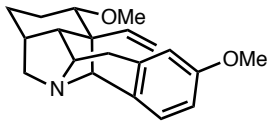

3.35

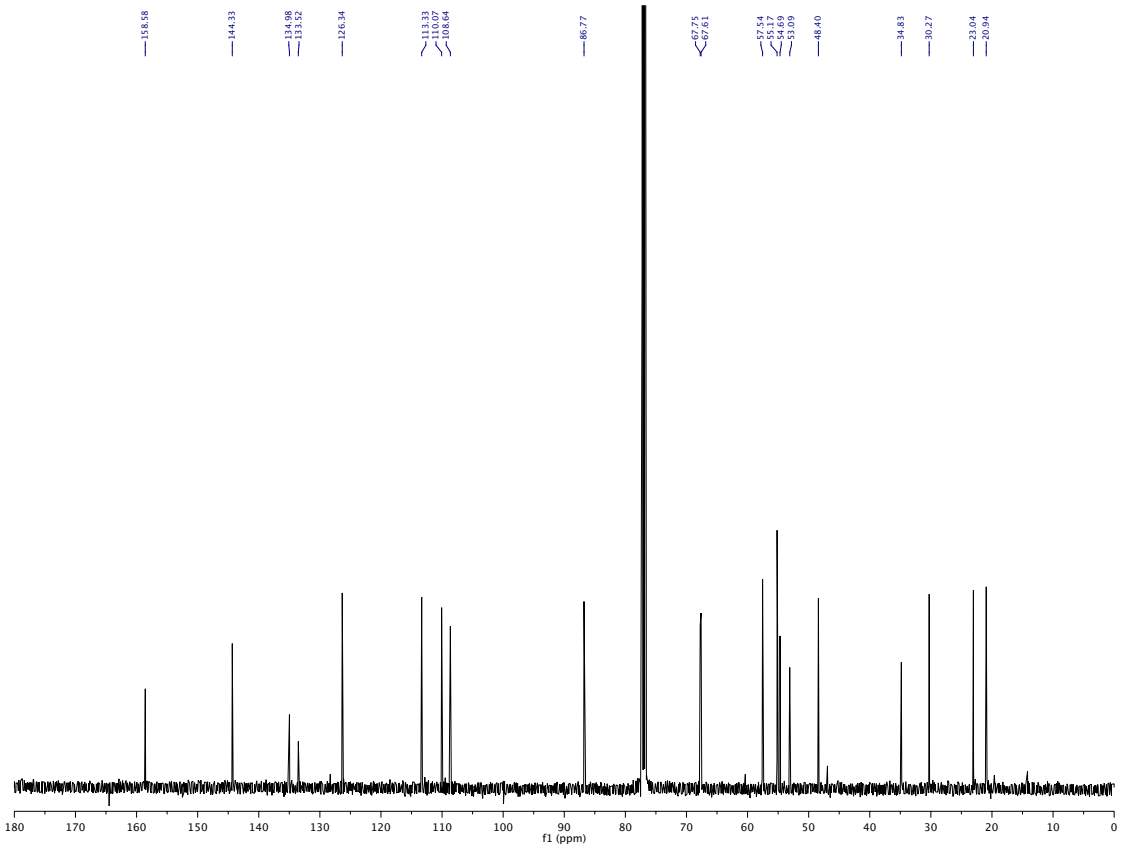

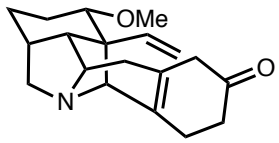
OMe
O
N

3.36

1.00
0.94
0.85
0.95
1.16
1.27
0.96
2.55
4.50
2.11
1.03
0.51
1.13
2.02
10.0 9.5 9.0 8.5 8.0 7.5 7.0 6.5 6.0 5.5 5.0 4.5 4.0 3.5 3.0 2.5 2.0 1.5 1.0 0.5 0.0 -0.5
f1 (ppm)

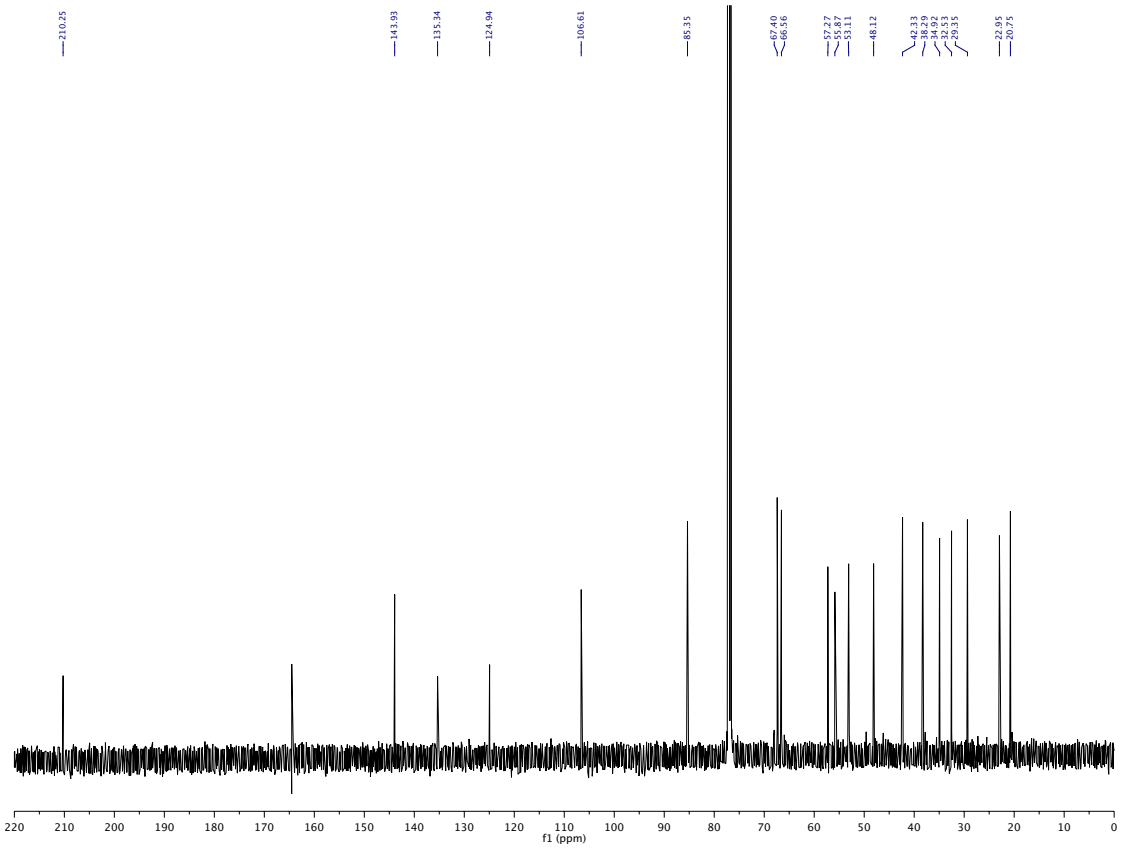
210.25
143.93
135.34
124.94
106.61
85.35
67.40
66.56
57.27
55.87
53.11
48.12
42.33
41.29
34.92
32.53
29.35
22.95
20.75
220 210 200 190 180 170 160 150 140 130 120 110 100 90 80 70 60 50 40 30 20 10 0
f1 (ppm)

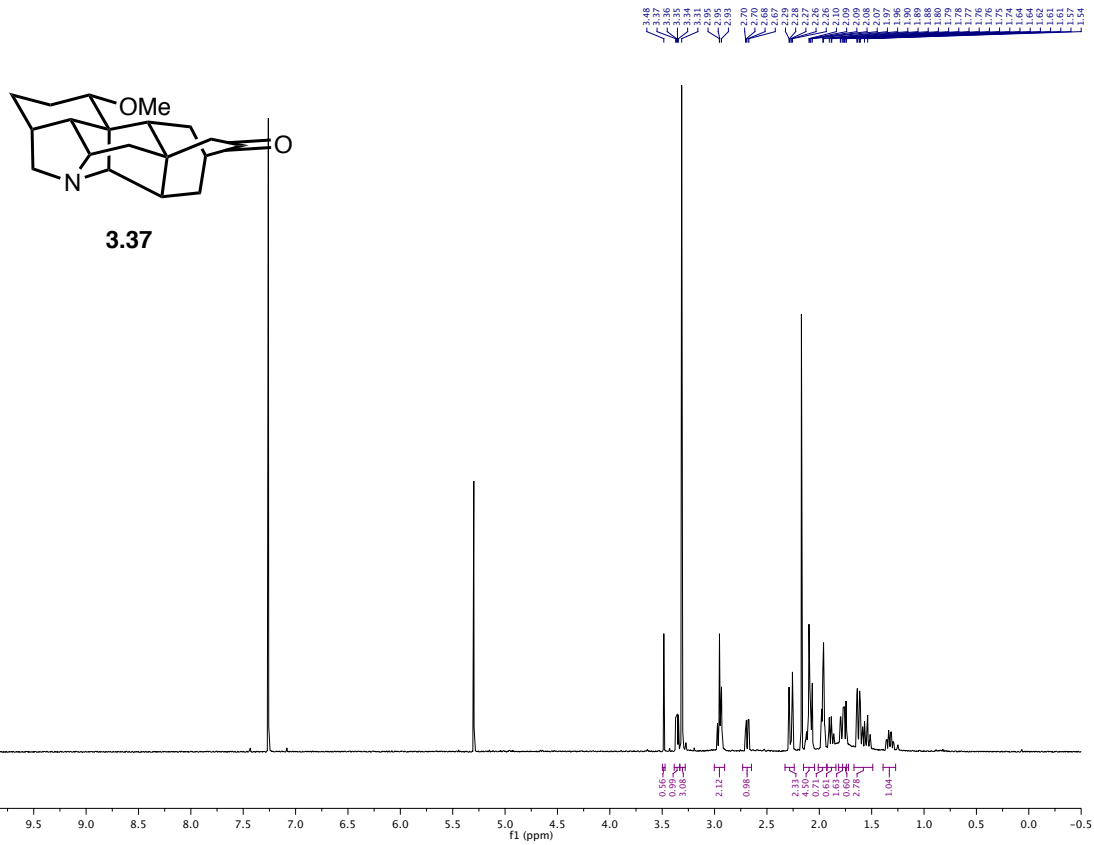

3.37

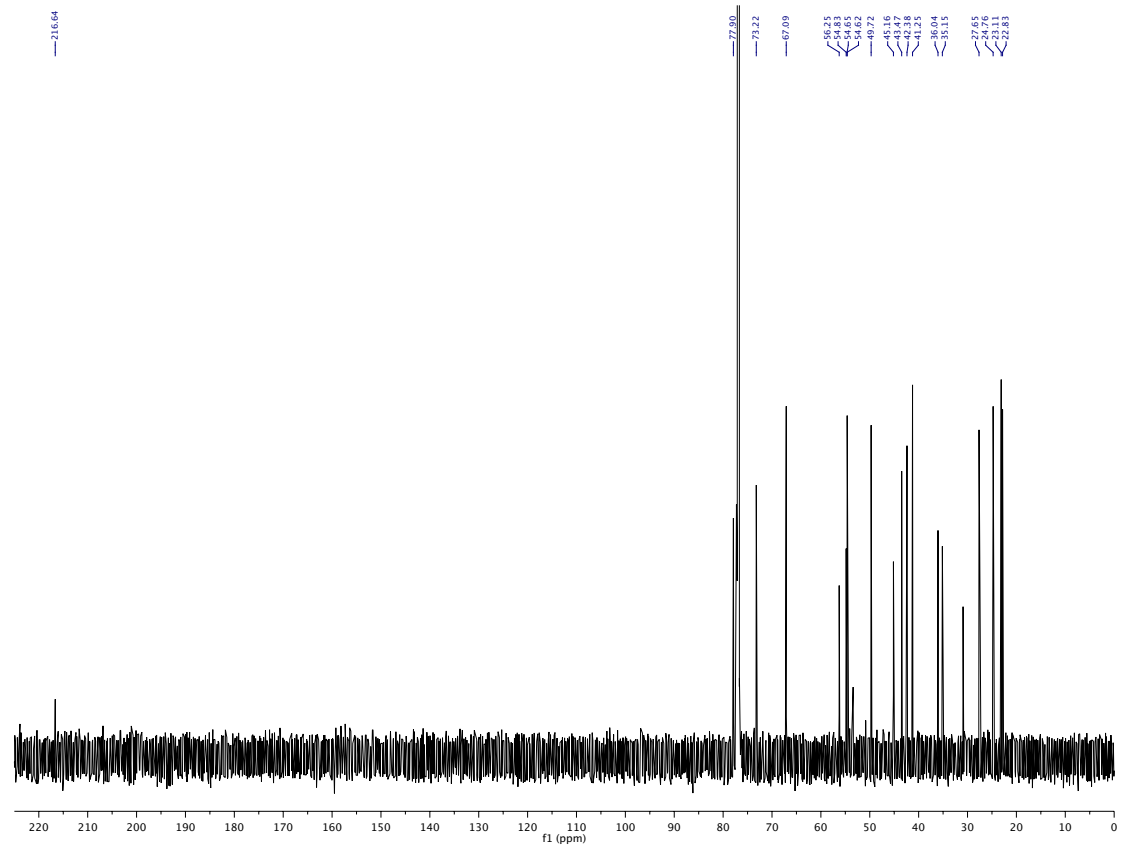

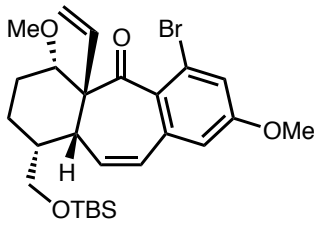
MeO
O
Br
OMe
H
OTBS

3.44

1.00
1.02
0.86
1.13
1.75
0.96
1.02
3.04
2.25
2.96
1.22
1.14
1.06
3.43
8.87
3.67
2.92
10.0 9.5 9.0 8.5 8.0 7.5 7.0 6.5 6.0 5.5 5.0 4.5 4.0 3.5 3.0 2.5 2.0 1.5 1.0 0.5 0.0 -0.5
f1 (ppm)

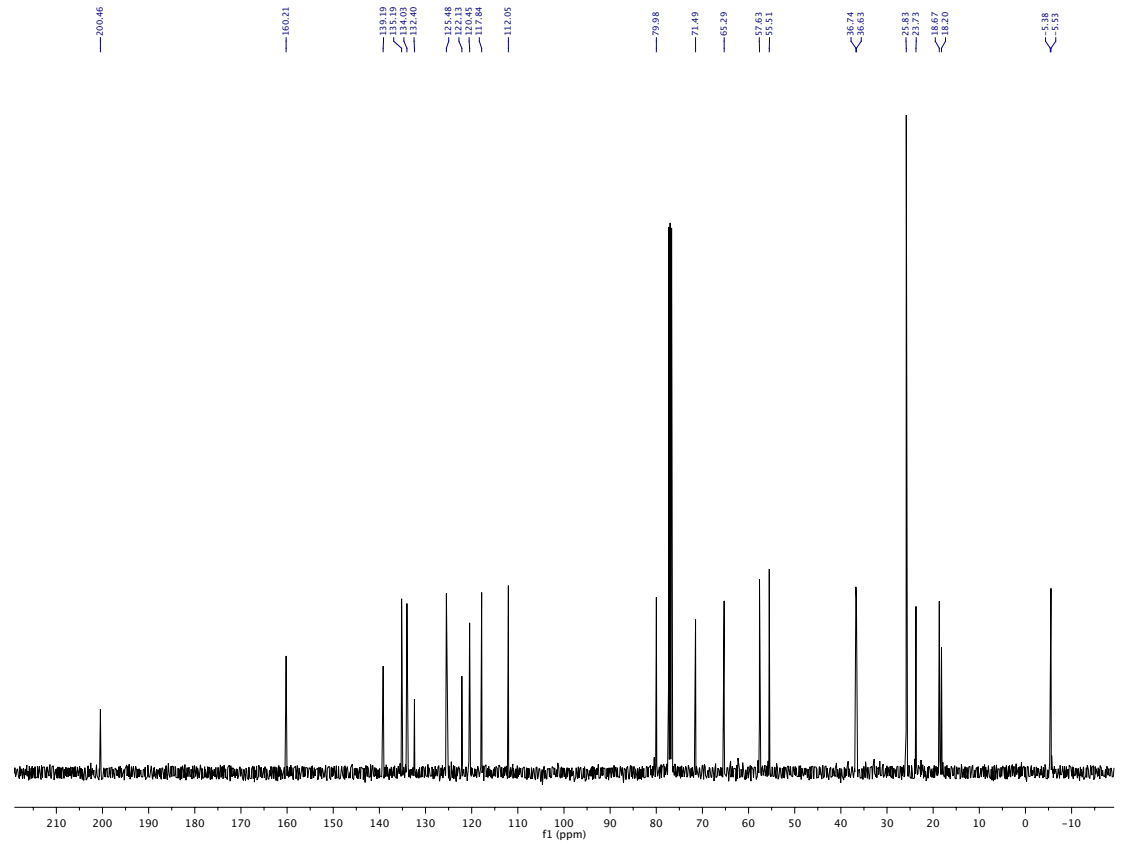
200.46
160.21
139.19
135.19
134.03
132.40
125.48
122.13
120.45
117.84
112.05
79.98
71.49
65.29
57.63
55.51
36.74
36.63
25.83
23.73
18.67
18.20
-5.38
-5.53
210 200 190 180 170 160 150 140 130 120 110 100 90 80 70 60 50 40 30 20 10 0 -10
f1 (ppm)

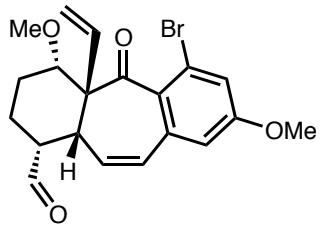
MeO
O
Br
OMe
H
O

3.43

1.00
0.98
0.99
0.78
1.02
1.88
1.30
0.97
0.01
0.99
2.90
1.01
1.13
1.25
1.07
0.99
10.0 9.5 9.0 8.5 8.0 7.5 7.0 6.5 6.0 5.5 5.0 4.5 4.0 3.5 3.0 2.5 2.0 1.5 1.0 0.5 0.0 -0.5
f1 (ppm)
203.55
199.14
160.33
138.44
134.18
133.42
131.75
126.14
122.28
120.61
118.17
112.06
79.16
70.99
57.46
55.44
47.59
35.40
22.68
15.80

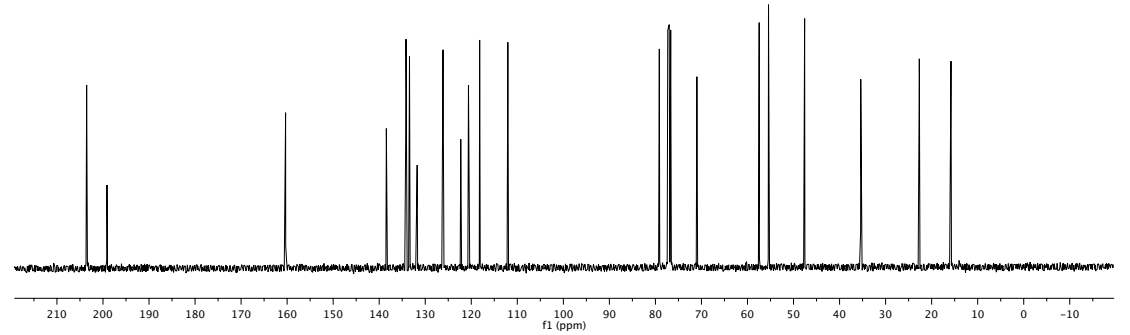
210 200 190 180 170 160 150 140 130 120 110 100 90 80 70 60 50 40 30 20 10 0 -10
f1 (ppm)

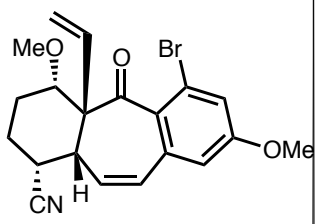
MeO
O
Br
OMe
CN
H

3.45

f1 (ppm)

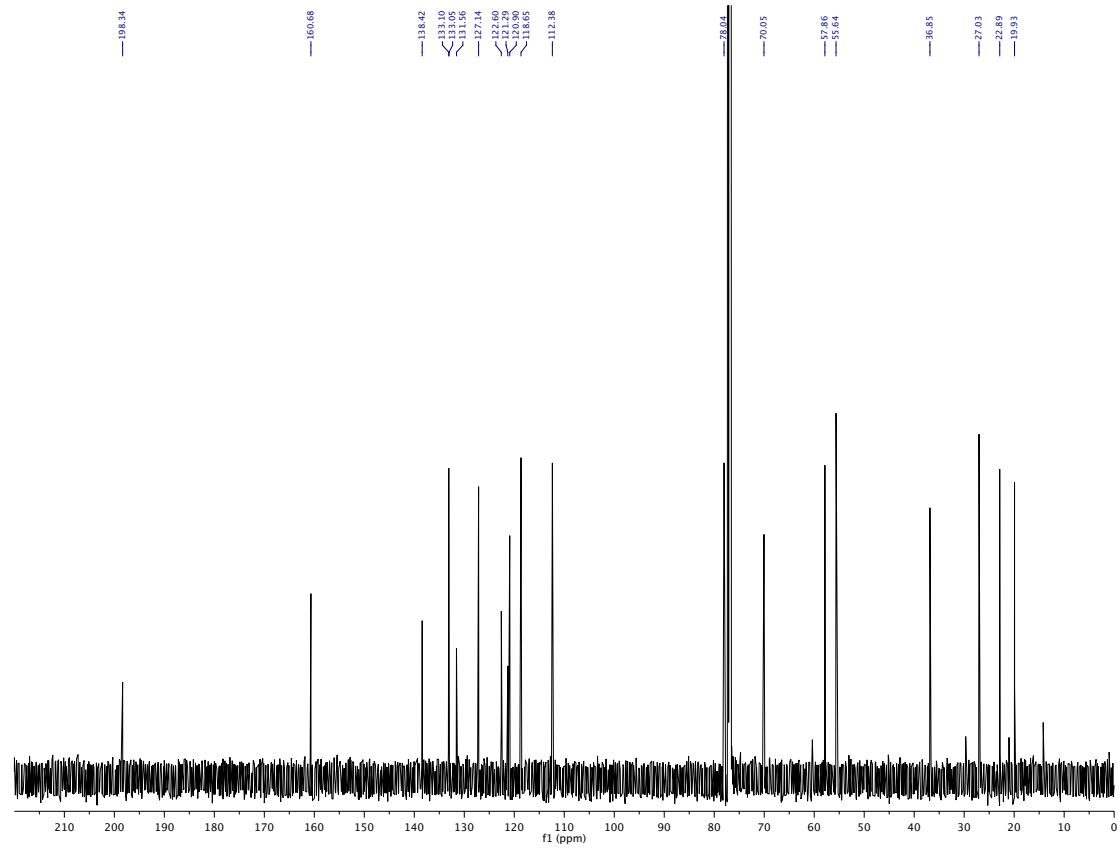
198.34
160.68
138.42
133.10
133.05
131.56
127.14
122.60
121.38
120.90
118.65
112.38
78.04
70.05
57.86
55.64
36.85
27.03
22.89
19.93
f1 (ppm)

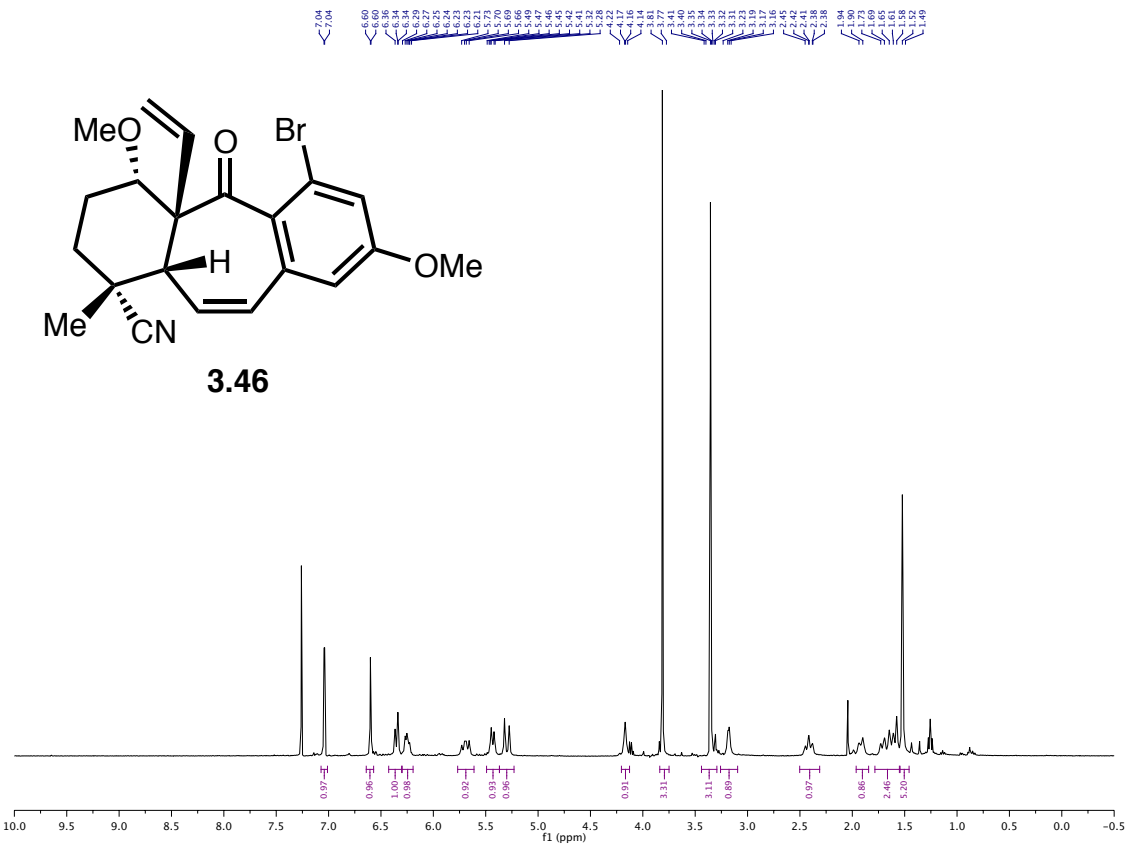

3.46

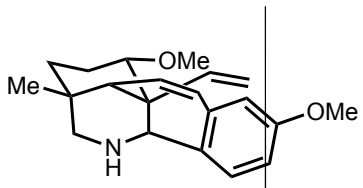
OMe
Me
OMe
N
H

3.48

1.02
1.08
1.07
1.05
1.09
1.07
1.51
1.49
1.09
3.20
3.43
1.08
2.43
1.11
1.06
1.26
1.21
1.20
3.42
10.0 9.5 9.0 8.5 8.0 7.5 7.0 6.5 6.0 5.5 5.0 4.5 4.0 3.5 3.0 2.5 2.0 1.5 1.0 0.5 0.0
f1 (ppm)

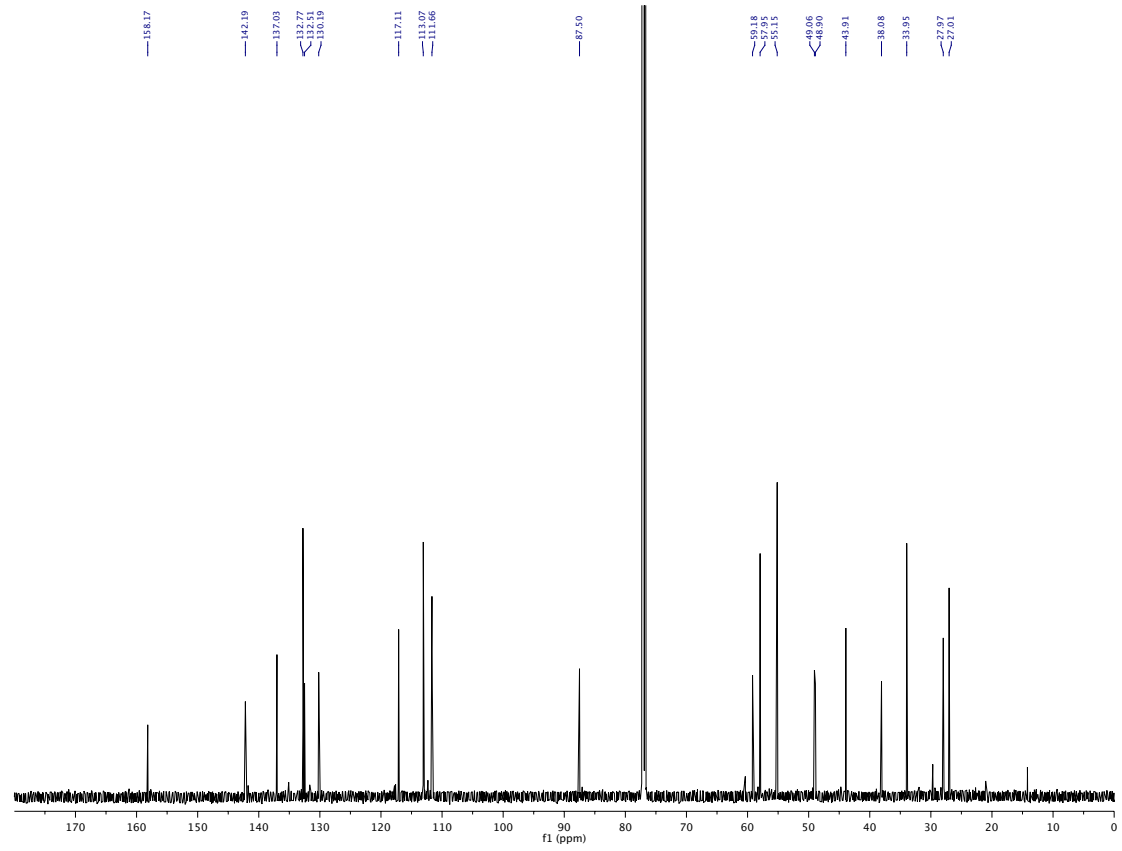
158.17
142.19
137.03
132.77
132.51
130.19
117.11
113.07
111.66
87.50
59.18
57.95
55.15
49.06
48.90
43.91
38.08
33.95
27.97
27.01
170 160 150 140 130 120 110 100 90 80 70 60 50 40 30 20 10 0
f1 (ppm)

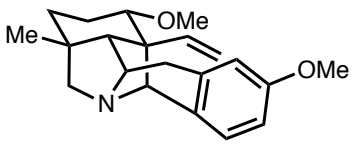

2.2

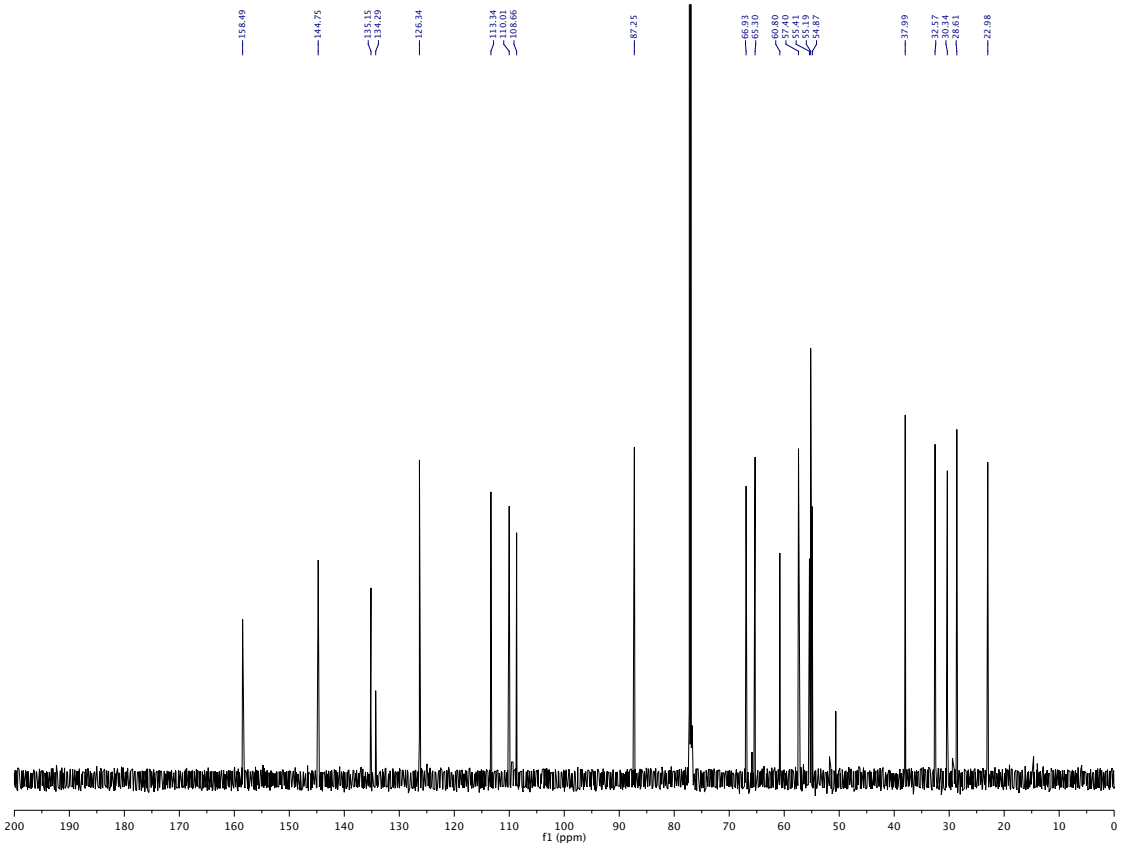

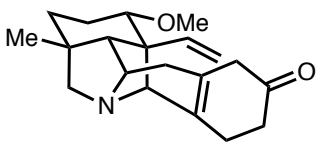
Me
OMe
O
N

3.49

0.89
1.01
1.01
4.72
0.85
1.43
2.40
1.12
1.12
2.18
0.99
2.11
3.36
f1 (ppm)

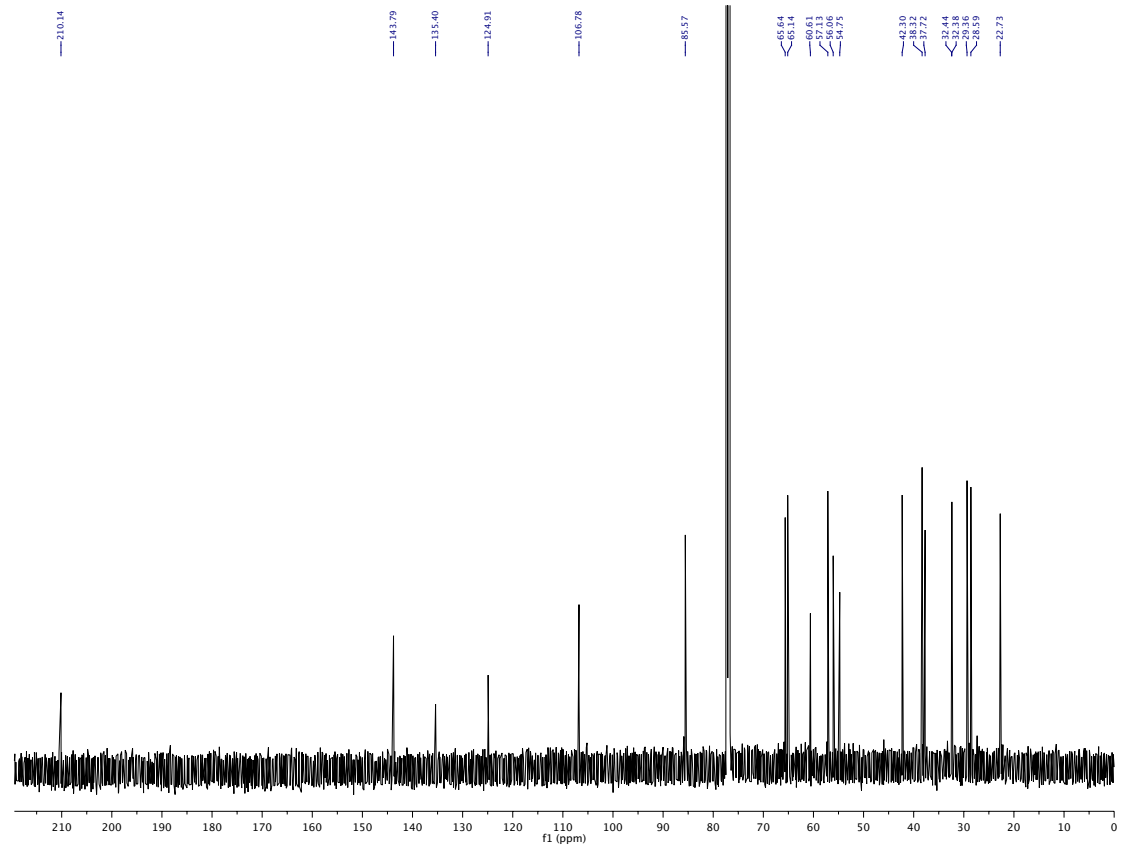
210.14
143.79
135.40
124.91
106.78
85.57
65.64
65.14
60.61
57.13
56.06
54.75
42.30
38.32
37.72
32.44
32.38
30.16
28.59
22.73
f1 (ppm)

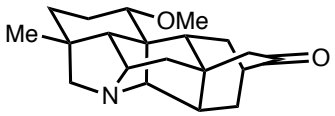
Me
OMe
O
N

3.50

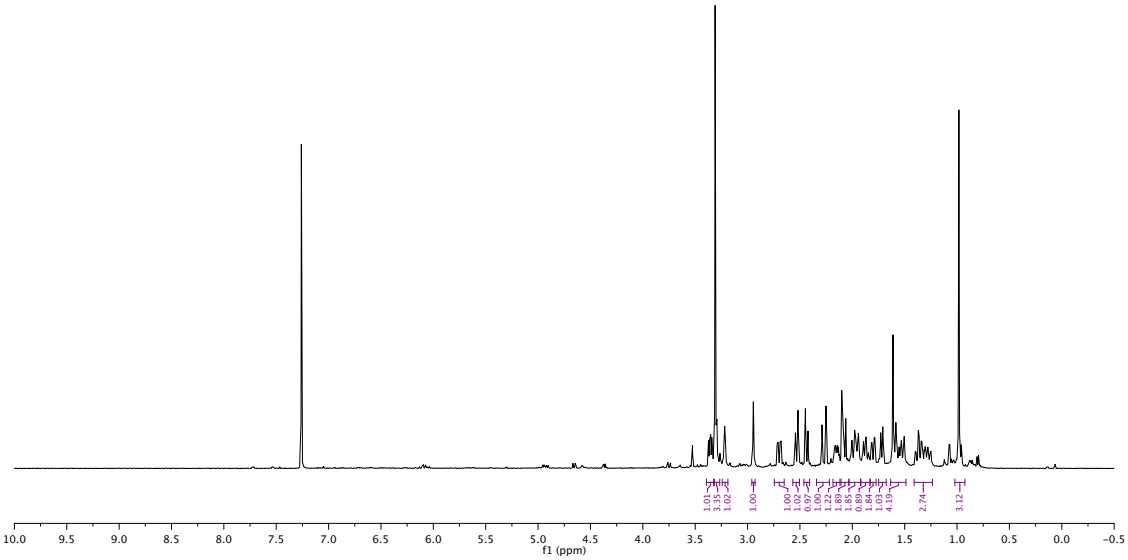
1.01
3.35
1.02
1.00
1.00
1.07
0.97
1.00
1.23
1.60
1.85
0.89
1.44
1.03
4.19
2.74
3.12
10.0 9.5 9.0 8.5 8.0 7.5 7.0 6.5 6.0 5.5 5.0 4.5 4.0 3.5 3.0 2.5 2.0 1.5 1.0 0.5 0.0 -0.5
f1 (ppm)

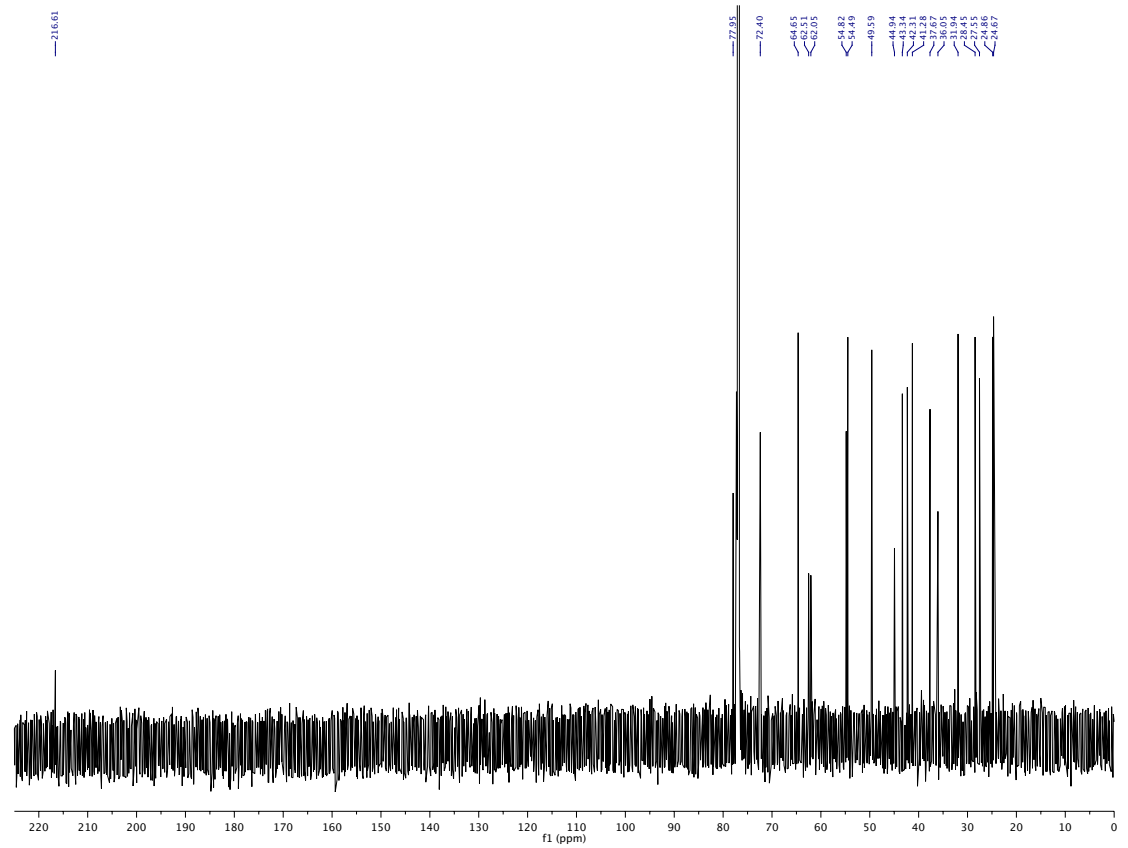
216.61
77.95
72.40
64.65
62.51
62.05
54.82
54.49
49.59
44.94
43.34
43.21
42.28
37.67
36.05
31.04
28.45
27.55
24.86
24.67
220 210 200 190 180 170 160 150 140 130 120 110 100 90 80 70 60 50 40 30 20 10 0
f1 (ppm)